Université de Montréal

Exposition à l'alcool pendant la période préimplantatoire : Conséquences sur l'épigénome et le développement embryonnaire

Par
Lisa-Marie Legault

Département de Biochimie et médecine moléculaire, Faculté de Médecine

Thèse présentée en vue de l'obtention du grade de Doctorat

en Biochimie

Août, 2023

Université de Montréal

Département de Biochimie et médecine moléculaire, Faculté de Médecine

---

Cette thèse intitulée

Exposition à l'alcool pendant la période préimplantatoire : Conséquences sur l'épigénome et le développement embryonnaire

Présenté par

Lisa-Marie Legault

A été évalué(e) par un jury composé des personnes suivantes

Mohan Malleshaiah
Président-rapporteur

Serge McGraw
Directeur de recherche

Martine Tétreault
Membre du jury

Luigi Bouchard
Examinateur externe

Résumé

Une exposition prénatale à l'alcool peut altérer le développement embryonnaire et causer le Trouble du Spectre de l'Alcoolisation Fœtale (TSAF). Les mécanismes moléculaires menant aux symptômes observés chez les enfants atteints sont toutefois méconnus. Plus encore, bien que les taux de consommation excessive d'alcool (*binge-drinking*) et de grossesses non-planifiées soient en hausse à travers le monde, les impacts d'une exposition prénatale à l'alcool pendant la préimplantation de l'embryon, sont inconnus et peu étudiés. Dans cette thèse, je souhaitais caractériser les impacts morphologiques d'une exposition à l'alcool pendant la préimplantation sur l'embryon en développement. De plus, je voulais définir les mécanismes moléculaires impliqués dans le cerveau antérieur ainsi que dans le placenta embryonnaire, en plus d'évaluer l'effet d'une exposition à l'alcool pendant la préimplantation sur certaines fonctions cognitives au stade post-natal.

Notre hypothèse de recherche est qu'une exposition à l'alcool de type aigu pendant la préimplantation entrainera des erreurs dans l'établissement du programme épigénétique embryonnaire, causant des altérations dans les profils de méthylation d'ADN et d'expression des gènes chez l'embryon et son placenta qui persisteront tout au long de la gestation. Plus encore, nous croyons que ces dérégulations moléculaires altèreront les fonctions cognitives à long terme chez les souriceaux exposés.

Pour répondre à ces questions, nous avons établi un modèle murin d'exposition à l'alcool de type aigu pendant la préimplantation en injectant des femelles gestantes au jour embryonnaire 2.5 (E2.5), correspondant au stade 8-cellules, avec deux doses de 2.5g/kg d'alcool séparées par 2 heures d'intervalle. Nous avons récolté des embryons à mi-gestation (E10.5), évaluer la morphologie puis nous avons isolé le cerveau antérieur pour étudier la méthylation d'ADN et l'expression génique. Nous avons aussi récolté des embryons en fin de gestation (E18.5) et leur placenta pour procéder à des analyses de méthylation d'ADN et de l'expression génique, en plus d'effectuer des analyses histologiques des placentas. Finalement, nous avons aussi laissé naître des souris issues de notre modèle d'exposition à l'alcool pendant la préimplantation pour évaluer certaines fonctions cognitives, notamment l'anxiété, la sociabilité et la mémoire, en procédant à des tests de comportement.

Nous avons d'abord observé une augmentation des anomalies morphologiques chez l'embryon à mi-gestation à la suite de l'exposition prénatale à l'alcool. Nous avons aussi découvert que l'exposition prénatale, pendant la préimplantation, engendrait des différences de méthylation d'ADN dans le cerveau antérieur à mi-gestation et en fin de gestation, dans plusieurs voies biologiques reliées au développement embryonnaire et au fonctionnement du système nerveux. La plupart des régions différentiellement méthylées (DMRs) et des gènes différentiellement exprimés (DEGs) étaient spécifiques à chaque sexe, avec peu de régions partagées entre les mâles et les femelles. Nous avons aussi identifié des DMRs et DEGs spécifiques à chaque sexe ou partagés entre les deux sexes, dans les placentas en fin de gestation en plus de démontrer une baisse du poids fœtal chez les embryons mâles exposés à l'alcool. Enfin, nous avons démontré que l'exposition prénatale pendant la préimplantation causait une baisse de la sociabilité et de la mémoire à court-terme, sans avoir d'effet sur le niveau d'anxiété des souris

En conclusion, nous avons démontré qu'une exposition prénatale à l'alcool en tout début de grossesse affecte le développement embryonnaire, via l'épigénome et le transcriptome du cerveau antérieur et du placenta, et entraine des conséquences à plus long terme sur les fonctions cognitives. En perspective, nous souhaitons établir les profils de méthylation d'ADN et d'expression génique précisément dans certains sous-types cellulaires du cerveau, dont les interneurones GABAergiques afin de mieux définir les mécanismes moléculaires derrière les altérations observées.

Mots-clés : Exposition prénatale à l'alcool, préimplantation, méthylation d'ADN, transcriptome, développement embryonnaire, environnement maternel, reprogrammation épigénétique, cerveau, placenta, différences spécifiques au sexe.

Abstract

Prenatal alcohol exposure can alter embryonic development and lead to Fetal Alcohol Spectrum Disorder (FASD). However, the molecular mechanisms underlying the symptoms in affected children remain poorly understood. Furthermore, despite the increasing rates of binge drinking and unplanned pregnancies worldwide, the impacts of prenatal alcohol exposure during the preimplantation stage of embryonic development are largely unknown and understudied.

In this thesis I aimed to characterize the morphological effects of alcohol exposure during preimplantation on developing embryos. Additionally, we sought to define the extent of DNA methylation defects and gene expression in the anterior brain and embryonic placenta. Furthermore, we aimed to evaluate the effects of our preimplantation alcohol exposure on certain cognitive functions in the postnatal stage.

Our research hypothesis is that acute alcohol exposure during preimplantation will lead to errors in establishing the embryonic epigenetic program, causing alterations in DNA methylation profiles and gene expression in both the embryo and its placenta, persisting throughout gestation. We also believed that these molecular dysregulations would result in long-term cognitive impairments in exposed pups.

To address these questions, we established a preclinical mouse model of acute alcohol exposure during preimplantation by injecting pregnant females on embryonic day 2.5 (E2.5), corresponding to the 8-cell stage, with two doses of 2.5g/kg of alcohol, separated by a 2-hour interval. We collected embryos at mid-gestation (E10.5), assessed for morphological defects and isolated the forebrain for DNA methylation and gene expression studies. We also collected embryos at late gestation (E18.5) along with their placenta for DNA methylation and gene expression analyses, as well as histological examinations of fixed placentas. Finally, we allowed mice from our preimplantation alcohol exposure model to be born and assessed specific cognitive functions such as anxiety, sociability, and memory through behavioral tests.

First, we observed an increase in morphological anomalies in mid-gestation embryos following prenatal alcohol exposure and discovered that prenatal exposure during preimplantation led to DNA methylation differences in the forebrain at mid-gestation and late gestation, affecting

various biological pathways related to embryonic development and nervous system function. Most of the differentially methylated regions (DMRs) and differentially expressed genes (DEGs) were sex-specific, with only few regions shared between males and females. We also identified sex-specific and shared DMRs and DEGs in late gestational placentas. Additionally, we demonstrated a decrease in fetal weight in male embryos and showed that preimplantation alcohol exposure caused reduced sociability and short-term memory without affecting the anxiety levels of the mice.

In conclusion, we have shown that early preimplantation alcohol exposure affects embryonic development through the epigenome and transcriptome of the anterior brain and placenta, leading to long-term cognitive consequences. Moving forward, we intend to establish DNA methylation and gene expression profiles specifically in certain brain cell subtypes, including GABAergic interneurons, to better define the molecular mechanisms underlying the observed alterations.

Keywords: Prenatal alcohol exposure, preimplantation, DNA methylation, transcriptome, embryonic development, maternal environment, epigenetic reprogramming, brain, placenta, sex-specific differences.

Table des matières

Liste des figures

Liste des sigles et abréviations

5hmC : 5-hydroxyméthylcytosine

5mC : 5-méthylcytosines

ADH : alcool déshydrogénase

CpG : Dinucléotide cytosine-phosphate-guanine

DEG : Gène différentiellement exprimé (*differentially expressed gene*)

DMR : Région différentiellement méthylée (*differentially methylated region*)

DNMT : *DNA methyltransferase*

DOHaD : *Developmental origins of health and disease*

EPA : exposition prénatale à l'alcool

hCG : hormone chorionique gonadotropine

ICR : *Imprinting control region*

MAT : S-adénosylméthionine synthétase

MTR : méthionine synthase

ng : nanogramme

PE : *paired-end*

RRBS : *Reduced representation bisulfite sequencing*

SAF : Syndrome de l'alcoolisation fœtale

SAM : S-adénosylméthionine

TET : Ten Eleven Translocation

TDA : Trouble d'attention

TDAH : Trouble d'attention et d'hyperactivité

TND : Troubles neurodéveloppementaux

TSAF : Trouble du spectre de l'alcoolisation fœtale

WGBS : *Whole genome bisulfite sequecing*

Remerciements

Je voudrais d'abord remercier Serge McGraw de m'avoir mentoré, encouragé et poussé à donner le meilleur tout au long de mon parcours. Merci de m'avoir accueilli dans ton labo fraichement ouvert comme stagiaire en 2015 et de m'avoir permis de continuer à la maitrise puis au doctorat. J'ai eu de la chance d'apprendre avec quelqu'un qui fait de la bonne science et de la bonne façon. Tu as toujours su me guider et me pousser à poursuivre, tout en me laissant assez de liberté pour forger mon autonomie scientifique. J'ai appris énormément à travers la découverte de nouvelles manips et les tentatives d'essayer quelque chose de nouveau. Tes conseils ont toujours été précieux, autant ceux reliés à la science qu'à l'ébénisterie et aux rénovations. Merci de m'avoir montré à avoir le souci du détail au millimètre près dans les posters et dans la préparation de librairies. Finalement, merci de m'avoir laissé gérer (dans une certaine mesure) tes comptes et le labo pendant aussi longtemps. J'ai appris énormément de cela à travers les années.

J'ai aussi eu la chance d'avoir eu de super collègues de laboratoire :

Karine, merci pour tes conseils scientifiques et de vie et d'avoir été une excellente partenaire de chialage et de rire;

Mélanie, merci d'avoir toujours remis en doute mes calculs de dilutions;

Elizabeth, merci d'avoir corrigé mon anglais aussi souvent et de m'avoir fait rire plus d'une fois avec tes différentes aventures de vie;

Alexandra, merci d'avoir été la seule bio-informaticienne qui voulait embarquer dans mes idées de graphiques bizarres;

Anthony, merci pour toutes les fois où tu m'as débloquée un code, même si c'était souvent une erreur stupide de ma part;

Josianne, merci pour ton aide avec les souris dans la dernière année;

Merci aussi à Fannie, Michelle, Diego et Thomas que j'ai appris à connaitre à travers une courte journée par semaine dans les derniers mois.

À votre façon, vous avez tous rendu mon PhD encore plus agréable.

Je voudrais aussi remercier mon comité de thèse, Dr Tony Antakly et Dr Sylvie Girard pour leur suivi annuel, ainsi que les membres de comité d'évaluation de ma thèse, Dr Mohan

Malleshaiah, Dr Martine Tétreault et Dr Luigi Bouchard de prendre le temps d'évaluer mon travail des dernières années.

Merci à Cyntia Duval pour les nombreuses discussions scientifiques et non-scientifiques et pour tes réponses à toutes mes questions de vie. Très contente de te retrouver en recherche, dans ton élément.

Merci à mes parents de n'avoir jamais mis en doute mes choix d'étude (pas ouvertement du moins) et de vous être intéressés à mon monde. Merci pour tout le temps passé avec Charlie dernièrement pour que je puisse terminer cet ouvrage dans les temps. Je suis chanceuse d'avoir des aussi bons parents! Ma sœur, Barb, merci pour tout ton temps de correction et de soutien, même quand tu en avais déjà pleins les bras. Laura, ta mère est une *superwoman*.

Finalement, je n'aurais jamais terminé ce doctorat sans le soutien, l'encouragement et l'amour de Laurie. Juste merci d'exister et d'avoir été là depuis le début de cette aventure. Merci de toujours comprendre le temps de surplus passé au labo, la présence constante du labo dans nos vies (même en vacances, même en congé de maternité), et d'avoir tout fait pour m'aider quand c'était nécessaire.

Charlie, ma fille. La vie est pleine de défis, mais surtout remplie de beaux accomplissements et de réussites. Travaille fort, fais toujours de ton mieux et choisis un domaine que tu aimes. Je serai toujours là pour toi et t'encourager à persévérer dans la vie. N'oublie jamais que je t'aime.

Chapitre 1 – Introduction

1.1 La méthylation d'ADN comme marque épigénétique

Les marques épigénétiques jouent un rôle crucial dans la manière dont une cellule perçoit et régule son propre génome en modifiant les schémas d'expression génique sans altérer la séquence d'ADN elle-même. Ces marques constituent un ensemble de modifications chimiques agissant de concert afin de modifier la structure, la compaction et l'accessibilité de la chromatine du génome (1). Les modifications épigénétiques sont nombreuses et incluent les modifications des histones et les micro-ARN, mais mes travaux de thèse se sont particulièrement concentrés sur la méthylation d'ADN. Les marques épigénétiques fluctuent et se modulent au cours du développement et de la vie afin de réguler l'expression génique à un temps donné (1). Elles peuvent aussi être modifiées en réponse à des expositions provenant de l'environnement, par exemple, à l'exposition à des contaminants chimiques ou par la consommation d'alcool pendant la grossesse (2-7).

La forme la plus connue de méthylation d'ADN est l'ajout d'un groupement méthyle sur le carbone situé en position 5' d'une cytosine d'un dinucléotide cytosine-guanine (CpG) (1, 8). Bien que moins étudié, il est toutefois aussi possible de retrouver de la méthylation sur des cytosines d'un dinucléotide autre que cytosine-guanine (méthylation non-CpG) comme sur les adénosines (CpA) (9). Les profils de méthylation d'ADN de l'ensemble du génome sont extrêmement dynamiques pendant le développement embryonnaire et à travers le vieillissement, en plus d'être variables en fonction du tissu, du type cellulaire, de l'âge et du sexe (1).

Comme les autres modifications épigénétiques, le rôle de la méthylation d'ADN dans la régulation de la transcription et de l'expression génique est crucial. De façon traditionnelle, la présence de méthylation sur les cytosines d'un promoteur riche en CpGs (*i.e* ilot CpG) était associée à un état de chromatine fermé – l'hétérochromatine – et donc à l'absence de transcription du gène (10). Au contraire, l'absence de méthylation à la même région signifiait plutôt un état de chromatine ouverte – l'euchromatine – et donc à une transcription active du gène (11, 12). Des études plus récentes démontrent toutefois que la présence ou l'absence de méthylation d'ADN, surtout dans les régions du corps du gène (*e.g.*, exon, intron) peuvent avoir des impacts variables

sur la modulation de la transcription en fonction du contexte génomique générale et de la localisation (13-15).

La présence de méthylation d'ADN joue aussi un rôle crucial dans l'inactivation du chromosome X chez la femelle ou dans la répression des rétrotransposons (1). Ces derniers, majoritairement composés de courtes séquences répétées (i.e. *repeat elements*) et souvent localisés dans des régions intergéniques, sont très importants pour la stabilité du génome et la régulation des gènes avoisinants (16, 17). La perte de méthylation aux rétrotransposons peut ultimement conduire à des anomalies chromosomiques étant donné que l'état passif maintenu par la présence de méthylation d'ADN prévient la transposition ou la recombinaison lors de la ségrégation des chromosomes (18). Plusieurs études ont aussi démontré que l'instabilité des rétrotransposons peut mener au développement de diverses formes de cancer (19-21).

Les enzymes ADN méthyltransférases (DNMTs) sont responsables de l'apposition de la méthylation d'ADN lors du développement embryonnaire et des divisions cellulaires. DNMT3a et DNMT3b sont toutes deux responsables de la méthylation *de novo*, c'est-à-dire qu'elles apposeront la méthylation sur des cytosines auparavant non-méthylées (22, 23). Ces deux enzymes sont ainsi essentielles lors du développement *in utero* afin de méthyler le génome embryonnaire (aussi discuté à la section 1.2.2). L'enzyme DNMT3L agit, pour sa part, comme cofacteur afin de stimuler l'action de DNMT3A et DNMT3B et jouerait aussi un rôle de régulateur dans l'établissement de l'empreinte génomique (24). DNMT3L seul ne possède aucune activité catalytique (24). Plusieurs modèles de souris *knock-out* pour une ou plusieurs de ces enzymes ont permis de bien étudier leur rôle crucial dans le développement embryonnaire et le bon établissement des profils de méthylation d'ADN de l'embryon et de son placenta. En effet, les souris DNMT3L-KO sont viables, mais infertiles en raison du mauvais établissement du paysage épigénétique dans les gamètes (23). Les embryons DNMT3A-KO se développent jusqu'à terme, mais meurent tôt après la naissance, alors que ceux DNMT3B-KO meurent *in utero*, environ à mi-gestation (23). Bien qu'ayant des rôles similaires, certaines études ont démontré que DNMT3A et DNMT3B ne sont pas totalement interchangeables. Dans le tissu extra-embryonnaire par exemple, l'absence de DNMT3A affecte très peu la méthylation d'ADN alors que l'absence de DNMT3B diminue de façon importante les niveaux de méthylation d'ADN (25). Au stade embryonnaire, un modèle de cellule *knock-out* pour DNMT3A ou DNMT3B a permis de démontrer que les régions visées par les deux enzymes sont

différentes et bien distinctes, DNMT3A étant absolument requise pour la méthylation *de novo* des gènes du groupe du Polycomb, un ensemble de gènes modulant la chromatine et crucial pour le développement embryonnaire, alors que DNMT3B avait un rôle prépondérant sur la méthylation du chromosome X (26, 27).

Une autre ADN méthyltransférase, DNMT1, est, pour sa part, responsable de méthyler l'ADN hémiméthylé, dont le brin parent est méthylé et le brin fille ne l'est pas (22, 28). C'est cette enzyme qui permet que la méthylation d'ADN reste une modification héritée à travers les divisions cellulaires. Lors du développement embryonnaire, DNMT1 est aussi responsable de maintenir la méthylation d'ADN sur certains gènes cruciaux, comme les gènes à empreinte lors de la phase de déméthylation de la reprogrammation épigénétique (29-31) (aussi discuter à la section 1.2.1). Les gènes à empreinte sont des gènes exprimés de façon monoallélique et dépendant de l'origine parentale. Pendant le développement embryonnaire, la méthylation sur l'allèle non-exprimé doit être maintenue afin de conserver l'empreinte parentale (29, 30, 32). Une erreur de l'empreinte épigénomique peut entrainer plusieurs maladies graves souvent reliées à des défauts développementaux, tels que le syndrome de Prader-Willi, associé à un défaut de l'empreinte du gène *SNRPN*, ou celui d'Angelman, associé à un défaut de l'empreinte du gène *UBE3A* (33). Environ une centaine de gènes à empreinte sont connus chez la souris et 70 chez l'humain (34-36). Un *knock-out* de l'enzyme DNMT1 entraine la mort embryonnaire dès le premier trimestre en raison de la perte du maintien de la méthylation dans l'ensemble des gènes à empreinte et certains autres gènes développementaux (37, 38). Dans un modèle de cellule souche embryonnaire murine, une perte transitoire de DNMT1 entraine des altérations importantes des profils de méthylation d'ADN des gènes à empreinte et de certaines sous-catégories de gènes réagissant de la même façon (30), incluant *Wnt5a*, important pour la régulation du développement embryonnaire (39-41), ou *Lhx6*, impliqué dans la cascade de migration des interneurones GABAergiques dans le cortex cérébral (42, 43). L'ensemble de ces études mettent bien en évidence le rôle crucial de la maintenance de la méthylation d'ADN par DNMT1 pendant le développement embryonnaire.

À l'opposé des ADN méthyltransférases, les enzymes TET – *Ten Eleven Translocation* – ont comme fonction principale la modification des marques de méthylation, en oxydant les 5-méthylcytosines (5mC) en 5-hydroxyméthylcytosine (5hmC), un état intermédiaire entre la présence et l'absence de méthylation (44, 45). Les TET sont importantes pour la maintenance de

la pluripotence des cellules souches, mais aussi lors de la préimplantation pendant le développement embryonnaire (1, 46).

1.2 Le développement embryonnaire

1.2.1 La période préimplantatoire

La préimplantation consiste en la période entre la fertilisation et l'implantation de l'embryon dans l'utérus. Même si cette période est relativement courte – environ 6 jours chez l'humain et 4 jours chez la souris – son importance est pourtant cruciale pour le bon développement embryonnaire (47, 48). Alors que l'embryon se déplace des trompes de Fallope vers l'utérus, son environnement subit aussi plusieurs changements, notamment au niveau du pH, des nutriments et des facteurs de croissance (49-51). Ces modifications de l'environnement embryonnaire sont nécessaires pour le reste de son développement et des perturbations externes pourrait entraver la poursuite de la grossesse. D'un point de vue épigénétique, la préimplantation correspond aussi au début du remodelage épigénétique comme nous allons le voir un peu plus loin.

1.2.1.1 Les premières divisions

Dès la fertilisation, nous assistons à une croissance rapide du nombre de cellules alors que le zygote, soit l'embryon 1-cellule, subit des divisions rapides et synchronisées où chaque cellule embryonnaire, les blastomères, sont répliqués. Ces blastomères sont entourés d'une zone pellucide (*zona pellucida*) constituant la barrière protectrice de l'embryon. Au stade 8-cellules, les cellules, maintenant polarisées grâce à la spécificité des interactions cellule-cellule, amorcent leur compaction qui se poursuivra au cours des divisions cellulaires subséquentes. Lors des divisions suivant le stade 16-cellules, les liens entre les cellules du blastomère deviendront quasi indétectables (52-55). Par la suite, des divisions asymétriques permettront le développement des deux premières lignées cellulaires distinctes, soit la masse de cellules internes (*inner cell mass*, ICM) qui mènera au développement de l'embryon et les cellules du trophectoderme (TE) qui mèneront au développement du placenta et des tissus extra-embryonnaires (56, 57). Grâce à un processus de cavitation, le blastocœle, une cavité remplie de fluide, entre autres sécrété par les cellules du trophoblaste, est formé lors des divisions subséquentes. Peu à peu, la zone pellucide s'ouvrira et le blastocyste, l'embryon d'environ 200 cellules, pourra prendre de l'expansion jusqu'à son implantation à l'endomètre de l'utérus (57, 58).

Pendant cette période préimplantatoire, le paysage épigénétique des cellules en pleine division subit aussi un important remodelage. Nous assistons, d'abord, à une vague de déméthylation des génomes parentaux qui débutent dès la fertilisation. Cette déméthylation affecte la majorité du génome à quelques exceptions près. Pendant la préimplantation, la reprogrammation épigénétique joue un rôle important dans la compaction de la morula et donc dans la formation du blastocyste. Par la suite, le remodelage des marques épigénétiques est nécessaire afin de permettre aux cellules embryonnaires de se différencier en tous les types cellulaires afin de former les différents tissus (59). L'acquisition par l'embryon de son propre méthylome lui permettra aussi de réguler la transcription génique des cellules pendant les processus de spécification et de différentiation pendant tout le développement (59-61).

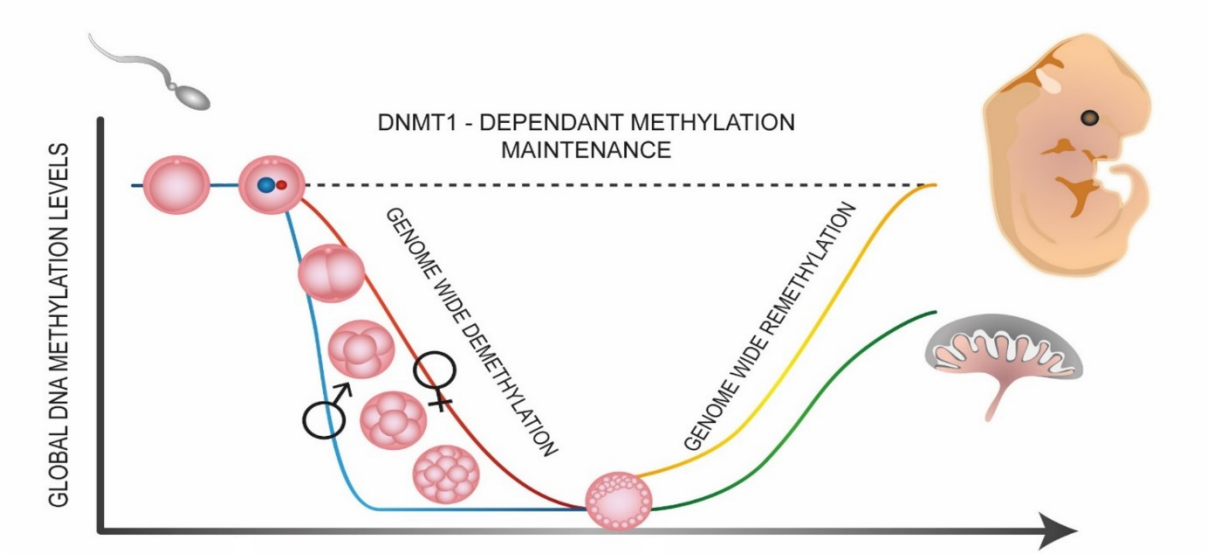

Figure 1. Reprogrammation épigénétique pendant le développement embryonnaire
Schéma de la vague de reprogrammation épigénétique débutant dès la fertilisation avec la déméthylation de l'allèle maternel (rouge) et paternel (bleu) pendant la préimplantation, puis reméthylation du génome embryonnaire dans les cellules de la masse interne (jaune) et cellule du trophectoderme (vert). Figure tirée de Legault et *al*., 2018 (62).

Plusieurs études ont permis de démontrer que la déméthylation de l'allèle maternel et paternel du génome embryonnaire ne se fait pas de façon synchronisée (59-61). Il faut d'abord souligner que le génome du sperme est très fortement méthylé (environ 85% des CpGs sont

méthylés) en raison de sa forte compaction, alors que le niveau de méthylation de l'ovocyte est seulement d'environ 30% (63). La déméthylation de l'allèle paternel débute dès la première division cellulaire. Deux mécanismes ont jusqu'à maintenant été proposés pour expliquer le processus de déméthylation. Le premier suggère que les enzymes TET serait responsable de la déméthylation dite active de l'allèle paternel (60, 61, 64, 65). Le second mécanisme, dit passif, suggère que les marques de méthylation du génome paternel ne sont pas transmises aux cellules filles pendant les divisions cellulaires et donc que leur dilution entraine leur perte (64, 66). Bien que le mécanisme exact demeure indéterminé, il est généralement accepté que les deux processus proposés agissent de concert, avec une prédominance de la déméthylation active, pour déméthyler l'allèle paternel (1). Pour ce qui est de l'allèle maternel, sa déméthylation se ferait plutôt de façon passive, via dilution des marques de méthylation puisque de nombreuses études ont démontré que la présence de la protéine DPPA3 (aussi appelé PGC7 ou STELLA) protègerait la méthylation ADN de l'allèle maternel contre l'oxydation des enzymes TET (60, 61, 64-67).

Alors que la majorité du génome des allèles parentaux seront déméthylés pendant la préimplantation, certaines régions bien spécifiques doivent toutefois échapper à cette étape. Ces régions, principalement les rétrotransposons, les gènes à empreinte et certains gènes agissant comme ceux-ci, doivent conserver les marques de méthylation établies dans les gamètes (29, 30, 32). Le maintien de la méthylation d'ADN aux régions de contrôle de l'empreinte (*imprinted control regions* – ICR) est d'ailleurs crucial pour le développement normal de l'embryon et comme mentionné à la section 1.1, la perte de l'empreinte épigénomique peut compromettre la survie de l'embryon (30, 68). Lors de tout le processus de reprogrammation épigénétique, le maintien de la méthylation à ces régions incombe à deux isoformes de DNMT1, soit DNMT1s (somatique) et DNMT1o (ovocyte) (69-73). Alors que DNMT1s sera actif pendant toute la préimplantation, l'activité de DNMT1o est spécifique au stade 8-cellules. Plusieurs études ont démontré que son absence ou d'autres perturbations de la méthylation à ce stade critique du développement embryonnaire pouvait entrainer des anomalies placentaires ou des anomalies cérébrales éventuellement léthales à mi-gestation (70, 73, 74).

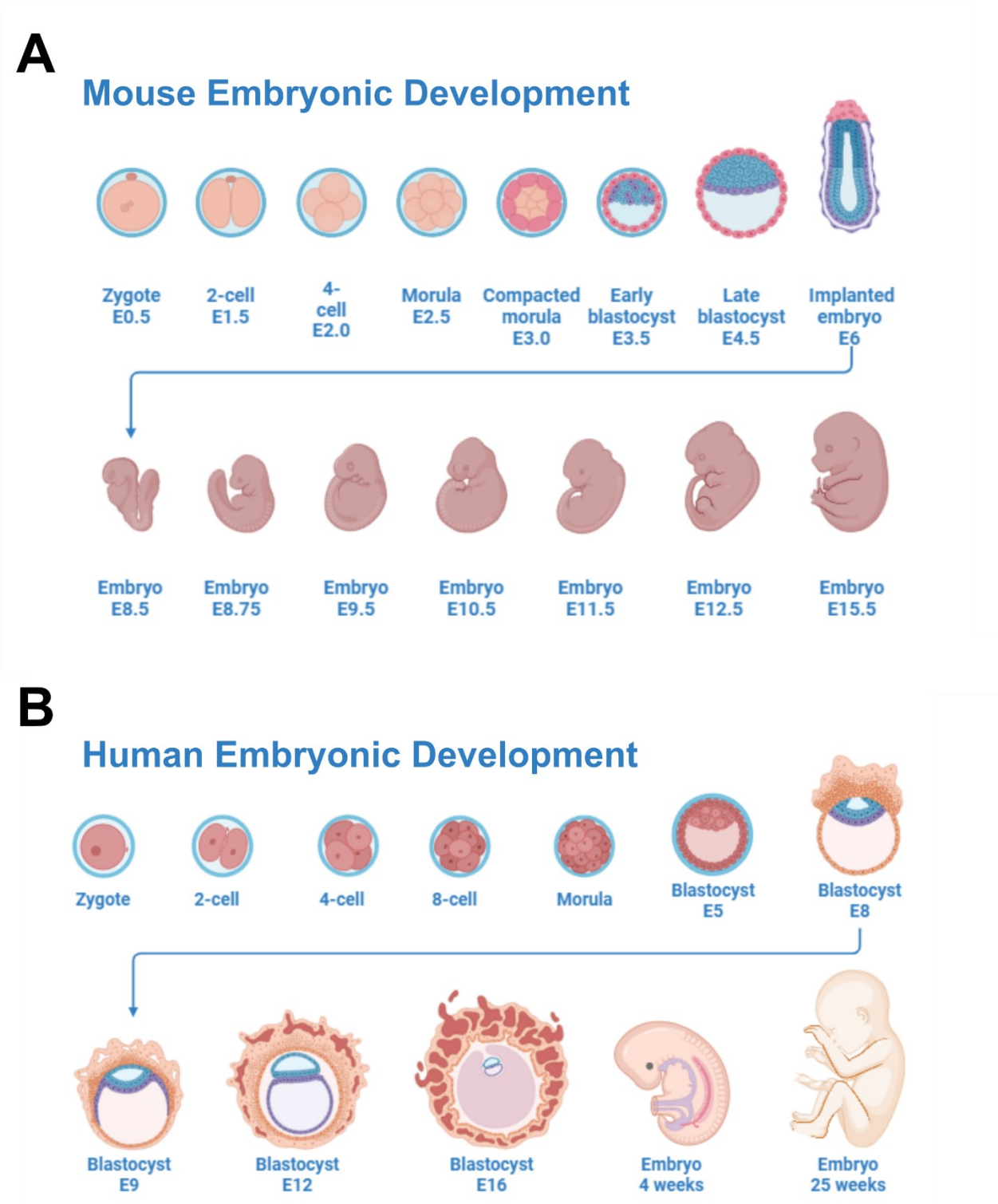

Figure 2. Développement embryonnaire chez la souris et l'humain

Schéma du développement embryonnaire chez la souris (**A**) et chez l'humain (**B**). Figure crée sur *BioRender.com*

1.2.2 La période post-implantatoire

Alors que l'embryon poursuit son développement via la spécification et la différenciation de divers types cellulaires en vue de la formation des différents organes, la reprogrammation épigénétique se poursuit aussi avec la reméthylation du jeune génome embryonnaire qui débute dès l'implantation. Le processus progressif requiert l'activité des enzymes DNMT3A, DNMT3B et DNMT3L qui méthyleront *de novo* le génome des cellules spécifiquement en fonction du sexe, du types cellulaires et du tissu où est localisée la cellule (59). La reméthylation est particulièrement rapide dans les cellules de la masse interne (75). Il a d'ailleurs été démontré chez la souris, qu'entre le jour embryonnaire 4.5 et 5.5, soit tout juste après l'implantation du blastocyste, la méthylation augmente d'environ 50% (8). Le corps du gène, les promoteurs pauvres en CpG ainsi que les différents éléments transposables seraient les premiers à être reméthylés après l'implantation alors que les promoteurs riches en CpG et les îlots CpG bénéficieraient d'une protection temporaire des mécanismes de méthylation *de novo*. Dans les cellules du trophectoderme, le processus de reméthylation serait tout aussi rapide, mais le niveau de méthylation atteint reste partiel par rapport à celui dans les cellules dérivées des cellules de la masse interne (75, 76). Nous avons également découvert des différences de méthylation entre l'embryon et le placenta à mi-gestation, révélant une méthylation différentielle dès l'implantation, qui persiste de manière asymétrique jusqu'à la fin de la gestation. Nous avons aussi pu mettre en perspective les rôles de compensation de DNMT3A et DNMT3B dans ces différences inter-tissus (voir annexe 1) (76).

1.2.2.1 Le développement du placenta

Le placenta est un organe bien distinct dont dépend la survie de l'embryon. Dérivé des cellules du trophectoderme, il se développera en parallèle à l'embryon après l'implantation et sera rapidement fonctionnel après le remodelage de cellules placentaires afin d'accomplir ses principales fonctions, soit d'acheminer les nutriments maternels et l'oxygène vers l'embryon et d'éliminer les déchets métaboliques embryonnaires (77). Le placenta primitif sera en effet fonctionnel dès le jour embryonnaire E10.5 chez la souris (E18 chez l'humain) pour être complètement mature au jour embryonnaire E14.5 chez la souris et E35 chez l'humain (77). En plus de ses fonctions d'échange fœto-maternel, le placenta sécrète aussi plusieurs hormones dès le début de son développement.

Au stade du blastocyste chez la souris, les cellules du trophectoderme forment une membrane externe de cellules polarisées. Rapidement après l'implantation, celles-ci formeront l'ectoderme extra-embryonnaire et le cône ectoplacentaire. Les premiers trophoblastes seront, par la suite, différenciés depuis les cellules externes du cône ectoplacentaire. Ces trophoblastes iront s'invaginer dans le décidua maternel afin d'entrer en contact avec le sang maternel (78). Au jour embryonnaire 6.5, pendant la gastrulation, l'amnion, le chorion et l'allantois seront formés à partir de l'ectoderme embryonnaire et extra-embryonnaire. Vers E8.5, le chorion interagira avec le cône ectoplacentaire pour fusionner avec l'allantois. Cette fusion est nécessaire pour la vascularisation du placenta élémentaire et la formation éventuelle du labyrinthe (77).

La structure du placenta sera ensuite mieux définie, particulièrement grâce à la différenciation des trophoblastes en différents sous-types cellulaires qui constitueront les couches du placenta (79). Toujours chez la souris, les syncytiotrophoblastes émergeront de la fusion de plusieurs trophoblastes. Ces cellules multinuclées formeront le labyrinthe du placenta à partir de plusieurs sites de vascularisation, permettant l'interaction entre les sinus de sang maternel et les capillaires de sang fœtal. Le labyrinthe compose la majeure partie du placenta et constitue le lieu des échanges de nutriments et d'oxygène. Afin de compléter le placenta, d'autres trophoblastes se différencieront en spongiotrophoblastes et en cellules de glycogène dans le but de former la zone jonctionnelle. Comme son nom l'indique, elle se situe entre le labyrinthe (côté fœtal) et le décidua (côté maternel) (80). Le placenta primitif est fonctionnel, mais toujours en formation vers E10.5, puis sera mature vers E14.5, chez les souris (77).

Le placenta est donc en contact étroit autant avec l'environnement maternel que l'environnement fœtal. Puisque ses cellules progénitrices, avant la différenciation entre les cellules de la masse interne et celle du trophectoderme, subissent aussi le remodelage épigénétique pendant la préimplantation, le placenta n'est pas à l'abri des perturbations pendant le remodelage épigénétique pouvant altérer son bon développement ou ses fonctions.

1.2.3 La vulnérabilité du développement embryonnaire

Le développement embryonnaire est un processus finement et strictement régulé au cours duquel la moindre perturbation peut compromettre la survie de l'embryon. Dès les années 80, plusieurs liens ont commencé à être fait entre un environnement *in utero* inadéquat et les risques sur la santé de l'enfant. Ces études ont mené le professeur David Barker a énoncé la théorie du

DOHaD, *Developmental Origins of Health and Disease,* évoquant que l'environnement pendant le développement embryonnaire influence la programmation fœtale et peut impacter de façon permanente la santé du bébé en augmentant, par exemple, le risque de développer certaines maladies (81). Dans sa première étude évoquant l'hypothèse DOHaD, le Dr Barker évoque qu'une nutrition inadéquate pendant la période fœtale entrainerait un sous-développement des fonctions endocrines du pancréas et augmenterait les chances de développer le diabète de type 2 (diabète *mellitus*) chez l'enfant à naître (81). Encore aujourd'hui, le concept DOHaD est une thématique de recherche à part entière et, bien qu'il inclue l'ensemble de la gestation, l'importance de la préimplantation sur la suite du développement embryonnaire est aussi bien reconnue.

Des perturbations en tout début de grossesse, soit pendant le développement préimplantatoire peuvent aussi entrainer des conséquences négatives à long terme sur l'embryon. Plusieurs études utilisant des modèles de culture *in vitro* l'ont d'abord démontré. Par exemple, un modèle de culture de cellules porcines avec une exposition au bromodichlorométhane a montré des perturbations des profils transcriptomiques et de méthylation d'ADN résultant en une diminution du taux de développement des blastocystes (3). Contrairement à certaines vieilles croyances, même si l'embryon n'est pas encore attaché à l'utérus et donc qu'aucun lien physique concret n'existe entre l'embryon et sa mère, l'environnement maternel peut tout de même atteindre le jeune embryon via les divers fluides du corps comme l'ont démontré plusieurs études *in vivo*, dont des études toxicologiques. Les effets du paraquat (gramoxone), un herbicide encore couramment utilisé, ont par exemple été étudiés dans un modèle d'exposition à différents stades de la préimplantation et ces recherches ont démontré des retards dans le développement embryonnaire (82).

La diète est aussi un facteur maternel primordial pour le bon développement embryonnaire, incluant pendant la préimplantation. L'importance d'une supplémentation adéquate en acide folique et les nombreuses études ayant servi à optimiser les recommandations actuelles en sont de bons exemples (83-89). La diète maternelle peut aussi entraîner des conséquences qui vont bien au-delà du développement embryonnaire. Une récente étude utilisant un modèle murin a par exemple démontré qu'une diète prénatale riche en gras exclusivement pendant la préimplantation entraine des dérégulations métaboliques cardiovasculaire en plus de changements moléculaires et cellulaires dans l'hippocampe de la progéniture une fois adulte (90). Ce type de résultat démontre

l'importance du concept du DOHaD et les recherches sur ce sujet, entre autres pendant la préimplantation.

Les technologies de reproduction assistée, comme la fécondation *in vitro*, ont aussi permis de démontrer à quel point l'intégrité du développement préimplantatoire est important pour l'embryon. Les techniques de reproduction assistée sont une des perturbations externes pendant la préimplantation où l'impact épigénétique est le mieux documenté. En effet plusieurs études chez la souris et le bovin ont démontré que certaines manipulations *in vitro* affectaient la méthylation sur plusieurs gènes à empreinte dont le locus *Igf2*/*H19* ou *Snrpn* (91-94). Chez l'humain, certaines méta-analyses ont démontré une augmentation de la prévalence de plusieurs maladies ou désordres de gènes à empreinte, tels que la maladie de Beckwith-Wiedemann associé aux gènes *CDKN1C*, *H19*, *IGF2* et *KNCNQ1OT1* ou le syndrome d'Angelman associé au gène *UBE3A* chez les enfants issus de la reproduction assistée (73, 95, 96). Certaines études ont aussi montré des changements plus globaux de la méthylation d'ADN dans le sang de cordon ombilical ou le placenta d'enfants issus de la reproduction assistée (97, 98).

Ces exemples de types d'éléments pouvant perturber la période préimplantatoire et leurs impacts sur l'embryon démontrent bien l'importance de cette courte fenêtre développementale en début de grossesse. Ayant malheureusement été longtemps sous-estimée, la préimplantation est maintenant de plus en plus étudiée permettant une meilleure compréhension de son rôle crucial.

1.3 Le Trouble du Spectre de l'Alcoolisation Fœtale

Une exposition prénatale à l'alcool (EPA) se produit lorsque la mère consomme de l'alcool pendant la grossesse. Bien que son mécanisme d'action ne soit pas encore entièrement connu, l'alcool, à la fois neurotoxique et tératogène, peut affecter de façon négative la différentiation et la prolifération cellulaire, voir même entrainer une mort cellulaire excessive (99-101). De plus, une exposition prénatale à l'alcool peut venir directement perturber certains mécanismes épigénétiques par son action dans le cycle de l'acide folique et auprès des DNMTs (102). Une exposition prénatale à l'alcool peut donc entrainer des conséquences importantes chez l'embryon et mener au Trouble du spectre de l'alcoolisation fœtale (TSAF) chez l'enfant à naître.

Le TSAF regroupe un grand nombre de pathologies et symptômes développementaux et neurodéveloppementaux résultant d'une consommation d'alcool maternelle pendant la grossesse

(103-106). Sa prévalence est très variée selon les régions du monde. De façon générale, les études épidémiologiques estiment qu'environ 1 à 5% de la population à travers le monde seraient atteints du TSAF (107-109). Dans certains pays où la consommation d'alcool est plus répandue et problématique, comme la Croatie ou l'Afrique du Sud, la prévalence du TSAF dépasse les 5%, allant jusqu'à une prévalence de 10% de la population qui serait atteint du TSAF (107, 108). Les études épidémiologiques estiment qu'environ une femme sur treize consommant de l'alcool pendant la grossesse donnera naissance à un enfant atteint d'un TSAF et donc, que 630 000 bébés naissent avec un TSAF à chaque année (108). L'intensité des symptômes du TSAF dépend de plusieurs facteurs, tels le type d'exposition (quantité, moment au cours du développement, fréquence, patron d'exposition), l'exposition à d'autres substances (drogue, tabac), la diète de la mère, certaines prédispositions génétiques ainsi que l'état de santé générale de la mère. Avec le taux croissant de consommation d'alcool chez les femmes en âge de procréer, particulièrement le taux de consommation excessive d'alcool (*binge drinking*), le nombre d'enfants atteints d'un TSAF est sujet à considérablement augmenter dans les prochaines années (107). Bien que la faible consommation d'alcool soit parfois banalisée dans la population, il est important de se rappeler qu'aucune quantité d'alcool n'est sécuritaire pour l'embryon pendant la grossesse et que les lignes directrices internationales mettent maintenant en garde des dangers de toute consommation maternelle d'alcool pendant la grossesse (110-113).

La forme grave du TSAF se nomme le Syndrome de l'alcoolisation fœtale (SAF) et est une forme visible d'une consommation d'alcool maternelle qui peut être détectée dès la naissance. En effet, les enfants atteints du SAF présenteront, dès leur plus jeune âge, des traits crânio-faciaux typiques de ce syndrome : fente palpébrale plus petite, hypoplasie du nez, lèvre supérieure plus mince et un philtrum hypoplasique (114, 115). En plus de ces caractéristiques physiques, les enfants avec un SAF sont aussi atteints de déficience intellectuelle sévère qui les affectera pour le reste de leur vie puisqu'aucun traitement n'existe à ce jour (114-117). Le SAF constitue environ 10% de tous les cas de TSAF, représentant environ 60 000 enfants par année (118, 119).

La majorité des enfants (environ 90%) ayant un TSAF présenteront l'un ou plusieurs symptômes associés avec des troubles neurodéveloppementaux (TND), incluant des déficits d'apprentissage, de langage, de mémoire ou encore un trouble du déficit de l'attention avec ou sans hyperactivité (TDA/TDAH). Les enfants peuvent aussi présenter un léger retard de croissance.

Chez les adultes avec un TSAF, des études ont aussi démontré une hausse de risque de maladie métabolique, immunitaire ou cardiovasculaire (107). Cependant, aucune caractéristique physique ne permet de les diagnostiquer dès la naissance et aucun test moléculaire permettant de démontrer qu'une exposition prénatale à l'alcool a perturbé le bon développement embryonnaire n'existe encore. Au Canada, les lignes directrices pour le diagnostic du TSAF sont basé sur le *4-Digit Diagnostic Code*, une approche systématique où l'enfant sera évalué par plusieurs médecins et intervenants sociaux lorsqu'il y a une suspicion d'exposition prénatale à l'alcool (120-122). Les enfants sont donc plus souvent d'âge scolaire, alors que les TND commencent à être plus envahissants, lorsqu'il est possible d'établir ou de présumer un diagnostic de TSAF (107). Il a toutefois été démontré qu'un diagnostic tôt dans la vie de l'enfant permettrait une intervention précoce ciblée et ainsi une amélioration des conséquences à long terme (123).

1.4 L'alcool, l'épigénome et le développement du cerveau

1.4.1 Le métabolisme du carbone

Bien avant l'avènement des technologies de séquençage à haut-débit, une première démonstration de l'impact d'une exposition à l'alcool sur l'épigénome fut faite en 1991 dans un article publié par Garro et *al* (124). Dans son étude, il démontre une baisse de l'activité enzymatique des ADN méthyltransférases (DNMTs) dans des cellules embryonnaires de souris exposées à l'alcool (124). Leurs travaux a aussi permis de découvrir que cet effet n'est pas dû à l'alcool même, mais plutôt aux acétaldéhydes, le principal métabolite généré par la dégradation d'alcool par l'alcool déshydrogénase (ADH) (124). Cette étude a été la première à révéler les effets néfastes de l'exposition prénatale à l'alcool sur l'épigénétique, tout en proposant une hypothèse explicative sur la perturbation de l'activité des DNMTs et ses conséquences sur les profils normaux de méthylation de l'ADN.

Des recherches subséquentes ont, par la suite, permis d'apprendre que l'acétaldéhyde n'affecte pas seulement l'activité enzymatique des DNMTs, mais débalancerait en fait tout le métabolisme du carbone (*1C metabolism*), qui inclut, entre autres, le cycle de l'acide folique et le cycle de la méthionine-homocystéine (102). En première ligne, l'acétaldéhyde diminue d'abord l'absorption du folate par les reins et l'intestin en réduisant l'activité d'un important transporteur de folate, RFC1 (125). Étant le principal donneur de groupement méthyle lors du développement

du cerveau et du système nerveux, le folate joue un rôle capital dans le développement embryonnaire, comme il fut démontré à de nombreuses reprises (126, 127). Un autre effet majeur sur le cycle du carbone est l'impact négatif de l'acétaldéhyde sur le mécanisme de régénération de la méthionine, entre autres, par l'inhibition de l'activité de la méthionine synthase (MTR) qui catalyse la conversion de l'homocystéine en méthionine (128). L'acétaldéhyde inhibe aussi l'action de la S-adénosylméthionine synthétase (MAT) qui convertit la méthionine en S-adénosylméthionine (SAM) (102). SAM est le principal donneur de groupement méthyle dans plusieurs réactions, dont la méthylation de l'ADN. Le niveau de méthionine et de SAM sont donc cruciaux afin de maintenir les profils de méthylation d'ADN. Cette importance est d'autant plus grande dans le contexte du développement embryonnaire où la vague de reprogrammation épigénétique requiert une dynamique précise des niveaux de méthylation d'ADN (102). En combinant la baisse du nombre de groupements méthyles et l'activité enzymatique réduite des DNMTs, l'exposition prénatale à l'alcool peut ainsi entraîner des conséquences désastreuses sur l'établissement et le maintien du paysage épigénétique embryonnaire et avoir des impacts à long terme sur le bon développement.

1.4.2 Le développement du système nerveux

Comme l'ensemble du développement embryonnaire, le développement du système nerveux se doit d'être strictement régulé. L'importance de la méthylation d'ADN lors de ce processus dans le maintien des marques de méthylation sur les gènes à empreinte et dans l'orchestration d'une dynamique précise de méthylation et déméthylation à des moments précis du développement sur les différents types cellulaires du cerveau afin de former les différentes structures a été démontrée à maintes reprises (129-132). En altérant les différents mécanismes menant à la méthylation d'ADN, l'exposition prénatale à l'alcool a donc le potentiel de perturber de façon importante le développement du système nerveux. Sachant que la très grande majorité des enfants atteints du TSAF ont des troubles neurodéveloppementaux, les dérèglements épigénétiques font fort possiblement partis du mécanisme. D'ailleurs, différentes études explorant l'impact de l'alcool sur le développement des cellules souches neurales ont démontré un ralentissement du cycle cellulaire pouvant entrainer à long terme des retards de croissance, des retards dans la différentiation cellulaire ainsi que des changements dans l'expression de certains gènes développementaux dont *Pax6* et *Nestin* (133-135).

Autant d'un point de vue cognitif que plus structural, certaines études affirment aussi que le cerveau antérieur jouerait un rôle important dans le développement de plusieurs phénotypes reliés au TSAF. Il a été démontré que cette région du cerveau exprime fortement certains gènes (e.g., *Emx1*, *Met*) reliés à la neurodégénération et divers phénotypes neurodéveloppementaux chez plusieurs enfants atteints du TSAF (136, 137). Structuralement, lors du développement embryonnaire, certaines portions du visage, dont le front, le nez et le philtrum se développe à partir des tissus adjacents au cerveau antérieur (138, 139). Des études d'imagerie ont d'ailleurs démontré que certaines anomalies crânio-faciales présentes chez les enfants atteints par la forme sévère du TSAF, le SAF, peuvent être issues d'anomalie structurale et développementale du cerveau antérieur (139, 140).

1.4.3 Étudier l'exposition prénatale à l'alcool

L'impact de l'alcool sur le développement cellulaire a d'abord commencé dans les années 90 dans des modèles *in vitro*, avec l'objectif étonnant de vouloir déterminer si l'ajout d'alcool au milieu de culture pouvait améliorer la croissance des cellules. En étudiant différents dosages, ces recherches ont rapidement démontré que l'ajout de très faible quantité d'alcool (0.05-0.1%) au milieu pouvait accélérer la formation du blastocyste, améliorer le processus de cavitation au stade morula et augmenter le taux de calcium intracellulaire (141-143). Ils ont cependant observé une inhibition complète du développement ou un ralentissement dans la formation de blastocystes avec des dosages plus élevés (0.4-1.6%), les conséquences variant selon la dose et en fonction du temps dans le développement lors de l'ajout d'alcool au milieu (141). Bien que pouvant montrer des effets intéressants lors de l'ajout de faible concentration d'alcool, il faut toutefois préciser que ces études n'ont pas regardé les possibles impacts délétères sur le paysage épigénétique, ni même la survie à long terme de ces embryons. Elles ont tout de même ouvert la voie à la recherche sur l'impact de l'exposition prénatale à l'alcool sur le développement embryonnaire et les mécanismes moléculaires. Il est important de noter que dans les protocoles de culture *in vitro* d'embryon, certaines hormones sont re-suspendues dans l'éthanol avant d'être ajoutées au milieu (144, 145).

À travers le temps et les avancées technologiques, des centaines d'études utilisant différents modèles *in vitro* et d'animaux ont permis de mieux caractériser certaines atteintes. L'utilisation d'animaux de recherche, particulièrement la souris ou le rat, afin de modéliser une exposition prénatale à l'alcool est énormément répandu dans la littérature. C'est en partie grâce à ses modèles que nous avons pu caractériser la variabilité des symptômes en fonction de différents facteurs en

plus de permettre l'analyse moléculaire précise de certains tissus, comme le cerveau, à la suite de l'exposition prénatale à l'alcool, chose qui est impossible avec l'humain. L'environnement contrôlé (i.e alimentation, profil génétique, exposition à d'autres substances) dans lequel les animaux de recherche évoluent en font aussi des outils puissants afin de déterminer l'impact de l'alcool seul. Nous avons, entre autres, révisé les différents modèles dans une revue de littérature (62), ce qui nous a permis de bien comprendre les différentes possibilités dans les modèles, ce qui avait été fait et les lacunes dans la recherche de l'impact de l'exposition prénatale à l'alcool sur l'épigénome de l'embryon.

Malheureusement, ces études ont démontré à de nombreuses reprises que les conséquences d'une exposition prénatale à l'alcool sont extrêmement variables en fonction de différents facteurs : la concentration d'alcool à laquelle l'embryon est exposé, la durée de l'exposition, la fréquence de l'exposition et surtout le moment de l'exposition dans le développement (révisé dans (62)). Par exemple, une étude utilisant un modèle de souris a fait une exposition unique de type *binge drinking*, soit la consommation d'une forte quantité d'alcool en peu de temps, à trois moments distincts pendant la gestation, correspondant environ aux 3 trimestres chez l'humain, puis ont récolté les cerveaux des embryons exposés *in utero* à l'âge adulte. Une analyse d'expression génique a démontré des altérations dans les cerveaux exposés à l'alcool en comparaison avec les cerveaux contrôles, distinctes selon le moment de l'exposition pendant la gestation (146). Les gènes dont l'expression sont altérés sont particulièrement enrichis dans des voies spécifiques en fonction du trimestre d'exposition : la prolifération cellulaire au 1er trimestre, la migration et la différenciation cellulaire au 2^{e} trimestre et la communication cellulaire et la neurotransmission au 3^{e} trimestre (146).

Une étude morphologique comparant deux doses d'alcool en début de gestation a aussi démontré des impacts au niveau du poids fœtal lorsque les embryons étaient exposés à la plus forte concentration (0.03mL/g d'EtOH 25%), mais pas lors de l'exposition avec une dose plus faible (147). Plusieurs études ont aussi démontré qu'une seule exposition prénatale à l'alcool de type *binge* pourrait entraîner des conséquences plus importantes sur l'embryon qu'une exposition plus soutenue de type chronique, mais avec une dose modérée en raison de la haute concentration d'alcool sanguine atteinte lors de ce type de consommation (148-150).

Ces nombreux éléments d'hétérogénéité dans les patrons d'exposition font en sorte qu'il est très difficile d'associer entre elles différentes études utilisant des modèles distincts afin de mieux définir les mécanismes derrière les conséquences néfaste de l'exposition prénatale à l'alcool. Chez l'humain, cette variabilité explique en grande partie l'ampleur et la diversité dans les nombreux symptômes chez les enfants atteints d'un TSAF, tout en rendant le diagnostic encore plus complexe.

1.4.3.1 L'exposition prénatale à l'alcool pendant la préimplantation

Bien que la littérature regorge d'études sur l'impact de l'exposition prénatale à l'alcool sur l'embryon dans différents contextes et différentes conditions, une période demeure sévèrement sous-étudiée : la préimplantation. Bien que certaines études investiguant l'impact d'une exposition prénatale à l'alcool de type chronique incluent la fenêtre préimplantatoire dans leur exposition, très peu d'études se sont attardées à l'impact d'une exposition prénatale à l'alcool strictement durant la préimplantation. Pourtant, viser spécifiquement une exposition pendant cette période permet de déterminer et de caractériser les conséquences uniquement associées à une exposition en tout début de grossesse, sans altération provenant d'une exposition à des stades ultérieurs du développement embryonnaire.

Les quelques études sur la préimplantation ont surtout étudié les conséquences directement sur le développement embryonnaire. Une étude ayant exposé à l'alcool des femelles souris gestantes pendant une des six premières journées de la gestation a, entre autres, démontré une augmentation d'anomalies crânio-faciales, une baisse du poids fœtal et une augmentation du poids du placenta chez des embryons au jour embryonnaire E15.5 (147). Un autre modèle murin dans le même article de recherche, cette fois avec une exposition au jour embryonnaire E2 et E6, a aussi montré des retards de croissance sévères chez les embryons exposés à l'alcool à E14, E16 et E18 (147). Des anomalies morphologiques, des retards de développement et des réductions des poids fœtaux et placentaires ont aussi été observés chez des embryons en fin de gestation (E19) après une exposition à l'alcool à E3 et E4 (151). L'ensemble de ces travaux ont été effectués en utilisant une dose dite aiguë, avec des niveaux d'alcool relativement élevés.

Avant le début de nos travaux, une seule étude avait étudié l'impact épigénétique d'une exposition prénatale à l'alcool pendant la préimplantation. Datant de 2009, l'article de Haycock et Ramsay a d'abord démontré que les embryons à mi-gestation (E10.5) présentaient des retards de

croissance et que les placentas étaient plus petits à la suite d'une exposition aiguë à l'alcool à E1.5 et E2.5 (132). Ils ont ensuite étudié la méthylation du gène à empreinte *H19* dans le placenta et l'embryon et découvert la perte de la méthylation sur l'allèle paternel de ce gène dans le placenta seulement (132). Uniquement ce locus a été étudié, ne permettant malheureusement pas de voir les potentiels dérèglements épigénétiques sur l'ensemble du génome embryonnaire et placentaire.

1.5 Lacune dans la littérature

Comme mentionné précédemment, très peu de recherches ont été menées jusqu'à récemment sur les impacts d'une exposition prénatale à l'alcool pendant la préimplantation sur le paysage épigénétique de l'embryon ou du placenta. Pourtant, il n'est plus à prouver l'importance de cette courte fenêtre développementale en début de grossesse et son immense vulnérabilité.

D'un point de vue humain et clinique, la période préimplantatoire passe toujours inaperçue au cours d'une grossesse. En effet, la première semaine de gestation est souvent une période où la femme ignore qu'elle est enceinte. Aucun test de grossesse ne permet de confirmer la grossesse aussi tôt puisque l'hormone gonadotrophine chorionique (hCG) est sécrétée seulement après l'implantation de l'embryon dans l'utérus (152). Des études ont estimé qu'à travers le monde, près de 40% des grossesses sont non-planifiées (153). Au Canada seulement, cela représente 160 000 grossesses par année, potentiellement à risque (153). Il y a donc un fort risque d'exposition prénatale involontaire en tout début de grossesse.

Comme mentionné précédemment, les statistiques sur la consommation d'alcool en général sont aussi en hausse chez les femmes, particulièrement la consommation dite excessive ou de type *binge drinking* (154). Correspondant à la prise de plus de quatre consommations à l'intérieur de 2h, ce type de consommation a augmenté de 17.5% chez les femmes entre 2005 et 2012 (155). Étant donné qu'une haute concentration d'alcool sanguine est atteinte lors de ce type de consommation, plusieurs études démontrent qu'une seule exposition prénatale à l'alcool de type *binge* pourrait entraîner des conséquences plus importantes sur l'embryon qu'une exposition plus soutenue de type chronique, mais avec une dose modérée (148-150). Ce type de patron d'exposition est d'ailleurs courant lors d'une exposition prénatale à l'alcool en tout début de grossesse, avant de savoir que la femme est enceinte (149, 150). En raison de ces chiffres et statistiques, plusieurs experts estiment que le taux d'enfants atteint du TSAF pourrait être en hausse au cours des prochaines années (155-157).

Grâce aux travaux de Haycock datant déjà de 2009, nous savons qu'une exposition de type *binge* pendant la préimplantation a le potentiel d'impacter l'épigénome, entre autres, la méthylation d'ADN. Malheureusement, cette étude s'est attardé à un gène seulement et grâce aux avancées techniques des dernières années, il est maintenant possible d'établir les profils de méthylation à travers le génome sur des structures embryonnaires isolées afin de mieux comprendre les impacts de l'exposition à l'alcool. Lorsqu'elles se produisent dans les premières cellules embryonnaires, certaines dérégulations causées par l'alcool, dans l'épigénome par exemple, peuvent s'intégrer à la mémoire cellulaire puis être transmises lors de divisions et différentiations subséquentes à une multitude de cellules de différents types. Ces altérations ont donc le potentiel à long terme d'altérer la régulation de l'expression génique par exemple et d'ainsi contribuer au développement de phénotypes en lien avec le TSAF. Ce phénomène contribue d'ailleurs à la complexité et à l'hétérogénéité des symptômes du TSAF en affectant de manière variable, voire aléatoire, les cellules en division et différentiation.

Une autre lacune en lien avec le TSAF est l'absence d'outil de diagnostic moléculaire. Alors que la détection des troubles neurodéveloppementaux est seulement possible plus tard dans la vie de l'enfant, seulement lorsqu'ils commencent à se manifester, l'atteinte moléculaire est pourtant présente dès la naissance. Bien que certaines études aient obtenu des résultats probants en cherchant des biomarqueurs moléculaires, dont des marqueurs épigénétiques, dans la salive ou des cellules épithéliales buccales, elles ont toutes été réalisées chez des enfants d'âge scolaire ou préscolaire dont les symptômes avaient déjà commencé à se manifester (158-160). Basé sur les recherches sur le sujet, nous croyons qu'un diagnostic précoce, dès la naissance, à l'aide d'une méthode moléculaire éprouvée permettrait de réduire considérablement les impacts sociaux sur la vie de l'enfant en assurant une prise en charge rapide, avant l'apparition de plusieurs symptômes.

Au cours des prochains chapitres, nous étudierons l'impact d'une exposition à l'alcool de type *binge* pendant la préimplantation sur le développement embryonnaire, sur le paysage épigénétique embryonnaire et placentaire ainsi que sur certaines fonctions cognitives chez la jeune souris.

1.6 Hypothèse et objectifs

Mon hypothèse de recherche est qu'une exposition prénatale à l'alcool pendant la préimplantation entrainera des altérations dans le remodelage du programme épigénétique fœtal qui génèreront des erreurs épigénétiques et transcriptomiques détectables pendant le développement embryonnaire et qui affecteront le développement plusieurs tissus dont le cerveau et le placenta.

Pour répondre à cette hypothèse, mon objectif principal est de définir et caractériser les anomalies développementales et épigénétiques causées par une exposition à l'alcool de type *binge* pendant la préimplantation.

Précisément, mes sous-objectifs sont :

1. Optimiser l'étude de la méthylation d'ADN à travers le génome à partir de la technique du *Reduced Representation Bisulfite Sequencing* (RRBS) afin de la rendre plus rapide et de réduire les duplicats générés par l'amplification PCR.

2. Déterminer si l'exposition prénatale à l'alcool pendant la période préimplantatoire entraine des anomalies morphologiques embryonnaires et des dérégulations dans la méthylation d'ADN dans le cerveau antérieur d'embryons à mi-gestation.

3. Déterminer si l'exposition prénatale à l'alcool pendant la période préimplantatoire entraine des anomalies morphologiques du placenta et des dérégulations dans la méthylation d'ADN et les profils transcriptomiques des placentas de souris en fin de gestation.

4. Déterminer si l'exposition prénatale à l'alcool pendant la période préimplantatoire entraine des dérégulations dans la méthylation d'ADN et les profils transcriptomiques des cerveaux antérieurs des embryons en fin de gestation et de vérifier l'impact sur certaines fonctions cognitives à long terme.

Chapitre 2 – Rapid Multiplexed Reduced Representation Bisulfite Sequencing Library Prep (rRRBS)

Mise en contexte et contribution de l'étudiant

Pour ce chapitre, nous avons d'abord choisi d'optimiser une technique déjà bien connue pour étudier la méthylation d'ADN, le RRBS, pour la rendre plus rapide et plus précise. Afin de limiter la génération de duplicats PCR, nous avons optimisé la méthode existante afin de la réaliser sur un appareil de type qPCR et de suivre en temps réel l'amplification. Nous avons surnommé notre protocole le rRRBS, soit le *rapid Reduced Representation Bisulfite Sequencing*. Cet article a été publié en 2019 dans la revue *Bio-Protocol* doi: 10.21769/BioProtoc.3171. (161)

Contribution :

J'ai optimisé le protocole de rRRBS à partir des protocoles existants avec l'aide du Dr. Donovan Chan et réalisé les expériences pour s'assurer de la robustesse de notre méthode en plus de réaliser le montage des figures. J'ai écrit le manuscrit avec Dr McGraw.

Rapid Multiplexed Reduced Representation Bisulfite Sequencing Library Prep (rRRBS)

Lisa-Marie Legault[1, 2], Donovan Chan[3] and Serge McGraw[1, 2, 4, *]

[1]CHU Sainte-Justine Research Center, Montréal, Quebec, Canada; [2]Department of Biochemistry and Molecular Medicine, Université de Montréal, Montréal, Quebec, Canada; [3]Research Institute of the McGill University Health Centre, Montréal, Quebec, Canada; [4]Department of Obstetrics & Gynecology, Université de Montréal, Montréal, Quebec, Canada

*For correspondence: Serge.McGraw@umontreal.ca

[Abstract] DNA methylation is a common mechanism of epigenetic regulation involved in transcriptional modulation and genome stability. With the evolution of next-generation sequencing technologies, establishing quantitative genome-wide DNA methylation profiles is becoming routine in many laboratories. However, many of these approaches take several days to accomplish and use subjective PCR methods to amplify sequencing libraries, which can induce amplification bias. Here we propose a rapid Reduced Representation Bisulfite Sequencing (rRRBS) protocol to minimize PCR amplification bias and reduce total time of multiplexed library construction. In this modified approach, the precise quantification of the final library amplification step is accomplished and monitored by qPCR, instead of using standard PCR and gel electrophoresis, to determine the appropriate number of cycles to perform. The main advantages of this rRRBS method are: i) Reduced amount of amplification enzyme used for library prep, ii) Reduced number of PCR cycles resulting in less PCR amplifications bias, and iii) Preparation of quality multiplexed rRRBS libraries in only ~2 days.

Keywords: DNA methylation, Reduced representation bisulfite sequencing, Epigenetics, Next-generation sequencing, Multiplex libraries

[Background] With the development of high-throughput sequencing technologies, evaluation of genome-wide DNA methylation profiles is more accessible than before. For the human genome, various commercial targeted methyl capture sequencing panels and methylation arrays are available and allow high-throughput, quantitative interrogation of methylation sites at single-nucleotide resolution. However, most of these commercial tools are not offered for other model species. Thus, cost-effective sequencing-based methods for genome-wide methylation analysis, not targeting species-specific genomic sequences, are still highly relevant and valuable especially when profiling large cohorts of samples. One of these techniques is Reduced Representation Bisulfite Sequencing (RRBS). This method enables you to quantitatively investigate the DNA methylation profile of ~10% of the overall CpGs, clustered in fragments composing approximately 1% of the genome, with a preference for CpG rich regions (e.g., CpG islands, promoters) (Gu et al., 2011; Meissner et al., 2005; Meissner et al., 2008; Smith, Gu, Bock, Gnirke, & Meissner, 2009).

Here, we present a rapid RRBS (rRRBS) protocol (Piché et al.) that significantly decreases hands-on time, allowing to perform the entire protocol in ~2 days compared to the 7 days usually needed (Boyle et al., 2012; Gu et al., 2011). Importantly, by using a qPCR amplification step, we now minimize amplification bias during multiplexed library construction (Figure 1). This method is suitable for DNA methylation studies from cells or tissues from any common research species (e.g., human, mouse, rat, zebrafish).

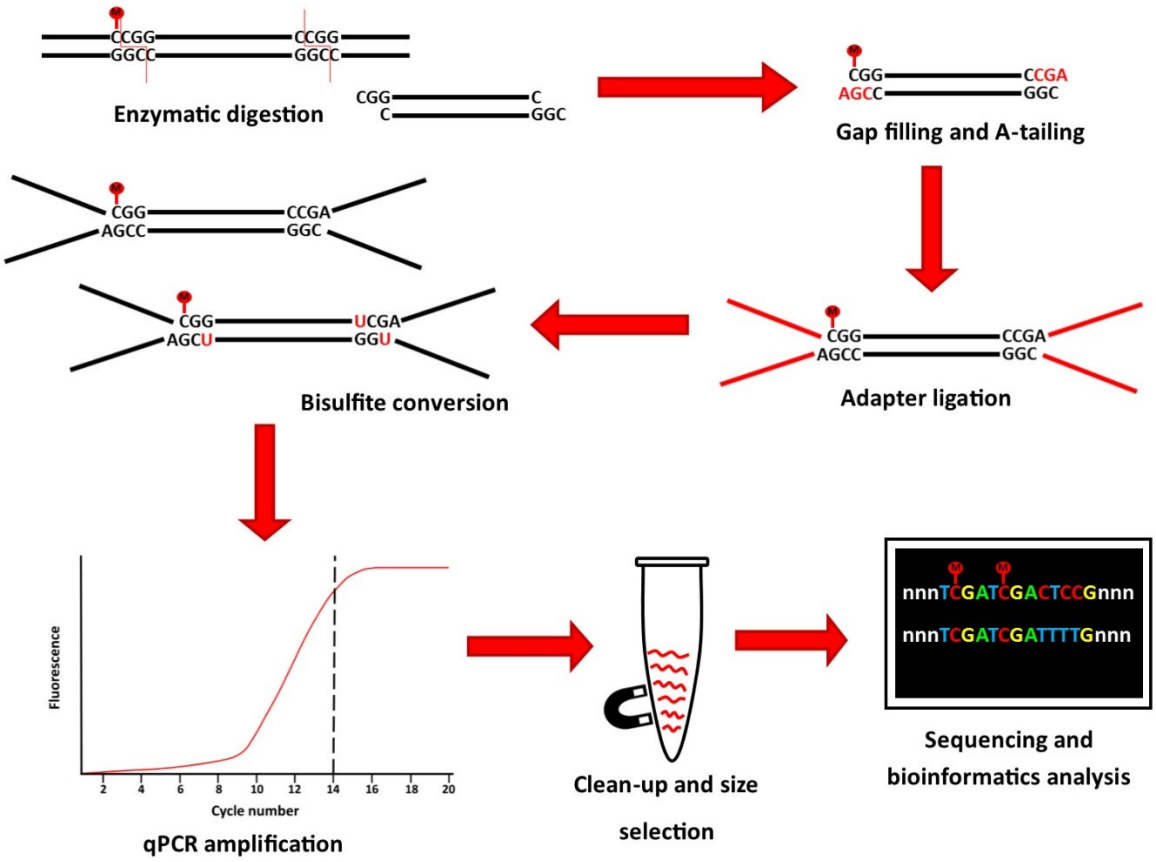

Figure 1. Graphical summary of the principal step of the rRRBS procedure

Materials and Reagents

1. Pipette tips
2. 1.5 ml microtubes
3. 0.2 ml strip tubes with individual caps
4. DNase/RNase-free tube
5. QIAamp DNA micro or mini kit (QIAGEN, catalog numbers: 56304 or 51306)
6. QuBit dsDNA BR assay kit (Thermo Fisher Scientific, catalog number: Q32853)
7. MspI 100 U/µl (New England Biolabs, catalog number: R0106M)
8. Klenow fragment 5,000 U/ml (New England Biolabs, catalog number: M0212L)
9. dNTP set (4 x 100 mM) (Thermo Fisher Scientific, catalog number: 10297018)
10. AMPure XP magnetic beads in PEG solution (Beckman Coulter, catalog number: A63881)

11. NEBNext® Multiplex Oligos for Illumina® (Methylated Adapter, Index Primers Set 1) (New England Biolabs, catalog number: E7535L)
12. T4 DNA ligase 2,000,000 units/ml (New England Biolabs, catalog number: M0202M)
13. EpiTect Fast bisulfite kit (QIAGEN, catalog number: 59826)
14. SYBR Green, 10,000x (Thermo Fisher Scientific, Invitrogen, catalog number: S7563)
15. KAPA HiFi Uracil+ 2x mastermix (Roche, catalog number: KK2802)
16. Bioanalyzer High Sensitivity DNA Assay (Agilent, catalog number: 5067-4626)
17. DNase/RNase free water
18. EB buffer (QIAGEN, catalog number: 19086)
19. NEBuffer 2 (New England Biolabs, catalog number: B7002S)
20. Ethanol 100%

Equipment

1. P10 pipet
2. QuBit fluorometric device (Thermo Fisher Scientific, catalog number: Q33226)
3. Vortex
4. Mini-centrifuge
5. Thermocycler
6. Heating block
7. DynaMag™-96 Side Magnet (Thermo Fisher Scientific, catalog number: 12331D)
8. DynaMag™-2 Magnet (Thermo Fisher Scientific, catalog number: 12321D)
9. qPCR machine
10. qPCR plates2100
11. Bioanalyzer instrument (Agilent, catalog number: G2939BA)
12. Illumina sequencing apparatus

Procedure (Figure 1)

A. DNA extraction and quantification

DNA is extracted from tissues or cultured cells using QIAGEN QIAamp DNA micro or mini kit, depending on the size of the original sample, following manufacturer's recommendations.

The Qubit fluorometric device with dsDNA BR assay kit is then used to quantify DNA samples. To ensure efficiency of bisulfite conversion (Procedure F), 0.5% of unmethylated λ phage DNA (Promega, Madison, WI) can be added as a spike-in with 500 ng of sample DNA to provide an internal control.

B. Enzymatic digestion

1. For each sample, in a 0.2 ml PCR tube from a strip tube with individual caps, dilute 500 ng of DNA in DNase/RNase-free water for a final volume of 26.8 µl.
   Note: Use 0.2 ml PCR strip tubes with individual caps at every step to avoid contamination of your samples.
2. Prepare a master mix of MspI enzyme by mixing 3 µl of 10x NEB Buffer 2 and 0.2 µl of 100 U/µl MspI enzyme per reaction (Table 1).

Table 1. Preparation of MspI digestion mix

Reagent	Volume for one reaction
10x NEB Buffer 2	3 µl
MspI 100 U/µl	0.2 µl

3. Add 3.2 µl of the master mix to each sample tube. Mix by pulse vortexing and briefly centrifuge (*i.e.,* spin down) reaction.
4. Incubate the digestion reaction in a thermocycler overnight at 37 °C, with lid set at 42 °C.

C. Gap filling and A-tailing

Gap filling and A-tailing are achieved using Klenow fragment and a dNTP mixture (10 mM dATP, 1 mM dCTP, 1 mM dGTP).

1. Prepare the dNTPs mixture by mixing 176 µl of DNase/RNase-free water, 20 µl of dATP (100 mM), 2 µl dCTP (100 mM) and 2 µl dGTP (100 mM). Aliquots of dNTPs can be stored at -20 °C for future rRRBS experiments.
2. For each sample, prepare a master mix by combining 1 µl of the dNTP mixture and 1 µl of Klenow fragment enzyme (Table 2).

Table 2. Preparation of gap filling and A-tailing mix

Reagent	Volume for one reaction
dNTP mixture (prepared at Step C1)	1 µl
Klenow enzyme 5,000 U/ml	1 µl

3. Without deactivating *MspI* digestion, add 2 µl of the master mix in each sample tube. Mix by pulse vortexing and briefly centrifuge.
4. Place tubes back in the thermocycler for a cycle of 20 min at 30 °C and 20 min at 37 °C. The lid should not be heated.

D. Beads clean-up

After the gap filling and A-tailing step, AMPure XP magnetic beads in PEG solution are used to clean up the reactions from previous reagents. To improve resuspension of the beads later on, warm up EB buffer in a heating block at 55 °C.

Note: Warming up the EB buffer at 55 °C will facilitate the resuspension of the beads, especially if they are over dried.

1. Add 64 µl of beads (2x ratio of beads [Note 1]) to each sample. Mix by slowly pipetting up and down at least 10 times.
2. Incubate mixture for 30 min at room temperature.
3. Add 0.2 ml tubes on a DynaMag^{TM}-96 Side magnet for 5 min. At this stage, DNA is bound to the AMPure XP magnetic beads.
4. Without disturbing the beads, carefully remove and discard the supernatant.
5. Wash the beads by adding 100 µl of 80% freshly prepared ethanol. Incubate 5 min and remove EtOH without disturbing the beads.
6. Repeat Step D5 for a second wash.
7. Remove the residual EtOH with a P10 pipet.
8. Dry the beads for about 5 min. Do not over dry (*i.e.,* bead ring appears cracked if over dried) as this will significantly decrease elution efficiency (Note 2).
9. Remove the tubes from the magnetic rack and resuspend the beads in 26 µl warmed EB buffer by repetitive pipetting, and incubate for 2 min at room temperature (not on the rack).
10. Place the tubes back in the magnetic rack and incubate for at least 5 min. Make sure all the beads are bound to the wall of the tube.

11. Carefully remove the supernatant without taking any beads and transfer into a new PCR tube.

E. Adapter ligation and beads clean-up

The next stage is to ligate the adapters for the future qPCR amplification and index fixation steps. Here, the NEBNext® Multiplex Oligos for Illumina® (Methylated Adapter, Index Primers Set 1) kit is used in combination with the T4 DNA ligase.

1. For each reaction, prepare a master mix of 8.5 µl of DNase/RNase-free water, 5 µl of T4 DNA ligase enzyme 10x buffer, 10 µl of NEB methylated adapters and 1.5 µl of T4 DNA ligase. It is crucial to use methylated adapters to avoid any incompatibility at the amplification step with the index primers. If non-methylated adapters are used, the bisulfite treatment will convert non-methylated cytosine into thymidine and this will interfere with the recognition of the adapter sequence in future reactions (Table 3).

Table 3. Preparation of adapter ligation mix

Reagent	Volume for one reaction
DNase/RNase free water	8.5 µl
T4 DNA ligase enzyme 10x buffer	5 µl
NEB methylated adapters	10 µl
T4 DNA ligase (2,000,000 U/ml)	1.5 µl

2. Add 25 µl of the master mix to each 26 µl DNA sample. Mix by pulse-vortexing and briefly centrifuge.
3. Incubate 20 min at 20 °C in a thermocycler with a non-heated lid.
4. Remove the tubes from the thermocycler and add 3 µl of USER enzyme to every reaction. Keep the reaction tubes at room temperature while adding the enzyme. Mix by pulse-vortexing, briefly centrifuge and place the tubes back in the thermocycler for 15 min at 37 °C with a non-heated lid.

Note: A second AMPure XP magnetic bead clean-up step is performed.

5. Add 55 µl of beads to each sample. Mix by slowly pipetting up and down at least 10 times.
6. Incubate 5 min at room temperature.

7. Place the tubes on a DynaMag^{TM}-96 Side magnet for 5 min. At this stage, DNA is captured by the beads.
8. Without disturbing the beads, carefully remove and discard the supernatant.
9. Wash the beads by adding 100 µl of 80% freshly prepared EtOH. Incubate 5 min and remove EtOH.
10. Repeat Step E9 for a second wash.
11. Remove the residual EtOH with a P10 pipet.
12. Dry the beads for about 5 min. Do not over dry (Note 2) .
13. Remove tubes from the magnetic rack, resuspend the beads in 25 µl warmed EB buffer, and incubate 2 min at room temperature (not on the magnetic rack).
14. Place the tubes back in the magnetic rack and incubate at least 5 min to make sure all the beads stick to the magnet.
15. Carefully remove the supernatant without taking any beads and put into a new PCR tube.

Note: The samples can be frozen (-20 °C) at this time to continue later (Note 3).

F. Bisulfite conversion

Sodium bisulfite DNA treatment allows for discrimination between methylated and unmethylated cytosines. Compared to previously described RRBS methods, we use the QIAGEN EpiTect Fast bisulfite kit, which significantly reduces time associated with this step.

Since sodium bisulfite-treated DNA is more sensitive to freezing and thawing, it is better to perform the bisulfite conversion and the amplification of rRRBS libraries without stopping to avoid any degradation (Note 3). (Table 4)

Table 4. Preparation of sodium bisulfite conversion reaction

Reagent	Volume to add per sample
Sodium bisulfite mix	85 µl
DNA protect buffer	25 µl

1. Add 85 µl of bisulfite mix to each 25 µl DNA sample. Pipet up and down at least 10 times.
2. Add 30 µl of DNA protect buffer. Mix by pulse-vortexing, briefly centrifuge and place tubes in the thermocycler.
3. Run 2 cycles: 95 °C for 5 min and 60 °C for 20 min as recommended by the manufacturer's protocol.

During the last minutes of incubation, a preparation of carrier RNA is made by mixing the appropriate quantity of carrier RNA with BL buffer following the indication from the kit handbook. For the second part of the bisulfite reaction procedure (*i.e.,* cleanup steps), follow the manufacturer's protocol. To elute the DNA, carefully add 15 µl of EB buffer in the middle of the column and incubate at room temperature for 5 minutes, then centrifuge for 1 min at full speed. Elution step is repeated with another 15 µl of EB buffer.

G. Amplification of rRRBS libraries

This step, one of the main improvements of our approach, uses a quantitative-PCR (qPCR) method to directly monitor the final amplification of rRRBS libraries to minimize the over cycling effect. In previous protocols, sample were tested with varying PCR cycle numbers to determine the minimal cycle number to be used in the final library preparation. For each sample, the appropriate number of cycles was determined by visualizing the PCR reactions on gel electrophoresis, and then a final library amplification step was performed on the rest of the samples. This protocol is therefore faster and accurately defines the appropriate number of PCR cycles required for library amplification.

1. Prepare a large-scale PCR mix reaction for each sample following the indication provided in Table 5. NEB Universal primer and Indexing primers are provided with the methylated adapter's kit. SYBR Green is diluted to 10x in water from 10,000x stock.

Table 5. Preparation of qPCR mix for library amplification

Reagent	**Mix per sample (200 µl)**
ddH_2O	60 µl
KAPA HiFi Uracil+ 2x mastermix	100 µl
Indexing primer	6 µl
NEB Universal primer	6 µl
Bisulfite converted DNA	24 µl
10x SYBR Green	4 µl

2. Divide the 200 µl reaction mix of each sample by distributing 25 µl in individual wells of a 8-strip PCR tube (0.2 ml). Insert PCR strips into the Roche LightCycler96 qPCR instrument and run under conditions indicated in Table 6.

Table 6. qPCR amplification protocol

Step	**Time**	**Temp (°C)**
1 – Denaturation	45 s	98
2.1 – Denaturation	15 s	98
2.2 – Annealing	30 s	57
2.3 – Extension	45 s	72
Stop during the exponential phase (after about 12-15 cycles)		
3 – Extend	7 min	72

3. Stop the qPCR reaction at the end of the linear phase of amplification, after about 12 to 15 cycles, before the plateau phase is reached (Figure 2).
   Note: When various libraries are amplified simultaneously, they might not all reach the plateau phase at the same time. Samples with adequate amplification can be quickly removed at the end of an amplification cycle, and transferred to another PCR machine for the final 7 min of extension step.

4. Perform a final extension step of 7 min at 72 °C.

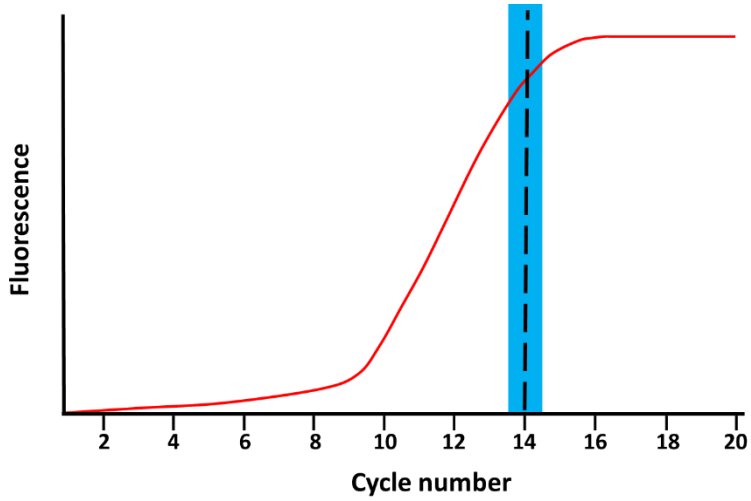

Figure 2. Schematic of qPCR library amplification plot. The red line represents the total amplified product accumulation at each qPCR cycle. The blue rectangle represents the period when the qPCR library amplification should be stopped; following the exponential phase and just before the plateau phase. Here for example, the rRRBS library amplification would have been stopped at cycle number 14, when the red line starts to curve.

H. Clean-up and size selection of rRRBS libraries

After amplification of rRRBS libraries by qPCR, a last clean-up step is performed using AMPure XP magnetic beads to remove reagent and primer-dimers.

1. For each sample, pool all 8 PCR reactions into a 1.5 ml low-binding DNase/RNase-free tube.
2. Calculate the precise volume of each reaction and add the same volume of beads to the PCR reaction to have a 1x ratio (Note 1) (*i.e.,* add 200 µl of beads if 200 µl of reaction remains after the PCR). Mix by pipetting up and down. The DNA/bead 1x ratio will remove most fragments below 200 bp and all smaller fragments below 100 bp.
3. Incubate 15 min at room temperature and gently tap the tube every 5 min to mix beads and DNA.
4. Place tubes in magnetic rack and let stand 10 min.
5. Carefully remove and discard the supernatant without disturbing the beads.
6. By keeping the tubes on the magnetic rack, wash the beads by adding 1 ml of 80% freshly prepared EtOH. Incubate 5 min and remove EtOH.
7. Repeat Step H6 for a second wash.

8. Remove the residual EtOH with a P20 pipet.
9. Dry the beads for about 10 min. Do not over dry (Note 2).
10. Remove the tube from the magnetic rack and resuspend the beads in 40 µl of pre-warmed EB buffer. Mix by pipetting, and incubate 5 min at room temperature (not on the rack).
11. Put the tubes back in the magnetic rack and incubate for at least 5 min to ensure all the beads stick to the magnet.
12. Carefully remove the supernatant without taking any beads and transfer the solution into a new 1.5 ml tube.

I. Quality control

Assess the quality and concentration of the sample by performing a High Sensitivity DNA Assay on the 2100 Bioanalyzer instrument.

Concentration varies depending on the original amount of input DNA and the efficiency of the different steps. The peak should be between 200 bp and 300 bp, and concentration at approximatively 5 ng/µl or higher. If a peak of primer-dimer is visible on the Bioanalyzer, at a length of about 75 bp, perform a second DNA/beads cleanup and repeat the Bioanalyzer quality assessment before.

Note: If you observe a peak at around 75 bp, perform a second DNA/beads clean-up with a 1x ratio of beads to get rid of all the primer-dimer as those smaller fragments can affect the quality of the sequencing.

J. Sequencing

Paired-end sequencing (> 100 bp read length) of libraries is performed on Illumina apparatus. The number of multiplex libraries per sequencing lane depends on the sequencing technology used and the species investigated (*i.e.,* total number of CpG of species) (Doherty & Couldrey, 2014). One should aim to obtain at least 20-30 million reads per sample for downstream bioinformatics analysis.

Data analysis

Various bioinformatics tools are widely available to analyze genome-wide DNA methylation sequencing data, and are usually customized depending on how data will be interpreted and visualized (e.g., single CpG methylation, tilling-window approach). Details of basic analysis are

detailed in previous papers (Magnus et al., 2014; McGraw et al., 2015; Piché et al.). Briefly, Trim Galore (Krueger, 2015) is use for sequence trimming and quality control, then reads are aligned to the reference genome using BSMAP (Xi & Li, 2009), which is specific for the alignment of bisulfite treated sequenced DNA. Methylation calls are obtain using BSMAP and differentially methylated regions across two conditions are obtain using the R package methylKit (Akalin et al., 2012). Differentially methylated sequences are annotated using HOMER v4.10 (Heinz et al., 2010). Final output processed data can be use in various other downstream analyses, such as functional annotation tools to highlight enrichment of specific biological (eg. DAVID (Dennis et al., 2003), Metascape (Tripathi et al., 2015)), or converted into specific formats, such as a bedgraph, in order to view methylation levels in various genome browsers (e.g., USCS genome browser, IGV (Thorvaldsdottir, Robinson, & Mesirov, 2013)).

Notes

1. The ratio of beads is crucial to ensure a good clean-up. To mark sure to add the right volume of beads, you can measure the exact volume of sample using a pipet at every clean-up step.
2. Bead ring appears cracked if you over dry it. The beads will be harder to resuspend and this will decrease nucleic acid elution efficiency.
3. Stopping point: It is recommended to stop after the adapter ligation step (Procedure E) or to go through all the protocol in the same day.

Acknowledgments

Research was funded by an NSERC discovery grant to SM. LML received scholarship from Fondation du CHU Sainte-Justine and Réseau Québécois en Reproduction. We thank Elizabeth Maurice-Elder for editing.

Competitive interests

The authors declare no conflict of interest.

References

Akalin, A., Kormaksson, M., Li, S., Garrett-Bakelman, F. E., Figueroa, M. E., Melnick, A., & Mason, C. E. (2012). methylKit: a comprehensive R package for the analysis of genome-wide DNA methylation profiles. *Genome Biol*, 13(10), R87. doi:10.1186/gb-2012-13-10-r87

Boyle, P., Clement, K., Gu, H., Smith, Z. D., Ziller, M., Fostel, J. L., . . . Meissner, A. (2012). Gel-free multiplexed reduced representation bisulfite sequencing for large-scale DNA methylation profiling. *Genome Biol*, 13(10), R92. doi:10.1186/gb-2012-13-10-r92

Dennis, G., Jr., Sherman, B. T., Hosack, D. A., Yang, J., Gao, W., Lane, H. C., & Lempicki, R. A. (2003). DAVID: Database for Annotation, Visualization, and Integrated Discovery. *Genome Biol*, 4(5), P3.

Doherty, R., & Couldrey, C. (2014). Exploring genome wide bisulfite sequencing for DNA methylation analysis in livestock: a technical assessment. *Front Genet*, 5, 126. doi:10.3389/fgene.2014.00126

Gu, H., Smith, Z. D., Bock, C., Boyle, P., Gnirke, A., & Meissner, A. (2011). Preparation of reduced representation bisulfite sequencing libraries for genome-scale DNA methylation profiling. *Nat Protoc*, 6(4), 468-481. doi:10.1038/nprot.2010.190

Heinz, S., Benner, C., Spann, N., Bertolino, E., Lin, Y. C., Laslo, P., . . . Glass, C. K. (2010). Simple combinations of lineage-determining transcription factors prime cis-regulatory elements required for macrophage and B cell identities. *Mol Cell*, 38(4), 576-589. doi:10.1016/j.molcel.2010.05.004

Krueger, F. (2015). Trim Galore!: A wrapper tool around Cutadapt and FastQC to consistently apply quality and adapter trimming to FastQ files: 0.4.

Magnus, N., Garnier, D., Meehan, B., McGraw, S., Lee, T. H., Caron, M., . . . Rak, J. (2014). Tissue factor expression provokes escape from tumor dormancy and leads to genomic alterations. *Proc Natl Acad Sci U S A*, 111(9), 3544-3549. doi:10.1073/pnas.1314118111

McGraw, S., Zhang, J. X., Farag, M., Chan, D., Caron, M., Konermann, C., . . . Trasler, J. M. (2015). Transient DNMT1 suppression reveals hidden heritable marks in the genome. *Nucleic Acids Res*, 43(3), 1485-1497. doi:10.1093/nar/gku1386

Meissner, A., Gnirke, A., Bell, G. W., Ramsahoye, B., Lander, E. S., & Jaenisch, R. (2005). Reduced representation bisulfite sequencing for comparative high-resolution DNA methylation analysis. *Nucleic Acids Res*, 33(18), 5868-5877. doi:10.1093/nar/gki901

Meissner, A., Mikkelsen, T. S., Gu, H., Wernig, M., Hanna, J., Sivachenko, A., . . . Lander, E. S. (2008). Genome-scale DNA methylation maps of pluripotent and differentiated cells. *Nature*, 454(7205), 766-770. doi:10.1038/nature07107

Piché, J., Gosset, N., Legault, L.-M., Pacis, A., Oneglia, A., Caron, M., . . . Andelfinger, G. Molecular signature of CAID syndrome: non-canonical roles of SGO1 in regulation of TGF-β signalling and epigenomics. *Cellular and Molecular Gastroenterology and Hepatology*. doi:10.1016/j.jcmgh.2018.10.011

Smith, Z. D., Gu, H., Bock, C., Gnirke, A., & Meissner, A. (2009). High-throughput bisulfite sequencing in mammalian genomes. Methods, 48(3), 226-232. doi:10.1016/j.ymeth.2009.05.003

Thorvaldsdottir, H., Robinson, J. T., & Mesirov, J. P. (2013). Integrative Genomics Viewer (IGV): high-performance genomics data visualization and exploration. *Brief Bioinform*, 14(2), 178-192. doi:10.1093/bib/bbs017

Tripathi, S., Pohl, M. O., Zhou, Y., Rodriguez-Frandsen, A., Wang, G., Stein, D. A., . . . Chanda, S. K. (2015). Meta- and Orthogonal Integration of Influenza "OMICs" Data Defines a Role for UBR4 in Virus Budding. *Cell Host Microbe*, 18(6), 723-735. doi:10.1016/j.chom.2015.11.002

Xi, Y., & Li, W. (2009). BSMAP: whole genome bisulfite sequence MAPping program. BMC *Bioinformatics*, 10, 232. doi:10.1186/1471-2105-10-232

Chapitre 3 – Pre-implantation alcohol exposure induces lasting sex-specific DNA methylation programming errors in the developing forebrain

Mise en contexte et contribution de l'étudiant

Dans ce premier article utilisant notre modèle murin d'exposition prénatale à l'alcool de type *binge*, pendant la préimplantation, nous caractérisons d'abord le modèle, entre autres en quantifiant le taux d'alcool dans le sang. Nous étudions par la suite l'impact de notre exposition sur le développement morphologique des embryons à mi-gestation (E10.5), puis nous investiguons l'impact sur les profils de méthylation d'ADN à grande échelle et l'expression génique de quelques gènes dans les cerveaux antérieurs (forebrains) de nos embryons à mi-gestation. Cet article a été publié dans le *journal Clinical Epigenetics* en 2021 doi: 10.1186/s13148-021-01151-0. (162)

Le matériel supplémentaire est disponible sur le site du journal https://clinicalepigeneticsjournal.biomedcentral.com/articles/10.1186/s13148-021-01151-0

Contribution :

J'ai établi le modèle murin, réalisé les injections, récolté les embryons et procédé à leur dissection avec l'aide de Mélanie Breton-Larrivée. J'ai réalisé toutes les expériences de méthylation, incluant les analyses qui ont été supervisées par Dr Maxime Caron et aidée par Alexandra Langford-Avelar et Anthony Lemieux. J'ai réalisé les expériences d'histologie et les analyses morphologiques, chapeautées par Dr Loydie Jerôme-Majewska. J'ai généré l'ensemble des figures et graphiques qui ont été assemblé avec l'aide du Dr Karine Doiron. J'ai collaboré à la rédaction du manuscrit avec Dr McGraw.

Pre-Implantation Alcohol Exposure Induces Lasting Sex-Specific DNA Methylation Programming Errors in the Developing Forebrain

Legault LM[1,2], Doiron K[1], Breton-Larrivée M[1,2], Langford-Avelar A[1,2], Lemieux A[1,2], Caron M[1], Jerome-Majewska LA[3,4], Sinnett D[1,5], McGraw S[1,2,6,#].

[1]CHU Sainte-Justine Research Center, Montreal, Canada.

[2]Department of Biochemistry and Molecular Medicine, Université de Montréal, Montreal, Canada.

[3]McGill University Health Centre Glen Site, Montreal, Canada.

[4]Department of Pediatrics, McGill University, Montreal, Canada.

[5]Department of Pediatrics, Université de Montréal, Montreal, Canada.

[6]Department of Obstetrics and Gynecology, Université de Montréal, Montreal, Canada.

[#]Corresponding author: serge.mcgraw@umontreal.ca

ABSTRACT

Background

Prenatal alcohol exposure is recognized for altering DNA methylation profiles of brain cells during development, and to be part of the molecular basis underpinning Fetal Alcohol Spectrum Disorder (FASD) etiology. However, we have negligible information on the effects of alcohol exposure during pre-implantation, the early embryonic window marked with dynamic DNA methylation reprogramming, and on how this may rewire the brain developmental program.

Results

Using a pre-clinical *in vivo* mouse model, we show that a binge-like alcohol exposure during pre-implantation at the 8-cell stage leads to surge in morphological brain defects and adverse developmental outcomes during fetal life. Genome-wide DNA methylation analyses of fetal forebrains uncovered sex-specific alterations, including partial loss of DNA methylation maintenance at imprinting control regions, and abnormal *de novo* DNA methylation profiles in various biological pathways (e.g., neural/brain development).

Conclusion

These findings support that alcohol-induced DNA methylation programming deviations during pre-implantation could contribute to the manifestation of neurodevelopmental phenotypes associated with FASD.

Keywords: Prenatal Exposure, Fetal Alcohol Spectrum Disorders, DNA methylation, Early Embryonic Development, Epigenetic Reprogramming, Imprinting.

INTRODUCTION

Fetal Alcohol Spectrum Disorders (FASD) encompasses the range of lifelong cognitive and physical disabilities observed in children born to mothers who consumed alcohol during pregnancy (1-4). Each year, 600 000 to 1 million children are born with FASD worldwide (5, 6). The most severe and physically visible form of the condition is known as Fetal Alcohol Syndrome (FAS), in ~10% of FASD cases, and associated with the full presentation of dysmorphic features including craniofacial malformations, growth deficits and structural brain pathologies. Depending on the amount, pattern and developmental period of prenatal alcohol exposure, children may not present with dysmorphic features, but still suffer from mild to severe FASD-related neurological disabilities, such as learning deficits and intellectual delays (1, 2). With the marked increase in rates of alcohol use and binge drinking behavior (7) among 18-34 year old women (8-14), added to the high number of unintended pregnancies worldwide (~40%; 85 million/year (15)), many women may inadvertently subject their developing embryos to acute levels of alcohol in first weeks of pregnancy. Although most studies state that alcohol consumption at all stages of pregnancy can cause FASD, pre-implantation is arguably the stage that is most prone to unintentional prenatal alcohol exposure since the human chorionic gonadotrophin (hCG) hormone, the main biomarker for pregnancy, is not yet detectable as it is only produced following implantation. Still, there is ample misinformation in the literature regarding the effects of alcohol exposure, and many other teratogen exposures, on pre-implantation embryos, and how this leads to an "*all-or-nothing*" developmental outcome.

An increasing body of evidence indicates that alcohol exposure during fetal brain development triggers lasting epigenetic alterations, including DNA methylation, in offspring long after the initial insult, supporting the role of epigenetics in FASD phenotypes (16-19). However, we remain unaware of how ethanol affects the early developmental window marked with dynamic changes in DNA methylation, and how interfering with this fundamental process may program future FASD-related neurological disabilities. During pre-implantation development, the period between oocyte fertilization and embryo implantation in the uterus, the epigenome undergoes a broad reprogramming that initiates the developmental program (20-26). We and others have shown that this essential reprogramming wave removes most DNA methylation signatures across the genome, except specific sequences that include imprinting control regions (ICRs), to trigger the embryonic developmental program (20, 27-29). DNA methylation marks are then reacquired in a

sex-, cell- and tissue-specific manner during the peri-implantation period, and marks continue to be modulated during lineage specification (30-33). Studies show that pre-implantation embryos can have sex-specific epigenetic responses to similar environmental challenges, leading to long-term sexual dimorphism in developmental programming trajectories (34-37).

One of the first indications of the direct link between ethanol exposure and aberrations in DNA methylation came from a mouse study showing that mid-gestation exposure at E9-E11 reduced global DNA methylation levels in E11 fetuses (17). This evidence gave rise to different FASD models using various levels of short or prolonged alcohol exposures at different stages of gestation. Ethanol exposure can either induce DNA methyltransferases (DNMTs) activity, through reactive oxygen species-dependent mechanisms (38, 39), or inhibit DNMTs activity, via direct action on DNMTs or on one-carbon metabolism that provides methyl groups (17, 40), which supports why both gain and loss of DNA methylation marks can be observed in FASD models. High levels of ethanol exposure on two consecutive days (E1.5, E2.5) altered DNA methylation of imprinted gene *H19,* a negative regulator of growth and proliferation, in the placenta at E10.5, yet this region showed no alteration in the embryo (41). Nonetheless, data remain very scarce on how alcohol exposure during the early stages of embryo development directly affects epigenetic reprogramming and permanently alters genome-wide DNA methylation.

In this study, we used a pre-clinical mouse model of prenatal alcohol exposure to specifically target pre-implantation embryos that are undergoing their epigenetic reprogramming wave. We show that this exposure leads to a surge in morphological brain defects during fetal life, and that exposed embryos with no visible abnormalities or developmental delays present lasting DNA methylation alterations in forebrain tissues, including sex-specific disparities in DNA methylation dysregulation.

RESULTS

Modeling early pre-implantation alcohol exposure increases phenotypic alterations in developing embryos.

To define the developmental and epigenetic (i.e., DNA methylation) impact of a binge alcohol exposure episode on early embryos undergoing the epigenetic reprogramming wave, we first established a pre-clinical mouse model to specifically expose pre-implantation embryos (E2.5)

to short, but elevated alcohol levels. To avoid possible confounding effects of gavage-associated stress, we used a well-recognized two-injection paradigm (42-45). Pregnant mice (C57BL/6) were subcutaneously injected at E2.5 (8-cell embryos) with two doses of 2.5g/kg ethanol (**EtOH-exposed**), or 0.15M saline (**control**), at 2h intervals (**Fig. 1A**). Pregnant females reached a peak blood alcohol concentration (**BAC**) of 284.27mg/dL (3h) with an average of 158.31mg/dL over a 4h window (**Fig. 1B**). In contrast with other chronic prenatal alcohol exposure models (46-49), this short but acute level of ethanol exposure on pre-implantation embryos did not affect average mid-gestational (E10.5) litter size (Ctrl; n=8.13 ± 2.58 vs EtOH-exposed; n=7.91 ± 2.86), or sex distribution (Ctrl and EtOH-exposed; 49% female vs 51% males). Similarly, early pre-implantation embryos subjected to binge-like alcohol levels did not show differences in mean morphological measurements at E10.5, however, we observed a significant increase in embryo-to-embryo variability for crown to rump length ($p<0.0001$), head height ($p<0.01$), occipital to nose diameter ($p<0.001$) and brain sagittal length ($p<0.05$) for EtOH-exposed embryos compared to controls. The greater intra-subject variability observed suggests that binge alcohol exposure levels during pre-implantation can alter the normal developmental programming of early embryos, thus causing abnormal morphological outcomes.

To define how a binge alcohol exposure episode during early pre-implantation can affect fetal development, we next investigated the morphological outcome of E10.5 embryos (control embryos: n=108 from 16 litters, EtOH-exposed: n=152 from 22 litters). As observed in **Fig. 2A**, early pre-implantation EtOH exposure leads to a significant increase in morphological defects or delayed development of mid-gestation embryos (19% vs 2%, $p<0.0001$). Types of defects observed in ethanol-exposed embryos included brain anomalies (e.g., forebrain or midbrain malformations) (10%), growth restriction or delayed development (5%), heart defects (2%), and other abnormal features (2%) (**Fig. 2B, Fig. 2C**). There was no sex-specific phenotypic divergence between EtOH-exposed male and female embryos for morphological defects (18% vs 20%, **Fig. S1**) or defect categories (**Fig. S1**). Compared to controls, we observed that binge alcohol exposure during pre-implantation leads to a larger proportion of E10.5 embryos with phenotypic alterations (29/152 vs 2/108, $p<0.0001$), and that embryos with phenotypic alterations are distributed across most ethanol-exposed litters (16/22 vs 2/16, $p<0.001$) (**Fig. 2D**) and not restricted to a small number of litters. Taken together, these results show that a binge alcohol exposure episode on pre-implantation embryos undergoing the epigenetic reprogramming wave does not interfere with normal processes

of implantation but leads to heterogeneity in morphological presentation during fetal life that mirrors the spectrum of clinical features associated to FASD.

Pre-implantation alcohol exposure causes alterations in forebrain DNA methylation profiles

To assess whether alcohol exposure during the embryonic epigenetic reprogramming wave dysregulates the normal programming of brain DNA methylation patterns during fetal development, we established genome-wide DNA methylation profiles using rRRBS on E10.5 mouse forebrains. To mirror the 90% of children with FASD that show no dysmorphic features but still suffer from mild to severe neurological disabilities (e.g., learning deficits, intellectual delays), we randomly selected 6 controls (3 males; 3 females) and 16 ethanol-exposed embryos (8 males; 8 females) of similar size (i.e., embryo size, head height, occipital to nose diameter, brain sagittal length) with no visible morphological defects (Fig. **S2**). Histological analysis revealed that ethanol-exposed embryos with no visible morphological defects or developmental delays had a general layout and distribution of brain cells that were comparable to controls (**Fig. S3A-B**), whereas ethanol-exposed embryo with delayed development were distinctly different (**Fig. S3C**). Furthermore, using markers for proliferation (Ki67 antigen) and apoptosis (cleaved Caspase-3), we confirmed that the early ethanol exposure did not promote an imbalance in cell proliferative response (**Fig. S4**) or cell death (**Fig. S5**) across brain regions of embryos with no apparent morphological defects. By removing embryos with abnormalities, developmental delays, or gross brain structure aberration, we further reduced potential DNA methylation variability that could be due to divergent forebrain cell type proportions between samples.

The first set of analyses was designed to define whether early pre-implantation alcohol exposure caused lasting DNA methylation alterations in developing E10.5 embryonic forebrains despite the absence of phenotypic presentation. To do so, we compared the average DNA methylation levels in 100 bp non-overlapping genomic windows (*tiles*; see methods section) between controls and ethanol-exposed samples. After removal of sex chromosomes, we identified 114 911 unique sequenced tiles containing 794 803 common CpGs across samples (min. 5 samples/condition, ≥10x sequencing depth). When tiles were classified according to their DNA methylation levels, we observed significant changes in the distribution of categories, including tiles ranging between 90-100% methylation for which we observed a decrease in ethanol-exposed forebrains compared to controls (26% vs 24%, $p<0.0001$ (**Fig. 3A**). Clustering of individual E10.5

forebrain samples by DNA methylation levels for the top 1% most variable tiles (n=1200) revealed three main subgroups; a first essentially composed of control samples (6/9; right in heatmap), a second mainly composed of ethanol-exposed female samples with similarities to controls patterns (5/6; middle in heatmap), and a third mostly composed of male ethanol-exposed samples with highly divergent patterns (6/7; left in heatmap) (**Fig. 3B**). We next identified regions of the genome that showed altered DNA methylation levels (±≥ 10% mean differences between tiles; see methods) as a result of the early pre-implantation alcohol exposure. Using such criteria, we identified 1509 differentially methylations regions (**DMRs**) with significant DNA methylation level decrease (n=1440) or increase (n=69) in EtOH-exposed forebrains compared to control forebrains (**Fig. 3C**). Differences in methylation levels ranged from 10%-55%, with most DMRs showing 10-15% (n=1086; 72%) or 15-20% (n=300; 20%) methylation change between EtOH-exposed and control forebrains (**Fig. 3D**). Most DMR-associated tiles with decreased methylation levels in EtOH-exposed samples (n=1239) were highly methylated (≥40-50%) in control samples, whereas DMRs that gained methylation in EtOH-exposed samples had variable levels in controls (**Fig. 3E**). The DMRs mainly overlapped with intergenic (43%) and genic (53%: introns; 37%, exons; 12%, and promoters; 4%) regions. Gene ontology enrichment analyses associated genic DMRs with various processes, including cell-to-cell signaling pathway, regulation of GTPase activity, positive regulation of nervous system development, tissue and embryonic morphogenesis, as well as regulation of neurological systems (**Fig. 3F**). When we looked at the DNA methylation levels between control and EtOH-exposed forebrains for genes associated to these enriched pathways (e.g,. *Lrch1*, *Cflar*, *Celsr1*, *Apoa1*, *Lpin1*, *Epha7*, *Foxa1*, *Egf*, *Il6*, *Nkx6-2*), we observed increased inter-individual variability in methylation levels for EtOH-exposed forebrains with some samples or genomic regions being more affected than others (**Fig. 3G**).

Overall, we showed that alcohol exposure during the embryonic epigenetic reprogramming wave triggers an array of DNA methylation alterations observed in forebrain of embryos that presented no visible abnormalities or developmental delays at E10.5.

Sex-specific DNA methylation alterations following pre-implantation alcohol exposure

We next sought to discern whether early pre-implantation alcohol exposure could have a sex-specific impact on later forebrain DNA methylation patterns. By analyzing male and female samples separately (min. 3 samples/condition/sex, ≥10x sequencing depth), we identified 83 424

and 126 857 unique sequenced tiles in male and female forebrains, respectively (**Fig. 4A**). Although there were lesser regions analyzed in males, they showed a larger number of DMRs following pre-implantation alcohol exposure (DMRs: males n=2 097, females n=1 273) (**Fig. S6**). In male EtOH-exposed forebrains, we found 2097 DMRs of which 1936 (92%) showed decreased methylation. Comparably, female EtOH-exposed forebrains revealed 1273 DMRs of which 1066 (84%) presented decreased methylation (**Fig. S6A-D**). We also observed contrasts between DMR number, as well as associated biological processes among sexes (**Fig. S6E**). However, we do not exclude that these results could be related to only a partial overlap in sequenced regions (n=46 475) between male and female forebrain samples (**Fig. 4A**).

To circumvent this issue, we focused on the 46 475 regions with sufficient sequencing coverage in both sexes encompassing 373 530 CpGs (**Fig. 4A**). We did not observe any differences in global DNA methylation levels between sexes in either controls or ethanol-exposed forebrains (males: 29.4% vs 28.7%, females: 29.4% vs 29.2%; not shown). However, when these common tiles (n= 46 475) were distributed according to their DNA methylation levels in control and ethanol-exposed forebrains, we observed a greater shift in tile distribution in male EtOH-exposed samples (**Fig. 4B**), suggesting a greater effect on males. Accordingly, among the 46 475 male-female common tiles, we identified 971 male-specific DMRs, 133 female-specific DMRs, and 111 DMRs that were present in both sexes (**Fig 4A**). Out of these 111 common DMRs, 100 had similar alteration profiles (i.e., n=99 DMRs with decreased methylation, n=1 DMR with increased methylation) in male and female EtOH-exposed forebrains (**Fig. 4C**). For the other DMRs (n=11), the alcohol exposure caused conflicting alteration profiles between sexes (e.g., decreased-methylation in males vs increased-methylation in females). For the most part, the common DMRs displayed low levels of methylation changes (10-15% range) for both sexes (42% for males, 79% for females), with methylation changes greater than 25% only present in male EtOH-exposed samples (**Fig. 4D**). When compared to the 46 475 common tiles analyzed, the 111 common DMRs were more enriched in intergenic regions and intron categories, as well as for LINE elements, whereas they were mostly depleted of CpG rich sequences (i.e. CpG islands). In addition, common DMRs in male and female EtOH-exposed forebrains showed various levels of DNA methylation for an assortment of genes, including *Tmem267* (putative oncogene), *Vwc2* (neural development and function), *Hcn4* (cardiac function), *Septin9* (cytoskeletal formation), *Gipc2* (gastrointestinal processes) and *Dlx2* (forebrain and craniofacial development) (**Fig. 4F**, **Fig. S7**).

When we turned our attention to male-specific (n=971) and female-specific (n=133) DMRs within the 46 475 common tiles, we observed that pre-implantation alcohol exposure had a more profound impact on male forebrains in terms of DMR number and level of methylation changes (**Figs. 4A**, **5A**). Although a portion of observed DMRs showed increased methylation (males 3%; n=31, females 23%; n=30), the majority of sex-specific DMRs were associated with a partial loss of DNA methylation (males n=940, females n=103) in all chromosomes. The only chromosomes that showed an enrichment ($p<0.0001$) in DMRs were female X-chromosomes (n=48/133). Most of these sex-specific DMRs showed low levels of alterations, in the 10-15% range (males n=627 DMRs; 65%, females n=112 DMRs; 84%), with males having a larger proportion of DMRs with >15% methylation changes (**Fig. 5B**). When we highlighted genomic features associated to these sex-specific DMRs, we observed more female-specific DMRs in promoter regions (17% vs 4%) and CpG rich regions (33% vs 8%) when compared to male-specific DMRs (**Fig. 5C**). When we focused on the distribution of CpG sites in a sequence context (i.e., CpG islands, shores, shelves), we noticed a significant loss of global methylation in male-specific DMRs for male EtOH-exposed forebrains, and similarly for female-specific in female EtOH-exposed forebrains (**Fig. 5D**). For female-specific DMRs, we noticed that DNA methylation levels in control forebrains are all higher in females compared to males. These higher methylation levels are mainly associated with the presence of methylation marks associated to the X-inactivation process in females (female-specific DMRs on X-chromosome: CpG islands 35/44; shores 9/36, shelves 0/6. **Fig. 5F** bottom for examples). The sex-specific DMRs resulting from pre-implantation alcohol exposure were related to divergent biological processes between males (e.g., muscle differentiation, cell projection organization) and females (e.g., receptor protein tyrosine kinase pathway, epithelial cell migration) (**Figs. 5E, 5F**).

We then evaluated whether early embryonic alcohol exposure led to expression errors in the forebrains of E10.5 embryos by focussing on a group of genes (with or without DMRs) implicated in the regulatory network coordinating the timing of GABAergic interneuron migration and forebrain formation. At the core of this network is the *Dlx* family of homeodomain transcription factors (50, 51). We show that *Dlx2* (DMR in gene body; males and females) and *Dlx1* (no DMRs) have small but significant changes in gene expression (*Dlx2*: males and females; *Dlx1*: females) (**Fig. S8A**), whereas for *Dlx5* and *Dlx6* (no DMRs), the expression remained unchanged (**Fig. S8B**). Upstream key regulator of MGE (medial ganglionic eminence)-derived GABAergic interneurons

(52-54), *Nkx2.1* (no DMRs) did not show expression alterations (**Fig. S8B**), however downstream transcription factors such as *Sox6* (DMR in gene body; males), and *Arx* (direct target of *Dlx2* (55, 56)), DMR in promoter; females) showed small but significant gene expression alteration (*Sox6*; males and females, *Arx*; males) (**Fig. S8A**).

Together, these results indicate that alcohol exposure in pre-implantation embryos in conjunction with epigenetic reprogramming leads to variable levels of sex-specific alterations, with male embryonic forebrains being more prone to DNA methylation alterations. This suggests that pre-implantation male embryos are more susceptible to the initial adverse exposure rendering them less efficient at re-establishing proper DNA methylation patterns during the *de novo* methylation wave, or that female embryonic cells are better at rectifying dysregulated DNA methylation patterns during development.

Pre-implantation alcohol exposure leads to partial loss of imprinted DNA methylation patterns

To further determine if a binge alcohol exposure episode on early embryos undergoing the epigenetic reprogramming wave is more adverse on the DNA methylation patterns of male or female embryos, we directed our attention to ICRs of imprinted genes, which are well known for their key roles in brain development and growth. We and others have shown that allele-specific methylation maintenance is required on ICRs during the reprogramming wave, as partial or complete loss of ICR profiles is permanent. Since our alcohol exposure specifically targets E2.5 embryos (8-cell stage), dysregulation in ICRs methylation maintenance would still be detectable in E10.5 forebrains. From the 46 475 commonly sequenced tiles, 28 were located within the ICRs of 9 imprinted genes. Our non-allele specific differential methylation analysis revealed that out of these 28 regions, 24 were differentially methylated in male EtOH-exposed forebrains. These 24 DMRs were associated to imprinted genes *H13*, *Nnat*, *Gnas*, *Kcnq1*, *Plagl1*, *Zrsr1*, *Peg13* and *Igf2r* (**Fig. 6A**). In females, only 2 of those 28 tiles showed altered levels in female EtOH-exposed forebrains, which were associated with *Gnas* and *Grb10*. We expanded our search for dysregulated ICR DNA methylation patterns within uniquely sequenced regions in male (n=36 949 tiles) and female (n=80 382 tiles) forebrains (**Fig. 4A**) to retrieve additional ICR-associated tiles. Again, in EtOH-exposed male forebrains, the majority of ICRs (10/13 tiles) showed altered DNA methylation patterns (**Fig. 6B**), which were associated with *Gnas*, *Snrpn*, *Peg3*, *Plagl1*, *Zrsr1* and *Impact.* Conversely, in EtOH-exposed female forebrains, we now observed a large portion of ICRs

(19/36 tiles) with dysregulated DNA methylation levels associated to various imprinted genes (i.e., *Gnas*, *Peg10*, *Inpp5f*, *Kcnq1*, *Snrpn*, *Grb10*, *Zrsr1*, *Peg13*, *Slc38a4*, *Igf2r* and *Impact*). When we plotted individual sample DNA methylation values for these ICR-associated DMRs, we again observed a high degree of heterogeneity in EtOH-forebrains with some samples showing altered DNA methylation levels (e.g., partial loss, complete loss), and others revealing normal control methylation values (**Fig. 6A-C**).

This partial loss of DNA methylation signatures within ICRs of male and female E10.5 EtOH-exposed forebrains was associated with small but significant deviation in expression level for a number of imprinted genes (e.g., *Gnas*, *Plagl1*, *Peg13*) (**Fig. S9A**). Whereas for others, although we observed similar ICR-associated DMRs, we did not detect any alteration in imprinted gene expression (e.g., *Impact*, *Peg10*, *Grb10*) for either male or female E10.5 EtOH-forebrains (**Fig. S9B**).

Both male and female EtOH-exposed forebrains showed variable levels of DNA methylation alterations in imprinted gene ICRs, which suggests that a binge-like alcohol exposure during pre-implantation interferes with the DNA methylation maintenance machinery during the epigenetic reprogramming wave. Finally, these results also suggest that male pre-implantation embryos are more susceptible to the initial adverse of alcohol exposure.

DISCUSSION

In this study, we showed that a binge alcohol exposure episode on early-stage embryos (8-cell; E2.5) leads to a surge in morphological brain defects and delayed development during fetal life, that are reminiscent of clinical features associated to FASD. As seen in children exposed to alcohol prenatally, a portion of ethanol-exposed embryos presented a spectrum of alcohol-induced macroscopic defects while the majority showed no noticeable dysmorphic features and not alterations. However, forebrain tissues from ethanol-exposed embryos with no visible macroscopic abnormalities, developmental delays, alteration in cell proliferative response or cell death still presented lasting genome-wide DNA methylation alterations in genes associated to various biological pathways, including neural/brain development, and tissue and embryonic morphogenesis. These ethanol-exposed embryos also showed partial loss of imprinted DNA

methylation patterns for various imprinted genes critical for fetal growth, development, and brain function. Moreover, we observed alcohol-induced sex-specific errors in DNA methylation patterns with male-embryos showing increased vulnerability.

Modeling early pre-implantation alcohol exposure

One of the challenges when modeling FASD is unscrambling direct and indirect outcomes associated with the amount, pattern (continuous vs. binge drinking), and developmental timing of alcohol exposure (18, 19, 45, 57-63). By targeting pre-implantation embryo, we observed that a binge-like alcohol exposure on a single embryonic cell type (8-cell stage blastomeres) leads to increased rate of macroscopic defects (e.g., brain anomalies, growth restriction, heart defects) across litters, with no impact on litter size or on sex-specific phenotypic representation during fetal life. These findings corroborate with pioneer work that reported abnormal fetal development without significant reduction in litter size following exposure during pre-implantation (64, 65). However, the acute dosage regimen paradigms used in those studies resulted in a much higher rate (67% to 100%) of embryonic abnormalities and severe growth retardation, as well as fetal death (41, 66). Nevertheless, such studies along with others (67) confirm that even prior to direct maternal-fetal interface exchanges via the placenta, alcohol can reach the developing pre-implantation embryos through the female reproductive track. In vitro studies support that pre-implantation embryos are sensitive and negatively affected by alcohol exposure (68). Although less investigated and understood than maternal exposure, studies suggest that alterations (e.g., epigenetic errors) initiated on the fathers' sperm are passed-on during fertilization to pre-implantation embryos, influence development beyond implantation, and lead to abnormal offspring development (e.g., fetal growth restriction, birth defects, placental defects) (58, 69-72).

It remains to be defined whether some of the milder abnormalities or delays that we observed at mid-gestation would become resolved or accentuated by birth, and whether embryos that presented no visible abnormalities or developmental delays but had DNA methylation alterations would show cognitive dysfunctions as observed in other FASD-models and children with FASD. In parallel, outlining if the dysregulation in DNA methylation profiles is associated with abnormal migration and organization of specific brain cell subtypes during development would further extend our understanding about the effect of early pre-implantation alcohol exposure on the neurobiological phenotype in offspring.

Pre-implantation alcohol exposure leads to partial loss of imprinted DNA methylation

Our genome-wide, high-resolution analysis of ethanol-induced DNA methylation alterations highlighted partial loss of DNA methylation maintenance within various 100bp tiles located across imprinting control regions (e.g., *Gnas*, *Zrsr1, Impact*) in E10.5 male and female forebrains. Then again, methylation alterations were not necessarily widespread across entire imprinting control regions, or in all individual ethanol-exposed embryos, suggesting only a slight reduction in DNMT1/DNMT1o maintenance activity. Concordantly, some imprinted genes showed alterations in their expression profiles (e.g., *Gnas*, *Plagl1*, *Peg13*) in both male and female EtOH-exposed forebrains, whereases others (e.g., *Impact*, *Peg10*, *Grb10*) were not affected. We know that temporary lack of DNA methylation maintenance by DNMT1o in 8-cell embryos (E2.5) leads to delays in development and to a wide range of lethal anatomical abnormalities that are associated with epigenetically mosaic embryos that failed to properly maintain normal imprinted methylation patterns at mid-gestation (73-75). In zebrafish, alcohol exposure during the two first days of embryo development led to reduced levels of *Dnmt1* expression (76), which could ultimately lead to a temporary reduction in methylation maintenance activity. Studies aiming at defining how pre-implantation embryos respond to environmental stimuli (e.g., assisted reproductive technologies, toxicants, ethanol) have broadly explored the impact on imprinted genes, but have mainly relied on evaluating DNA methylation levels of imprinting control regions using targeted approaches (i.e., specific genomic loci) (41, 77, 78). Although informative, conclusions are often based on profiling DNA methylation levels of a limited number of CpG sites associated to a handful of genes. For instance, modeling binge alcohol exposure during two consecutive days (E1.5, E2.5) led to decreased fetal and placental weight by E10.5, but only to a partial loss of DNA methylation in the *H19* —a negative regulator of growth and proliferation— imprinting control region (only 17 CpG analysed) in the placenta. Although only a portion of one ICR was evaluated, these results insinuated that embryonic imprinted methylation was not affected by such early pre-implantation alcohol exposure.

Since imprinted genes are well recognized in regulating essential neurodevelopmental processes, including neural differentiation, migration and cell survival (79), we can presume that the forebrain of ethanol-exposed embryos with severe macroscopic defects and developmental delays would have broader loss of imprinted DNA methylation patterns compared to those with no visible abnormalities. However, the fact that morphologically normal forebrain tissues derived

from ethanol-exposed pre-implantation embryos reveal widespread low-level DNA methylation alterations with increased inter-individual variability in imprinted control regions supports that failure in maintaining accurate methylation imprints could contribute to the invisible nature of FASD.

Pre-implantation alcohol exposure initiates sex-specific DNA methylation programming errors

We demonstrated that exposing 8-cell embryos to alcohol is detrimental for future forebrain autosomal and X-chromosome DNA methylation patterns. Furthermore, such an early embryonic exposure leads to sex-specific DNA methylation alterations with male embryos being more susceptible to alterations. Early embryonic developmental stages are marked by a series of molecular events that are crucial for the proper establishment of the developmental program, as well as the *de novo* genome-wide DNA methylation signatures that are conserved throughout development (29, 80). A considerable amount of evidence shows that interfering with this process *in vivo* or *in vitro* leads to sex-specific long-term effects in the offspring (36, 72, 81-87). Although the mechanism remains unclear, we know that molecular events in early-stage embryos are marked with sex-specific discrepancies. For instance, mammalian pre-implantation embryos display differential expression of sex chromosome and autosomal transcripts, leading to extensive transcriptional sexual dimorphism (88, 89). In mouse, sex-biased gene expression (n=69; mainly X-linked) is detected as early as the 8-cell stage with substantial variation between individual embryos, and with female embryos expressing higher transcript levels. Then, just prior to the *de novo* re-methylation wave, the sex chromosomes seem to further drive this sexual dimorphism in transcriptional regulation for hundreds of autosomal genes, with *Dnmt3a* and *Dnmt3b* showing higher expression in male blastocyst (90). This is consistent with sex-specific acquisition of DNA methylation reported in bovine blastocyst, with males showing increased levels (89, 91). Thus, the alcohol-induced sex-specific DNA methylation alterations resulting from an early embryonic alcohol exposure model are mostly initiated at the 8-cell stage because of the male-female differences in transcriptional regulation. The DNA methylation alterations would then trigger a series of events that would negatively impact the re-establishment of genome-wide *de novo* DNA methylation profiles occurring between E3.5 and E6.5 in a sex-specific manner, with males being more affected. Once established, these abnormal *de novo* DNA methylation profiles would be maintained or would initiate further DNA methylation alterations during subsequent developmental stages. Since the sex-specific alterations observed in the forebrains are linked to

divergent biological pathways, this could lead to sex-specific neurocognitive impairments in offspring. Although such observations have been made in children with FASD, with males appearing to be more vulnerable to the irreversible effects of fetal alcohol exposure (e.g., cranial and facial malformations, learning disabilities, social and memory disabilities, and altered brain structure and function) (reviewed in (92)), further studies are needed to explore the long-term degree and impact of the sexual dimorphism in this pre-implantation alcohol exposure paradigm.

Pre-implantation alcohol exposure and impact on neurodevelopment

One common phenotype observed in human FASD and animal models of prenatal alcohol exposure is the interference of alcohol on the development of the central nervous system (structural or functional abnormalities). We observed DNA methylation alterations in promoters and bodies of genes implicated in brain and nervous system function and development (e.g., *Dlx2, Epha7*, *Foxa1, Nkx6, Vwc2*, *Sox6*). For example, *Dlx2* (Distal-Less Homeobox 2), is part of a transcription factor family (*Dlx1/2*; *Dlx3/4*; *Dlx5/6*) that is a critical molecular determinant for forebrain and craniofacial development, as well as for coordinating the timing of GABA(gamma-aminobutyric acid)ergic interneuron migration and process formation (93-96). *Dlx2 is* required to promote the expression of several downstream factors including other *Dlx* genes and *Arx* (directly activated by *Dlx2*) (56), an X-linked gene that also controls cortical interneuron migration and differentiation (97), which incidentally showed altered DNA methylation in female ethanol-exposed forebrains. Ethanol-exposed forebrains showed reduced methylation in *Dlx2* (gene body) and *Arx* (promoter), which correlated with reduced *Dlx2* and *Arx* expression, whereas the average expression of *Dlx5* and *Dlx6* (no DMRs) remained unchanged. Mice lacking *Dlx1/*2 have profound deficits in tangential migration of GABAergic cortical interneurons and neurite growth. Similarly, prenatal stress-induced anxiety in mouse leads to GABAergic interneuron deficiency-associated dysregulation of promoter DNA methylation levels of *Gad67* (glutamic acid decarboxylase 67), an enzyme critical for GABA synthesis (the principal inhibitory neurotransmitter). In prenatal alcohol exposure models targeting different brain developmental time points, the migration and positioning of GABAergic cortical interneurons are profoundly impaired, leading to subsequent cortical dysfunction (98-102). We know that cortical interneuron dysfunction, associated with impaired development, migration, or function of interneurons, results in interneuronopathies that contribute to multiple neurodevelopmental disorders including autism, epilepsy, schizophrenia, and FASD (103-105). We also know that GABAergic interneurons are particularly responsive to adverse

maternal exposures during in utero periods of developmental plasticity; from the moment these cells arise, to the shaping of cortical circuits (101, 105). Our data suggest that early embryonic alcohol exposure triggers alterations in the epigenome that leave lasting signals that could lead to pathological plasticity in the developing brain. We need to further define whether GABAergic interneurons, or other cortical neurons, are particularly vulnerable to early embryonic alcohol-induced epigenetic programming errors, and whether this could drive interneuronopathies or neurodevelopmental impairments associated with FASD.

Study Limitation

One limitation to our study is the absence of information about the dose-dependency of alcohol exposure with regards to the phenotypes and molecular consequences observed. Since higher peak blood alcohol concentrations have been shown to play a critical role in the extent of prenatal alcohol exposure-related damages (17, 18, 45, 48, 66, 86, 106), we can presume that similar observations would be observed using our paradigm. Nonetheless, the impact of low-dose and early prenatal alcohol exposure should not be overlooked, as they have been associated to increase the risk of mental illness regardless of a FAS or FASD diagnosis in human (review in (107)). To fully comprehend the wide range of detrimental consequences (visible and invisible) associated to dose-dependency of alcohol exposure during pre-implantation will require a thorough investigation across pre- and post-natal development.

CONCLUSION

We showed that pre-implantation alcohol exposure is detrimental for normal development and leads to a broad spectrum of adverse outcomes that closely replicate clinical facets observed in children with FASD. Specifically, we demonstrated that a binge-like drinking episode while pre-implantation embryos are in the mist of their reprogramming wave leads to two main categories of lasting programming errors: the partial loss of DNA methylation at several imprinted control regions, and the abnormal re-establishment of *de novo* DNA methylation profiles in key biological pathways (e.g., neural/brain development, tissue and embryonic morphogenesis). Further studies in peri-implantation embryos, when DNA methylation is globally reacquired, and in specific cell subtypes during key neocortex developmental time points will provide a better understanding of

the fundamental mechanisms leading to these DNA methylation programming errors and their implication in neurodevelopmental FASD-related deficits. Importantly, our data demonstrate that pre-implantation alcohol exposure does not lead to an "all-or-nothing" response, as morphologically normal embryos still presented conserved and sex-specific DNA methylation alterations in forebrain tissues, which could be indicative of the particular sexual dimorphism in cognitive dysfunctions associated with FASD. Thus, our study provides strong scientific evidence to refute the "all-or-nothing'' principle and supports the potential contribution of early embryonic epigenetic alterations to the manifestation of neurodevelopmental phenotypes observed in a portion of children with FASD.

METHODS

Pre-implantation embryo binge-like ethanol exposure model

Animal work was approved by the Comité Institutionnel de Bonnes Pratiques Animales en Recherche (CIBPAR) of the CHU Ste-Justine Research Center under the guidance of the Canadian Council on Animal Care (CCAC). Female C57BL/6 mice (8-week-old) were mated with same age C57BL/6 males (Charles River laboratories). Females that showed copulatory plugs the next morning were considered pregnant with day 0.5 embryos (E0.5). They were separated from the males and housed together in a 12h light/dark cycle with unlimited access to food and water.

Using a recognized prenatal binge-like alcohol exposure paradigm (41, 45, 66, 106), pregnant females (E2.5) were injected with 2 subsequent doses of 2.5g/kg ethanol 50% (ethanol-exposed group) or an equivalent volume of saline (control group) at 2 hours intervals. Female with the same treatment were housed together and had negligible handling during the gestation.

Blood alcohol concentration quantification

Blood alcohol concentration associated with our pre-implantation binge-like alcohol exposure paradigm was quantified over a 4h period. To avoid supplementary stress on experimental animals, a different subset of pregnant E2.5 females (n=12) was used for this experiment. Ethanol-exposed females (n=3) were euthanized at each time point (1, 2, 3 and 4h), blood was collected, samples were centrifuged to separate serum and plasma, and alcohol was quantified using the

EnzyChrome Ethanol Assay kit (BioAssays Systems/Cedarlane) following manufacturer's recommendations (1:5 plasma dilution).

Morphological analysis

At E10.5, pregnant females were euthanized, and embryos were collected and dissected for morphological evaluation using Leica stereo microscope. Using LasX software, measurements of the crown-rump length (top of the head to the end of the tail), occipital to nose length (occipital part of the head to the nasal process), height of the head (top of the head to the beginning of the torso) and length of the midbrain (occipital part to the midbrain/forebrain limit) were done. Similarly, morphological defects (e.g., severe developmental delay or growth restriction, brain or head malformation, heart anomaly or any other unexpected feature) were evaluated (108-110). Three embryos (n=3) revealed more than 2 morphological defects and were placed in the category of their main defect (delayed n=2, brain malformation n=1). Embryos that hatched (Ctrl n= 23; EtOH n=21) from the yolk sac during dissection were excluded of both measurements and morphological analyses due to the possible deformation induced by the pressure on the embryo during the expulsion. The sex of each embryo was determined by qPCR using expression of *Ddx3,* on yolk sac DNA. Statistical analyses were done using GraphPad prism (version 8.4.3) for t-test with Welch correction and f-test for variance or R (version 3.5.0) for chi-square and proportional z-test.

Histological analysis and immunostaining

Following collection, whole E10.5 embryos were fixed in 4% paraformaldehyde (PFA), post-fixed in EtOH 70% for 48h and paraffin embedded (111). Whole embryos were sectioned at 5µM and corresponding sections were stained with hematoxylin and eosin (112) to determine gross morphology, or for Cleaved Caspase-3 (Cell Signaling #9579S) or Ki67 (Abcam # AB15580) following manufacturer's protocol and counterstained with hematoxylin. Imaging was done using Zeiss Zen Axioscan Slide Scanner system . Images processing and quantification were performed using ImageJ. Three similar sub regions of forebrain and midbrain (0.02mm^2 each) were quantified across all samples. Statistical analyses were done using GraphPad prism (version 8.4.3) for t-test with Welch correction.

DNA extraction and Reduced Representation Bisulfite Sequencing

Following morphological analyses, embryonic E10.5 forebrains were isolated, flash frozen and kept at -80°C. Genomic DNA was extracted from forebrains using the QIAamp DNA Micro kit (Qiagen #56304) following manufacturer's recommendations. Extracted DNA was quantified using QuBit fluorimeter apparel with the Broad range DNA assay kit (ThermoFisher #Q32853). The sex of each DNA sample was again validated by *Ddx3* qPCR. DNA samples from forebrains with no apparent morphological defects were randomly selected, using 6 control embryos (3 males and 3 females, from 3 different litters) and 16 ethanol-exposed embryos (8 males and 8 females, from 6 different litters). EtOH-exposed and control embryo groups were similar in size and morphology (**Fig. S2**). Genomic DNA was used to produce rapid Reduced Representation Bisulfite Sequencing (rRRBS) libraries as previously described (27, 113-116). Briefly, 500ng of DNA was digested with *Msp1* restriction enzyme, adapters were attached to DNA fragments followed by sodium bisulfite conversion and amplification/indexation of libraries. Libraries were quantified using QuBit fluorimeter apparel with the High Sensitivity DNA assay kit (ThermoFisher #Q32854). Quality control was assessed using BioAnalyzer and paired-end sequencing was done on Illumina HiSeq 2500 at the Genome Québec core facility. We obtained between 19M and 41M raw reads for each sample (**Table S1**).

Bioinformatics analysis

Data processing, alignment (mm10 genome) and methylation calls were performed using our established pipeline (27, 114-116) which includes tools such as Trim Galore (version 0.3.3) (117), BSMAP (version 2.90) (118) and R (version 3.5.0) (**Table S1**). Differentially methylated regions were obtained with MethylKit (version 1.8.1) (119) using the Benjamini-Hochberg false discovery rate (FDR) procedure. Fixed parameters were used, including 100bp stepwise tiling windows, a minimum of 2 CpGs per tile and a threshold of $q<0.01$. DNA methylation level is calculated as the average methylation of all CpGs within a tile for all the samples within a condition (**Fig. 3**: minimum 5 samples/condition, ≥10x sequencing depth; **Fig. 4-6** & **Fig. S6-S7**: minimum 3 samples/condition/sex, ≥10x sequencing depth). The number of CpGs per tile and bisulfite conversion rate (>97%) were obtained using a custom Perl script.

Annotation of the analysed tiles was done using Homer (version 4.10.1) with mm10 reference genome. Gene ontology enrichment analysis was performed with Metascape (120) online

tool using only differentially methylated tiles located in genic regions. Repeats and CpG islands coordinates were obtained from UCSC table browser databases (mm10 genome). CpG context tracks (CpG shores and CpG shelves) were built by adding up respectively 0-2kb and 2-4kb from the CpG islands coordinates as previously describes (114, 121).

RNA extraction and expression analysis by quantitative PCR (qPCR)

Quantitative gene expression analyses were performed as previously (122, 123). Briefly, embryonic E10.5 forebrains were isolated, flash frozen and kept at -80°C until RNA extraction. RNA was extracted using RNeasy Mini kit (Qiagen #74004) following manufacturer's recommendations. Extracted RNA was quantified using QuBit fluorimeter apparel with the High Sensitivity RNA assay kit (ThermoFisher #Q32852). 600ng of RNA was used for cDNA conversion using SuperScript IV Reverse Transcriptase (ThermoFisher #18090010). For each gene (primer sequence **Table S2**), qPCR reactions were performed in triplicate on 5ng of cDNA using SensiFAST SYBR No-ROX (Bioline #BIO-98005) on a LightCycler 96 (Roche Life Science). Gene expression analysis and normalization was done using the $2^{-\Delta\Delta Ct}$ method using *Hprt1* and *Pgk1* as reference genes. Statistical analyses were done using GraphPad prism (version 8.4.3) for t-test with Welch correction.

Figures and legends

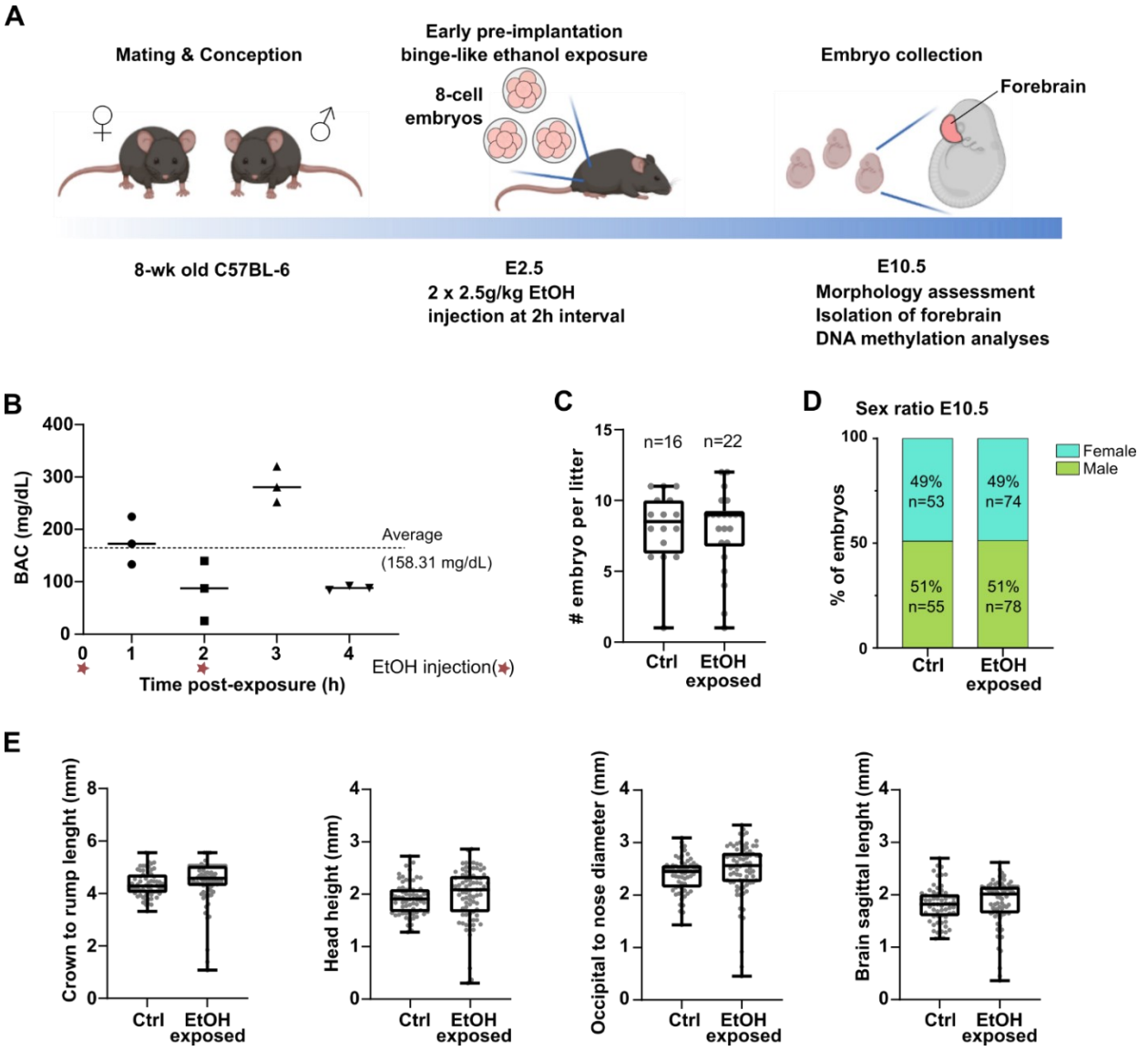

Figure 1. Early pre-implantation alcohol exposure affects mouse embryonic development at mid-gestation. A) Schematic description of binge alcohol exposure model during pre-implantation embryo development, and analyses performed at mid-gestation. Pregnant females were exposed to EtOH (2x 2.5g/kg EtOH) or Saline (Ctrl) (equivalent volume to ethanol) by subcutaneous injections (2h interval) to precisely target E2.5 stage embryos (~8-cell stage). E10.5 embryos were collected for morphological assessment; forebrain was isolated for genome-wide DNA methylation analyses. **B)** Quantification of blood alcohol concentration in pregnant females following EtOH exposure at E2.5. Red stars indicate the two EtOH injection time points. Peak level (284mg/dL) was observed at 3h post-exposure, with an average of 158.31 mg/dL over 4hrs. **C)** Number of E10.5 embryos per litter in Ctrl (n=16 litters; average 8.13 embryos/litter) and EtOH-exposed (n=22 litters; average

7.91 embryos/litter). **D)** Male and female embryo sex ratios of litters presented in panel C), with number of embryos shown in bar graph. **E)** Embryonic (E10.5) measurements: crown-rump length, head height, occipital-nose length and brain sagittal length. Control embryos: (n=63, 8 litters), ethanol-exposed embryos (n=76, 11 litters). No significant difference of the means; t-test with Welch's correction, but higher variance in EtOH-exposed; F-test.

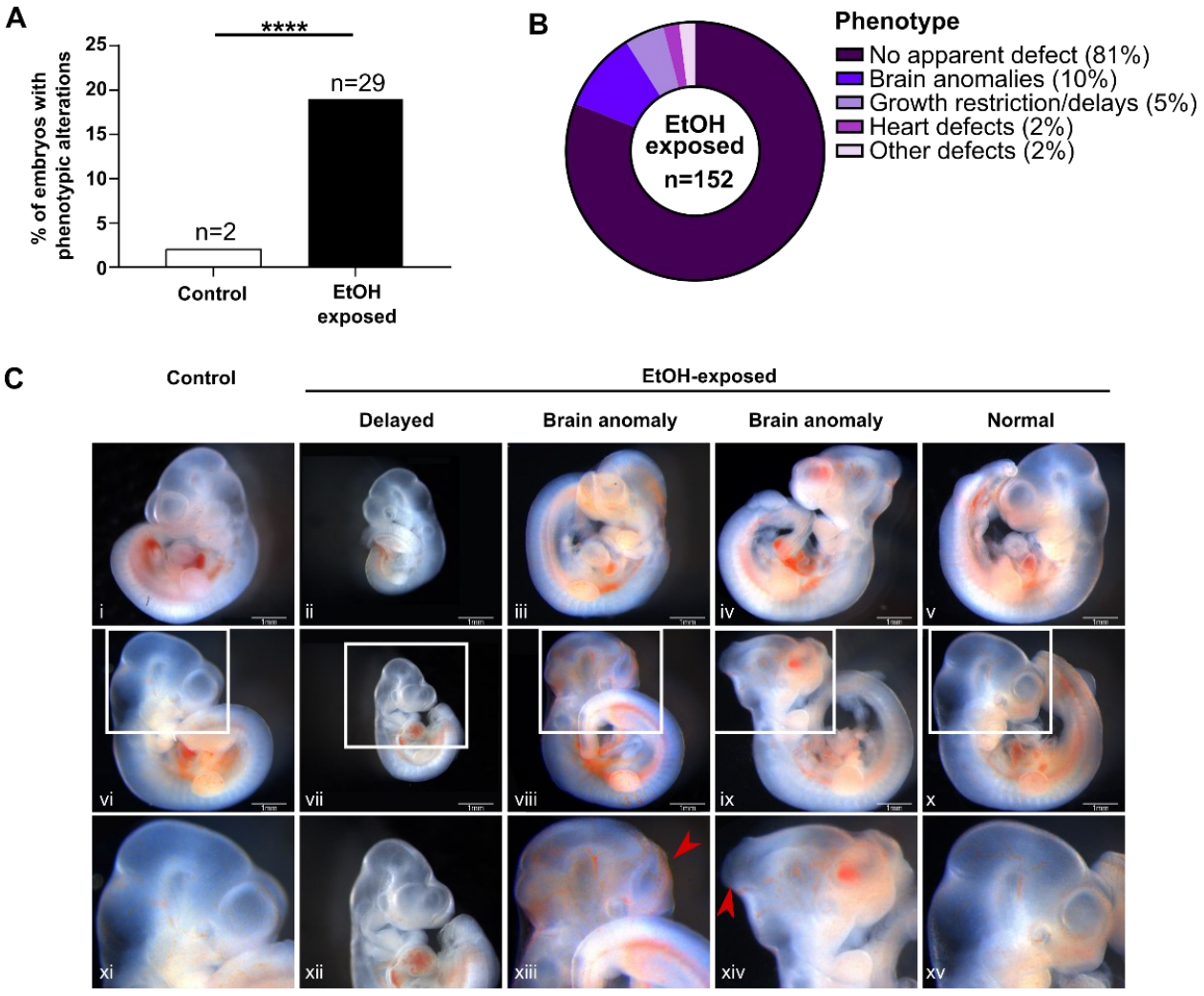

D

	Ctrl	EtOH exposed	x^2 value	p-value
Embryos with phenotypic alterations	2/108	29/152	17.84	<0.0001
Mothers with at least one altered embryo	2/16	16/22	13.48	<0.001

Figure 2. Increased phenotypic alterations in developing embryos following early pre-implantation alcohol exposure. **A)** Percentage of E10.5 embryos with phenotypic alterations (Ctrl: 2%; n=2/108, EtOH-exposed: 19%; n=29/152, ****p<0.0001; chi-square test). **B**) Classification and proportion of phenotypic alterations observed in EtOH-exposed embryos. **C)** Examples of primary phenotypic alterations observed in EtOH-exposed embryos. Views from both side of the embryo and zoom on the head for control (i, vi, xi) and EtOH-exposed embryos with severe developmental delays (ii, vii, xii), brain malformations (iii, viii, xiii, iv, ix, xiv) and no apparent defects (v, x, xv). **D)** Number of embryos with alterations and number of litters with at least one affected embryo. ***p<0.001; chi-square test.

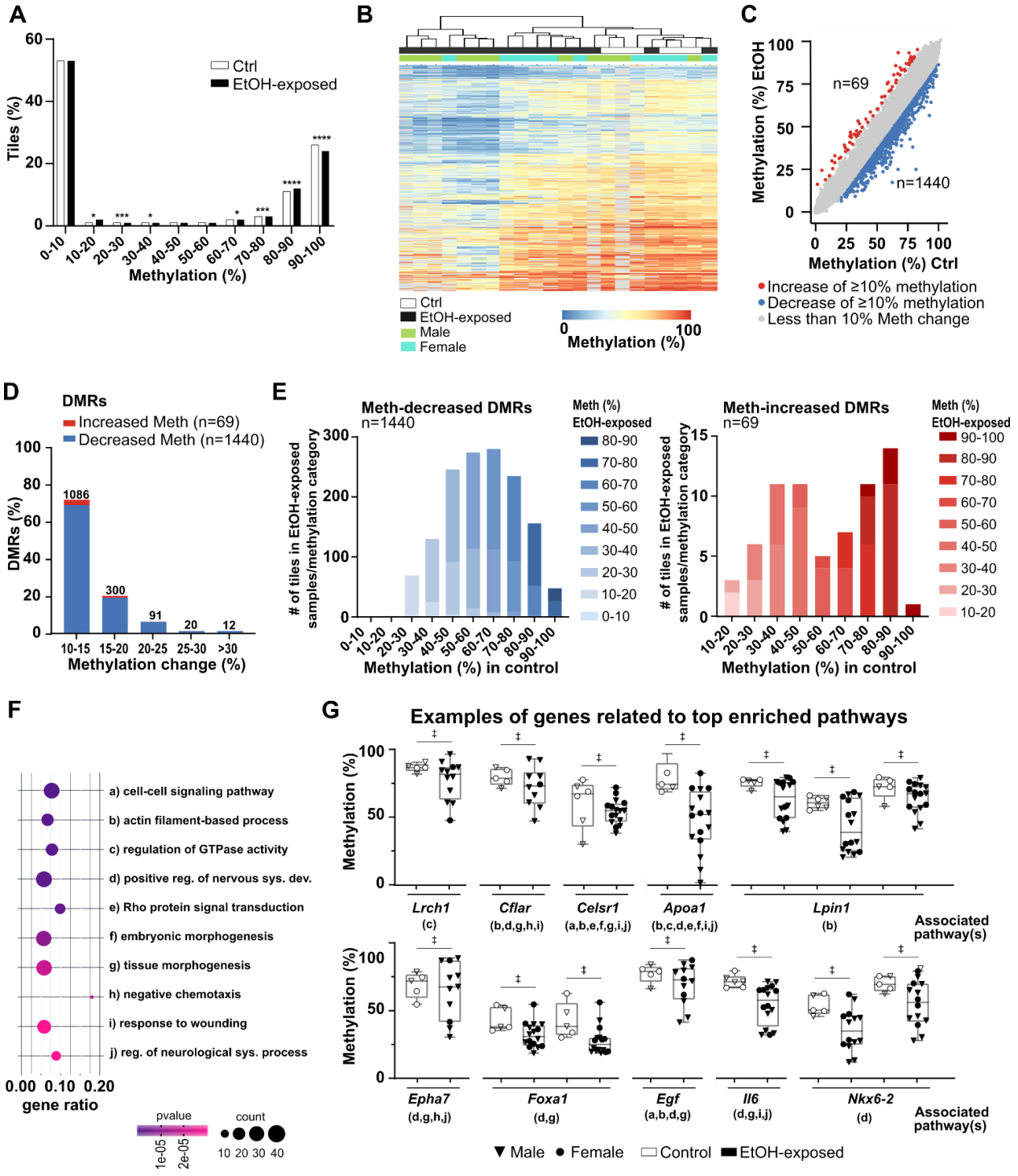

Figure 3. **Early pre-implantation alcohol exposure triggers DNA methylation alterations in developing embryonic forebrain.** Genome-wide CpG methylation analyses of E10.5 control (n=6) and ethanol-exposed (n=16) forebrains. **A)** Distribution of genomic tiles (100bp) (all-tiles; n=114 911) across ranges of CpG methylation levels in control and EtOH-exposed samples.

****p<0.0001, ***p<0.001, *p<0.05; z-test proportion test. **B)** Heatmap showing CpG methylation levels for the top1% most variable tiles (n=1 200) between control and EtOH-exposed forebrains. Gray lines in heatmap have no associated methylation values because of lack of sufficient sequencing coverage in sample. **C)** Scatterplot representing the differentially methylated regions (DMRs) between control and EtOH-exposed forebrains (see methods section for details). Red dots represent the tiles with a methylation increase of at least 10% in EtOH-exposed compared to control forebrains (n=69); blue dots represent the tiles with a methylation decrease of at least 10% in EtOH-exposed compared to control forebrains (n=1 440); grey dots represent the tiles with changes less than 10% in EtOH-exposed compared to control forebrains (n=113 402). **D)** Proportion of DMRs associated with the changes of CpG methylation levels between control and EtOH-exposed E10.5 forebrains. **E)** Comparison of CpG methylation levels of specific DMRs-associated tiles in EtOH-exposed versus control forebrains. Blue bar graph represents the comparison for decreased-methylation DMRs (n=1 440); red bar graph represents comparison for the increased-methylation DMRs (n=69). **F)** Functional enrichment analysis showing top 10 enriched pathways for decreased- and increased-methylation DMRs located in genic regions (n=710 unique gene DMRs), based on Metascape analysis for pathways and p-value. The size of the dot represents the number of DMR-associated genes in a pathway, and gene ratio represents the number of DMR-associated genes with regards to the number of genes in a pathway. **G)** Examples of CpG methylation levels of individual samples for DMR-associated genes related to the top enriched pathways. Letters under gene name relate to the pathways in F). ǂ represents significant differences in CpG methylation levels of DMRs (e.g., ±>10% methylation difference, q<0.01) between control and EtOH-exposed embryos (see methods section for details).

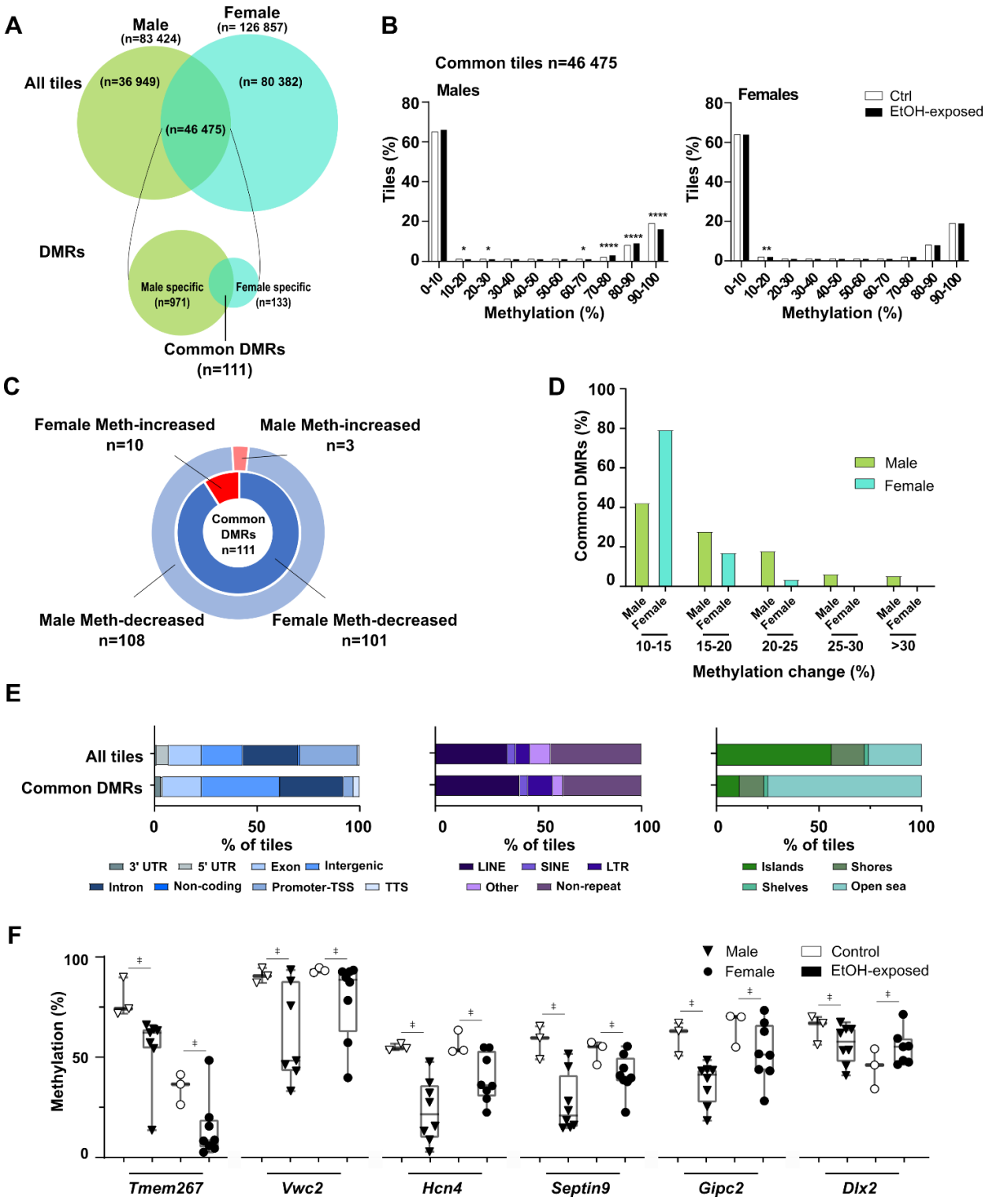

Figure 4. Sex-related changes in embryonic forebrain DNA methylation mediated by early pre-implantation ethanol exposure. A) Schematic design of sex-related genome-wide CpG methylation analysis in male (Ctrl n=3, EtOH n=8) and female (Ctrl n=3, EtOH n=8) E10.5

forebrain samples. Identification of all-tiles associated with either male samples (n=83 424), female samples (n=126 857), male-female common samples (n=46 475), as well as male-specific (n=971), female-specific (n=133) and common (n=144) DMRs (see methods section for details). **B)** Distribution of genomic tiles (100bp) (common tiles; n=46 475) across ranges (10%) of CpG methylation in male and female control and EtOH-exposed samples. ****p<0.0001, **p<0.01, *p<0.05; z-test proportion test. **C)** Distribution of common DMRs (n=111) with increased or decreased CpG methylation in male (outer circle) and female (inner circle) samples. **D)** Proportion of common DMRs associated with the changes of CpG methylation levels between control and EtOH-exposed in male and female forebrains. **E)** Percentage of tiles associated with various genomic features: genomic annotation (left), repeat elements (middle) and CpG-rich context (right) in common all-tiles (n=46 475) and common DMRs (n=111). **F)** Examples of CpG methylation levels of individual samples of common DMRs in male and female samples. ǂ represents significant differences in CpG methylation levels of DMRs (e.g., ±>10% methylation difference, q<0.01) between control and EtOH-exposed embryos (see methods section for details).

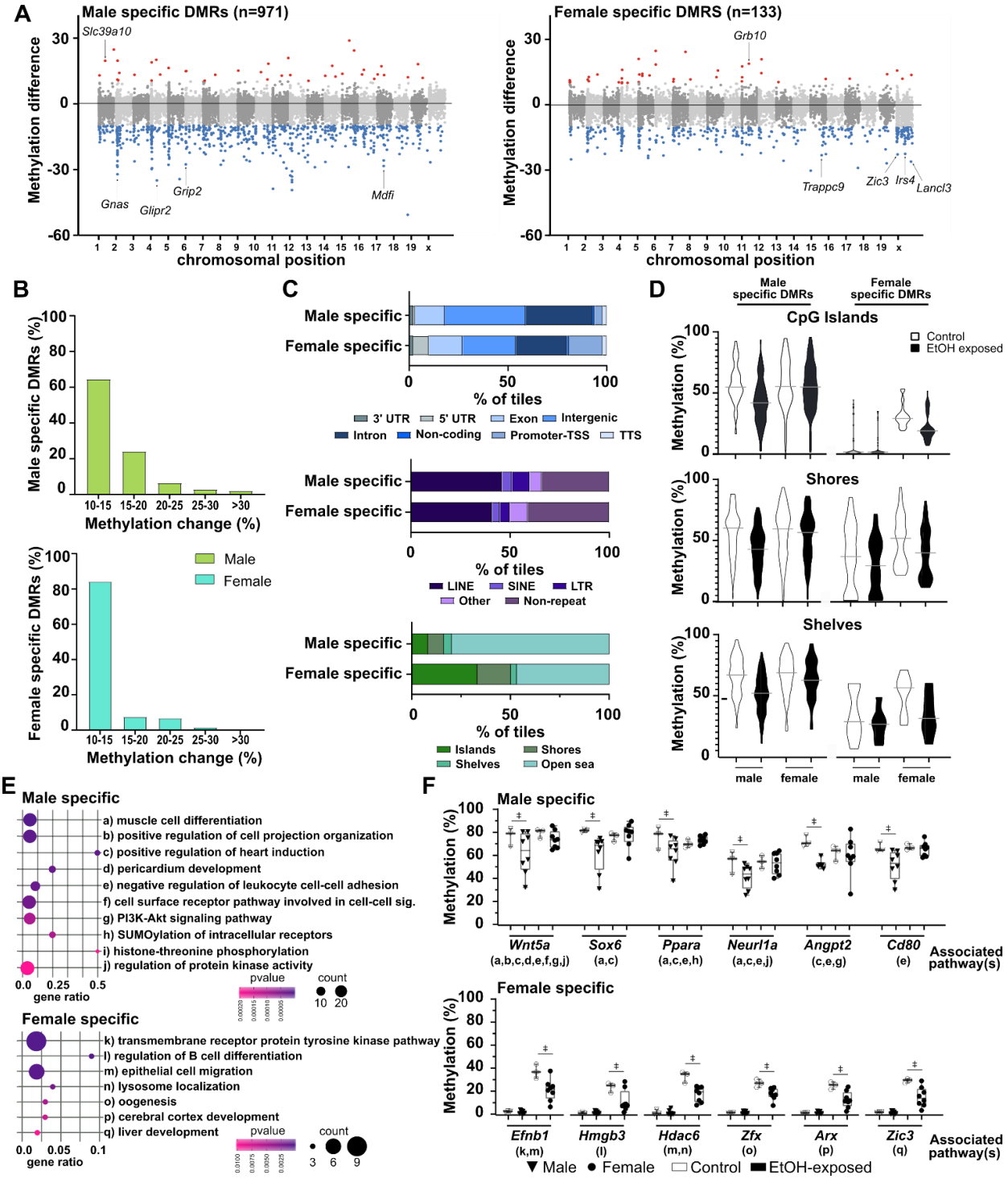

Figure 5. Early pre-implantation ethanol exposure induces sex-specific DNA methylation alterations in developing embryonic forebrain. Identification of male and female sex-specific DMRs in ethanol-exposed E10.5 forebrains is described in Fig.4A. **A)** Manhattan plot showing differences of CpG methylation by chromosomal position for male-specific (n=971; left graph) and

female-specific (n=133; right graph) DMRs. Red dots represent DMRs with increased-methylation in EtOH-exposed forebrains (n=31; right graph and n=30; left graph); blue dots represent DMRs with decreased methylation in EtOH-exposed forebrains (n=940; right graph and n=103; left graph); grey dots represent tiles with less than 10% methylation differences between EtOH-exposed and control forebrains (n=45 504; right graph and n=46 342; left graph). **B)** Proportion of sex-specific DMRs (upper graph; male n=971, lower graph; female n=133) associated with changes in CpG methylation levels between control and EtOH-exposed E10.5 forebrains. **C)** Percentage of sex-specific DMR-associated tiles (male n=971, female n=133) across various genomic features: genomic annotation (top), repeat elements (middle) and CpG-rich context (bottom). **D)** Percentage of CpG methylation levels of male- and female-specific DMRs based on the distribution of CpG sites in CpG islands, CpG shores and CpG shelves. **E)** Functional enrichment analysis showing top enriched pathways for male- (top 10 pathways, n=508 unique gene DMRs) and female-specific DMRs (n=87 unique gene DMRs), based on Metascape analysis for pathways and p-value. The size of the dot represents the number of DMR-associated genes in pathways, and gene ratio represents the number of DMR-associated genes with regards to the number of genes in a pathway. **F)** Examples of CpG methylation levels of individual samples for sex-specific DMR-associated genes related to the top enriched pathways in E). Letters under gene name relate to the pathways in E). ǂ represents significant differences in CpG methylation levels of DMRs (e.g., ±>10% methylation difference, $q<0.01$) between control and EtOH-exposed embryos (see methods section for details).

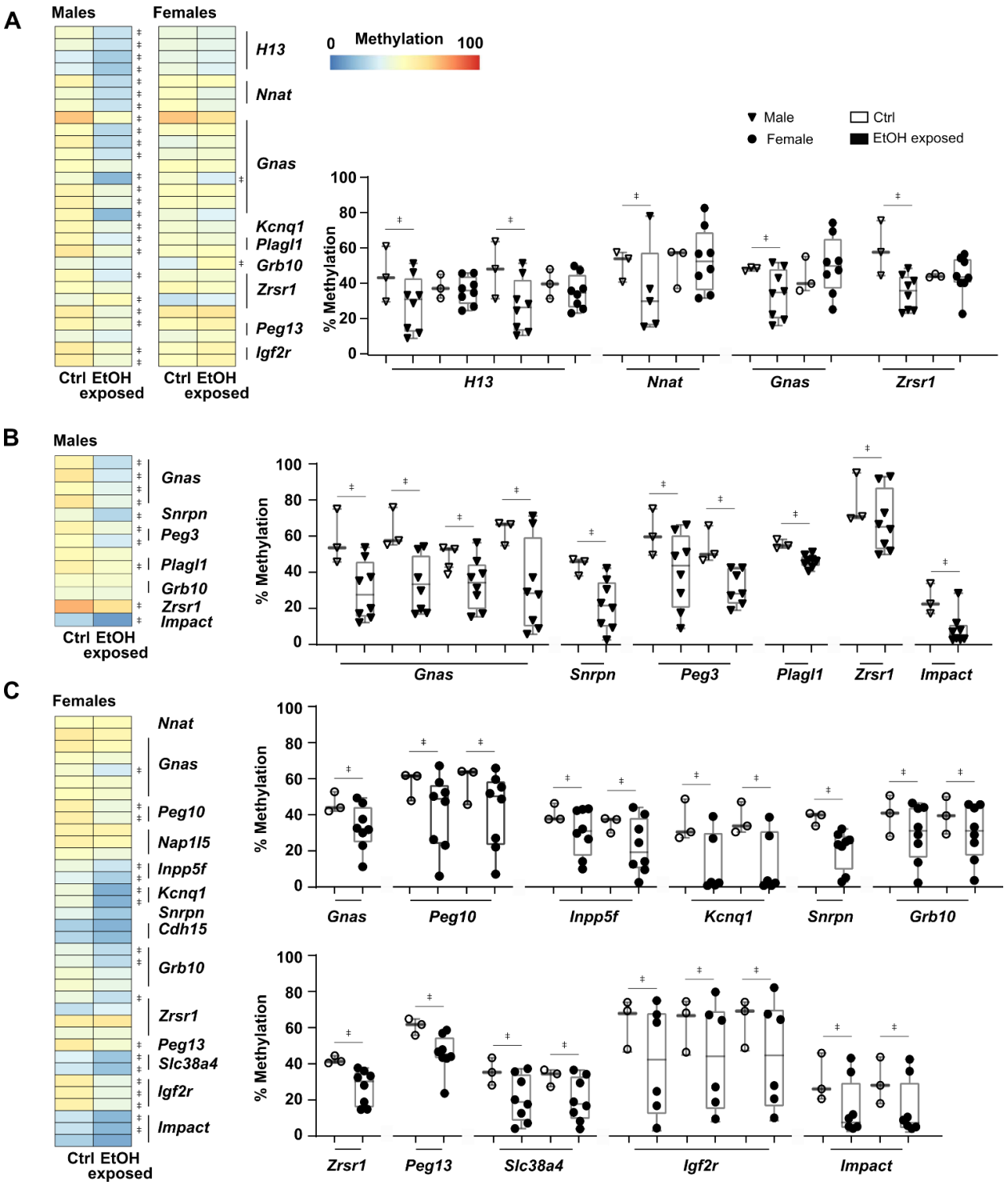

Figure 6. **Early pre-implantation ethanol exposure leads to partial loss of DNA methylation maintenance across imprinting control regions. A-C)** Heatmaps representing CpG methylation levels for control versus EtOH-exposed samples in regions (100bp tiles) located within defined imprinting control regions. Examples of CpG methylation levels of individual samples in

imprinting control regions associated tiles are shown. ǂ represents significant differences in CpG methylation levels of DMRs (e.g., ±>10% methylation difference, q<0.01) between control and EtOH-exposed embryos (see methods section for details). **A)** Imprinting control regions (n=28 tiles) analyzed (sufficient sequencing coverage) in both male and female samples (control vs EtOH-exposed). **B)** Imprinting control regions (n=13 tiles) analyzed only in males (lack of proper sequencing coverage in females). **C)** Imprinting control regions (n=36 tiles) analyzed only in females (lack of proper sequencing coverage in males).

Supplemental Figures

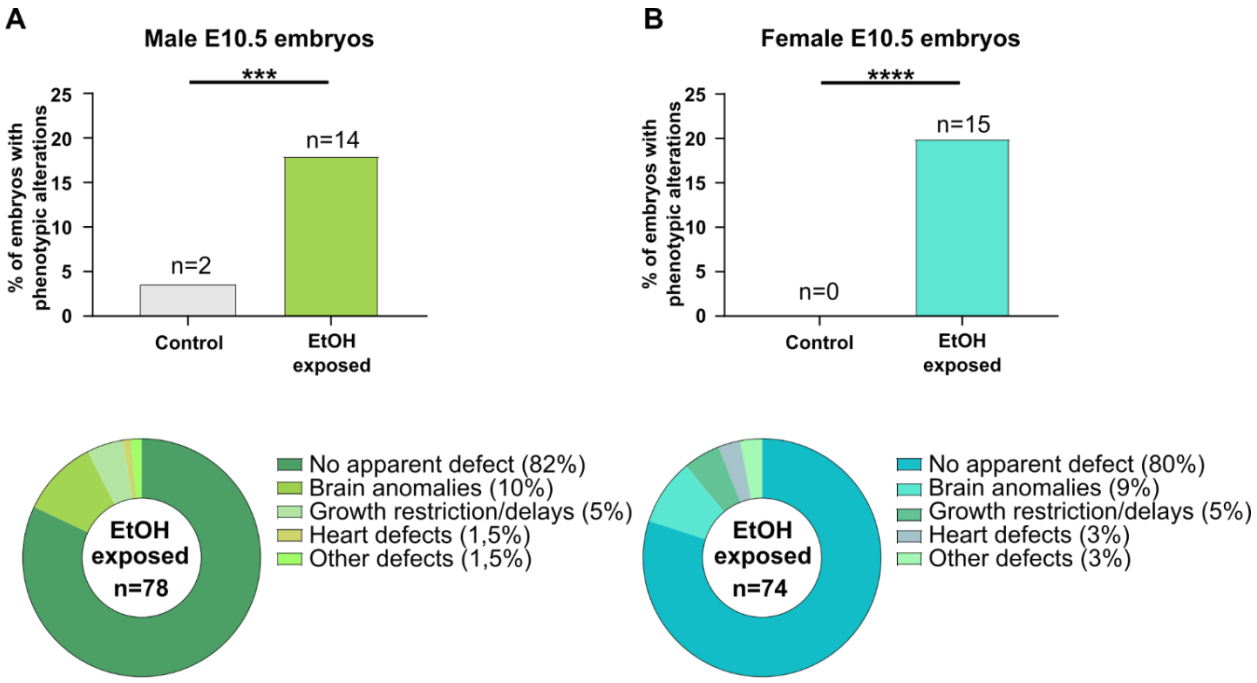

	Ctrl	EtOH exposed	x^2 value	p-value
Embryos with phenotypic alterations	2/55	14/78	13.73	<0.001
Mothers with at least one altered embryo	2/16	10/22	4.66	<0.01

	Ctrl	EtOH exposed	x^2 value	p-value
Embryos with phenotypic alterations	0/53	15/74	12.61	<0.001
Mothers with at least one altered embryo	0/16	13/22	6.17	<0.01

Figure S1. No difference in phenotypic alterations between male and female developing embryos following early pre-implantation alcohol exposure. **A)** Percentage of E10.5 male embryos with phenotypic alterations (Ctrl: 4%; n=2/55, EtOH-exposed: 18%; n=14/78, ***p<0.001; chi-square test) (upper graph). Classification and proportion of phenotypic alterations observed in EtOH-exposed male embryos (middle graph). Number of male embryos with alterations, and number of litters with at least one affected embryo. **p<0.01; chi-square test (lower table). **B**) Percentage of E10.5 female embryos with phenotypic alterations (Ctrl: 0%; n=0/53, EtOH-exposed: 20%; n=15/75, ***p<0.001; chi-square test) (upper graph). Classification and proportion of phenotypic alterations observed in EtOH-exposed female embryos (middle graph). Number of female embryos with alterations, and number of litters with at least one affected embryo. *p<0.05; chi-square test (lower table).

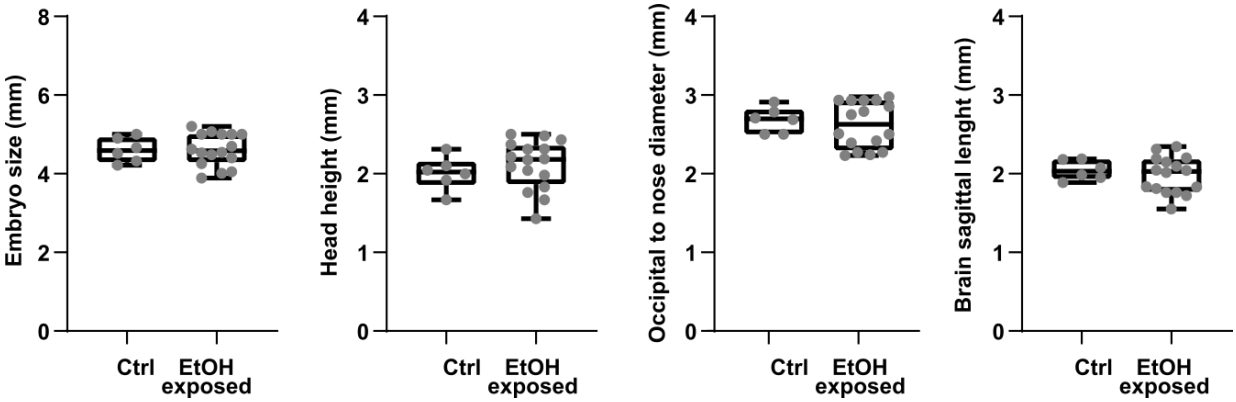

Figure S2. Embryonic measurements of E10.5 embryos used to perform Rapid Reduced Representation Bisulfite Sequencing (rRRBS) on forebrains. Crown-rump length, head height, occipital-nose length and brain sagittal length. Control embryos: (n=6, 3 litters), EtOH-exposed embryos (n=16, 6 litters). No significant difference; t-test with Welch's correction.

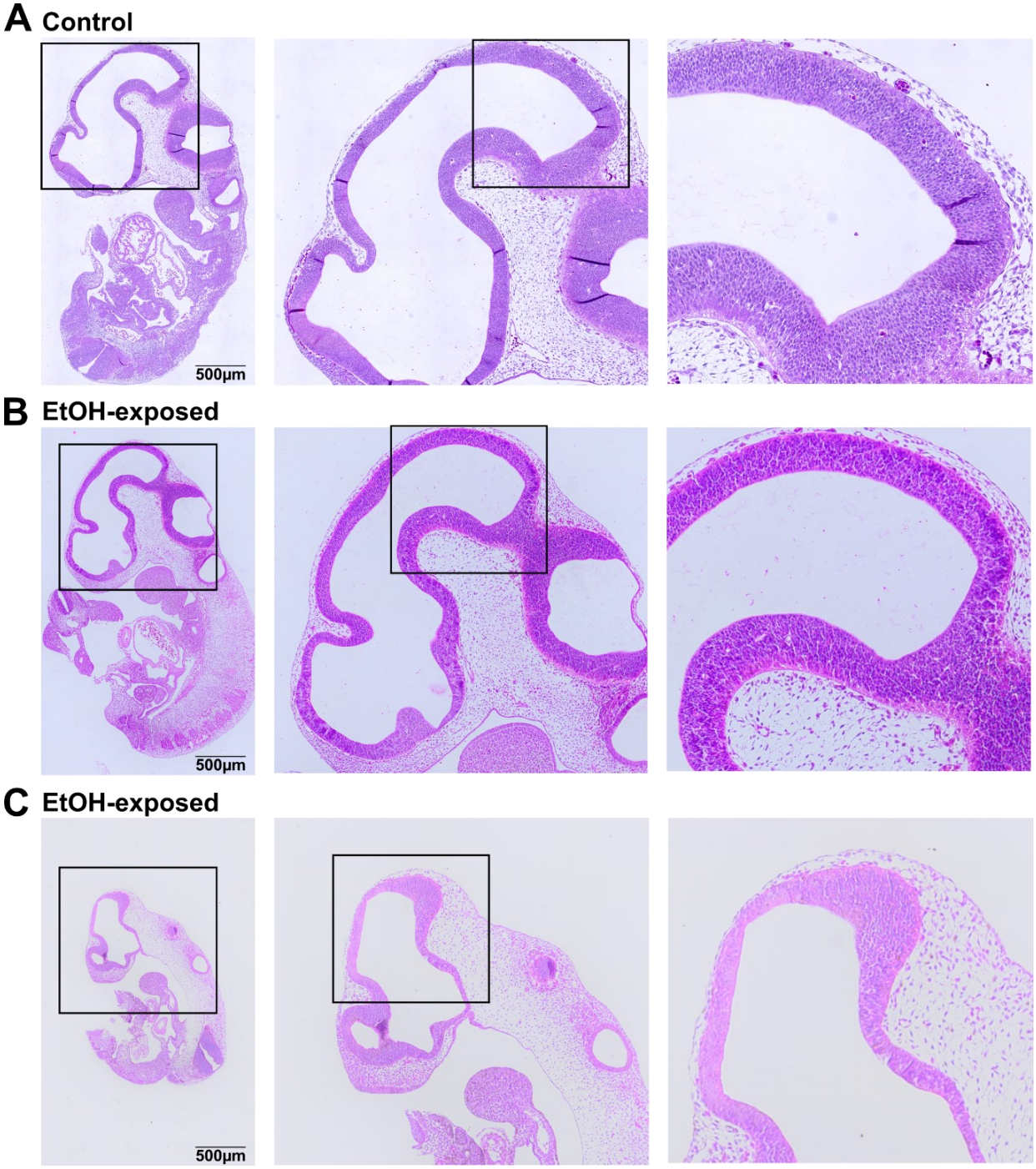

Figure S3. Early pre-implantation alcohol exposure does not alter overall brain cell structural organization in mid-gestation embryos. Hematoxylin and eosin (H&E) staining in control and ethanol-exposed E10.5 embryos (Male: ctrl n= 9, EtOH-exposed n=11; Female: ctrl n= 9, EtOH-exposed n=11). Representative images of H&E-stained sections of (A) control and (B, C) ethanol-exposed embryos, with focus on head area and sub-section of brain. A) Control male

embryo. B) Male ethanol-exposed embryo without any morphological defect observed during dissection. C) Female ethanol-exposed embryo with a delayed development.

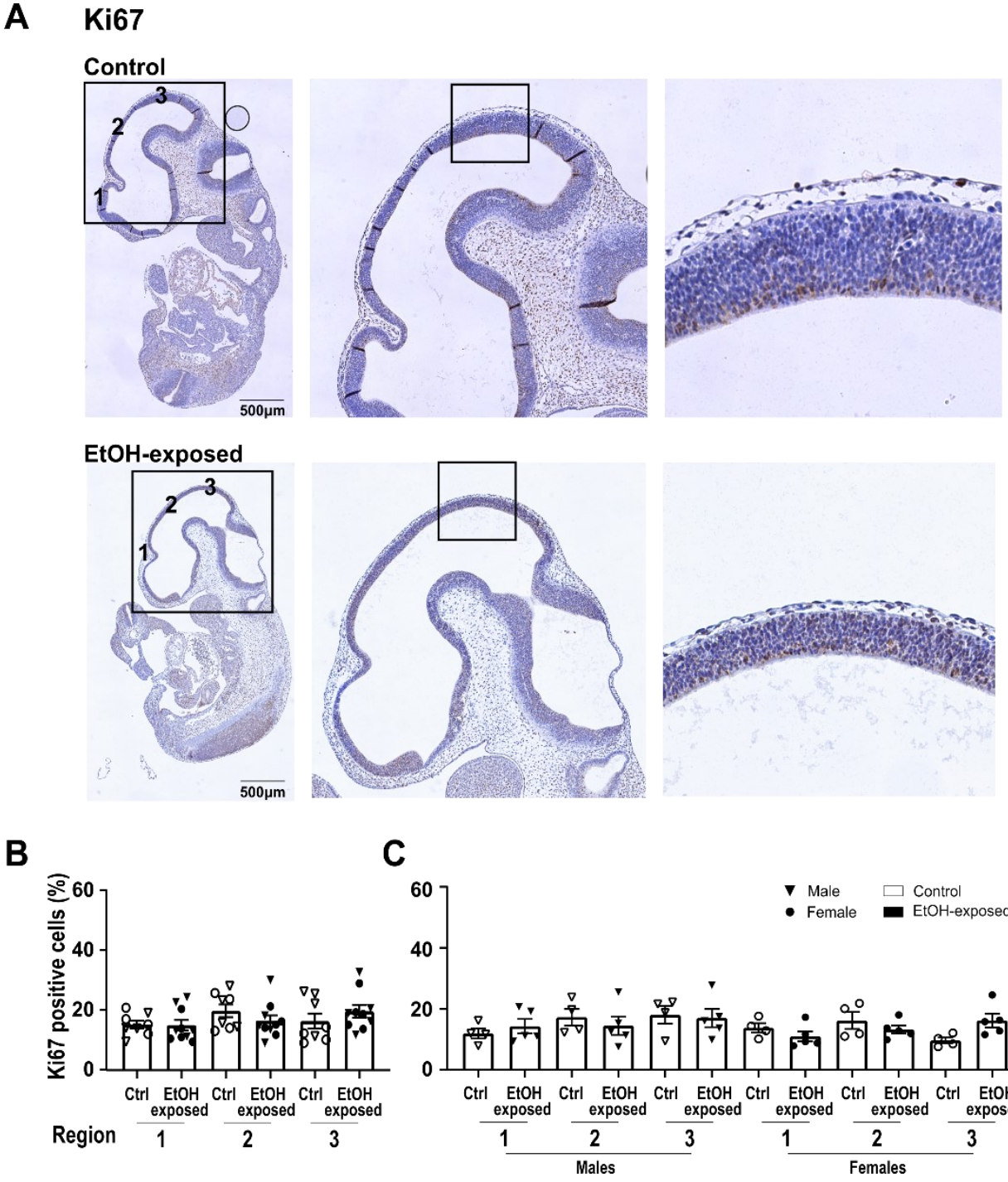

Figure S4. Early pre-implantation alcohol exposure does not modify brain cell proliferative state in mid-gestation embryos. Immunohistochemical staining for Ki67 (brown) and counterstaining with hematoxylin (blue) in control and ethanol-exposed embryos. A) Representative distribution of Ki67 positive cells in sagittal sections of E10.5 embryos. Left panel shows the three brain regions used to quantify Ki67 positive cells. Details of framed areas are

shown in middle and right panels. B) Percentage (%) of Ki67 positive cells across brain regions in control and ethanol-exposed (no apparent morphological defects) embryos (males and females). Bars represent mean ± SEM. C) Sex-specific quantification of Ki67 positive cells. Data from B) separated in male and female samples; male (Ctrl n= 4, EtOH-exposed n=5), female (Ctrl n= 4, EtOH-exposed n=5). Bars represent mean ± SEM.

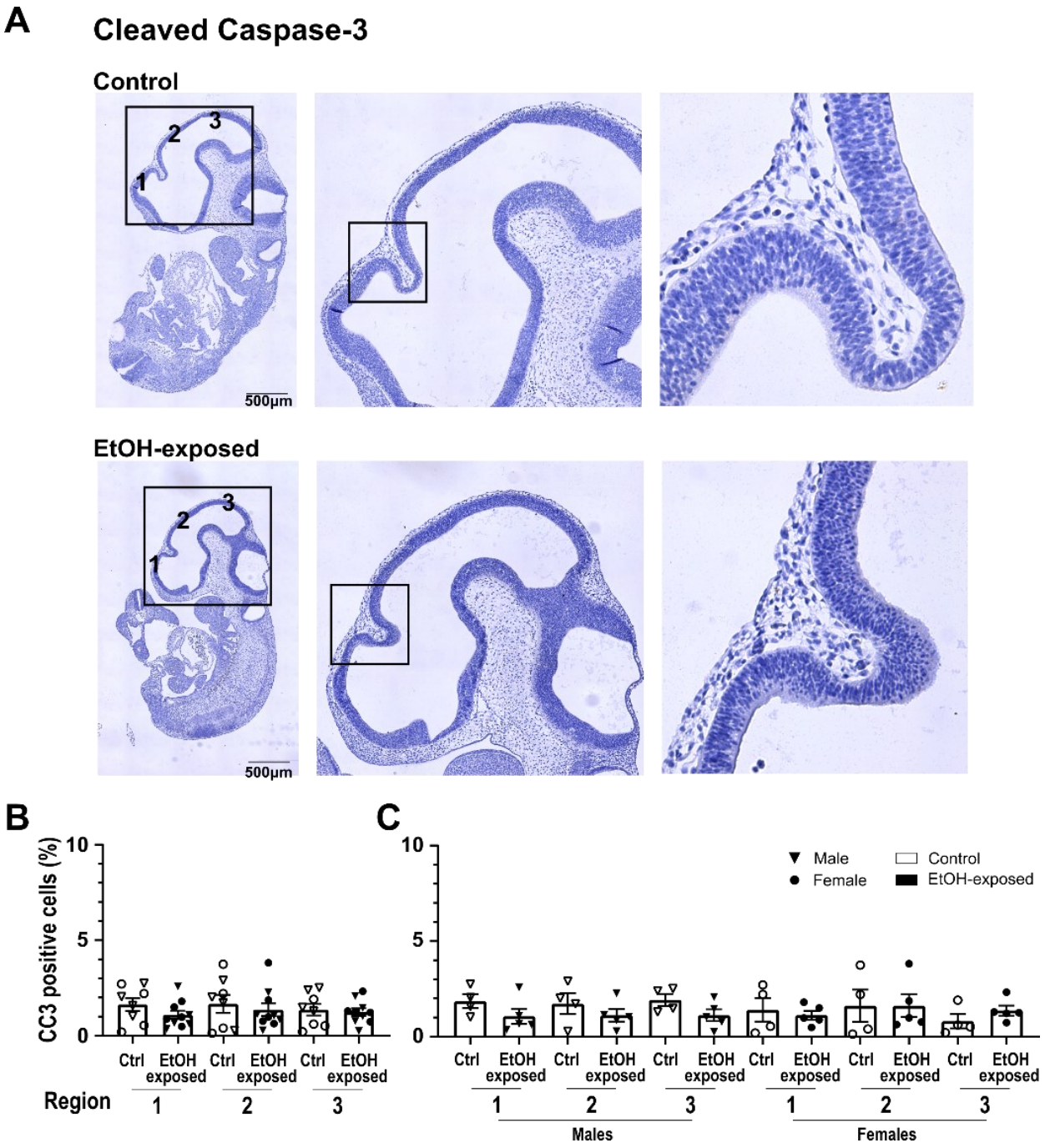

Figure S5. Early pre-implantation alcohol exposure does not increase brain cell apoptosis in mid-gestation embryos. Immunohistochemical staining for cleaved Caspase-3 (brown) and counterstaining with hematoxylin (blue) in control and ethanol-exposed embryos. A) Representative distribution of cleaved Caspase-3 (CC3) positive cells in sagittal sections of E10.5 embryos. Left panel shows the three brain regions used to quantify cleaved Caspase-3 positive cells. Details of framed areas are shown in middle and right panels. B) Percentage (%) of cleaved

Caspase-3 positive cells across brain regions in control and ethanol-exposed (no apparent morphological defects) embryo (males and females). Bars represent mean ± SEM. C) Sex-specific quantification of cleaved Caspase-3 positive cells. Data from B) separated in male and female samples; male (Ctrl n= 4, EtOH-exposed n=5), female (Ctrl n= 4, EtOH-exposed n=5). Bars represent mean ± SEM.

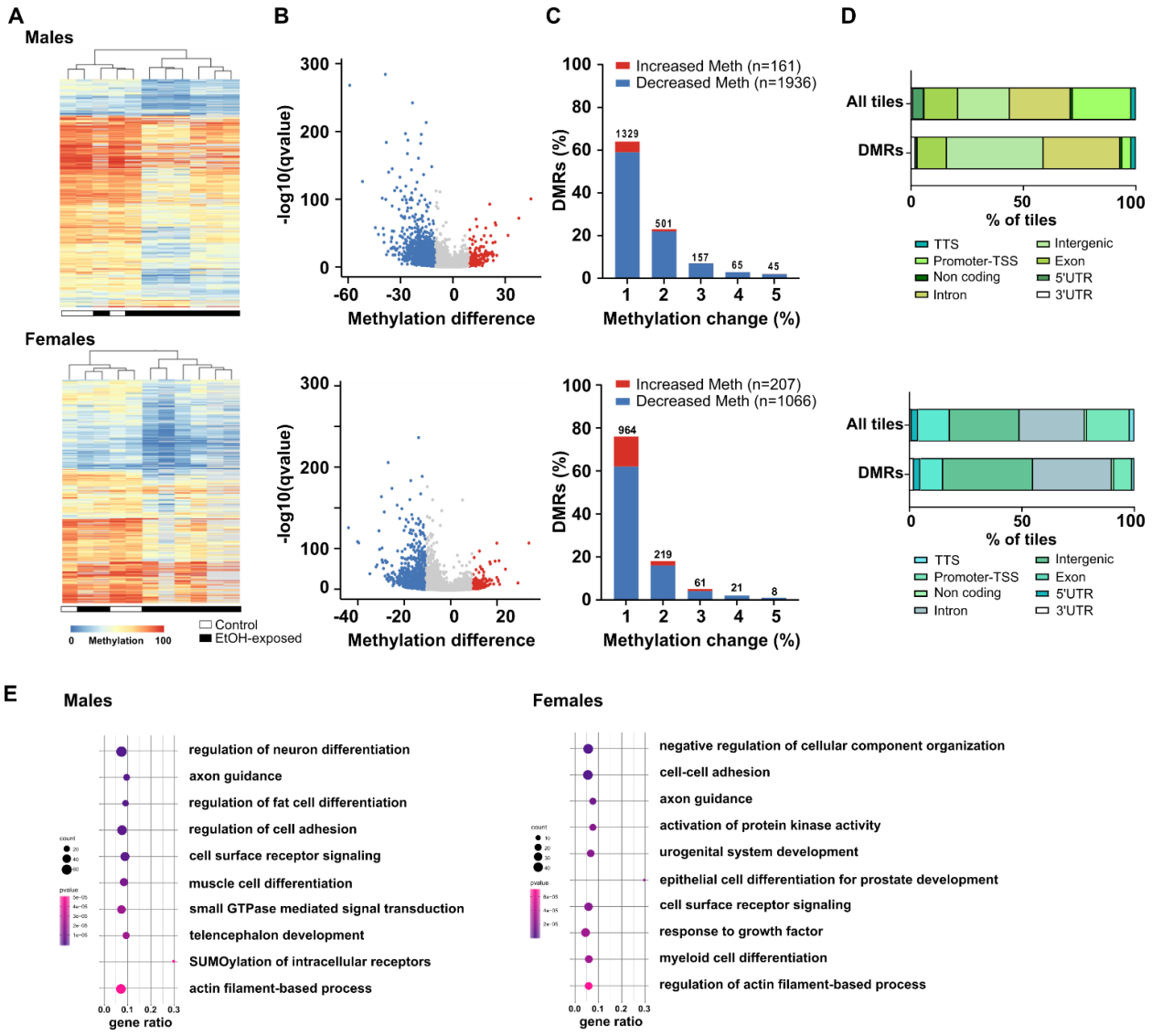

Figure S6. Early pre-implantation alcohol exposure triggers DNA methylation alterations in developing embryonic forebrain of males and females. Genome-wide CpG methylation analyses of male E10.5 control (n=3) and ethanol-exposed (n=8) forebrains (upper graphs) and females E10.5 control (n=3) and ethanol-exposed (n=8) forebrains (lower graphs). **A)** Heatmap showing CpG methylation levels for the DMRs (Males n=2 097; Females n=1 273) between control and EtOH-exposed forebrains. **B)** Volcano plot representing the differentially methylated regions (DMRs) between control and EtOH-exposed forebrains (see methods section for details). Red dots represent the tiles with a methylation increase of at least 10% in EtOH-exposed compared to control forebrains (Males n=161; Females n=1207); blue dots represent the tiles with a methylation decrease of at least 10% in EtOH-exposed compared to control forebrains (Males n=1 936; Females

n= 1 066); grey dots represent the tiles with changes less than 10% in EtOH-exposed compared to control forebrains (Males n=81 327; Females n=125 584). **C)** Proportion of DMRs associated with the changes of CpG methylation levels between control and EtOH-exposed E10.5 forebrains. **D)** Pie chart of genomic annotations for All tiles (Males n=83 424; Females n=126 857) and DMRs (Males n=2 097 and Females (n=1 273).

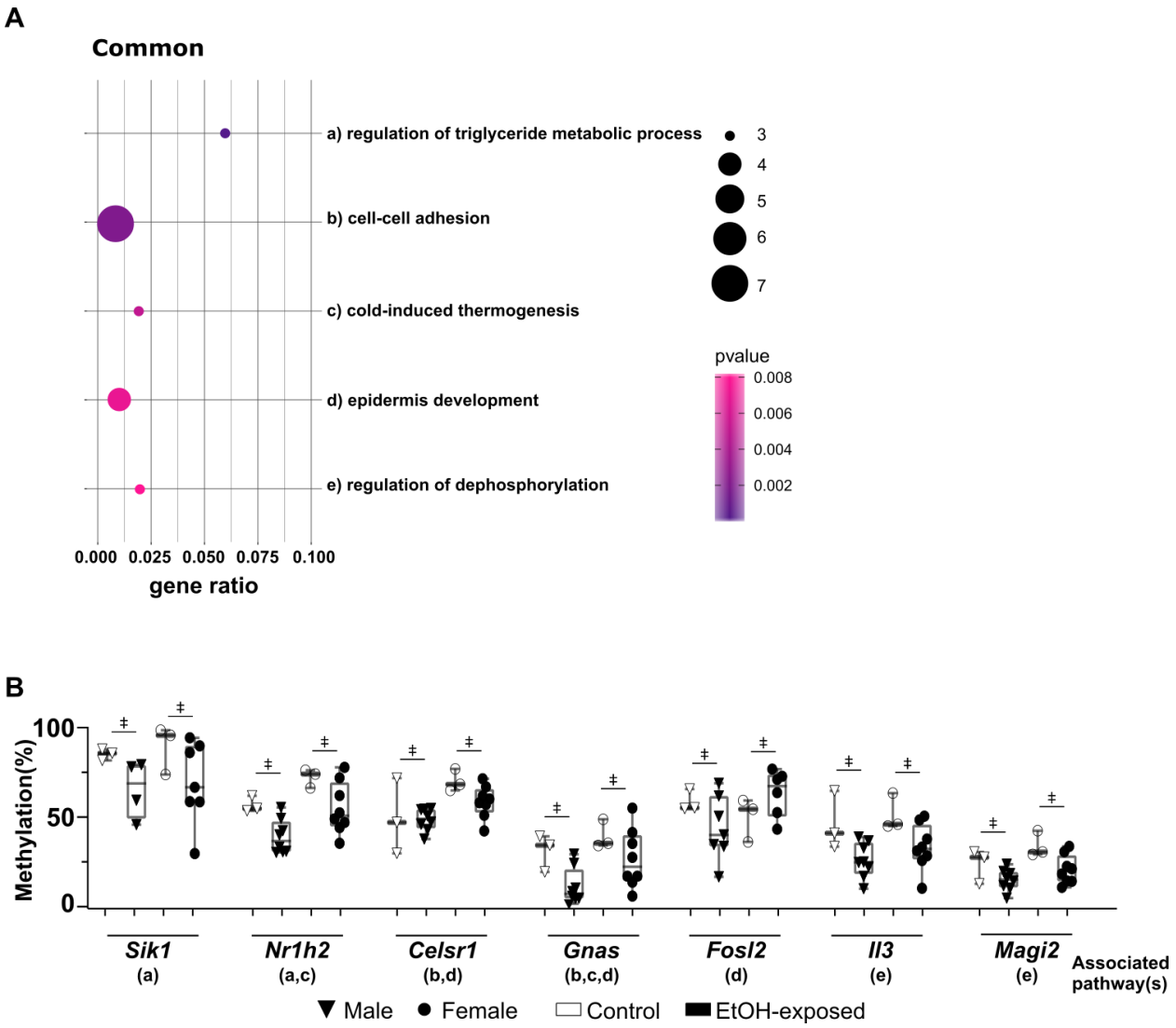

Figure S7. Functional enrichment analysis of common DMRs. A) Functional enrichment analysis showing the top enriched pathways for common DMRs (n=60 unique gene DMRs), based on Metascape analysis for pathways and p-value. The size of the dot represents the number of DMR-associated genes in pathways, and gene ratio represents the number of DMR-associated genes with regards to the number of genes in a pathway. **B)** Examples of CpG methylation levels of individual samples for sex-specific DMR-associated genes related to the top enriched pathways in A). Letters under gene name relate to the pathways in A). ǂ represents significant differences in CpG methylation levels of DMRs (e.g., ±>10% methylation difference, q<0.01) between control and EtOH-exposed embryos (see methods section for details).

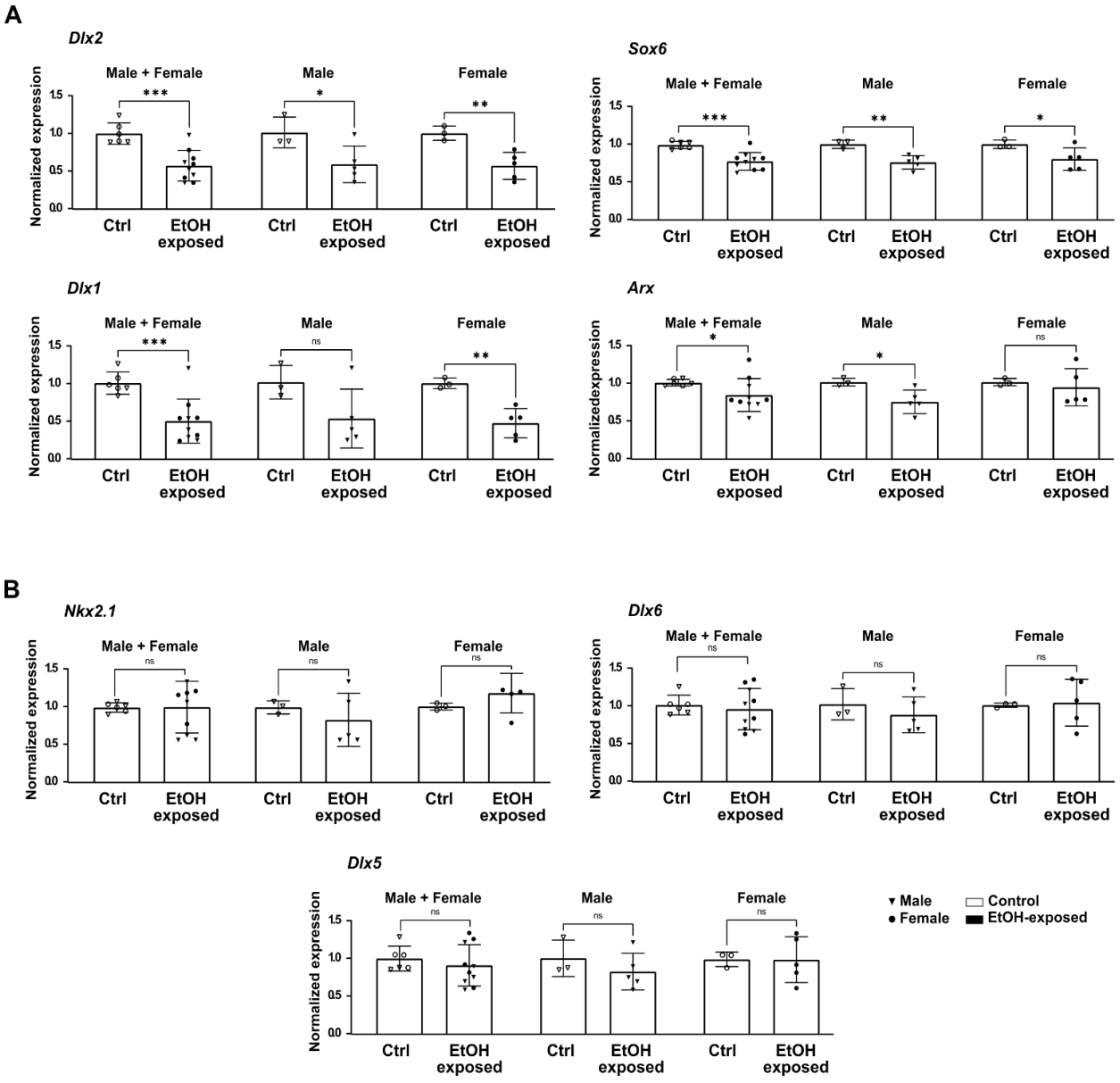

Figure S8. Relative gene expression in forebrains following early embryonic ethanol exposure. Selected genes associated, directly or indirectly, to the *Dlx* family of homeodomain transcription factors, which is at the core of the gene regulatory network that controls general aspects in the development of GABAergic interneurons (50,51). Quantitative Real Time PCR (qPCR) analyses of E10.5 control and EtOH-exposed forebrains showing : A) altered expression for genes associated to DMRs (*Dlx2*, *Sox6*, *Arx*) and normal DNA methylation profiles (*Dlx1*), and B) normal gene expression and normal DNA methylation profiles (*Nkx2.1*, *Dlx6*, *Dlx5*). Samples used for quantification: male Ctrl n= 3 and EtOH-exposed n=5; female Ctrl n= 3 and EtOH-exposed

n=5. Gene expression was normalized using control genes *Hprt1* and *Pgk1*. Bars represent mean ± SD. * p≤0.05, ** p≤0.01, ***p≤0.001, ns: non significative.

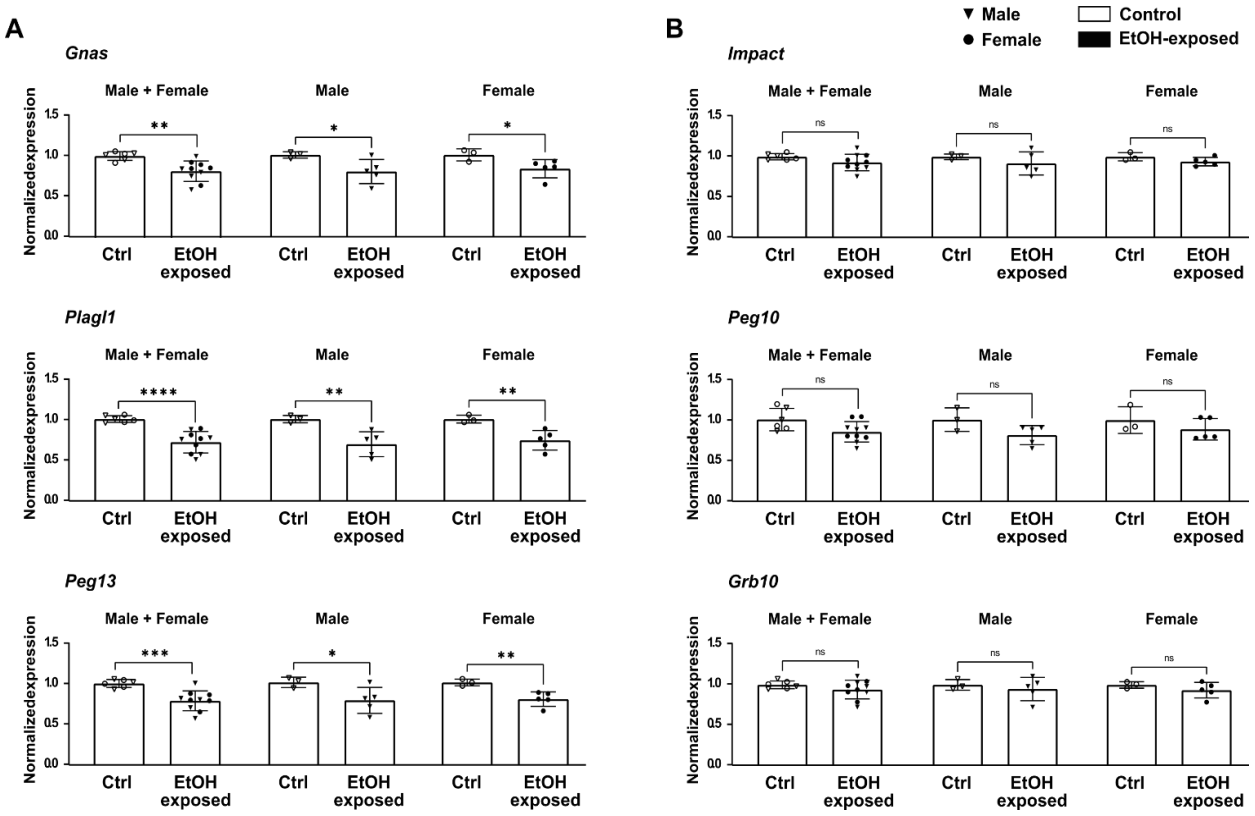

Figure S9. Relative expression of imprinting genes in forebrains following early embryonic ethanol exposure. Selection of imprinted genes that presented DNA methylation differences (i.e., DMRs) in their ICRs in both males and females E10.5 EtOH-exposed forebrains. Quantitative Real Time PCR (qPCR) analyses of E10.5 control and EtOH-exposed forebrains showing : A) altered expression, and B) no alteration in gene expression. Samples used for quantification: male Ctrl n= 3 and EtOH-exposed n=5; female Ctrl n= 3 and EtOH-exposed n=5. Gene expression was normalized using control genes *Hprt1* and *Pgk1*. Bars represent mean ± SD. * p≤0.05, ** p≤0.01, ***p≤0.001, ****p≤0.0001, ns: non significative.

Table S1. Sequencing information for RRBS data.

Sample	#Raw reads	Alignment %	#CpGs at 10X
Ctl-1	21 997 747	75	974 474
Ctl-2	20 433 987	78	1 500 815
Ctl-3	26 320 922	75	719 769
Ctl-4	23 030 420	79	1 066 382
Ctl-5	24 468 312	79	965 737
Ctl-6	27 783 216	79	1 058 976
EtOH-1	19 896 764	84	766 792
EtOH-2	30 101 522	81	1 066 501
EtOH-3	24 052 738	80	932 801
EtOH-4	26 671 945	84	859 007
EtOH-5	24 362 110	80	1 019 589
EtOH-6	28 346 140	80	1 061 420
EtOH-7	21 250 969	81	724 247
EtOH-8	39 781 961	87	1 390 455
EtOH-9	41 482 260	83	1 624 216
EtOH-10	22 864 202	81	853 155
EtOH-11	39 019 936	81	1 480 644
EtOH-12	24 787 442	81	875 794
EtOH-13	20 102 140	85	1 017 251
EtOH-14	25 365 210	81	936 405
EtOH-15	26 574 342	77	1 635 345
EtOH-16	23 808 905	83	842 291

Table S2. Primer sequences

Gene	Forward	Reverse
Arx	GCTCTCCTCCTACTGCATCG	CTCCCAGAAGCCTCATTTTG
Dlx1	TGTCTCCTTCTCCCATGTCC	TGCTGACCGAGTTGACGTAG
Dlx2	TGGGCTCCTACCAGTACCAC	TTGTTGACCGGAGACGAACT
Dlx5	TCTCAGGAATCGCCAACTTT	GAGCGCTTTGCCATAAGAAG
Dlx6	GGAGGCAACTCCTACAACCA	GACTGGAGGTAAGGGCTGTG
Gnas	CATTCTGAGCGTGATGAACG	ATCCTCCCACAGAGCCTTG
Grb10	GCTTCTCCATCTGTGAAGTGG	AAGACCACTGCGAGATTTTCA
Hprt1	CTGGTGAAAAGGACCTCTCGAA	CTGAAGTACTCATTATAGTCAAGGGCAT
Impact	ACTTCATGGATGACCCCAAAT	TGATAAGAAGGCGGTGCTGTA
Nkx2.1	AAAGCACACGACTCCGTTCT	CTCCATGCCCACTTTCTTGT
Peg10	GGACCCCTCATCCTTCGT	GTTGGCGTCTTTTGGTTCTT
Peg13	TAAAGTGCCCTGATCCGAAC	ATTTCAAACCTGCCAACCTG
Pgk1	CTGACTTTGGACAAGCTGGACG	GCAGCCTTGATCCTTTGGTTG
Plagl1	AATGTGGCAAGTCCTTCGTCAC	TGGTTCTTCAGGTGGTCCTTCC
Sox6	CAGCCCATGATGAACAGAAA	AGTTGCTGCTGTTGTCTTGC

DATA AVAILABILITY AND MATERIALS

The data from this study have been submitted to the Gene Expression Omnibus (GSE162765).

REFERENCES

1. May PA, Baete A, Russo J, Elliott AJ, Blankenship J, Kalberg WO, et al. Prevalence and characteristics of fetal alcohol spectrum disorders. Pediatrics. 2014;134(5):855-66.
2. Welch-Carre E. The neurodevelopmental consequences of prenatal alcohol exposure. Adv Neonatal Care. 2005;5(4):217-29.
3. Cook JL, Green CR, Lilley CM, Anderson SM, Baldwin ME, Chudley AE, et al. Fetal alcohol spectrum disorder: a guideline for diagnosis across the lifespan. Cmaj. 2016;188(3):191-7.
4. Legault LM, Bertrand-Lehouillier V, McGraw S. Pre-implantation alcohol exposure and developmental programming of FASD: an epigenetic perspective. Biochem Cell Biol. 2018;96(2):117-30.
5. Lange S, Probst C, Gmel G, Rehm J, Burd L, Popova S. Global Prevalence of Fetal Alcohol Spectrum Disorder Among Children and Youth: A Systematic Review and Meta-analysis. JAMA Pediatr. 2017;171(10):948-56.
6. Popova S, Lange S, Probst C, Gmel G, Rehm J. Estimation of national, regional, and global prevalence of alcohol use during pregnancy and fetal alcohol syndrome: a systematic review and meta-analysis. Lancet Glob Health. 2017;5(3):e290-e9.
7. Dwyer-Lindgren L, Flaxman AD, Ng M, Hansen GM, Murray CJ, Mokdad AH. Drinking Patterns in US Counties From 2002 to 2012. Am J Public Health. 2015;105(6):1120-7.
8. Grucza RA, Norberg K, Bucholz KK, Bierut LJ. Correspondence between secular changes in alcohol dependence and age of drinking onset among women in the United States. Alcohol Clin Exp Res. 2008;32(8):1493-501.
9. Lim SS, Vos T, Flaxman AD, Danaei G, Shibuya K, Adair-Rohani H, et al. A comparative risk assessment of burden of disease and injury attributable to 67 risk factors and risk factor clusters in 21 regions, 1990-2010: a systematic analysis for the Global Burden of Disease Study 2010. Lancet. 2012;380(9859):2224-60.
10. Popova S, Lange S, Probst C, Parunashvili N, Rehm J. Prevalence of alcohol consumption during pregnancy and Fetal Alcohol Spectrum Disorders among the general and Aboriginal populations in Canada and the United States. Eur J Med Genet. 2016.
11. Popova S, Lange S, Probst C, Shield K, Kraicer-Melamed H, Ferreira-Borges C, et al. Actual and predicted prevalence of alcohol consumption during pregnancy in the WHO African Region. Trop Med Int Health. 2016;21(10):1209-39.
12. Tan CH, Denny CH, Cheal NE, Sniezek JE, Kanny D. Alcohol use and binge drinking among women of childbearing age - United States, 2011-2013. MMWR Morb Mortal Wkly Rep. 2015;64(37):1042-6.
13. Thomas G. Levels and patterns of alcohol use in Canada. Alcohol Price Policy Series. Report 1. Ottawa, ON: Canadian Centre on Substance Abuse. 2012;http://www.ccsa.ca/Resource%20Library/CCSA-Patterns-Alcohol-Use-Policy-Canada-2012-en.pdf.

14. Wilsnack SC, Wilsnack RW, Kantor LW. Focus on: women and the costs of alcohol use. Alcohol Res. 2013;35(2):219-28.
15. Sedgh G, Singh S, Hussain R. Intended and unintended pregnancies worldwide in 2012 and recent trends. Stud Fam Plann. 2014;45(3):301-14.
16. Öztürk NC, Resendiz M, Öztürk H, Zhou FC. DNA Methylation program in normal and alcohol-induced thinning cortex. Alcohol. 2017;60:135-47.
17. Garro AJ, McBeth DL, Lima V, Lieber CS. Ethanol consumption inhibits fetal DNA methylation in mice: implications for the fetal alcohol syndrome. Alcohol Clin Exp Res. 1991;15(3):395-8.
18. Chater-Diehl EJ, Laufer BI, Castellani CA, Alberry BL, Singh SM. Alteration of Gene Expression, DNA Methylation, and Histone Methylation in Free Radical Scavenging Networks in Adult Mouse Hippocampus following Fetal Alcohol Exposure. PLoS One. 2016;11(5):e0154836.
19. Laufer BI, Kapalanga J, Castellani CA, Diehl EJ, Yan L, Singh SM. Associative DNA methylation changes in children with prenatal alcohol exposure. Epigenomics. 2015;7(8):1259-74.
20. McGraw S, Oakes CC, Martel J, Cirio MC, de Zeeuw P, Mak W, et al. Loss of DNMT1o disrupts imprinted X chromosome inactivation and accentuates placental defects in females. PLoS Genet. 2013;9(11):e1003873.
21. Breton-Larrivée M, Elder E, McGraw S. DNA methylation, environmental exposures and early embryo development. Anim Reprod. 2019;16(3):465-74.
22. McGraw S, Trasler IM. Oocyte epigenetics and the risks for imprinting disorders associated with assisted reproduction. Biology and Pathology of the Oocyte: Role in Fertility, Medicine and Nuclear Reprograming. 2013:384.
23. Zhu P, Guo H, Ren Y, Hou Y, Dong J, Li R, et al. Single-cell DNA methylome sequencing of human preimplantation embryos. Nat Genet. 2018;50(1):12-9.
24. Farthing CR, Ficz G, Ng RK, Chan CF, Andrews S, Dean W, et al. Global mapping of DNA methylation in mouse promoters reveals epigenetic reprogramming of pluripotency genes. PLoS Genet. 2008;4(6):e1000116.
25. Oswald J, Engemann S, Lane N, Mayer W, Olek A, Fundele R, et al. Active demethylation of the paternal genome in the mouse zygote. Curr Biol. 2000;10(8):475-8.
26. Peat JR, Dean W, Clark SJ, Krueger F, Smallwood SA, Ficz G, et al. Genome-wide bisulfite sequencing in zygotes identifies demethylation targets and maps the contribution of TET3 oxidation. Cell Rep. 2014;9(6):1990-2000.
27. McGraw S, Zhang JX, Farag M, Chan D, Caron M, Konermann C, et al. Transient DNMT1 suppression reveals hidden heritable marks in the genome. Nucleic Acids Res. 2015;43(3):1485-97.
28. Reik W, Dean W, Walter J. Epigenetic reprogramming in mammalian development. Science. 2001;293(5532):1089-93.
29. Messerschmidt DM, Knowles BB, Solter D. DNA methylation dynamics during epigenetic reprogramming in the germline and preimplantation embryos. Genes Dev. 2014;28(8):812-28.
30. Kazakevych J, Sayols S, Messner B, Krienke C, Soshnikova N. Dynamic changes in chromatin states during specification and differentiation of adult intestinal stem cells. Nucleic Acids Res. 2017;45(10):5770-84.
31. Liu J, Banerjee A, Herring CA, Attalla J, Hu R, Xu Y, et al. Neurog3-Independent Methylation Is the Earliest Detectable Mark Distinguishing Pancreatic Progenitor Identity. Dev Cell. 2019;48(1):49-63.e7.

32. Sanosaka T, Imamura T, Hamazaki N, Chai M, Igarashi K, Ideta-Otsuka M, et al. DNA Methylome Analysis Identifies Transcription Factor-Based Epigenomic Signatures of Multilineage Competence in Neural Stem/Progenitor Cells. Cell Rep. 2017;20(12):2992-3003.
33. Zhang Y, Xiang Y, Yin Q, Du Z, Peng X, Wang Q, et al. Dynamic epigenomic landscapes during early lineage specification in mouse embryos. Nat Genet. 2018;50(1):96-105.
34. Pérez-Cerezales S, Ramos-Ibeas P, Rizos D, Lonergan P, Bermejo-Alvarez P, Gutiérrez-Adán A. Early sex-dependent differences in response to environmental stress. Reproduction. 2018;155(1):R39-r51.
35. Bermejo-Alvarez P, Rizos D, Lonergan P, Gutierrez-Adan A. Transcriptional sexual dimorphism during preimplantation embryo development and its consequences for developmental competence and adult health and disease. Reproduction. 2011;141(5):563-70.
36. Donjacour A, Liu X, Lin W, Simbulan R, Rinaudo PF. In vitro fertilization affects growth and glucose metabolism in a sex-specific manner in an outbred mouse model. Biol Reprod. 2014;90(4):80.
37. Lowe R, Gemma C, Rakyan VK, Holland ML. Sexually dimorphic gene expression emerges with embryonic genome activation and is dynamic throughout development. BMC Genomics. 2015;16(1):295.
38. Miozzo F, Arnould H, de Thonel A, Schang AL, Sabéran-Djoneidi D, Baudry A, et al. Alcohol exposure promotes DNA methyltransferase DNMT3A upregulation through reactive oxygen species-dependent mechanisms. Cell Stress Chaperones. 2018;23(1):115-26.
39. Wu D, Cederbaum AI. Alcohol, oxidative stress, and free radical damage. Alcohol Res Health. 2003;27(4):277-84.
40. Mandal C, Halder D, Jung KH, Chai YG. Gestational Alcohol Exposure Altered DNA Methylation Status in the Developing Fetus. Int J Mol Sci. 2017;18(7).
41. Haycock PC, Ramsay M. Exposure of mouse embryos to ethanol during preimplantation development: effect on DNA methylation in the h19 imprinting control region. Biol Reprod. 2009;81(4):618-27.
42. Patten AR, Fontaine CJ, Christie BR. A comparison of the different animal models of fetal alcohol spectrum disorders and their use in studying complex behaviors. Front Pediatr. 2014;2:93.
43. Perkins A, Lehmann C, Lawrence RC, Kelly SJ. Alcohol exposure during development: Impact on the epigenome. Int J Dev Neurosci. 2013;31(6):391-7.
44. Boschen KE, Criss KJ, Palamarchouk V, Roth TL, Klintsova AY. Effects of developmental alcohol exposure vs. intubation stress on BDNF and TrkB expression in the hippocampus and frontal cortex of neonatal rats. Int J Dev Neurosci. 2015;43:16-24.
45. Mantha K, Laufer BI, Singh SM. Molecular changes during neurodevelopment following second-trimester binge ethanol exposure in a mouse model of fetal alcohol spectrum disorder: from immediate effects to long-term adaptation. Dev Neurosci. 2014;36(1):29-43.
46. Abel E. Effects of ethanol on pregnant rats and their offspring. Psychopharmacology. 1978;57(1):5-11.
47. Sulik KK, Johnston MC, Webb MA. Fetal alcohol syndrome: embryogenesis in a mouse model. Science. 1981;214(4523):936-8.
48. El Shawa H, Abbott CW, 3rd, Huffman KJ. Prenatal ethanol exposure disrupts intraneocortical circuitry, cortical gene expression, and behavior in a mouse model of FASD. J Neurosci. 2013;33(48):18893-905.
49. Ghimire SR, Dhungel S, Rai D, Jha CB, Saxena AK, Maskey D. Effect of prenatal exposure of alcohol in the morphology of developing rat embryo. Nepal Med Coll J. 2008;10(1):38-40.

50. Le TN, Zhou QP, Cobos I, Zhang S, Zagozewski J, Japoni S, et al. GABAergic Interneuron Differentiation in the Basal Forebrain Is Mediated through Direct Regulation of Glutamic Acid Decarboxylase Isoforms by Dlx Homeobox Transcription Factors. J Neurosci. 2017;37(36):8816-29.
51. Lim L, Mi D, Llorca A, Marín O. Development and Functional Diversification of Cortical Interneurons. Neuron. 2018;100(2):294-313.
52. Sussel L, Marin O, Kimura S, Rubenstein JL. Loss of Nkx2.1 homeobox gene function results in a ventral to dorsal molecular respecification within the basal telencephalon: evidence for a transformation of the pallidum into the striatum. Development. 1999;126(15):3359-70.
53. Nóbrega-Pereira S, Kessaris N, Du T, Kimura S, Anderson SA, Marín O. Postmitotic Nkx2-1 controls the migration of telencephalic interneurons by direct repression of guidance receptors. Neuron. 2008;59(5):733-45.
54. Alzu'bi A, Lindsay S, Kerwin J, Looi SJ, Khalil F, Clowry GJ. Distinct cortical and sub-cortical neurogenic domains for GABAergic interneuron precursor transcription factors NKX2.1, OLIG2 and COUP-TFII in early fetal human telencephalon. Brain Structure and Function. 2017;222(5):2309-28.
55. Kitamura K, Yanazawa M, Sugiyama N, Miura H, Iizuka-Kogo A, Kusaka M, et al. Mutation of ARX causes abnormal development of forebrain and testes in mice and X-linked lissencephaly with abnormal genitalia in humans. Nat Genet. 2002;32(3):359-69.
56. Colasante G, Collombat P, Raimondi V, Bonanomi D, Ferrai C, Maira M, et al. Arx is a direct target of Dlx2 and thereby contributes to the tangential migration of GABAergic interneurons. J Neurosci. 2008;28(42):10674-86.
57. Lunde ER, Washburn SE, Golding MC, Bake S, Miranda RC, Ramadoss J. Alcohol-Induced Developmental Origins of Adult-Onset Diseases. Alcohol Clin Exp Res. 2016;40(7):1403-14.
58. Chang RC, Skiles WM, Chronister SS, Wang H, Sutton GI, Bedi YS, et al. DNA methylation-independent growth restriction and altered developmental programming in a mouse model of preconception male alcohol exposure. Epigenetics. 2017;12(10):841-53.
59. Laufer BI, Chater-Diehl EJ, Kapalanga J, Singh SM. Long-term alterations to DNA methylation as a biomarker of prenatal alcohol exposure: From mouse models to human children with fetal alcohol spectrum disorders. Alcohol. 2017;60:67-75.
60. Lussier AA, Morin AM, MacIsaac JL, Salmon J, Weinberg J, Reynolds JN, et al. DNA methylation as a predictor of fetal alcohol spectrum disorder. Clin Epigenetics. 2018;10:5.
61. Portales-Casamar E, Lussier AA, Jones MJ, MacIsaac JL, Edgar RD, Mah SM, et al. DNA methylation signature of human fetal alcohol spectrum disorder. Epigenetics Chromatin. 2016;9:25.
62. Petrelli B, Weinberg J, Hicks GG. Effects of prenatal alcohol exposure (PAE): insights into FASD using mouse models of PAE. Biochem Cell Biol. 2018;96(2):131-47.
63. Liyanage VR, Zachariah RM, Davie JR, Rastegar M. Ethanol deregulates Mecp2/MeCP2 in differentiating neural stem cells via interplay between 5-methylcytosine and 5-hydroxymethylcytosine at the Mecp2 regulatory elements. Exp Neurol. 2015;265:102-17.
64. Wiebold JL, Becker WC. In-vivo and in-vitro effects of ethanol on mouse preimplantation embryos. J Reprod Fertil. 1987;80(1):49-57.
65. Abel EL. Prenatal effects of alcohol on growth: a brief overview. Fed Proc. 1985;44(7):2318-22.
66. Padmanabhan R, Hameed MS. Effects of acute doses of ethanol administered at pre-implantation stages on fetal development in the mouse. Drug Alcohol Depend. 1988;22(1-2):91-100.

67. Sandor S, Gârban Z, Checiu M, Daradics L. The presence of ethanol in the oviductal and uterine luminal fluids of alcoholized rats. Morphol Embryol (Bucur). 1981;27(4):303-9.
68. Pagé-Larivière F, Campagna C, Sirard MA. Mechanisms Involved in Porcine Early Embryo Survival following Ethanol Exposure. Toxicol Sci. 2017;156(1):289-99.
69. Mustapha TA, Chang RC, Garcia-Rhodes D, Pendleton D, Johnson NM, Golding MC. Gestational exposure to particulate air pollution exacerbates the growth phenotypes induced by preconception paternal alcohol use: a multiplex model of exposure. Environ Epigenet. 2020;6(1):dvaa011.
70. Chang RC, Thomas KN, Bedi YS, Golding MC. Programmed increases in LXRα induced by paternal alcohol use enhance offspring metabolic adaptation to high-fat diet induced obesity. Mol Metab. 2019;30:161-72.
71. Bedi Y, Chang RC, Gibbs R, Clement TM, Golding MC. Alterations in sperm-inherited noncoding RNAs associate with late-term fetal growth restriction induced by preconception paternal alcohol use. Reprod Toxicol. 2019;87:11-20.
72. Chang RC, Wang H, Bedi Y, Golding MC. Preconception paternal alcohol exposure exerts sex-specific effects on offspring growth and long-term metabolic programming. Epigenetics Chromatin. 2019;12(1):9.
73. Cirio MC, Martel J, Mann M, Toppings M, Bartolomei M, Trasler J, et al. DNA methyltransferase 1o functions during preimplantation development to preclude a profound level of epigenetic variation. Dev Biol. 2008;324(1):139-50.
74. Toppings M, Castro C, Mills PH, Reinhart B, Schatten G, Ahrens ET, et al. Profound phenotypic variation among mice deficient in the maintenance of genomic imprints. Hum Reprod. 2008;23(4):807-18.
75. Cirio MC, Ratnam S, Ding F, Reinhart B, Navara C, Chaillet JR. Preimplantation expression of the somatic form of Dnmt1 suggests a role in the inheritance of genomic imprints. BMC Dev Biol. 2008;8:9.
76. Dasmahapatra AK, Khan IA. DNA methyltransferase expressions in Japanese rice fish (Oryzias latipes) embryogenesis is developmentally regulated and modulated by ethanol and 5-azacytidine. Comp Biochem Physiol C Toxicol Pharmacol. 2015;176-177:1-9.
77. Kindsfather AJ, Czekalski MA, Pressimone CA, Erisman MP, Mann MRW. Perturbations in imprinted methylation from assisted reproductive technologies but not advanced maternal age in mouse preimplantation embryos. Clin Epigenetics. 2019;11(1):162.
78. Market-Velker BA, Zhang L, Magri LS, Bonvissuto AC, Mann MR. Dual effects of superovulation: loss of maternal and paternal imprinted methylation in a dose-dependent manner. Hum Mol Genet. 2010;19(1):36-51.
79. Ho-Shing O, Dulac C. Influences of genomic imprinting on brain function and behavior. Current opinion in behavioral sciences. 2019;25:66-76.
80. Seisenberger S, Peat JR, Hore TA, Santos F, Dean W, Reik W. Reprogramming DNA methylation in the mammalian life cycle: building and breaking epigenetic barriers. Philos Trans R Soc Lond B Biol Sci. 2013;368(1609):20110330.
81. Whidden L, Martel J, Rahimi S, Chaillet JR, Chan D, Trasler JM. Compromised oocyte quality and assisted reproduction contribute to sex-specific effects on offspring outcomes and epigenetic patterning. Hum Mol Genet. 2016;25(21):4649-60.
82. Tan K, Wang Z, Zhang Z, An L, Tian J. IVF affects embryonic development in a sex-biased manner in mice. Reproduction. 2016;151(4):443-53.
83. Skuse DH. Imprinting, the X-chromosome, and the male brain: explaining sex differences in the liability to autism. Pediatric research. 2000;47(1):9-.

84. Hart R, Norman RJ. The longer-term health outcomes for children born as a result of IVF treatment: Part I--General health outcomes. Hum Reprod Update. 2013;19(3):232-43.
85. Källén B, Finnström O, Lindam A, Nilsson E, Nygren KG, Olausson PO. Cancer risk in children and young adults conceived by in vitro fertilization. Pediatrics. 2010;126(2):270-6.
86. Kenton JA, Castillo VK, Kehrer PE, Brigman JL. Moderate Prenatal Alcohol Exposure Impairs Visual-Spatial Discrimination in a Sex-Specific Manner: Effects of Testing Order and Difficulty on Learning Performance. Alcohol Clin Exp Res. 2020.
87. de Ávila MAP, Gonçalves RM, Nascimento ECC, Cabral LDM, Vilela FC, Giusti-Paiva A. Prenatal exposure to alcohol impairs social play behavior in adolescent male mice. Neurotoxicology. 2020;79:142-9.
88. Petropoulos S, Edsgärd D, Reinius B, Deng Q, Panula SP, Codeluppi S, et al. Single-Cell RNA-Seq Reveals Lineage and X Chromosome Dynamics in Human Preimplantation Embryos. Cell. 2016;165(4):1012-26.
89. Bermejo-Alvarez P, Rizos D, Rath D, Lonergan P, Gutierrez-Adan A. Epigenetic differences between male and female bovine blastocysts produced in vitro. Physiol Genomics. 2008;32(2):264-72.
90. Bermejo-Alvarez P, Rizos D, Rath D, Lonergan P, Gutierrez-Adan A. Sex determines the expression level of one third of the actively expressed genes in bovine blastocysts. Proc Natl Acad Sci U S A. 2010;107(8):3394-9.
91. Gebert C, Wrenzycki C, Herrmann D, Gröger D, Thiel J, Reinhardt R, et al. DNA methylation in the IGF2 intragenic DMR is re-established in a sex-specific manner in bovine blastocysts after somatic cloning. Genomics. 2009;94(1):63-9.
92. Terasaki LS, Gomez J, Schwarz JM. An examination of sex differences in the effects of early-life opiate and alcohol exposure. Philos Trans R Soc Lond B Biol Sci. 2016;371(1688):20150123.
93. Hernández-Miranda LR, Parnavelas JG, Chiara F. Molecules and mechanisms involved in the generation and migration of cortical interneurons. ASN Neuro. 2010;2(2):e00031.
94. Yun K, Fischman S, Johnson J, Hrabe de Angelis M, Weinmaster G, Rubenstein JL. Modulation of the notch signaling by Mash1 and Dlx1/2 regulates sequential specification and differentiation of progenitor cell types in the subcortical telencephalon. Development. 2002;129(21):5029-40.
95. Anderson SA, Eisenstat DD, Shi L, Rubenstein JL. Interneuron migration from basal forebrain to neocortex: dependence on Dlx genes. Science. 1997;278(5337):474-6.
96. Cobos I, Borello U, Rubenstein JL. Dlx transcription factors promote migration through repression of axon and dendrite growth. Neuron. 2007;54(6):873-88.
97. Friocourt G, Parnavelas JG. Identification of Arx targets unveils new candidates for controlling cortical interneuron migration and differentiation. Front Cell Neurosci. 2011;5:28.
98. Bird CW, Taylor DH, Pinkowski NJ, Chavez GJ, Valenzuela CF. Long-term Reductions in the Population of GABAergic Interneurons in the Mouse Hippocampus following Developmental Ethanol Exposure. Neuroscience. 2018;383:60-73.
99. Cunningham LA, Newville J, Li L, Tapia P, Allan AM, Valenzuela CF. Prenatal Alcohol Exposure Leads to Enhanced Serine 9 Phosphorylation of Glycogen Synthase Kinase-3β (GSK-3β) in the Hippocampal Dentate Gyrus of Adult Mouse. Alcohol Clin Exp Res. 2017;41(11):1907-16.
100. Larsen ZH, Chander P, Joyner JA, Floruta CM, Demeter TL, Weick JP. Effects of Ethanol on Cellular Composition and Network Excitability of Human Pluripotent Stem Cell-Derived Neurons. Alcohol Clin Exp Res. 2016;40(11):2339-50.

101. Cuzon VC, Yeh PW, Yanagawa Y, Obata K, Yeh HH. Ethanol consumption during early pregnancy alters the disposition of tangentially migrating GABAergic interneurons in the fetal cortex. J Neurosci. 2008;28(8):1854-64.
102. Skorput AG, Lee SM, Yeh PW, Yeh HH. The NKCC1 antagonist bumetanide mitigates interneuronopathy associated with ethanol exposure in utero. Elife. 2019;8.
103. Paterno R, Casalia M, Baraban SC. Interneuron deficits in neurodevelopmental disorders: Implications for disease pathology and interneuron-based therapies. Eur J Paediatr Neurol. 2020;24:81-8.
104. Rossignol E. Genetics and function of neocortical GABAergic interneurons in neurodevelopmental disorders. Neural Plast. 2011;2011:649325.
105. Skorput AG, Gupta VP, Yeh PW, Yeh HH. Persistent Interneuronopathy in the Prefrontal Cortex of Young Adult Offspring Exposed to Ethanol In Utero. J Neurosci. 2015;35(31):10977-88.
106. Kleiber ML, Mantha K, Stringer RL, Singh SM. Neurodevelopmental alcohol exposure elicits long-term changes to gene expression that alter distinct molecular pathways dependent on timing of exposure. J Neurodev Disord. 2013;5(1):6.
107. Burgess DJ, Moritz KM. Prenatal alcohol exposure and developmental programming of mental illness. Journal of developmental origins of health and disease. 2020;11(3):211-21.
108. Christensen KE, Hou W, Bahous RH, Deng L, Malysheva OV, Arning E, et al. Moderate folic acid supplementation and MTHFD1-synthetase deficiency in mice, a model for the R653Q variant, result in embryonic defects and abnormal placental development. Am J Clin Nutr. 2016;104(5):1459-69.
109. Christensen KE, Deng L, Leung KY, Arning E, Bottiglieri T, Malysheva OV, et al. A novel mouse model for genetic variation in 10-formyltetrahydrofolate synthetase exhibits disturbed purine synthesis with impacts on pregnancy and embryonic development. Hum Mol Genet. 2013;22(18):3705-19.
110. Theiler K. The house mouse: atlas of embryonic development: Springer Science & Business Media; 2013.
111. Li L, Jayabal S, Ghorbani M, Legault LM, McGraw S, Watt AJ, et al. ATAT1 regulates forebrain development and stress-induced tubulin hyperacetylation. Cell Mol Life Sci. 2019;76(18):3621-40.
112. Shaffer B, McGraw S, Xiao SC, Chan D, Trasler J, Chaillet JR. The DNMT1 intrinsically disordered domain regulates genomic methylation during development. Genetics. 2015;199(2):533-41.
113. Legault L-M, Chan D, McGraw S. Rapid multiplexed reduced representation bisulfite sequencing library prep (rRRBS). Bio-Protocol. 2019;9:4.
114. Legault LM, Doiron K, Lemieux A, Caron M, Chan D, Lopes FL, et al. Developmental genome-wide DNA methylation asymmetry between mouse placenta and embryo. Epigenetics. 2020;15(8):800-15.
115. Pierre WC, Legault LM, Londono I, McGraw S, Lodygensky GA. Alteration of the brain methylation landscape following postnatal inflammatory injury in rat pups. Faseb j. 2020;34(1):432-45.
116. Piché J, Gosset N, Legault LM, Pacis A, Oneglia A, Caron M, et al. Molecular Signature of CAID Syndrome: Noncanonical Roles of SGO1 in Regulation of TGF-β Signaling and Epigenomics. Cell Mol Gastroenterol Hepatol. 2019;7(2):411-31.
117. Krueger F. Trim Galore: a wrapper tool around Cutadapt and FastQC to consistently apply quality and adapter trimming to FastQ files, with some extra functionality for MspI-digested

RRBS-type (Reduced Representation Bisufite-Seq) libraries. URL http://www bioinformatics babraham ac uk/projects/trim_galore/(Date of access: 28/04/2016). 2012.
118. Xi Y, Li W. BSMAP: whole genome bisulfite sequence MAPping program. BMC Bioinformatics. 2009;10:232.
119. Akalin A, Kormaksson M, Li S, Garrett-Bakelman FE, Figueroa ME, Melnick A, et al. methylKit: a comprehensive R package for the analysis of genome-wide DNA methylation profiles. Genome Biol. 2012;13(10):R87.
120. Zhou Y, Zhou B, Pache L, Chang M, Khodabakhshi AH, Tanaseichuk O, et al. Metascape provides a biologist-oriented resource for the analysis of systems-level datasets. Nat Commun. 2019;10(1):1523.
121. Bibikova M, Barnes B, Tsan C, Ho V, Klotzle B, Le JM, et al. High density DNA methylation array with single CpG site resolution. Genomics. 2011;98(4):288-95.
122. Da Costa EM, Armaos G, McInnes G, Beaudry A, Moquin-Beaudry G, Bertrand-Lehouillier V, et al. Heart failure drug proscillaridin A targets MYC overexpressing leukemia through global loss of lysine acetylation. J Exp Clin Cancer Res. 2019;38(1):251.
123. McGraw S, Vigneault C, Sirard MA. Temporal expression of factors involved in chromatin remodeling and in gene regulation during early bovine in vitro embryo development. Reproduction. 2007;133(3):597-608.

ACKNOWLEDGMENTS

We thank the McGraw lab for critical comments and suggestions, as well as Elizabeth Maurice-Elder for editing.

FUNDING

This work was supported by a research grant to SM from the Sickkids Foundation and Fonds de Recherche du Québec en Santé (FRQS). LML is supported by Canadian Institutes of Health Research (CIHR) scholarship. MBL and KD are supported by FRQS scholarship / fellowship. ALA is supported by Université de Montréal and Réseau Québécois en Reproduction (RQR) scholarships. AL is supported by Université de Montréal and Centre de Recherche en Reproduction et Fertilité (CRRF) scholarships. SM is supported by FRQS – Junior 2 salary award.

AUTHOR INFORMATION

Affiliations

CHU Sainte-Justine Research Center, 3175 Chemin de la Côte-Sainte-Catherine, Montréal, QC H3T 1C5, Canada

Lisa-Marie Legault, Karine Doiron, Mélanie Breton Larrivée, Alexandra Langford-Avelar, Anthony Lemieux, Maxime Caron, Daniel Sinnett, Serge McGraw

Department of Biochemistry and Molecular Medicine, Université de Montréal, 2900 Boulevard Edouard-Montpetit, Montréal, QC H3T 1J4, Canada.

Lisa-Marie Legault, Mélanie Breton Larrivée, Alexandra Langford-Avelar, Anthony Lemieux, Serge McGraw

McGill University Health Centre Glen Site, 1001 Boulevard Décarie, Montréal, QC H4A 3J1, Canada.

Loydie Jerome-Majewska

Department of Pediatrics, McGill University, 1001 Boulevard Décarie, Montréal, QC H4A 3J1, Canada.

Loydie Jerome-Majewska

Department of Pediatrics, Université de Montréal, 2900 Boulevard Edouard-Montpetit, Montréal, QC H3T 1J4, Canada.

Daniel Sinnett

Department of Obstetrics and Gynecology, Université de Montréal, 2900 Boulevard Edouard-Montpetit, Montréal, QC H3T 1J4, Canada.

Serge McGraw

Contributions

LML and SM conceptualized the study. LML and MBL contributed in data acquisition. LML, KD, ALA, AL, MC, LJM and DS participated in data analysis. LML, KD and SM wrote the manuscript. All authors read and approved the final manuscript.

Corresponding author

Correspondence to Serge McGraw

ETHICS DECLARATION

Consent for publication

Not applicable

Competing interests

No competing interests declared.

Chapitre 4 – Early preimplantation binge alcohol exposure induces sex-specific changes in DNA methylation and gene expression in the mouse placenta

Mise en contexte et contribution de l'étudiant

Pour ce chapitre, nous avons voulu déterminer si notre exposition prénatale à l'alcool pendant la préimplantation entrainait des dérégulations épigénétiques et transcriptomiques dans le placenta en fin de gestation. Pour ce faire, nous avons récolté des placentas en fin de gestation (E18.5) et procédé à des analyses histologiques, en plus de nos analyses de méthylation d'ADN et d'expression des gènes. Finalement, nous avons aussi utilisé une approche d'apprentissage automatique (*machine learning*) afin de déterminer si nous pouvions établir une signature basée sur les profils de méthylation d'ADN à la suite d'une exposition prénatale à l'alcool pendant la préimplantation qui permettrait éventuellement de servir d'outil diagnostic. Cet article en préparation est aussi disponible sur la plateforme bioRxiv https://doi.org/10.1101/2023.09.30.560198.

Contributions :

J'ai effectué les expériences avec les souris, la récolte et la dissection d'embryons avec l'aide de Mélanie Breton-Larrivée. J'ai réalisé les expériences d'histologie, de méthylation (Methyl-Seq) et l'extraction d'ARN pour les librairies de mRNA-seq réalisé par la plateforme de Génome Québec. L'ensemble des données brutes ont été analysé par Alexandra Langford-Avelar. J'ai ensuite réalisé les analyses sous-jacentes avec son aide et celle d'Anthony Lemieux. Fannie Filion-Bienvenue a réalisé les expériences de *machine learning* et généré les figures correspondantes. J'ai généré l'ensemble des graphiques et figures (sauf celle provenant de l'analyse de *machine learning*) et fait l'assemblage final. J'ai écrit le manuscrit avec l'aide du Dr McGraw.

Early preimplantation binge alcohol exposure induces sex-specific changes in DNA methylation and gene expression in the mouse placenta

Lisa-Marie Legault[1,2], Mélanie Breton-Larrivée[1,2], Fannie Filion-Bienvenue[1,2], Anthony Lemieux[1], Alexandra Langford-Avelar[1,2], Serge McGraw[1,2,3,#]

[1]CHU Ste-Justine Research Center, Montréal, QC, Canada

[2]Department of Biochemistry and Molecular Medicine, Université de Montréal, QC, Canada

[3]Department of Obstetrics and Gynecology, Université de Montréal, QC, Canada

[#]Corresponding author : Serge McGraw

CHU Ste-Justine Research Center, 3175 Chemin de la Côte-Sainte-Catherine, Montréal, QC H3T 1C5, Canada

514-344-4931

serge.mcgraw@umontreal.ca (corresponding author)

Competing interests

The authors have declared that no conflict of interest exists.

ABSTRACT

The placenta is vital for proper embryonic development and successful pregnancy. Preimplantation alcohol exposure has the potential of negatively impacting embryonic development and long-term health, leading to Fetal Alcohol Spectrum Disorder. We and others have demonstrated adverse effects of preimplantation alcohol exposure on embryo morphology and molecular profiles at late gestation, but studies on the placenta are remarkably lacking. Here, using our established pre-clinical mouse model, we assessed the impact of binge-like preimplantation alcohol exposure on late-gestation placenta morphology, DNA methylation and transcription in a sex-specific manner. Overall placenta morphology was not affected. However, we uncovered sex-specific differentially methylated regions (DMRs; n=991 in male; n=1 309 in female) and differentially expressed genes (DEGs; n=1 046 in male; n=340 in female) in placentas. Only 21 DMRs and 54 DEGs were common to both sexes but showed enrichment for pathways related to growth factor response. Using LASSO regression, we were able to precisely discriminate control and ethanol-exposed placentas based on specific DNA methylation patterns. This is the first study to demonstrate that preimplantation alcohol exposure alters DNA methylation and transcriptomic profiles in placentas at late gestation and identify a placental DNA methylation signature that could be used for prenatal alcohol exposure detection.

INTRODUCTION

The placenta is a transient organ that plays a vital role in supplying oxygen, essential nutrients, hormones, and metabolites to the developing fetus (1). Although commonly misconceived as a maternal organ, the placenta is a fetal organ that emerges from the trophectoderm cells, that originate from the same pool of early embryonic blastomere cells. During early development, the inner cell mass and trophectoderm separate into distinct lineages, and the placenta develops alongside the embryo. In mice, placental remodeling occurs as the chorion fuses with the allantois, followed by trophoblast differentiation and the formation of the labyrinth structure (1). This remodeling process typically ends by mid-gestation, at embryonic day E10.5 in mice and day 18 in humans (1, 2). Proper development and adequate function of the placenta are crucial for the progression of pregnancy. Any abnormality in placental structure or dysfunction can lead to a range of adverse pregnancy outcomes, including preterm birth, intrauterine growth restriction, or preeclampsia (3, 4). In addition to these complications, research has highlighted the connection between embryonic growth delays and placental dysfunction (3, 4).

Prenatal alcohol exposure is a leading yet preventable cause of birth defects and neurodevelopmental issues worldwide (5). It can lead to a range of problems affecting development, cognition, and behavior that can persist throughout a person's lifetime. Fetal Alcohol Spectrum Disorder (FASD) is the term used to describe these conditions resulting from alcohol exposure at any given time during pregnancy (5). FASD can manifest as a variety of symptoms, including cognitive impairments, learning difficulties, behavioral issues, and, in severe cases, profound intellectual disabilities and craniofacial abnormalities (5). Each year, approximately 630 000 newborns are affected by FASD worldwide (6). The severity and variability of symptoms depend on multiple factors, including the timing, amount, and pattern of alcohol exposure during pregnancy (5). Maternal health, exposure to other harmful substances, and diet are additional factors that can impact the severity of the disorder (5). At present, there is no molecular diagnostic tool for FASD, and most cases are identified in childhood during school-age years when neurodevelopmental symptoms become noticeable. Late detection often leads to a need for lifelong health and social care for individuals with FASD. Nonetheless, early diagnosis and management hold the potential to alleviate the impact of FASD (5).

The preimplantation period is a critical phase in embryonic development. During this short period, the epigenome undergoes significant remodeling, involving the erasure and reprogramming of DNA methylation marks from parental gametes, to initiate the developmental program (7). Since pregnancy is typically detectable only after implantation, when human chorionic gonadotropin hormone (hCG) production begins, there is a 6-day window of high risk for prenatal alcohol exposure during the preimplantation development stage (8). Given the increasing alcohol use, including binge drinking, among women of childbearing age (18-34 years) (9), and the substantial number of unplanned pregnancies worldwide (approximately 40%) (10), it is essential to investigate the impact of alcohol during this critical phase. Despite its critical importance for proper embryonic development and its heightened susceptibility to adverse environmental exposures, the preimplantation period has been understudied in relation to prenatal alcohol exposure, with only a few models focusing exclusively on this early developmental time-point.

In a recent study using a preclinical mouse model of early preimplantation binge-like alcohol exposure, we reported sex-specific DNA methylation changes in the forebrain of mid-gestation embryos (E10.5) (11). We also observed an increased incidence of morphological defects, including growth delays, in the group of embryos exposed to ethanol at E10.5 and E18.5 (11, 12). Despite these findings, there is still a significant knowledge gap regarding the effects of early preimplantation alcohol exposure on both the embryo and placenta.

Here, we used a mouse model of early prenatal alcohol exposure during the preimplantation period to define the impact on the placenta at late gestation. While we didn't observe any change in placental morphometrics or morphology, suggesting no significant alterations in cell types, we found significant decreases in fetal weight, specifically in male embryos. Additionally, we identified sex-specific disruptions in DNA methylation and gene expression in the placenta. These disruptions affected crucial developmental pathways related to growth regulation, inflammation, cytoskeleton organization, and serotonin uptake.

RESULTS

Early preimplantation alcohol exposure does not induce morphometric changes in the placenta but induces lower embryo weight in males.

In this study, we examined the effect of early preimplantation binge alcohol exposure on various aspects of late placenta development using an established FASD mouse model (11). Briefly, to simulate short-term exposure to a high level of alcohol, pregnant females were given two doses of 2.5g/kg ethanol at 2-hour intervals during preimplantation, at the 8-cell stage (E2.5). We previously showed that this paradigm increases alcohol blood level to an average of 158.31mg/dl (11). At late gestation (E18.5), we collected embryos and placentas to assess the overall impact of alcohol on gestational outcomes, focusing first on basic morphometric measurements. All measurements were compared within same sex.

We analyzed the impact of early preimplantation alcohol exposure on the sex ratio and observed that while 55% (n=47/86) of control embryos were males, the ethanol-exposed group had a slightly higher proportion of males (61%; n=62/101) without significant difference (Fig1A). Additionally, there were no significant effect of early preimplantation alcohol exposure on litter size, on the number of males and females per litter (Fig1B), as well as on placental area and weight (Fig1C-D). We observed a small but significant decrease in fetal weight among male embryos exposed to ethanol compared to control group (1.195g average in controls vs 1.134g average in ethanol-exposed; $p<0.01$), while no such decrease was observed in females (Fig1E). Despite the significant reduction of fetal weight in male embryos, the placental efficiency (fetal to placental weight ratio) is similar in controls and ethanol-exposed embryos for both sexes (Fig1F). To obtain a comprehensive view, we analyzed the morphometric measurements per litter for all four parameters and did not find any significant differences between control and ethanol-exposed litters (Fig S1).

To assess the impact of preimplantation alcohol exposure on global placenta cell composition, we next measured the area and thickness for the junctional zone and the labyrinth using H&E staining of E18.5 placenta cross sections. Comparing the control and ethanol-exposed groups, we did not observe any significant difference in the area or thickness of both the junctional zone and labyrinth, nor in the ratios of their respective area/thickness to total area/thickness (Fig S2A-I). However, we found a significant increase of variance in the female groups for the ratio of the area of the junctional zone on the total area (*F* test, $p<0.05$), as well as in the thickness of the junctional zone (*F* test, $p<0.05$; Fig S2B;E).

Overall, these findings suggest that early preimplantation alcohol exposure does not have a severe impact on placenta morphology during late gestation. However, it does have a developmental effect on male embryos.

Altered DNA methylation in late-gestation placentas exposed to alcohol during preimplantation.

To examine the impact of preimplantation alcohol exposure on DNA methylation patterns in late-gestation placentas, we performed a genome-wide DNA methylation analysis. We randomly selected 6 control placentas (3 males and 3 females) and 10 ethanol-exposed placentas (5 males and 5 females) with normal morphometric measurements and no visible morphological defects. The corresponding embryos also exhibited normal morphometric measurements and no visible morphological defects.

After establishing sex-specific DNA methylation profiles in E18.5 placentas, we compared the average DNA methylation levels in 100 bp non-overlapping windows (tiles) between control and ethanol-exposed male or female placentas, each with a minimum of 3 samples per condition and a sequencing depth of at least 10x. We identified a set of 751 083 tiles with sufficient coverage in both male and female placentas, allowing us to investigate shared and sex-specific DNA methylation differences induced by early alcohol exposure (Fig S3A-B).

We observed a noticeable shift in the distribution of the 751 083 tiles based on their DNA methylation values in both control and ethanol-exposed placenta of males and females (Fig S3C). Specifically, female ethanol-exposed placentas showed an increased number of tiles with higher methylation levels (70-80%, 80-90%, 90-100%) compared to control placentas, while there was a decrease in the number of tiles with lower methylation levels (10-20%, 20-30%, 30-40%). A similar pattern was observed in male ethanol-exposed placentas, although to a lesser extent. Among the 751 083 shared tiles, we identified 991 differentially methylated regions (DMRs) exclusively altered in males, 1 309 DMRs exclusively altered in females, and only 21 shared DMRs that showed alterations in both sexes in response to early alcohol exposure (Fig S3A). These findings highlight the sex-specific influence of early preimplantation alcohol exposure on DNA methylation patterns in E18.5 placentas.

Sex-specific DNA methylation dysregulation in the late-gestation placenta following early preimplantation alcohol exposure.

To gain a better understanding of the long-term sex-specific impact of early preimplantation alcohol exposure on placenta DNA methylation profiles, we focused on the dysregulation associated only to male or female samples. Our sex-specific analysis revealed distinct patterns: male ethanol-exposed placentas exhibited 991 DMRs, while female ethanol-exposed placentas showed 1 309 DMRs (Fig 2A;C; Fig S3A; Table 1). Male placentas had nearly equal distribution of DMRs with increased (n=540; 54%) and decreased (n=451; 46%) methylation in response to ethanol exposure (Fig 2A). In contrast, female placentas predominantly exhibited DMRs with increased methylation (increased n=988; 75%, decreased n= 321; 25%) (Fig 2C). In both sexes, the majority of the DMRs were annotated as introns (male 41%; female 42%) or intergenic regions (male 39%; female 37%) (Fig 2B;D). However we observed wider DNA methylation change between control and ethanol-exposed placentas in DMRs located in non-coding regions (average methylation in controls 44%; ethanol-exposed 51%) and DMRs located in exons (average methylation in controls 47%; ethanol-exposed 52%) in males, while for female DMRs, wider change was observed for DMRs located in 3' untranslated regions (UTR; average methylation in controls 53%; ethanol-exposed 63%) or introns (average methylation in controls 45%; ethanol-exposed 54%; Fig 2B;D)

Upon analyzing the distribution of sex-specific DMRs across different CpG methylation levels, we observed a consistent trend in both sexes. Regions with higher methylation levels tended to gain methylation following ethanol exposure, while regions with lower methylation levels tended to lose methylation (Fig 2E;G). This trend was particularly pronounced in female-specific DMRs, where we observed significant differences in the distribution of the 1 309 tiles across nearly all methylation categories (Fig 2G). Most of these sex-specific DMRs exhibited modest methylation changes of around 10-15%. In terms of magnitude, a greater proportion of female-specific DMRs (12%) exhibited methylation changes exceeding 20%, compared to male-specific DMRs (9%) (Fig 2F;H). However, the number of DMRs with methylation differences higher than 30% was quite low in both sexes, with only ~1% for female-specific DMRs (n=15) and 0.4% for male-specific DMRs (n=4).

To gain insight into the pathways associated with sex-specific DMRs in ethanol-exposed placentas, we performed a gene ontology enrichment analysis for both males and females. First, we removed all intergenic-associated tiles from our datasets. In male DMRs, we analyzed 607 regions representing 542 unique genes. Notable enriched pathways included cell junction assembly (*Cttn*, *Mapt*), response to growth factors (*Fgf1*, *Zeb2*), negative regulation of synaptic transmission (*Cttn*, *Mapt*), organic hydroxy compound biosynthetic process (*Slc11a2*, *Star*), and phenol-containing compound biosynthetic process (*Hdc*, *Nr4a2*) (Fig 2I). For female-specific DMRs, we analyzed 821 regions corresponding to 749 unique genes. The top enriched pathways differed from the male-specific pathways and included plasma membrane bounded cell projection morphogenesis (*Ank3*, *Cdh11*), regulation of inflammatory response (*Bcl6*, *Foxj1*), alpha-beta T cell differentiation (*Bcl6*, *Foxj1*), negative regulation of cell migration (*Rbp4*), and negative regulation of cell population proliferation (*Foxj1*, *Wnt5a*) (Fig 3I-J). Other examples of specific DMRs for males and females are shown (Fig 2J), with males-specific DMRs (left panel) including *Klhl29* (Biological process), *Mfge8* (Apoptosis and phagocytose process), *Scarb2* (Lipid activity) and *Tnfrsf11a* (Signaling activity), and females-specific DMRs (right panel) including *Mfsd2a* (Lipid metabolism), *Aagab* (Protein transport), *Ccdc57* (Centriole assembly), *Myrfl* (Protein processing), *Ncam2* (Cell adhesion) and *Rps6kl1* (Protein phosphorylation).

These findings reveal that early preimplantation alcohol exposure results in sex-specific DNA methylation dysregulation in late-gestation placentas, with females showing a higher susceptibility. Furthermore, these sex-specific alterations in DNA methylation are associated with specific biological pathways.

Female ethanol-exposed placentas tend to lose methylation in CpG rich regions.

To explore if local genomic sequence contributes to the intrinsic sex-specific susceptibility of DMRs, we explored the CpG context using publicly available CpG island tracks and categorized DMRs into CpG islands, CpG shores (+/- 2kb from CpG islands), CpG shelves (+/- 2kb from CpG shores) or labeled them as "open sea" if not located in any of these categories. As shown in Figure S4A, the majority of male and female DMRs were found in open sea regions characterized by low CpG content. We found that the highest proportion of DMRs located in CpG islands (i.e., CpG rich regions) were for DMRs with increased methylation in male (13%; n=68) and decreased methylation in female (14%; n=45;) placentas. DMRs with decreased methylation in female

placentas also showed the highest proportion in CpG shores (28%; n=89), with other groups having similar proportions (16-18%) (Fig S4A). The highest increased or decreased levels were found in open sea regions and shores, with the lowest mainly found in CpG islands (Fig S4B).

To evaluate the methylation differences of sex-specific DMRs based on their CpG context more broadly, we compared the methylation profiles of DMRs located in CpG islands (high CpG content), annotated in promoters (mid CpG content), and repeat regions (low CpG content) (Fig S4C). We observed a generally higher level of methylation in ethanol-exposed placentas from male DMRs located in CpG islands. This difference became smaller as the CpG density decreased, consistent with the fact that DMRs in repeat regions, like open sea regions, contained regions with both decrease and increase methylation level in ethanol-exposed placentas compared to controls. Interestingly, we observed the opposite trend when examining the methylation profiles of female DMRs across different annotations. While we observed a generally lower methylation level in ethanol-exposed placentas in DMRs located in CpG islands, the methylation level became higher in female ethanol-exposed placentas compared to controls in DMRs located in promoters and especially those in repeat regions (Fig S4C; bottom panels).

Taken together, our findings suggest that early preimplantation alcohol exposure impacts the placenta in different CpG density locations and in a sex-specific manner.

Affected regions in both male and female late-gestation placentas following early preimplantation alcohol exposure are related to growth development.

Although our primary focus was to identify sex-specific DMRs resulting from early preimplantation alcohol exposure in the placenta, we also observed shared affected regions between sexes. We identified a total of 21 DMRs (Table 2), most (n=16 DMRs) of which exhibit methylation differences below 15% between ethanol-exposed and control placentas, with the largest difference being 23% between the conditions (Fig 3A). Regions of interest included DMRs located in genes such as *Galp* (neuropeptide signaling), *Psd3* (protein transduction) or *Wwox* (apoptotic signaling) (Fig 3B). The direction of DNA methylation changes (decrease or increase) in ethanol-exposed placentas was consistent for 17 DMRs in both sexes, while 4 DMRs displayed divergent changes (Fig 3A). Among the 21 DMRs, 12 are in promoters or intragenic regions. Gene ontology analysis reveals that the regulation of growth pathway is enriched, notably because of the presence of *Clstn3*, *Soc5*, and *Tro* (Fig 3C-D).

To gather a broader understanding of how preimplantation alcohol exposure alters DNA methylation patterns of specific genes in both male and female placentas, we performed DMR comparison based on gene annotation instead of genomic position. Following exclusion of intergenic DMRs, we compared a total of 607 male-specific DMRs (n=542 genes) to 821 female-specific DMRs (n=749 genes) located in promoters and intragenic regions. Along with the 21 shared DMRs previously described, we uncovered 69 shared genes in 89 DMRs with DNA methylation differences in male and female ethanol-exposed placentas (Fig S5A). Again, the direction of DNA methylation changes in ethanol-exposed placentas was consistent in both sexes for a subset of DMRs (n=39), while 50 DMRs displayed divergent changes (Fig S5A-B). Gene ontology enrichment analysis revealed pathways related to reproductive process, cell morphogenesis, transmembrane transport activity, myeloid cell development, and response to growth factors with regions associated to *Bmp6*, *Prdm14*, *Ptprk*, and *Runx1* being affected (Fig S5C-D).

These analyses indicate that the dysregulated pathways shared between male and female placentas in response to preimplantation alcohol exposure likely contribute to the adverse effects observed in male and female embryonic development.

Early preimplantation alcohol exposure leads to sex-specific gene expression alterations in late-gestation placentas.

To further our understanding of the molecular impact of preimplantation alcohol exposure on the late gestation placenta, we performed gene expression profiling using mRNA-seq. We used a significance threshold of $p<0.05$ to identify differentially expressed genes (DEGs), with the aim of identifying small but significant changes between ethanol-exposed and control placentas. Out of 31 235 expressed genes, we identified a total of 1 046 male-specific DEGs, 340 female-specific DEGs, and 54 DEGs shared between both sexes (Fig 4A-D; FigS6A-B; Table 3). In males, 498 genes showed decreased expression in ethanol-exposed placentas, while 548 genes showed increased expression (Fig 4A;C). Although females showed a greater number of DMRs compared to males, we did not see such a trend for genes expression. Of the 340 genes with altered expression in ethanol-exposed female placentas, 185 DEGs showed decreased expression and 155 genes exhibited increased expression (Fig 4B;D). Examples of male- and female-specific DEGs are shown (Fig 4G-H).

Our functional enrichment investigation for male- and female-specific differentially expressed genes revealed biological pathways that were divergent. For instance, the 1 046 males DEGs were related to regulation of cell migration (*Aqp1*, *Rhoc*), cytoskeleton organization (*Apoa1*, *Bmp10*), cell-substrate adhesion (*Adam8*, *Utrn*), cell junction organization (*Ank6*, *Cdh6*), and blood vessel development (*Flt4*, *Slc16a1*) (Fig 4E). Whereas the 340 female DEGs showed enrichment in pathways involved in regulation of cell adhesion (*Itgb3*, *Ret*), serotonin uptake (*Slc22a2*, *Snca*), piRNA metabolic process (*Fkbp6*, *Piwil2*), megakaryocyte development and platelet production (*Gata2*, *Gata4*), and locomotory behavior (*Chrna4*, *Efnb3*) (Fig 4F).

Early preimplantation alcohol exposure leads to non-sex-specific gene expression alterations in late-gestation placentas.

As for DMRs, we also identified genes (n=54; Table 4) that showed similar differential expression in both male and female ethanol-exposed placentas following the early alcohol exposure. For most genes (e.g., *Cited2*, *Luzp1*, *Timp2*, *Pmp22*, *Krt14*), we observed comparable changes in normalized read counts and fold change in both sexes (Fig S7A-C). While almost every shared DEGs (50 of 54) show similar decrease or increase in expression in both sexes, 4 genes showed divergent changes in males and females, including *Ifit2* (response to interferon-alpha) and *Krt14* (cytoskeleton organization) (Fig S7D). For *Ifit2*, we also denote that the level of expression in the control condition is different between males and females (Fig S7D).

To better understand the functional pathways associated with DEGs that are not specific to male or female placentas, we performed a gene ontology analysis. The analysis revealed enrichment in several pathways, including neuromuscular junction development (*Musk*, *Pmp22*), sphingolipid biosynthetic process (*B3gnt5*, *St8sia5*), artery development (*Chd7*, *Luzp1*), and matrix organization (*Foxf2*, *Kif9*) (Fig S7E). Furthermore, we identified additional DEGs of interest. For example, *Bhlhe41*, associated with muscle development, and *Cited2*, involved in decidualization, placenta, cardiac, and cortex development, showed decreased expression in ethanol-exposed placentas. On the other hand, *Scel*, related to the regulation of the *Wnt* signaling pathway, and *Syt14*, involved in synaptic transmission, exhibited increased expression in ethanol-exposed placentas (Fig S7F). These specific DEGs highlight potential molecular mechanisms and pathways affected by preimplantation alcohol exposure in the placenta regardless of sex.

These findings provide insights into the biological processes that may be impacted in both male and female placenta by preimplantation alcohol exposure, suggesting potential negative consequences of placental dysfunction on embryonic development.

Early preimplantation alcohol exposure does not strictly impact genes crucial for placenta development or placenta imprinting genes at late gestation.

To evaluate the impact of early alcohol exposure on genes that are crucial for placental development, we analyzed our DNA methylation and gene expression datasets using curated gene lists sourced from the literature (13).

Out of the 205 placental genes initially considered, 193 were present in our DNA methylation dataset, accounting for 7 327 tiles present in promoters and intragenic regions (Fig S8A). These represented only 6 DMRs: 3 DMRs in males (*Epas1*, *Id1*, and *Peg10*) and 3 DMRs in females (*Flt1*, *Ppard*, and *Serpine1*). All 205 placental genes were covered in our transcriptomic dataset, revealing dysregulation of 19 genes in males and 8 genes in females following ethanol exposure (Figure S8B). Only one DEG, *Cited2*, was altered in both male and female placentas (FigS7B;C;F and Fig S8B). Additionally, we observed that *Peg10* exhibited increased DNA methylation (intronic DMR) and increased expression in male ethanol-exposed placentas, with the *Peg10* DMR overlapping the imprinting control region (ICR) of the gene (Fig S8A).

To further investigate the impact of preimplantation alcohol exposure on imprinted genes, we examined a curated list of 105 genes known to be regulated by genomic imprinting in the placenta (14-19). From these genes, we identified 17 DMRs located in promoters or intragenic regions, associated to 11 genes, and altered in male ethanol-exposed placentas (Fig S9A;C; Table S1). 12 of these DMRs (7 different genes) are located directly in the imprinting control region of the corresponding gene. Furthermore, we observed 18 imprinted genes with differential expression in male placentas (Fig S8B; Table S1). In contrast, female ethanol-exposed placentas showed fewer DNA methylation changes, with only 9 DMRs representing 9 different genes affected from which only one gene, *Slc22a2*, showed differential expression (Fig S9A-B; Table S1). Detailed examples of DMR and DEG levels for male and female placentas are provided (Fig S9C-D).

These results reveal that although several placental and imprinted genes exhibited dysregulated DNA methylation levels or expression following early preimplantation alcohol

exposure, the dysregulation was not widespread. These findings align with the morphometric analyses, which did not reveal any significant placental malformation or dysfunction.

Sex-specific regions are showing both DNA methylation and gene expression alterations in the placenta at late-gestation following early preimplantation alcohol-exposure.

To explore the relationship between dysregulated DNA methylation and gene expression profiles in the placenta after preimplantation alcohol exposure, we next conducted a comparative analysis between our lists of DMRs and gene expression profiles. For this analysis, we focused on intragenic DMRs, excluding intergenic regions. We compared the genes associated with 607 male DMRs (542 unique genes), 821 female DMRs (749 unique genes), and 12 shared DMRs (11 unique genes) with their respective gene expression profiles.

Of the 12 shared DMRs representing 11 unique genes, only *Clstn3* and *Tro* exhibited gene expression changes in male ethanol-exposed placentas (Fig S10A-B), with no expression changes observed in females. In males, we identified 46 DMRs located in 40 unique genes that displayed both DNA methylation changes and gene expression dysregulation in ethanol-exposed placentas (Fig5A). The majority of these DMRs (78%; n=36) exhibited DNA methylation changes ranging from 10% to 20% and small expression changes (|log2FC| <0.5) (FigS11A). Notably, regions/genes with altered methylation and expression included *Apoc1* (lipid activity), *Carmil1* (actin filament processes), *Slc16a3* (encode the MCT4 protein; transmembrane transport, placental organization and vascularization) and *Zfhx3* (growth factors and development) (Fig 5B).

In females we identified 16 DMRs, located in 15 unique genes, that showed both differential methylation and transcriptomic alterations in ethanol-exposed placentas (Figure 5C). 11 of these DMRs (69%) showed greater than 20% methylation difference, while 7 genes (47%) showed gene expression differences over |log2FC| >0.5 in ethanol-exposed placentas (Fig S11B). Some noteworthy regions displaying DNA methylation and expression changes in female ethanol-exposed placentas include *Chd7* (cardiac, muscle, and neuronal development), *Cux2* (neuronal pathways and functions, including cortical interneurons development), *Elovl2* (fatty acid processes) and *Mfsd2a* (establishment of the blood-brain barrier) (Fig 5D).

These results provide valuable insight into the long-term impact of preimplantation alcohol exposure on several genes and emphasize the significance of sex-specific DNA methylation dysregulation in shaping gene expression patterns in male and female placentas.

DNA methylation dysregulation in the placenta as a biomarker for early preimplantation alcohol exposure.

To address the absence of a reliable way to detect prenatal alcohol exposure and fetal alcohol spectrum disorder (FASD) shortly after birth, we explored the potential of using specific molecular patterns present in placentas exposed to ethanol. We employed a machine learning technique called LASSO (Least Absolute Shrinkage and Selection Operator) regression to create a diagnostic model using identifiable markers found in our transcriptomic or DNA methylation data. To enhance accuracy and effectiveness, we trained the model using both male and female samples together, increasing our statistical strength and refining the analytical process.

First, we used gene expression profiles and performed the LASSO regression to establish specific transcriptomic signatures for ethanol-exposed placentas. Despite presenting significant statistical parameters such as Wilcoxon *p*-value and area under the ROC curve (AUC), the 20 DEGs identified are not distinguishable enough between the conditions to establish a good transcriptomic signature of preimplantation alcohol exposure in the late-gestation placentas, with small Euclidean distance between samples of the two conditions and poor statistical coefficient importance (Fig S12A-C).

We then used our DNA methylation profiles to perform the LASSO regression and identify a set of DNA methylation patterns forming a specific signature for placentas exposed to ethanol. This signature consisted of 24 DMRs that exhibited significant statistical parameters, allowing to effectively discriminate ethanol-exposed samples from controls for both principal component analysis (PCA) and Euclidean distance calculations (Fig 6A-B). These 24 DMRs were located in both intragenic (n=15) and intergenic (n=9) regions, with each DMR having a different level of importance based on statistical parameters, notably LASSO coefficient, Wilcoxon *p*-value and area under the ROC curve (AUC) generated by the LASSO analysis (Fig 6C). The most significant DMR in the signature was located in an intergenic region close to the *Nup35* gene. Additionally, there were DMRs in genes like *B3galt1*, *Kcng1*, *Mir3960*, *Mir6940*, *Psd3*, and *Sesn1*, along with intergenic DMRs close to *Bicd1*, *Gatsl2*, and *Zeb2* genes (Fig 6C-D).

These results highlight that a specific DNA methylation pattern in the placenta is better at identifying preimplantation alcohol exposure when compared to transcriptomic profiles. This emphasizes the potential of a distinctive DNA methylation signature in the placenta as a dependable molecular tool for detecting early embryonic prenatal alcohol exposure at birth.

DISCUSSION

In this study, our aim was to uncover the effects of early prenatal alcohol exposure during the preimplantation stage on molecular and developmental aspects of the placenta at late gestation. Through our analyses, we highlighted for the first-time sex-specific alterations in DNA methylation and gene expression patterns in late-gestation placentas exposed to alcohol. Interestingly, despite these molecular changes, the overall development of the placenta appeared unaffected. Through machine learning, we successfully identified a DNA methylation signature for identifying offspring exposed to alcohol during the early embryonic stages.

Sex-specific impact of preimplantation alcohol exposure on fetal growth and related pathways.

Prenatal alcohol exposure was previously shown to alter embryonic development in different contexts, by inducing fetal growth restriction or growth delay (5, 11, 12). With our model of preimplantation alcohol exposure, we found that the impact of preimplantation alcohol exposure on growth and related pathways was more pronounced in our male ethanol-exposed samples. We observed dysregulation in genes involved in the regulation of growth, cytoskeleton organization, placental development, and vascularization specifically in the male ethanol-exposed group. Furthermore, we noted a reduction in fetal weight only in male embryos, indicating that males may be more susceptible to growth retardation following preimplantation alcohol exposure. However, it is worth noting that previous studies from our group using our model of preimplantation alcohol exposure showed a similar percentage of growth-delayed embryos in both males and females (approximately 5% in each sex) at mid-gestation (11). One hypothesis that could explain this discrepancy between male and female at different developmental stages is that some female embryos with growth delays at mid-gestation may have had the ability and resources to catch up on their development and eventually achieve a similar fetal weight to control embryos in later

development. Existing literature suggests that female embryos generally exhibit greater adaptability to adverse *in utero* environment than male embryos, by being able to mediate their development even with altered resource availability (20-22). We observed many genes related to regulation of growth or development presenting dysregulated methylation and/or expression patterns in male ethanol-exposed placentas, such as *Bmp6*, *Fgf1*, *Fgf2*, *Slc16a3*, *Tro*, *Clstn3*, and *Zfhx3* that were previously reported in the literature to be directly linked to embryonic growth restriction. For instance, a study recently showed that injection of *Fgf2* (down-expressed in our male ethanol-exposed placentas) in a rat model of preeclampsia was shown to improve the clinical outcomes, including an attenuation of fetal growth restriction (23). Mutation of *Fgf1* (increased methylation in our male ethanol-exposed placentas) was also previously linked to preeclampsia in human (24), while *Bmp6* (decreased methylation in our male ethanol-exposed placentas) was previously reported as being down-expressed in fetal kidneys of rat presenting intrauterine growth restriction (IUGR) in a model of induced hypertension by chronic administration of insulin (25). Molecular alterations observed in those specific genes in our male ethanol-exposed placentas may significantly contribute to the inability of male embryos to achieve normal development and reach a similar fetal weight than control embryos throughout gestation.

Preimplantation alcohol exposure had a greater impact on imprinted and placenta developmental genes in male placentas.

Methylation patterns of imprinted genes at the differentially methylated regions, as well as the DNA methylation and expression of genes crucial for placental development, can significantly influence proper embryo development. Despite placental development being largely completed by late gestation, aberrant epigenetic and transcriptomic profiles of key genes can disrupt placental function, especially if those dysregulations were already present at earlier developmental stages (26). Although the histological analysis of the junctional and labyrinth zones showed comparable results between ethanol-exposed and control placentas in both sexes, we observed more alterations in imprinted or placenta developmental genes in male ethanol-exposed placentas compared to females.

Among the dysregulated genes, we observed differential methylation and expression of the imprinted gene *Grb10* in male ethanol-exposed placentas. The incorrect imprinted status of *Grb10*, especially at the imprinting control region, can directly affect embryonic development, as this gene

acts as a growth restrictor (27). The increased expression of *Grb10* observed in male ethanol-exposed placentas can therefore directly impact embryo growth development. Additionally, we observed both DNA methylation and gene expression dysregulation in the *H19*/*Igf2* cluster, including increased expression of the gene *Igf2r* in male ethanol-exposed placentas and increased methylation level in the ICR of the gene *Airn*. Similar to *Grb10*, *Igf2r* has been shown to negatively regulate embryo growth development (27, 28). This imprinted cluster was also identified in a previous study using a similar paradigm of alcohol exposure during preimplantation. In their study, Haycock & Ramsay showed decreased DNA methylation level at the ICR of *H19* in the placenta at mid-gestation (29). Moreover, they also observed a significant decrease in both ethanol-exposed fetal and placental weights also at mid-gestation and found a strong correlation between DNA methylation of the paternal allele of the *H19* locus and weights loss in the ethanol-exposed group (29). The abnormal methylation and expression profiles of imprinted genes can collectively impact proper embryo development and contribute to the observed reduction in fetal weight in males in our own observations.

Analysis of placenta developmental genes also revealed a higher number of genes with altered expression profiles in male ethanol-exposed placentas. Notably, we observed increased expression of *Dnmt3l*, a coactivator of *Dnmt3a* and *Dnmt3b*, which are responsible for *de novo* DNA methylation (30). During placenta development, *Dnmt3l* is essential for establishing proper maternal gene imprinting profiles and is highly expressed in trophoblasts (30-32). While the impact of *Dnmt3l* overexpression in the placenta is unknown, studies have demonstrated morphological defects and abnormal trophoblast patterns in *Dnmt3l* knockout mice, providing further evidence of its critical role in proper embryonic development (33, 34). Given its role in the establishment of genomic imprinting during development (30), we cannot exclude the potential impact of dysregulated *Dnmt3l* expression on the incorrect DNA methylation and transcriptomic profiles observed in certain imprinted genes, such as the maternally methylated genes *Peg10*, *Jade1*, or *Zrsr1* in male ethanol-exposed placentas.

Dysregulation of the placental epigenetic and transcriptomic landscape could play a role on proper embryonic brain development.

The placenta-brain axis has received considerable attention in recent years, and it is now well-established that placental dysregulation can lead to adverse effects on brain development and

function. Neurodevelopmental disorders and intellectual disabilities are commonly observed in Fetal Alcohol Spectrum Disorders (FASD), resulting from disruptions during brain development and incomplete maturation (5). While the impact of endocrine placental dysfunctions on brain development is increasingly understood, the role of placental epigenetic and transcriptomic dysregulation has been less explored. Among the many gene ontology enrichments observed in our data, two main pathways emerged that could directly affect normal brain development in embryos. Firstly, we found that male-specific DMRs were enriched in a pathway related to synaptic transmission, with dysregulated genes such as *Asic1*, *Cbln1*, and *Plk2*. Additionally, transcriptomic analysis revealed that one of the main pathways enriched in female ethanol-exposed placentas was related to serotonin metabolism. Serotonin is a neurotransmitter that regulates neurodevelopment during embryonic development, and the placenta plays a neuroendocrine role by producing and providing serotonin to the developing forebrain (35). Studies have shown that placental insufficiency, including inadequate serotonin supply to the embryo, is associated with the development of mental health issues and reduced cognitive abilities (35).

Among the affected genes in our model, *Itgb3*, which was down-regulated in female ethanol-exposed placentas, has been shown to have adverse effects on vascularization structure in the placenta when knocked out in a sheep model, compromising nutrient transport (36). It is also directly involved in serotonin uptake by interacting with different serotonin transporters (37). Another affected gene, *Slc22a2* (*Oct2*), was overexpressed in female ethanol-exposed placentas. Apart from its normal imprinting in the placenta, this gene has been implicated in serotonin clearance (38). Together, these two genes could negatively modulate serotonin uptake in the developing brain through altered endocrine function of the placenta and disrupted communication, further emphasizing the impact of the placenta on the health and proper development of the embryo.

Distinct patterns of DNA methylation dysregulation in female and male ethanol-exposed placentas.

DNA methylation analysis of late-gestation placentas following preimplantation alcohol exposure uncovered sex-specific regions with altered methylation. Moreover, we also observed different patterns of alteration depending on the sex. While male ethanol-exposed placentas showed a similar number of regions presenting increased and decreased methylation in ethanol-exposed placentas, female ethanol-exposed placentas displayed a high proportion of regions with increased

methylation. Interestingly, when categorizing those DMRs based on their proximity to CpG islands, we observed that almost half of the regions showing a decrease in methylation in the female ethanol-exposed placentas were located in CpG islands, CpG shores or CpG shelves, while the vast majority of female DMRs with increased methylation were located on "Open sea" regions. Both decreased and increased male DMRs were mostly located in Open sea regions. This suggests a sex-specific effect on DNA methylation based on CpG content following preimplantation alcohol exposure.

In a recent study of ours, we discovered a sex-biased profile of DNA methylation in genome-wide regions of control placentas at E18.5, indicating differential methylation patterns between male and female placentas (13). When comparing the DMRs following preimplantation alcohol exposure with sex-biased regions, we found that 115 male DMRs and 188 female DMRs were also sex-biased at late gestation. Importantly, these DMRs and sex-biased regions exhibited distinct distributions of CpG content based on sex. Notably, we observed a higher proportion of female sex-biased DMRs in CpG islands and shores than male sex-biased DMRs (13).

These sex-biased DNA methylation profiles during embryonic development could help explain the sex-specific dysregulations observed in both DNA methylation and gene expression. It is known that sex-biased differences exist during early development (13, 21), and the divergent profiles of DNA methylation may contribute to the observed sex-specific DMRs in late-gestation placenta. One possible assumption is that these specific regions may be more vulnerable to harmful exposures from the maternal environment due to their sex-specificity during development. Epigenetic dysregulations in these specific regions may progress differently in male and female cells, resulting in sex-specific DMRs in the placenta at late gestation following preimplantation alcohol exposure.

Further studies investigating the evolution of DNA methylation dysregulations in the placenta and trophectoderm cells during early development could provide insights into the variability of sex-biased regions when prenatal alcohol exposure occurs during preimplantation. Understanding the dynamics and mechanisms underlying these sex-specific effects will contribute to our knowledge of how prenatal alcohol exposure impacts placental function and subsequent developmental outcomes in a sex-dependent manner.

DNA methylation dysregulations in the placenta as a biomarker for early preimplantation alcohol exposure.

Finding a molecular diagnostic tool for early detection of FASD would be an unprecedented advance in the treatment and care of affected babies. In recent years, promising results published from 2 distinct research groups in Canada showed DNA methylation alterations in buccal swabs (buccal epithelial cells) from children with confirmed FASD (39-41). Moreover, one of these studies used their epigenetic signature with a machine learning approach to train and further efficiently validate the identification of confirmed FASD cases (41). Although these cells being easily accessible and requiring no invasive procedure to obtain, their epigenome will vary across ages and may generate some bias in the generation of accurate DNA methylation signatures. Moreover, the high renewal rate of these surface cells might not homogeneously show the altered epigenetic modifications caused by prenatal alcohol exposure. The heterogeneity of the prenatal alcohol exposure paradigms and their effect on the epigenome of buccal epithelial cells also constitute an obstacle in establishing a universal DNA methylation signature. Tissues or cell types more directly exposed to alcohol during gestation might be a more promising alternative. In this perspective, the placenta could be an effective avenue to detect FASD at birth when there is a suspicion of prenatal alcohol exposure since its development occurs rapidly during gestation. A previous study using preconception and gestational exposure to cannabis also observed common DNA methylation dysregulations in the placenta and the brain of exposed embryos (42), showing that the placenta might effectively mirror some epigenetic alterations present in the brain. In our study, we showed that even if the alcohol exposure happens as early as the 8-cell stage, lasting DNA methylation changes occur in the placenta. Furthermore, we were able to establish a unique signature to perfectly separate control and ethanol-exposed samples with machine learning. The short life of the placenta might also best represent epigenetic alterations caused by prenatal alcohol exposure happening at any time during gestation. The placenta must be thought as an organ having a high potential to teach us more about what transpired during pregnancy and how it may have affected embryonic development. By developing one or multiple divergent epigenetic signatures – based on different prenatal alcohol exposure paradigms and patterns – in the placenta at birth, we could establish a reliable diagnostic tool, based on molecular modifications and guarantee an optimal support system to FASD children from their early life.

CONCLUSION

With this study, we showed that early preimplantation alcohol exposure can alter molecular profiles of the mouse placenta at late gestation. More precisely, our study provides valuable insights into the sex-specific epigenetic and transcriptomic consequences of early prenatal alcohol exposure on the placenta, contributing to a better understanding of its potential effects on placental function and fetal development. Furthermore, this study highlighted for the first time that DNA methylation profiles of the placenta could be an excellent molecular diagnostic tool for early detection of FASD. Further studies based on our model will enable to decipher mechanisms of sex-specific placenta DNA methylation and gene expression alterations on both embryonic development and long-term implications.

METHOD

Preimplantation alcohol exposure mouse model

8-week-old female C57BL/6 mice were mated with same age C57BL/6 males (Charles River laboratories). The presence of visible copulatory plug the following morning confirmed pregnancy with day 0.5 embryos (E0.5). Pregnant females were separated from the males and housed together (n=2-3) in a 12 h light/dark cycle with unrestricted access to food and water. Like our previously published preimplantation binge-like alcohol exposure model (11), pregnant females at embryonic day E2.5 (8-cell stage) were injected with 2 doses of 2.5g/kg of 50% ethanol, while control groups received an equivalent volume of saline at 2h intervals. The pregnant females were housed under similar conditions with limited handling during gestation.

Tissue collection and Analysis

At E18.5, pregnant females were euthanized, the embryos and placentas were collected. The maternal tissue layer was removed from the placenta. The weight of embryos and placentas were recorded, and the placenta area was calculated using Leica stereo microscope and Leica LasX software. Placentas were flash frozen in liquid nitrogen and kept at -80°C for subsequent DNA and RNA extraction. The sex of each embryo and placenta was determined by probing for the *Ddx3x*

and *Ddx3y* genes by qPCR (LightCycler 96, Roche) of digested DNA obtained from the tail of each embryo (11, 12).

Histological analysis

Placentas were collected at E18.5 with the maternal decidua to facilitate handling. Placentas were fixed in 4% paraformaldehyde (PFA), post-fixed in 70% ethanol for 48h, and then divided into two identical sections for paraffin embedding. Cross-sections of 5µm thickness were stained with hematoxylin and eosin (H&E) (11) to measure junctional and labyrinth zones and imaging was done using the Zeiss Zen Axioscan Slide Scanner. Image processing and zone measurements were performed using ImageJ.

DNA/RNA extraction and library preparation

A total of 6 control placentas (3 males and 3 females from 3 different litters) and 10 ethanol-exposed placentas (5 males and 5 females from 5 different litters) were randomly selected from normal looking embryos and placentas. Whole placentas were ground, and an equivalent amount of powder from each sample was used to extract DNA using QIAamp DNA Micro kit (Qiagen #56304) and RNA using RNeasy Mini kit (Qiagen #74004), following manufacturer's recommendations. DNA and RNA extracts were quantified using QuBit fluorimeter apparatus using the Broad range DNA assay kit (ThermoFisher #Q32853) or the High Sensitivity RNA assay kit (ThermoFisher #Q32852).

DNA was used to produce methyl-seq libraries using the SureSelectXT Methyl-Seq Target Enrichment System with the mouse enrichment panel (Agilent #G9651B and #5191-6704) following manufacturer's recommendations, with an input of 1µg of DNA per sample. After final amplification/indexation, libraries were quantified using QuBit fluorimeter with the High Sensitivity DNA assay kit (ThermoFisher #Q32854) and quality was assessed by BioAnalyzer before paired-end sequencing on NovaSeq6000 S4 at the Genome Quebec core facility. Each library generated between 112M and 139M reads.

High-quality RNA (500 ng) was used to produce mRNA-seq libraries using NEBNext mRNA stranded library kit by the Genome Quebec core facility, followed by paired-end sequencing on NovaSeq6000 S4. Between 26M and 43M reads were obtained for each sequenced library.

Bioinformatics analysis

For Methyl-Seq sequencing results, analysis was performed using the GenPipes Methyl-Seq pipeline (v3.3.0) (43). Reads were aligned to the mouse reference genome (mm10) and methylation calls were obtained with Bismark (v0.18.1) (44). The R package MethylKit (version 1.8.1) (45) was used to obtain differentially methylated regions (DMRs) employing the Benjamini–Hochberg false discovery rate (FDR) procedure. Fixed parameters, such as 100 bp stepwise tiling windows, a minimum of 10% of difference in DNA methylation level between conditions and a threshold of $q < 0.01$ were applied. DNA methylation levels were calculated as the average methylation of all CpGs within a tile for all the samples within a condition (minimum 3 samples/condition/sex ≥10X sequencing depth) (11, 46). The bisulfite conversion rate (> 96%) and the number of CpGs per tile were obtained using a custom Perl script (11).

Annotation of all analyzed tiles was conducted using Homer (version 4.10.1) with the mouse mm10 reference genome (47). Gene ontology enrichment analyses were performed using the Metascape tool (48) with differentially methylated tiles located in genic regions as input. We obtained the coordinates of CpG islands from the UCSC table browser database (mm10 genome) (49). Additionally, we created CpG content tracks, namely CpG shores and CpG shelves, by extending 0-2 kb and 2-4 kb, respectively, from the CpG islands coordinates, as described previously (11, 46). The statistical analyses were performed using R (version 3.5.0) or GraphPad Prism (version 9.5.0).

For mRNA-seq data, post-sequencing bioinformatics analysis was performed on the mouse reference genome (mm10) using GenPipes RNA-Seq pipeline (v4.1.2) (43) with tools such as Trimmomatic (v0.36) (50), STAR (v2.5.3) (51), Picard (v2.9.0) and BWA (v0.7.12) (52). Gene counts matrix and differentially expressed genes (DEGs) were obtained using the R package DESeq2 (v1.24.0) (53). Genes with p-value <0.05 were considered significant.

For the establishment of a molecular signature of early preimplantation alcohol exposure, we used L1-regularized linear regression (Lasso) (54, 55) with cross-validation for the gene expression and DNA methylation profiles. The Curse of dimensionality (i.e., challenges stemming from training models on datasets with a large number of features relative to samples) was then addressed with the Synthetic Minority Over-sampling Technique (SMOTE) to counteract sample imbalances (56). A random forest classifier was trained on these balanced datasets to emphasize

the significance of the selected DEGs and DMRs in classification. The specific regions used to establish the signature were identified as being among the top-ranking based on the feature importance metric. The efficacy of these identified biomarkers in differentiating the two groups was subsequently substantiated through a two-sample t-test and a Wilcoxon rank-sum test while Receiver Operating Characteristic (ROC) curves were used to assess the discriminatory capacity of each biomarker (55).

Statistics

Statistical analysis that were not included in bioinformatic pipelines were performed using R (version 3.5.0) or GraphPad Prism (version 9.5.0). Statistical significance was calculated using unpaired *t* test with Welch's correction and including a *F* test for variance. All data are shown as the mean ± standard deviation (SD). *p*-value <0.05 were considered significant.

Study approval

All animal work conducted in this study was approved by the CHU Ste-Justine Research Center *Comité Institutionnel de Bonnes Pratiques Animales en Recherche* (CIBPAR) under the guidance of the Canadian Council on Animal Care (CCAC).

AUTHOR CONTRIBUTIONS

LML and SM designed the study. LML and MBL conducted experiments and contributed to data acquisition. LML, FFB, AL and ALA participated in data analysis. LML and SM wrote the manuscript. All authors read and approved the final manuscript.

ACKNOWLEDGEMENTS

We thank the McGraw lab for critical comments and suggestions, Elizabeth Maurice-Elder and Thomas Dupas for editing as well as the staff of the Centre de Recherche du CHU Sainte-Justine animal facility for their assistance.

REFERENCES

1. Hemberger M, Hanna CW, Dean W. Mechanisms of early placental development in mouse and humans. Nature reviews Genetics. 2020;21(1):27-43.
2. Simmons DG, Natale DR, Begay V, Hughes M, Leutz A, Cross JC. Early patterning of the chorion leads to the trilaminar trophoblast cell structure in the placental labyrinth. Development (Cambridge, England). 2008;135(12):2083-91.
3. Coussons-Read ME. Effects of prenatal stress on pregnancy and human development: mechanisms and pathways. Obstetric medicine. 2013;6(2):52-7.
4. Wadhwa PD, Entringer S, Buss C, Lu MC. The contribution of maternal stress to preterm birth: issues and considerations. Clinics in perinatology. 2011;38(3):351-84.
5. Popova S, Charness ME, Burd L, Crawford A, Hoyme HE, Mukherjee RAS, et al. Fetal alcohol spectrum disorders. Nature reviews Disease primers. 2023;9(1):11.
6. Lange S, Probst C, Gmel G, Rehm J, Burd L, Popova S. Global Prevalence of Fetal Alcohol Spectrum Disorder Among Children and Youth: A Systematic Review and Meta-analysis. JAMA pediatrics. 2017;171(10):948-56.
7. Canovas S, Ross PJ. Epigenetics in preimplantation mammalian development. Theriogenology. 2016;86(1):69-79.
8. Cole LA. New discoveries on the biology and detection of human chorionic gonadotropin. Reproductive biology and endocrinology : RB&E. 2009;7:8.
9. Organization WH. Global status report on alcohol and health 2018: World Health Organization; 2019.
10. Sedgh G, Singh S, Hussain R. Intended and unintended pregnancies worldwide in 2012 and recent trends. Studies in family planning. 2014;45(3):301-14.
11. Legault LM, Doiron K, Breton-Larrivée M, Langford-Avelar A, Lemieux A, Caron M, et al. Pre-implantation alcohol exposure induces lasting sex-specific DNA methylation programming errors in the developing forebrain. Clinical epigenetics. 2021;13(1):164.
12. Breton-Larrivée M, Elder E, Legault LM, Langford-Avelar A, MacFarlane AJ, McGraw S. Mitigating the detrimental developmental impact of early fetal alcohol exposure using a maternal methyl donor-enriched diet. FASEB journal : official publication of the Federation of American Societies for Experimental Biology. 2023;37(4):e22829.
13. Legault LM Breton-Larrivée M, Langford-Avelar A, Lemieux A, McGraw S. Sex-specific differences in DNA methylation and gene expression in late-gestation mouse placentas Biology of sex differences. Under review.
14. Coan PM, Burton GJ, Ferguson-Smith AC. Imprinted genes in the placenta--a review. Placenta. 2005;26 Suppl A:S10-20.
15. Proudhon C, Bourc'his D. Identification and resolution of artifacts in the interpretation of imprinted gene expression. Briefings in functional genomics. 2010;9(5-6):374-84.

16. Wang X, Soloway PD, Clark AG. A survey for novel imprinted genes in the mouse placenta by mRNA-seq. Genetics. 2011;189(1):109-22.
17. Lefebvre L. The placental imprintome and imprinted gene function in the trophoblast glycogen cell lineage. Reproductive biomedicine online. 2012;25(1):44-57.
18. Golding MC, Magri LS, Zhang L, Lalone SA, Higgins MJ, Mann MR. Depletion of Kcnq1ot1 non-coding RNA does not affect imprinting maintenance in stem cells. Development (Cambridge, England). 2011;138(17):3667-78.
19. Okae H, Hiura H, Nishida Y, Funayama R, Tanaka S, Chiba H, et al. Re-investigation and RNA sequencing-based identification of genes with placenta-specific imprinted expression. Human molecular genetics. 2012;21(3):548-58.
20. Christians JK, Ahmadzadeh-Seddeighi S, Bilal A, Bogdanovic A, Ho R, Leung EV, et al. Sex differences in the effects of prematurity and/or low birthweight on neurodevelopmental outcomes: systematic review and meta-analyses. Biology of sex differences. 2023;14(1):47.
21. Meakin AS, Cuffe JSM, Darby JRT, Morrison JL, Clifton VL. Let's Talk about Placental Sex, Baby: Understanding Mechanisms That Drive Female- and Male-Specific Fetal Growth and Developmental Outcomes. International journal of molecular sciences. 2021;22(12).
22. Bale TL. The placenta and neurodevelopment: sex differences in prenatal vulnerability. Dialogues in clinical neuroscience. 2016;18(4):459-64.
23. Martinez-Fierro ML, Garza-Veloz I, Castañeda-Lopez ME, Wasike D, Castruita-De la Rosa C, Rodriguez-Sanchez IP, et al. Evaluation of the Effect of the Fibroblast Growth Factor Type 2 (FGF-2) Administration on Placental Gene Expression in a Murine Model of Preeclampsia Induced by L-NAME. International journal of molecular sciences. 2022;23(17).
24. Marwa BA, Raguema N, Zitouni H, Feten HB, Olfa K, Elfeleh R, et al. FGF1 and FGF2 mutations in preeclampsia and related features. Placenta. 2016;43:81-5.
25. Bursztyn M, Gross ML, Goltser-Dubner T, Koleganova N, Birman T, Smith Y, et al. Adult hypertension in intrauterine growth-restricted offspring of hyperinsulinemic rats: evidence of subtle renal damage. Hypertension (Dallas, Tex : 1979). 2006;48(4):717-23.
26. Apicella C, Ruano CSM, Méhats C, Miralles F, Vaiman D. The Role of Epigenetics in Placental Development and the Etiology of Preeclampsia. International journal of molecular sciences. 2019;20(11).
27. Plasschaert RN, Bartolomei MS. Genomic imprinting in development, growth, behavior and stem cells. Development (Cambridge, England). 2014;141(9):1805-13.
28. Sleutels F, Tjon G, Ludwig T, Barlow DP. Imprinted silencing of Slc22a2 and Slc22a3 does not need transcriptional overlap between Igf2r and Air. The EMBO journal. 2003;22(14):3696-704.
29. Haycock PC, Ramsay M. Exposure of mouse embryos to ethanol during preimplantation development: effect on DNA methylation in the h19 imprinting control region. Biology of reproduction. 2009;81(4):618-27.
30. Bourc'his D, Xu GL, Lin CS, Bollman B, Bestor TH. Dnmt3L and the establishment of maternal genomic imprints. Science (New York, NY). 2001;294(5551):2536-9.

31. Logan PC, Mitchell MD, Lobie PE. DNA methyltransferases and TETs in the regulation of differentiation and invasiveness of extra-villous trophoblasts. Frontiers in genetics. 2013;4:265.
32. Joh K. Transcription-dependent DNA methylation at the imprinted Zrsr1-DMR. bioRxiv. 2018:249524.
33. Arima T, Hata K, Tanaka S, Kusumi M, Li E, Kato K, et al. Loss of the maternal imprint in Dnmt3Lmat-/- mice leads to a differentiation defect in the extraembryonic tissue. Developmental biology. 2006;297(2):361-73.
34. Andrews S, Krueger C, Mellado-Lopez M, Hemberger M, Dean W, Perez-Garcia V, et al. Mechanisms and function of de novo DNA methylation in placental development reveals an essential role for DNMT3B. Nature communications. 2023;14(1):371.
35. Rosenfeld CS. Placental serotonin signaling, pregnancy outcomes, and regulation of fetal brain development†. Biology of reproduction. 2020;102(3):532-8.
36. Frank JW, Steinhauser CB, Wang X, Burghardt RC, Bazer FW, Johnson GA. Loss of ITGB3 in ovine conceptuses decreases conceptus expression of NOS3 and SPP1: implications for the developing placental vasculature†. Biology of reproduction. 2021;104(3):657-68.
37. Whyte A, Jessen T, Varney S, Carneiro AM. Serotonin transporter and integrin beta 3 genes interact to modulate serotonin uptake in mouse brain. Neurochemistry international. 2014;73:122-6.
38. Bacq A, Balasse L, Biala G, Guiard B, Gardier AM, Schinkel A, et al. Organic cation transporter 2 controls brain norepinephrine and serotonin clearance and antidepressant response. Molecular psychiatry. 2012;17(9):926-39.
39. Laufer BI, Kapalanga J, Castellani CA, Diehl EJ, Yan L, Singh SM. Associative DNA methylation changes in children with prenatal alcohol exposure. Epigenomics. 2015;7(8):1259-74.
40. Portales-Casamar E, Lussier AA, Jones MJ, MacIsaac JL, Edgar RD, Mah SM, et al. DNA methylation signature of human fetal alcohol spectrum disorder. Epigenetics & chromatin. 2016;9:25.
41. Lussier AA, Morin AM, MacIsaac JL, Salmon J, Weinberg J, Reynolds JN, et al. DNA methylation as a predictor of fetal alcohol spectrum disorder. Clinical epigenetics. 2018;10:5.
42. Laufer BI, Neier K, Valenzuela AE, Yasui DH, Schmidt RJ, Lein PJ, et al. Placenta and fetal brain share a neurodevelopmental disorder DNA methylation profile in a mouse model of prenatal PCB exposure. Cell reports. 2022;38(9):110442.
43. Bourgey M, Dali R, Eveleigh R, Chen KC, Letourneau L, Fillon J, et al. GenPipes: an open-source framework for distributed and scalable genomic analyses. GigaScience. 2019;8(6).
44. Krueger F, Andrews SR. Bismark: a flexible aligner and methylation caller for Bisulfite-Seq applications. Bioinformatics (Oxford, England). 2011;27(11):1571-2.
45. Akalin A, Kormaksson M, Li S, Garrett-Bakelman FE, Figueroa ME, Melnick A, et al. methylKit: a comprehensive R package for the analysis of genome-wide DNA methylation profiles. Genome biology. 2012;13(10):R87.

46. Legault LM, Doiron K, Lemieux A, Caron M, Chan D, Lopes FL, et al. Developmental genome-wide DNA methylation asymmetry between mouse placenta and embryo. Epigenetics. 2020;15(8):800-15.
47. Heinz S, Benner C, Spann N, Bertolino E, Lin YC, Laslo P, et al. Simple combinations of lineage-determining transcription factors prime cis-regulatory elements required for macrophage and B cell identities. Molecular cell. 2010;38(4):576-89.
48. Zhou Y, Zhou B, Pache L, Chang M, Khodabakhshi AH, Tanaseichuk O, et al. Metascape provides a biologist-oriented resource for the analysis of systems-level datasets. Nature communications. 2019;10(1):1523.
49. Karolchik D, Hinrichs AS, Furey TS, Roskin KM, Sugnet CW, Haussler D, et al. The UCSC Table Browser data retrieval tool. Nucleic acids research. 2004;32(Database issue):D493-6.
50. Bolger AM, Lohse M, Usadel B. Trimmomatic: a flexible trimmer for Illumina sequence data. Bioinformatics (Oxford, England). 2014;30(15):2114-20.
51. Dobin A, Davis CA, Schlesinger F, Drenkow J, Zaleski C, Jha S, et al. STAR: ultrafast universal RNA-seq aligner. Bioinformatics (Oxford, England). 2013;29(1):15-21.
52. Li H, Durbin R. Fast and accurate short read alignment with Burrows-Wheeler transform. Bioinformatics (Oxford, England). 2009;25(14):1754-60.
53. Love MI, Huber W, Anders S. Moderated estimation of fold change and dispersion for RNA-seq data with DESeq2. Genome biology. 2014;15(12):550.
54. Xu Y, Wang X, Huang Y, Ye D, Chi P. A LASSO-based survival prediction model for patients with synchronous colorectal carcinomas based on SEER. Translational cancer research. 2022;11(8):2795-809.
55. Sohn I, Kim J, Jung SH, Park C. Gradient lasso for Cox proportional hazards model. Bioinformatics (Oxford, England). 2009;25(14):1775-81.
56. Taft LM, Evans RS, Shyu CR, Egger MJ, Chawla N, Mitchell JA, et al. Countering imbalanced datasets to improve adverse drug event predictive models in labor and delivery. Journal of biomedical informatics. 2009;42(2):356-64.

Tables

Table 1 : Sex-specific top 10 decrease- and increase-DMRs

Male-specific DMRs			
Condition	**Gene Name**	**Methylation change (%)**	**Annotation**
Decrease in EtOH-exposed	*(Hmox2)*	-33,13	Intergenic
Decrease in EtOH-exposed	*Trappc9*	-31,79	Intron
Decrease in EtOH-exposed	*Arsg*	-28,90	Intron
Decrease in EtOH-exposed	*Mir148b*	-28,61	Intron
Decrease in EtOH-exposed	*(Cplx2)*	-28,02	Intergenic

Decrease in EtOH-exposed	*Mrpl45*	-27,29	3' UTR
Decrease in EtOH-exposed	*(Slc1a5)*	-26,62	Intergenic
Decrease in EtOH-exposed	*(Cdh15)*	-26,58	Intergenic
Decrease in EtOH-exposed	*a*	-26,54	Intron
Decrease in EtOH-exposed	*Cacna2d3*	-25,99	Intron
Increase in EtOH-exposed	*Snai2*	36,27	Intron
Increase in EtOH-exposed	*Egln3*	29,58	Intron
Increase in EtOH-exposed	*(Ctrc)*	28,57	Intergenic
Increase in EtOH-exposed	*(Snai1)*	28,13	Intergenic
Increase in EtOH-exposed	*Pik3r4*	27,20	Exon
Increase in EtOH-exposed	*Me1*	27,06	Intron
Increase in EtOH-exposed	*Rubcnl*	26,94	Intron
Increase in EtOH-exposed	*(Chrna5)*	26,47	Intergenic
Increase in EtOH-exposed	*Ilf3*	25,76	3'UTR
Increase in EtOH-exposed	*(Tmem150cos)*	25,49	Intergenic
Female-specific DMRs			
Condition	**Gene Name**	**Methylation change (%)**	**Annotation**
Decrease in EtOH-exposed	*(Pla2g4d)*	-39,54	Intergenic
Decrease in EtOH-exposed	*Mfsd2a*	-37,35	Intron
Decrease in EtOH-exposed	*Pygo1*	-31,79	Intron
Decrease in EtOH-exposed	*(Plau)*	-29,63	Intergenic
Decrease in EtOH-exposed	*(Jun)*	-29,28	Intergenic
Decrease in EtOH-exposed	*Msx1os*	-28,73	Non-coding
Decrease in EtOH-exposed	*(Zfp57)*	-28,31	Intergenic
Decrease in EtOH-exposed	*Capza2*	-26,06	Intron
Decrease in EtOH-exposed	*(Hpf1)*	-25,90	Intergenic
Decrease in EtOH-exposed	*Traf6*	-25,16	Intron
Increase in EtOH-exposed	*(Ssbp3)*	37,50	Intergenic
Increase in EtOH-exposed	*Jdp2*	34,63	TTS
Increase in EtOH-exposed	*(Sox5os3)*	33,91	Intergenic
Increase in EtOH-exposed	*(Fam98b)*	32,86	Intergenic
Increase in EtOH-exposed	*(Usp7)*	32,66	Intergenic
Increase in EtOH-exposed	*Fgf12*	32,61	Intron
Increase in EtOH-exposed	*(Kpna1)*	32,06	Intergenic
Increase in EtOH-exposed	*Fam105a*	31,71	Intron
Increase in EtOH-exposed	*(Ppif)*	30,73	Intergenic
Increase in EtOH-exposed	*(Pax9)*	30,45	Intergenic

Table 2 : Shared top 10 decrease- and increase-DMRs

Shared top DMRs					
Condition Male	**Gene Name**	**Methylation change (%) Male**	**Condition Female**	**Methylation change (%) Female**	**Annotation**
Decrease in EtOH-exposed	Cdk8	-23,33	Decrease in EtOH-exposed	-12,21	Intron
Decrease in EtOH-exposed	(Mirt1)	-13,04	Decrease in EtOH-exposed	-12,24	Intergenic
Decrease in EtOH-exposed	Hs3st2	-12,54	Decrease in EtOH-exposed	-10,83	Exon
Decrease in EtOH-exposed	Tmem267	-12,51	Decrease in EtOH-exposed	-10,67	Promoter-TSS
Decrease in EtOH-exposed	Rbm3os	-10,07	Increase in EtOH-exposed	15,50	Promoter-TSS
Increase in EtOH-exposed	(Ifngas1)	15,22	Decrease in EtOH-exposed	-20,68	Intergenic
Increase in EtOH-exposed	(Slc22a19)	10,02	Decrease in EtOH-exposed	-10,61	Intergenic
Increase in EtOH-exposed	Tro	10,12	Increase in EtOH-exposed	13,77	Promoter-TSS
Increase in EtOH-exposed	Galp	15,12	Increase in EtOH-exposed	10,21	Exon
Increase in EtOH-exposed	(Spry1)	15,01	Increase in EtOH-exposed	15,70	Intergenic
Increase in EtOH-exposed	Clstn3	13,36	Increase in EtOH-exposed	15,06	Exon
Increase in EtOH-exposed	(Spry1)	13,08	Increase in EtOH-exposed	12,83	Intergenic
Increase in EtOH-exposed	Spry1	13,00	Increase in EtOH-exposed	16,15	Intergenic
Increase in EtOH-exposed	(Spry1)	12,05	Increase in EtOH-exposed	11,63	Intergenic
Increase in EtOH-exposed	Socs5	11,55	Increase in EtOH-exposed	13,67	Intron
Increase in EtOH-exposed	Psd3	11,40	Increase in EtOH-exposed	10,02	Intron
Increase in EtOH-exposed	Socs5	11,02	Increase in EtOH-exposed	11,20	Exon
Increase in EtOH-exposed	Wwox	10,80	Increase in EtOH-exposed	10,94	Intron
Increase in EtOH-exposed	(Trh)	10,18	Increase in EtOH-exposed	11,33	Intergenic

Table 3 : Sex-specific top 10 decrease- and increase- DEGs

Male-specific DEGs			
Condition	**Gene Name**	**Log2 fold change**	**p-value**
Decrease in EtOH-exposed	*Ear1*	-5,66	0,04
Decrease in EtOH-exposed	*Klk15*	-4,67	0,00
Decrease in EtOH-exposed	*Kap*	-4,31	0,01

Decrease in EtOH-exposed	*Ang2*	-4,03	0,05
Decrease in EtOH-exposed	*Pcdhb8*	-3,93	0,04
Decrease in EtOH-exposed	*Jsrp1*	-3,74	0,01
Decrease in EtOH-exposed	*Cdc20b*	-3,64	0,04
Decrease in EtOH-exposed	*Aadacl3*	-3,53	0,04
Decrease in EtOH-exposed	*Shisa3*	-3,11	0,01
Decrease in EtOH-exposed	*Crabp1*	-3,05	0,00
Increase in EtOH-exposed	*Lrrc4b*	4,38	0,01
Increase in EtOH-exposed	*C8a*	3,51	0,01
Increase in EtOH-exposed	*Alb*	3,43	0,02
Increase in EtOH-exposed	*Krt77*	3,34	0,04
Increase in EtOH-exposed	*Gria1*	3,24	0,03
Increase in EtOH-exposed	*Stmn3*	3,08	0,03
Increase in EtOH-exposed	*Fgg*	3,03	0,02
Increase in EtOH-exposed	*Trpm2*	2,95	0,02
Increase in EtOH-exposed	*Spink3*	2,94	0,03
Increase in EtOH-exposed	*Krt6b*	2,93	0,01
Female-specific DEGs			
Condition	**Gene Name**	**Log2 fold change**	***p*-value**
Decrease in EtOH-exposed	*Ddn*	-3,88	0,04
Decrease in EtOH-exposed	*Caly*	-3,86	0,04
Decrease in EtOH-exposed	*Serpinb2*	-2,89	0,01
Decrease in EtOH-exposed	*Dsc1*	-2,81	0,01
Decrease in EtOH-exposed	*Cyp2b19*	-2,63	0,00
Decrease in EtOH-exposed	*Cyp2ab1*	-2,46	0,02
Decrease in EtOH-exposed	*Dsg3*	-1,96	0,00
Decrease in EtOH-exposed	*Serpina3c*	-1,96	0,04
Decrease in EtOH-exposed	*Nol4*	-1,86	0,05
Decrease in EtOH-exposed	*Marco*	-1,74	0,03
Increase in EtOH-exposed	*Serpina1c*	4,96	0,00
Increase in EtOH-exposed	*Mir296*	4,73	0,00
Increase in EtOH-exposed	*Oprm1*	4,06	0,03
Increase in EtOH-exposed	*Klk1b8*	4,06	0,02
Increase in EtOH-exposed	*Fgf23*	4,04	0,04
Increase in EtOH-exposed	*Dmrt3*	3,86	0,03
Increase in EtOH-exposed	*St6galnac1*	3,67	0,05
Increase in EtOH-exposed	*Myot*	3,24	0,05
Increase in EtOH-exposed	*C6*	3,10	0,03
Increase in EtOH-exposed	*Pigr*	3,08	0,02

Table 4 : Shared top 10 decrease- and increase-DEGs

Shared top DEGs						
Condition Male	**Gene Name**	**Log2 fold change Male**	**p-value Male**	**Condition Female**	**Log2 fold change Female**	**p-value Female**
Decrease in EtOH-exposed	*Dok7*	-0,92	0,00	Decrease in EtOH-exposed	-0,60	0,03
Decrease in EtOH-exposed	*Spata2l*	-0,36	0,04	Decrease in EtOH-exposed	-0,39	0,04
Decrease in EtOH-exposed	*Foxf2*	-0,55	0,03	Decrease in EtOH-exposed	-0,38	0,02
Decrease in EtOH-exposed	*Chchd10*	-0,41	0,01	Decrease in EtOH-exposed	-0,33	0,01
Decrease in EtOH-exposed	*Timp2*	-0,44	0,04	Decrease in EtOH-exposed	-0,33	0,01
Decrease in EtOH-exposed	*Gpr156*	-0,52	0,01	Decrease in EtOH-exposed	-0,33	0,01
Decrease in EtOH-exposed	*Map2k6*	-0,37	0,02	Decrease in EtOH-exposed	-0,31	0,05
Decrease in EtOH-exposed	*St8sia5*	-0,61	0,00	Decrease in EtOH-exposed	-0,29	0,04
Decrease in EtOH-exposed	*Ypel3*	-0,32	0,00	Decrease in EtOH-exposed	-0,23	0,03
Decrease in EtOH-exposed	*Ifit2*	-0,43	0,02	Increase in EtOH-exposed	0,33	0,04
Increase in EtOH-exposed	*Dsc3*	1,74	0,05	Decrease in EtOH-exposed	-2,10	0,03
Increase in EtOH-exposed	*Dnajc6*	1,22	0,03	Increase in EtOH-exposed	0,87	0,04
Increase in EtOH-exposed	*Syt14*	0,60	0,00	Increase in EtOH-exposed	0,60	0,01
Increase in EtOH-exposed	*Pm20d1*	0,51	0,01	Increase in EtOH-exposed	0,55	0,00
Increase in EtOH-exposed	*Tceal7*	0,50	0,02	Increase in EtOH-exposed	0,51	0,01
Increase in EtOH-exposed	*Pdzk1ip1*	0,69	0,00	Increase in EtOH-exposed	0,47	0,04
Increase in EtOH-exposed	*Serpinb1a*	0,59	0,03	Increase in EtOH-exposed	0,46	0,02
Increase in EtOH-exposed	*Musk*	0,54	0,00	Increase in EtOH-exposed	0,40	0,04
Increase in EtOH-exposed	*Gsta3*	0,64	0,01	Increase in EtOH-exposed	0,40	0,04
Increase in EtOH-exposed	*Scel*	0,53	0,00	Increase in EtOH-exposed	0,28	0,04

Figures and legends

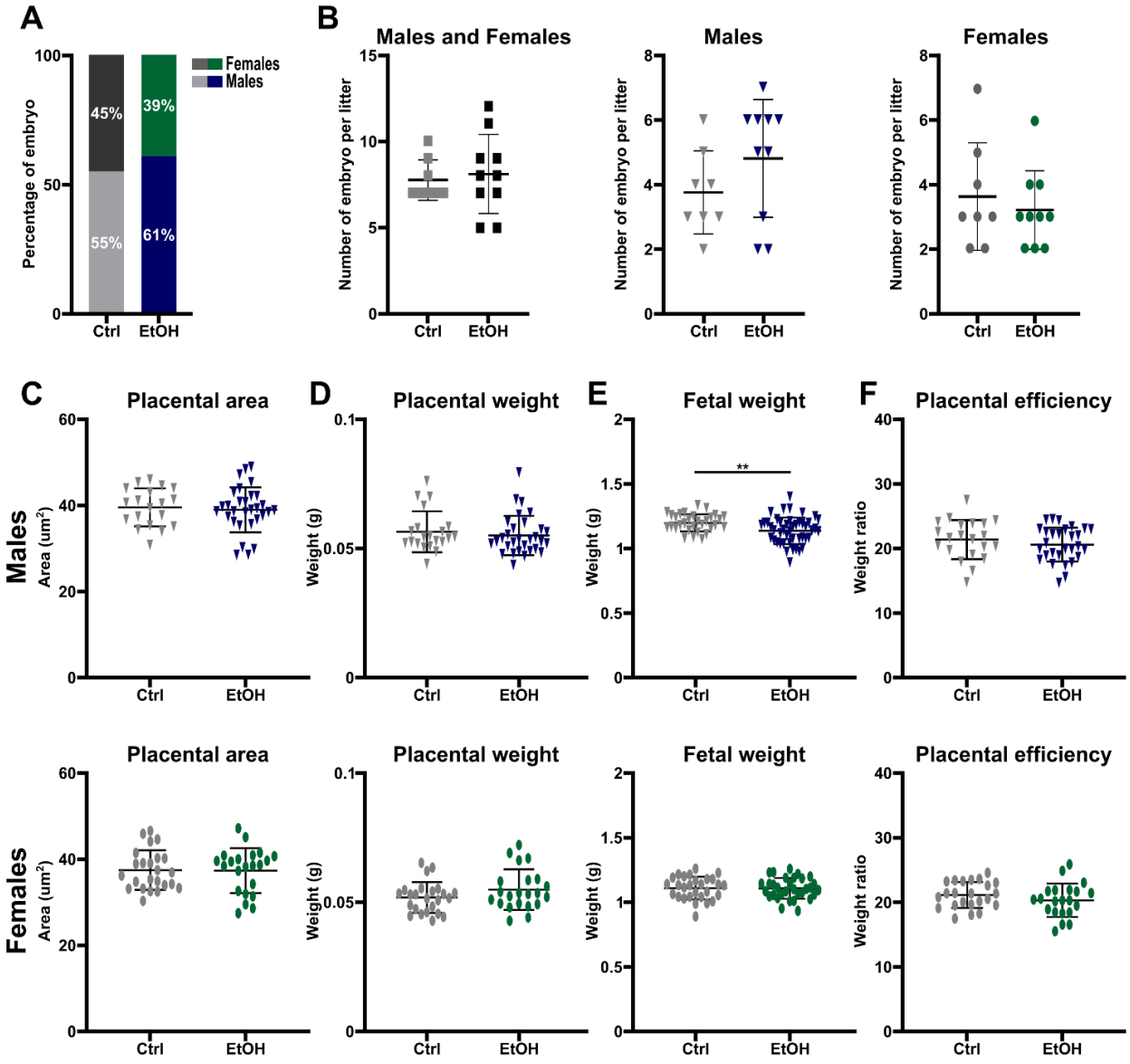

Figure 1: Absence of morphometric alterations in E18.5 placentas following preimplantation alcohol exposure.

A) Male and female embryo sex ratio of litters (control: males n = 47, females n = 39; ethanol-exposed: males n = 62, females n = 39). Percentage of embryos shown in bar graph. **B)** Number of E18.5 total embryos per litter in control (n = 8 litters; average 7.75 embryos/litter) and ethanol-exposed (n = 10 litters; average 8.10 embryos/litter) (left); number of male embryos per litter in controls (n = 8 litters; average 3.75 embryos/litter) and ethanol-exposed (n = 10 litters; average 4.80 embryos/litter) (center) and number of female embryos per litter in controls (n = 8 litters; average 3.63 embryos/litter) and ethanol-exposed (n = 10 litters; average 3.20 embryos/litter). **C)**

Placental surface area measurements in males (top) and females (bottom) at E18.5. Control embryos: (males n = 19; 6 litters; females n = 24; 6 litters), ethanol-exposed embryos (males n = 30; 6 litters; females n = 22; 6 litters). **D)** Placental weight in males (top) and females (bottom) at E18.5. Control embryos: (males n = 19; 6 litters; females n = 24; 6 litters), ethanol-exposed embryos (males n = 30; 6 litters; females n = 22; 6 litters). **E)** Fetal weight in males (top) and females (bottom) at E18.5. Control embryos: (males n = 31; 8 litters; females n = 28; 8 litters), ethanol-exposed embryos (males n = 46; 10 litters; females n = 32; 8 litters). **F)** Placental efficiency (fetal to placental weight ratio) in males (top) and females (bottom) at E18.5. Control embryos: (males n = 19; 6 litters; females n = 24; 6 litters), ethanol-exposed embryos (males n = 30; 6 litters; females n = 22; 6 litters). All data are represented as mean ± standard deviation (SD). Significant difference was assessed with *t* test by Welch's correction. **: $p<0.01$.

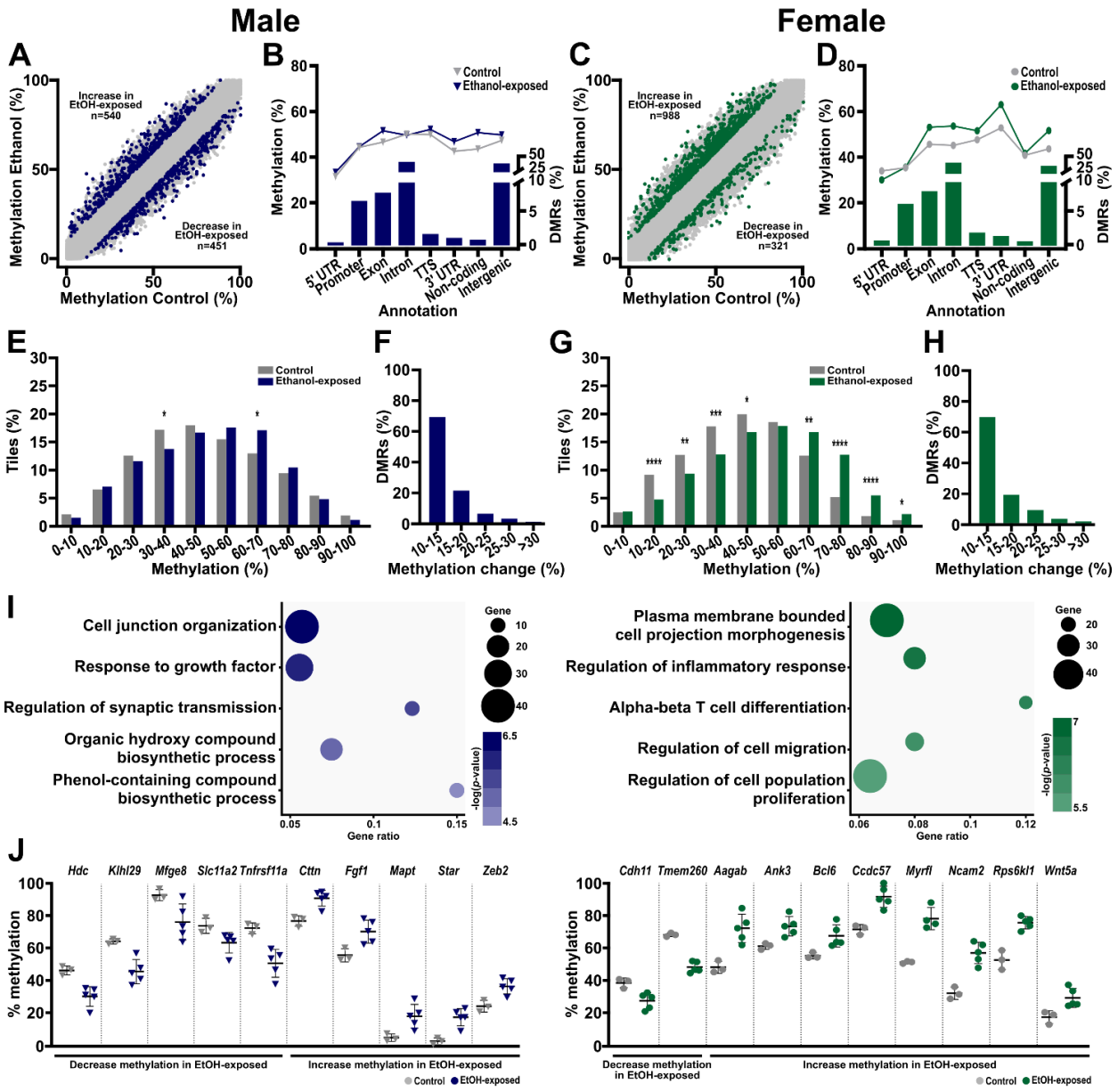

Figure 2: Sex-specific DNA methylation dysregulation in the placenta following early preimplantation alcohol exposure.

A) Scatterplot representing the DMRs between control and ethanol-exposed male placentas. Blue dots represent the tiles with a methylation change of at least 10% in ethanol-exposed compared to control placentas (n=991). **B)** CpG methylation levels in control and ethanol-exposed male placentas based on DMR annotation (left *Y*-axis) and DMR distribution across genomic annotations (right *Y*-axis). **C)** Scatterplot representing the DMRs between control and ethanol-exposed female placentas. Green dots represent the tiles with a methylation change of at least 10% in ethanol-

exposed compared to control placentas (n=1 309). **D)** CpG methylation levels in control and ethanol-exposed female placentas based on DMR annotation (left *Y*-axis) and DMR distribution across genomic annotations (right *Y*-axis). **E)** Tile distribution across ranges of DNA methylation levels in male control and ethanol-exposed DMRs (n=991). **F)** Proportion of male DMRs (n=991) associated with changes of CpG methylation levels between control and ethanol-exposed placentas. **G)** Tile distribution across ranges of DNA methylation levels in female control and ethanol-exposed DMRs (n=1 309). **H)** Proportion of female DMRs (n=1 309) associated with changes of CpG methylation levels between control and ethanol-exposed placentas. **I)** Functional enrichment analysis showing top enriched pathways for male DMRs (n=542 unique gene DMRs ; left, blue) and female DMRs (n=749 unique gene DMRs ; right, green) based on Metascape analysis for pathways and p value. **J)** Graph showing the CpG methylation levels in control and ethanol-exposed male (left; grey/blue) and female (right; grey/green) placentas for top changed DMRs or DMRs associated to top enriched pathways showed in **I)**. Data are represented as mean ± standard deviation (SD).

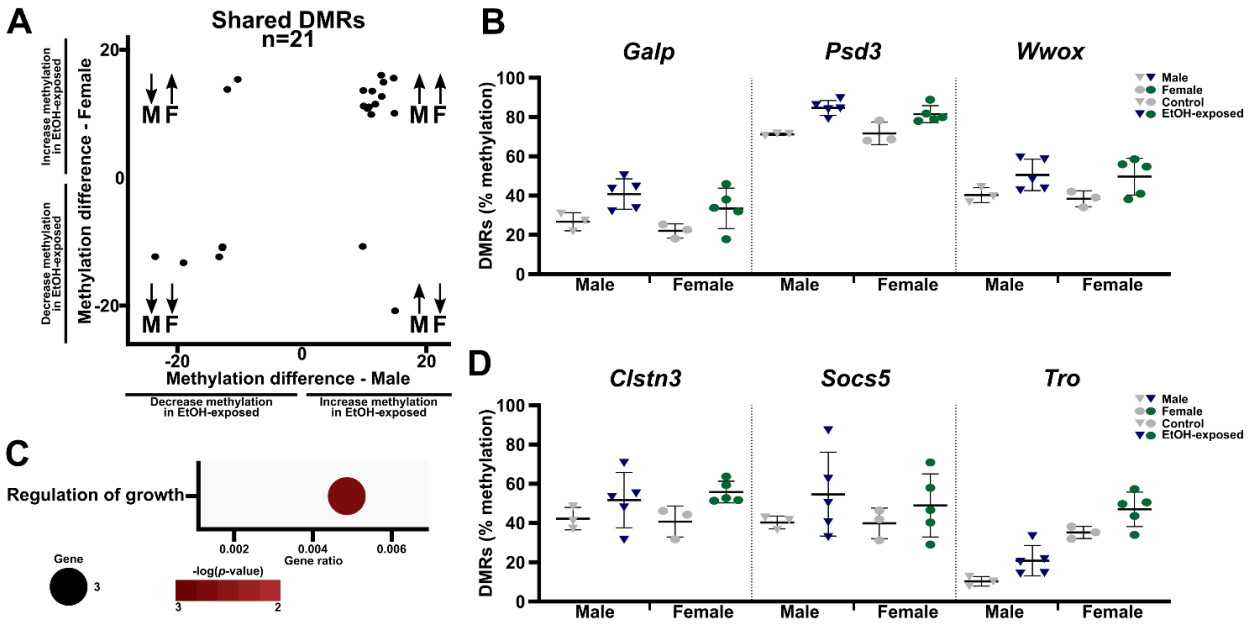

Figure 3: Regions presenting differential DNA methylation in ethanol-exposed male and female placentas are enriched in genes related to growth.

A) Scatterplot representing the percentage of change of the 21 shared DMRs between males (X axis) and females (Y axis). **B)** Graph showing the CpG methylation levels, of shared DMRs, in control and ethanol-exposed male (left; grey/blue) and female (right; grey/green) placentas. Data are represented as mean ± standard deviation (SD). **C)** Functional enrichment analysis showing top enriched pathways for shared DMRs (n=11 unique gene DMRs) based on Metascape analysis for pathways and p value. **D)** Graph showing the CpG methylation levels in control and ethanol-exposed male (left dots; grey/blue) and female (right dots; grey/green) placentas in DMRs located in genes related to regulation of growth as described by Metascape enrichment analysis in **C)**. Data are represented as mean ± standard deviation (SD).

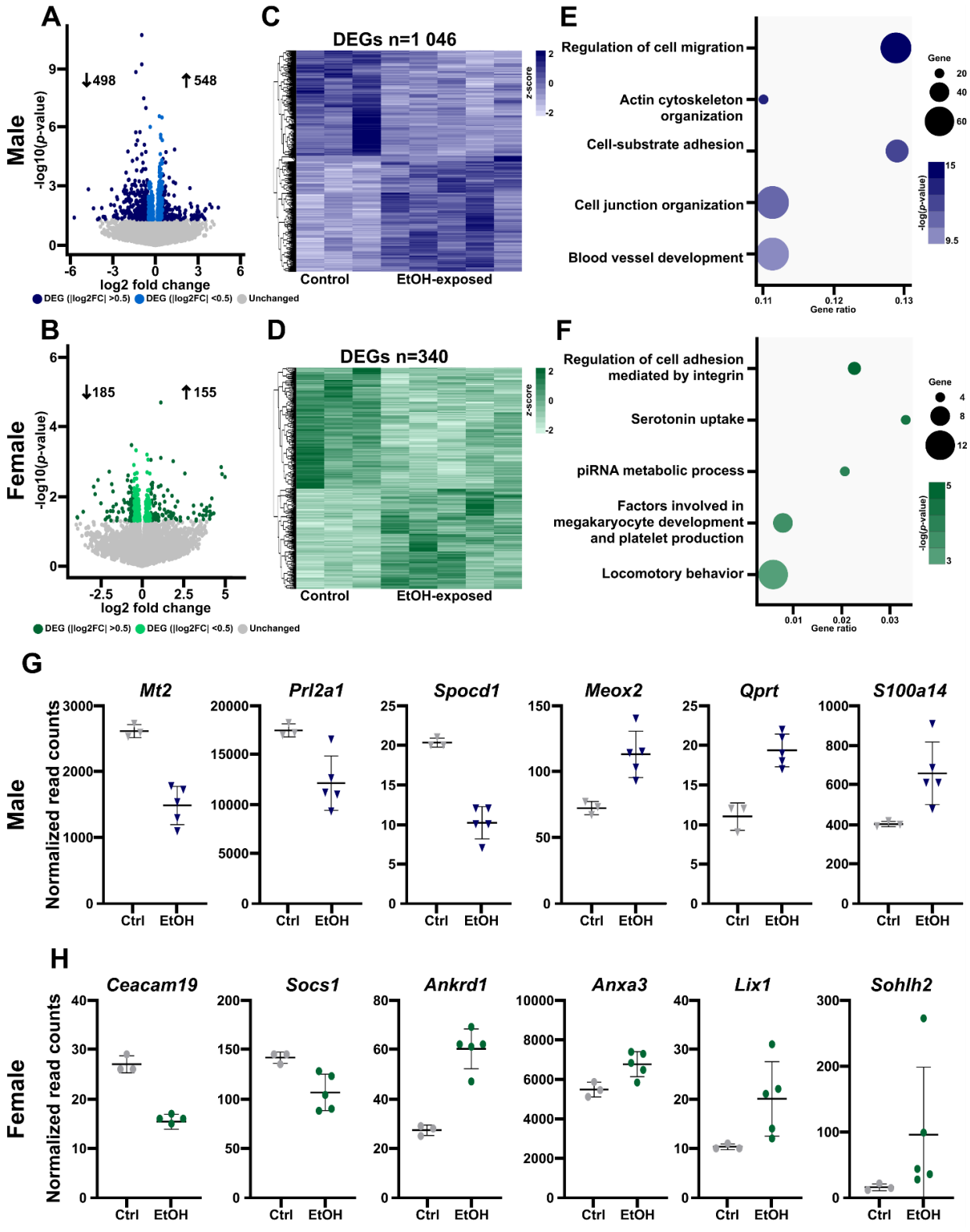

Figure 4: Gene expression profiles are especially affected in the male placenta following preimplantation alcohol exposure

A) and **B)** Differential expression analyses between control and ethanol-exposed placenta in males (A) and females (B). All colored dots represent statistically significant differentially expressed genes ($p<0.05$; males n = 1 046; females n = 340). Darker dots represent differentially expressed genes with log2 fold change values higher than 0.5 (males n = 359 ; females n = 157). **C)** and **D)** Heatmaps showing gene expression level (z score) of the 1 046 differentially expressed genes between control and ethanol-exposed male placentas (C) and the 340 differentially expressed genes in female placentas (D). **E)** and **F)** Functional enrichment analysis showing top enriched pathways for male DEG (E, n = 1 046) and female DEG (F, n = 340) based on Metascape analysis for pathways and p-value. **G)** and **H)** Representation (normalized read counts) of genes with altered expression in male (G) and female (H) ethanol-exposed placentas. Data are represented as mean ± standard deviation (SD).

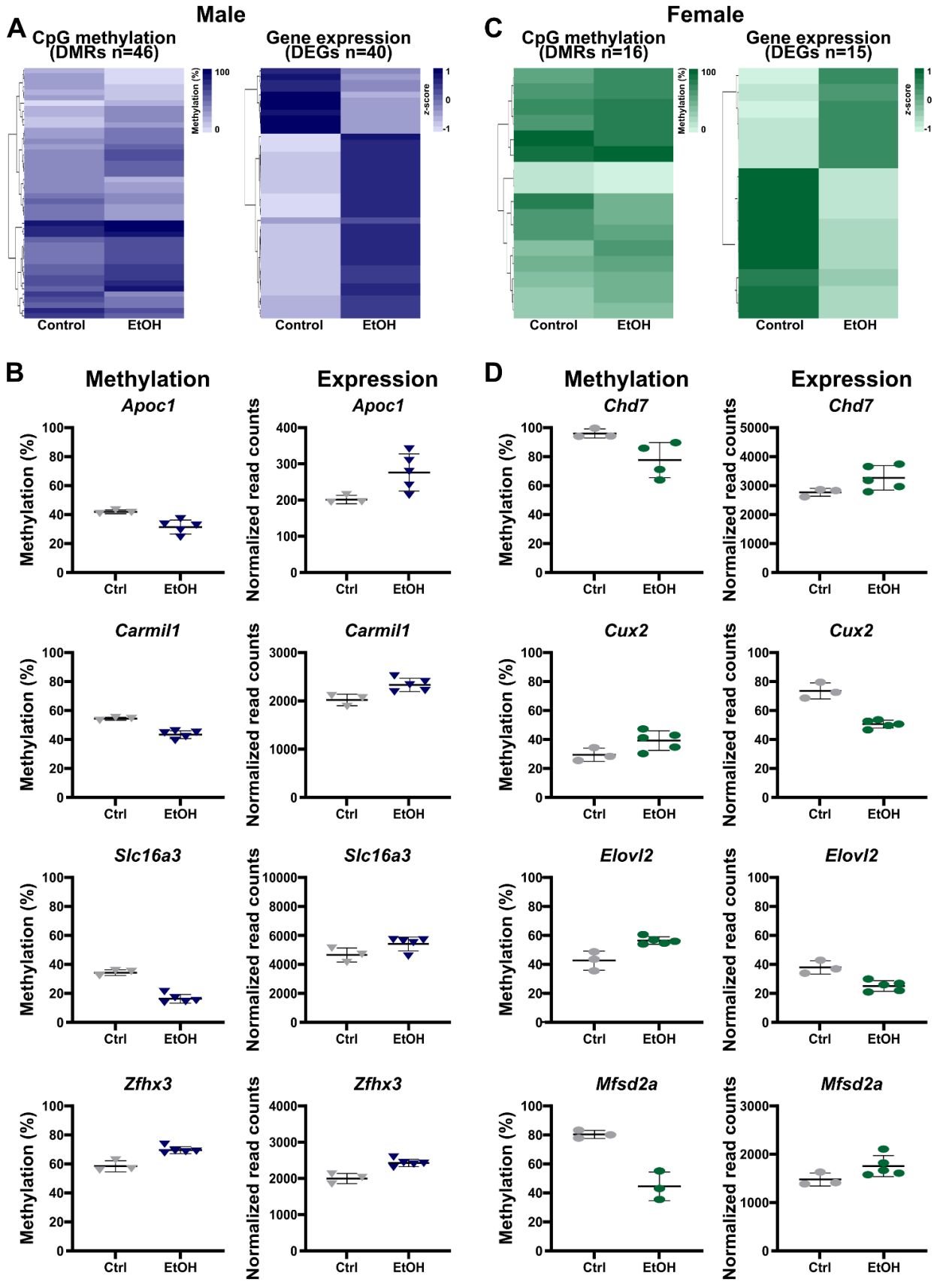
A
Male
CpG methylation (DMRs n=46)
Gene expression (DEGs n=40)
Methylation (%)
z-score
Control
EtOH
C
Female
CpG methylation (DMRs n=16)
Gene expression (DEGs n=15)
B
Methylation
Expression
Apoc1
Carmil1
Slc16a3
Zfhx3
D
Chd7
Cux2
Elovl2
Mfsd2a
Normalized read counts
Ctrl
EtOH

Figure 5 Sex-specific regions show both DNA methylation and gene expression alterations in the placenta at late-gestation in response to early preimplantation alcohol-exposure

A) and **C)** Heatmaps showing CpG methylation level (left heatmap) and gene expression levels (*z*-score; right heatmap) in genic regions (methylation) and genes (expression) presenting both DNA methylation (DMRs) and gene expression alterations (DEGs) between control and ethanol-exposed placentas in males (A; n= 46 DMRs, n= 42 DEG) and females (B; n= 16 DMRs, n= 15 DEG). **B)** and **D)** Representation (normalized read counts) of DEGs and DMRs in male (B) and female (D) placentas. Data are represented as mean ± standard deviation (SD).

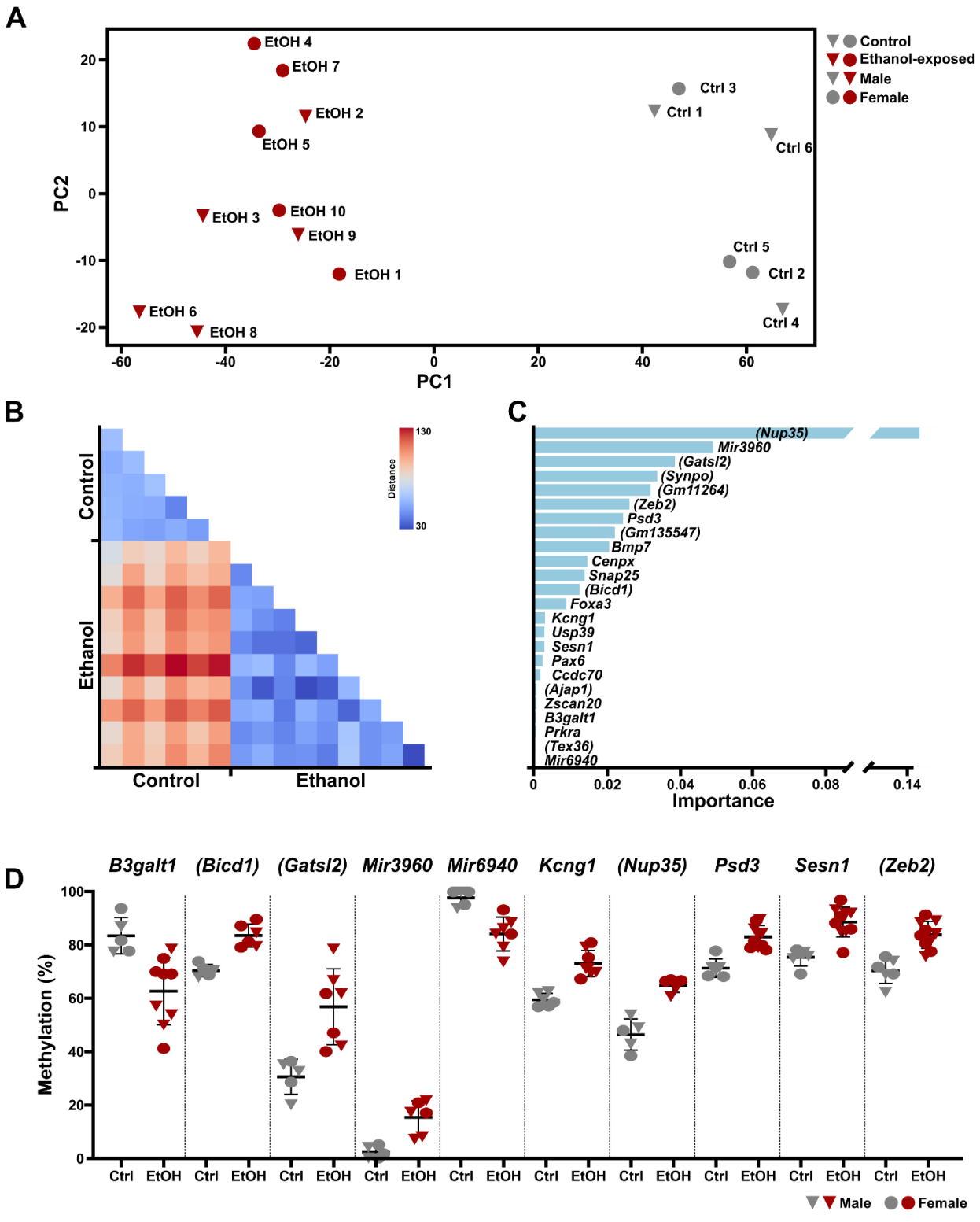

Figure 6: DNA methylation dysregulation signature in the late-gestation placenta as biomarkers of preimplantation alcohol exposure

A) Principal component analysis showing the clustering of control and ethanol-exposed samples based on their CpG methylation levels in the 24 regions (DMRs) identified as possible biomarkers. **B)** Heatmap of Eucledian distance of each control and ethanol-sample based on their CpG methylation level in the 24 regions identified as biomarkers. **C)** Feature importance plot of each region identified as biomarker based on LASSO analysis. Genes in brackets refer to the closest gene to which an intergenic DMR is located. **D)** Graph showing the CpG methylation level in control and ethanol-exposed male and female placental DMRs identified as biomarkers. Genes in brackets refer to the closest gene to which an intergenic DMR is located.

Supplementary figures and legends

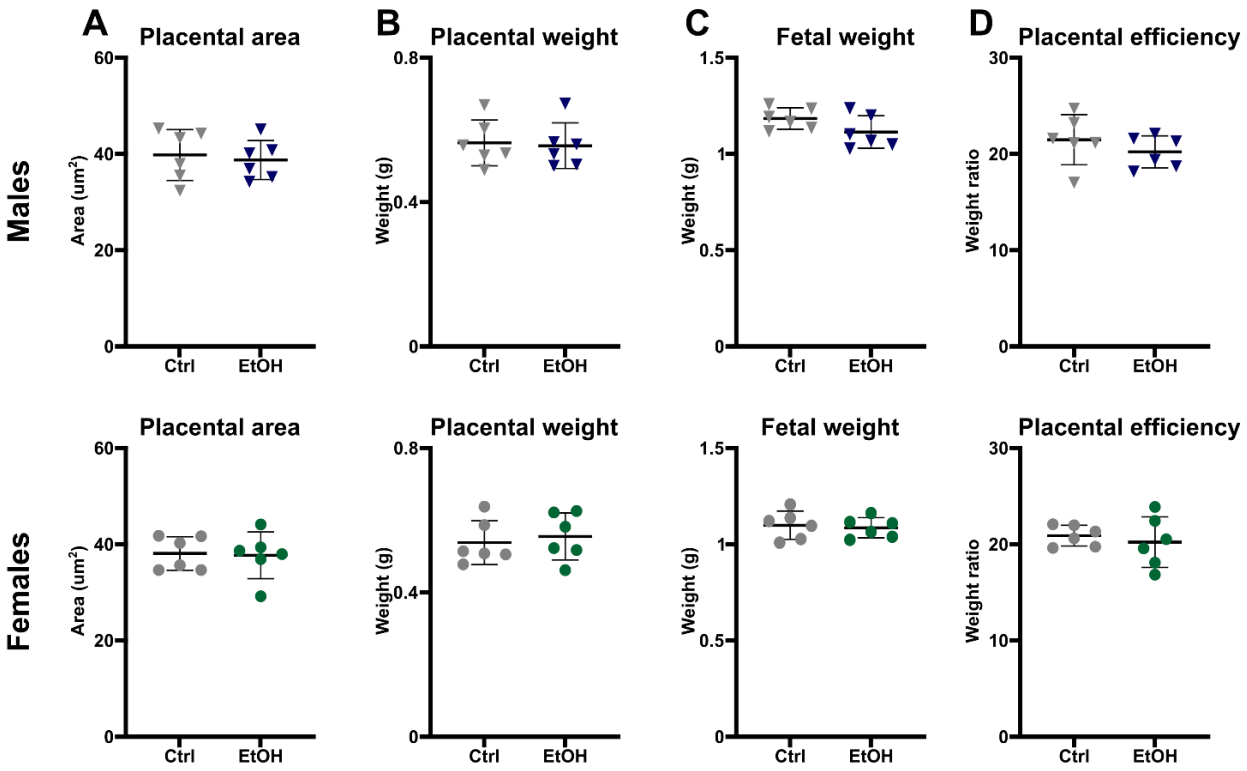

Figure Supp 1: Morphometric measurements on placentas and embryos

A) Average placental surface area measurements per litter in males (top) and females (bottom) at E18.5. Control embryos: (males n = 6 litters, 2-6 embryos per litter; females n = 6 litters, 2-7 embryos per litter), ethanol-exposed embryos (males n = 6 litters, 2-7 embryos per litter; females n = 6 litters, 2-6 embryos per litter). **B)** Average placental weight per litter in males (top) and females (bottom) at E18.5. Control embryos: (males n = 6 litters, 2-6 embryos per litter; females n = 6 litters, 2-7 embryos per litter), ethanol-exposed embryos (males n = 6 litters, 2-7 embryos per

litter; females n = 6 litters, 2-6 embryos per litter). **C)** Average fetal weight per litter in males (top) and females (bottom) at E18.5. Control embryos: (males n = 8 litters, 2-6 embryos per litter; females n = 8 litters, 2-7 embryos per litter), ethanol-exposed embryos (males n = 10 litters, 2-7 embryos per litter; females n = 10 litters, 2-6 embryos per litter). **D)** Average placental efficiency per litter (fetal to placental weight ratio) in males (top) and females (bottom) at E18.5. Control embryos: (males n = 6 litters, 2-6 embryos per litter; females n = 6 litters, 2-7 embryos per litter), ethanol-exposed embryos (males n = 6 litters, 2-7 embryos per litter; females n = 6 litters, 2-6 embryos per litter). All data are represented as mean ± standard deviation (SD). Significant difference was assessed by *t* test with Welch's correction.

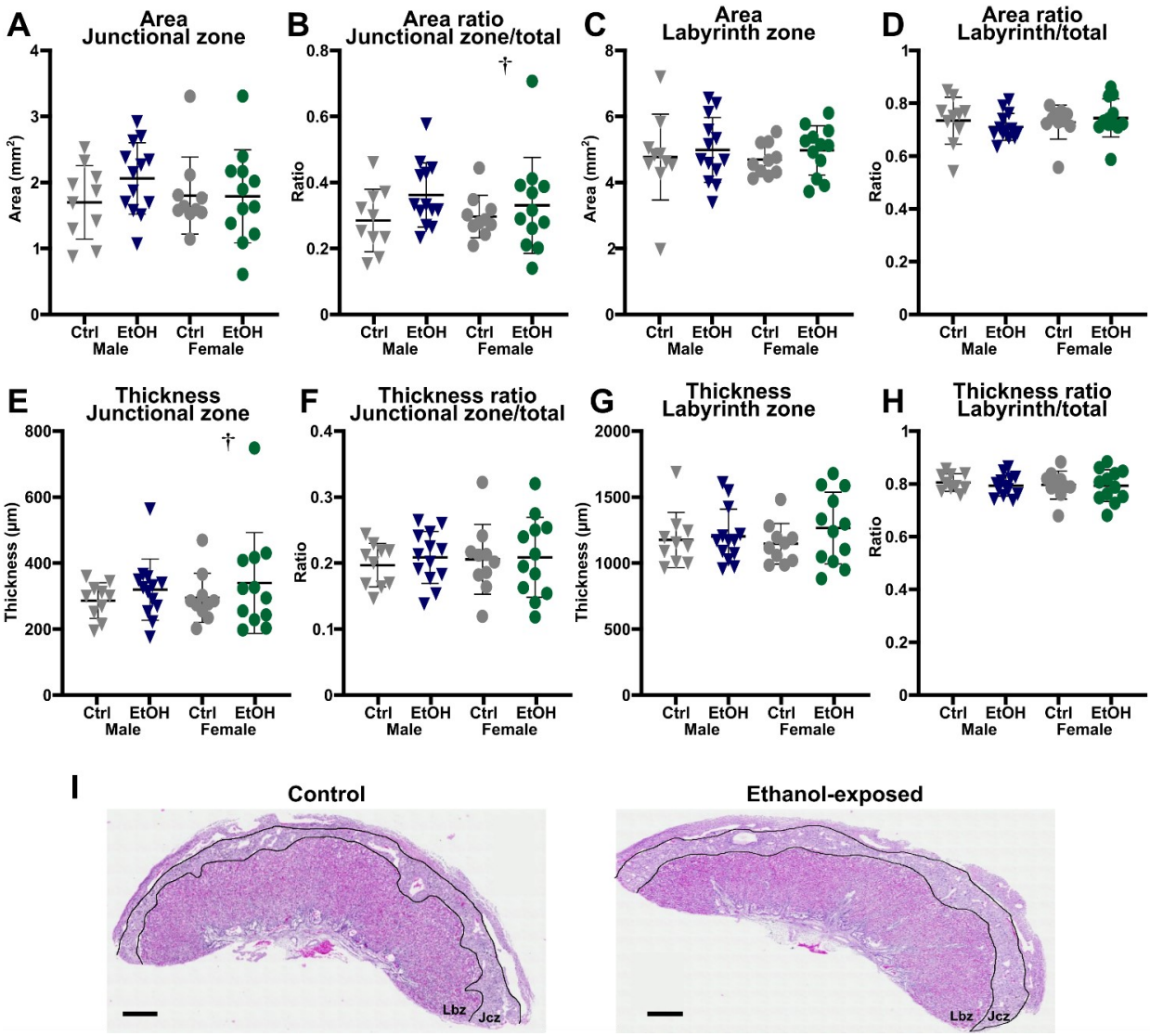

Figure Supp2: Increased variability in female ethanol-exposed placenta morphometrics

A) Histological morphometric measurements of E18.5 placentas based on cross section of the placenta: Area of junctional zone (Jcz). **B)** Ratio of the area of the junctional zone on the total placenta area. **C)** Area of the labyrinth zone (Lbz). **D)** Ratio of the area of the labyrinth zone on the total placenta area. **E)** Thickness of junctional zone. **F)** Ratio of the thickness of the junctional zone on the total placenta thickness. **G)** Thickness of the labyrinth zone. **H)** Ratio of the thickness of the labyrinth zone on the total placenta thickness. All data are represented as mean ± standard deviation (SD). Significant difference assessed with *t* test with Welch's correction and *F* test for the variance analysis. **I)** Representative example of H&E staining in controls (left) and ethanol-

exposed (right). The junctional zone (Jcz) and the the labyrinth zone (Lbz) are delimited by black lines. † Higher variance in ethanol-exposed placentas; *F* test $p<0.05$.

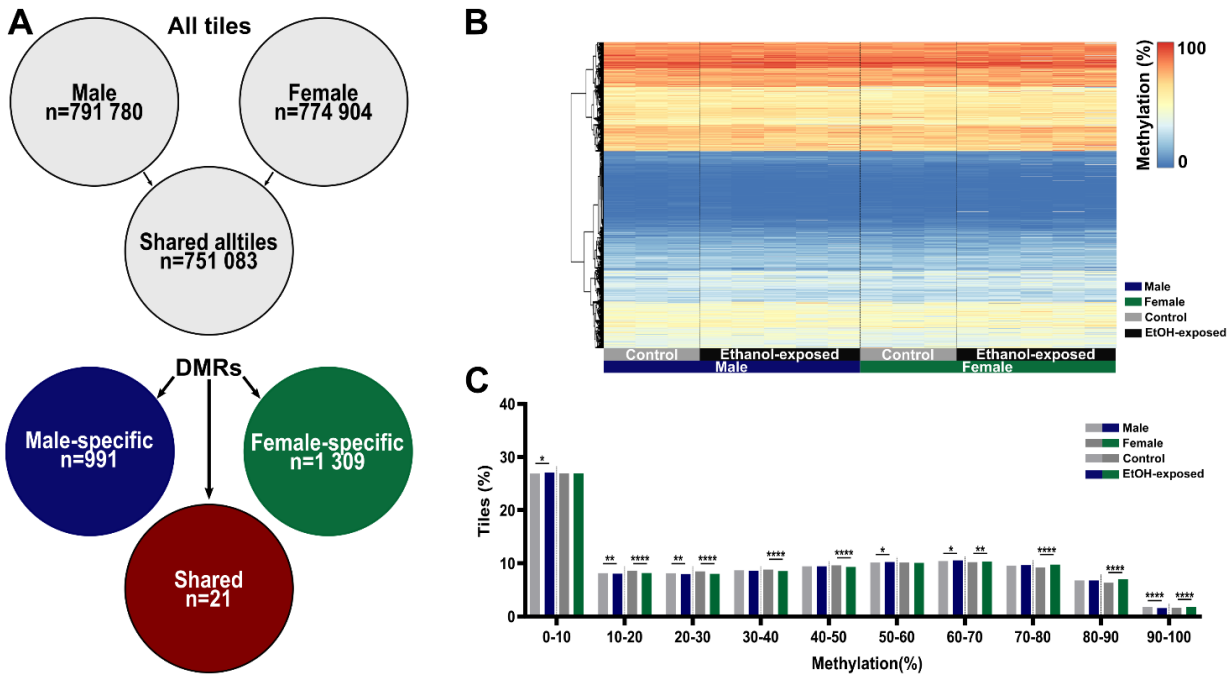

Figure Supp 3: Establishing DNA methylation profiles in E18.5 late-gestation placentas exposed to alcohol

A) Schematic design of sex-related genome-wide CpG methylation analysis in male (Ctrl n = 3, EtOH n = 5) and female (Ctrl n = 3, EtOH n =5) E18.5 placentas. Identification of all-tiles associated with either male samples (n = 791 780), female samples (n = 774 904), shared in male and female samples (n = 751 083), as well as male-specific (n = 991), female-specific (n = 1 309) and common (n = 21) DMRs (see "Methods" section for details). **B)** Heatmap showing DNA methylation levels for a random subset of tiles (~1% of 751 083 total tiles; 100b, coverage >10X) for individual male and female control and ethanol-exposed placenta samples. No clustering applied. **C)** Tile distribution across ranges of DNA methylation levels in male and female control and ethanol-exposed placentas (shared tiles; n = 751 083). ****p < 0.0001, **p < 0.01, *p < 0.05 *z*-test proportion test.

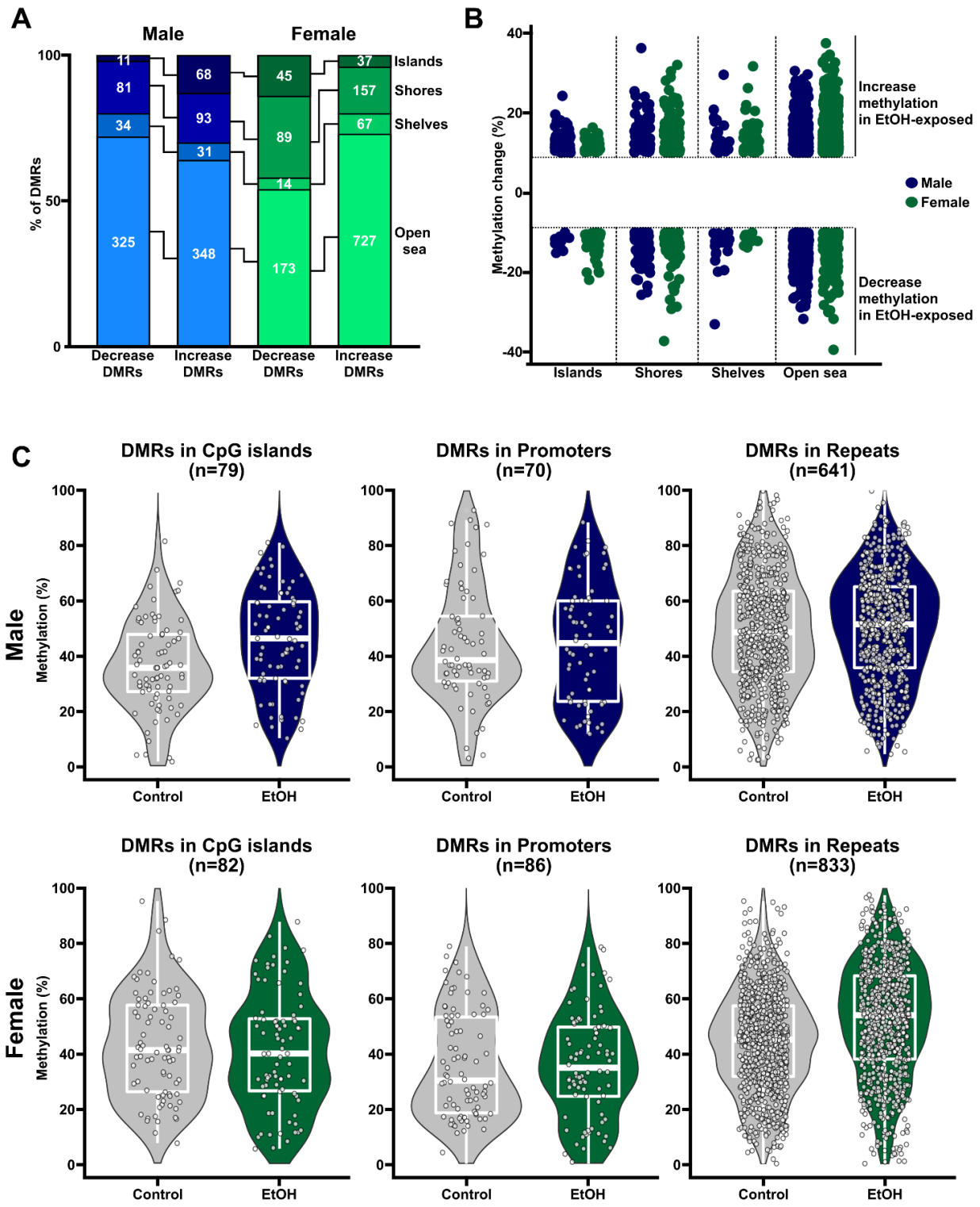

Figure Supp 4: Female ethanol-exposed placentas tend to loose methylation in CpG rich regions.

A) Distribution of the DMRs between control and ethanol-exposed in male (blue) and female (green) placentas based on their proximity to CpG rich regions (CpG island; CGI). Regions are defined as shore: up to ±2kb from CGIs, shelf: ±2–4kb from CGIs, and open sea: ±≥4kb from CGIs. **B)** Methylation difference of male (blue) and female (green) DMRs based on their proximity to CpG rich regions. **C)** DNA methylation distribution in male (blue; top) and female (green; bottom) in different CpG density contexts (CpG islands, promoters, repeats).

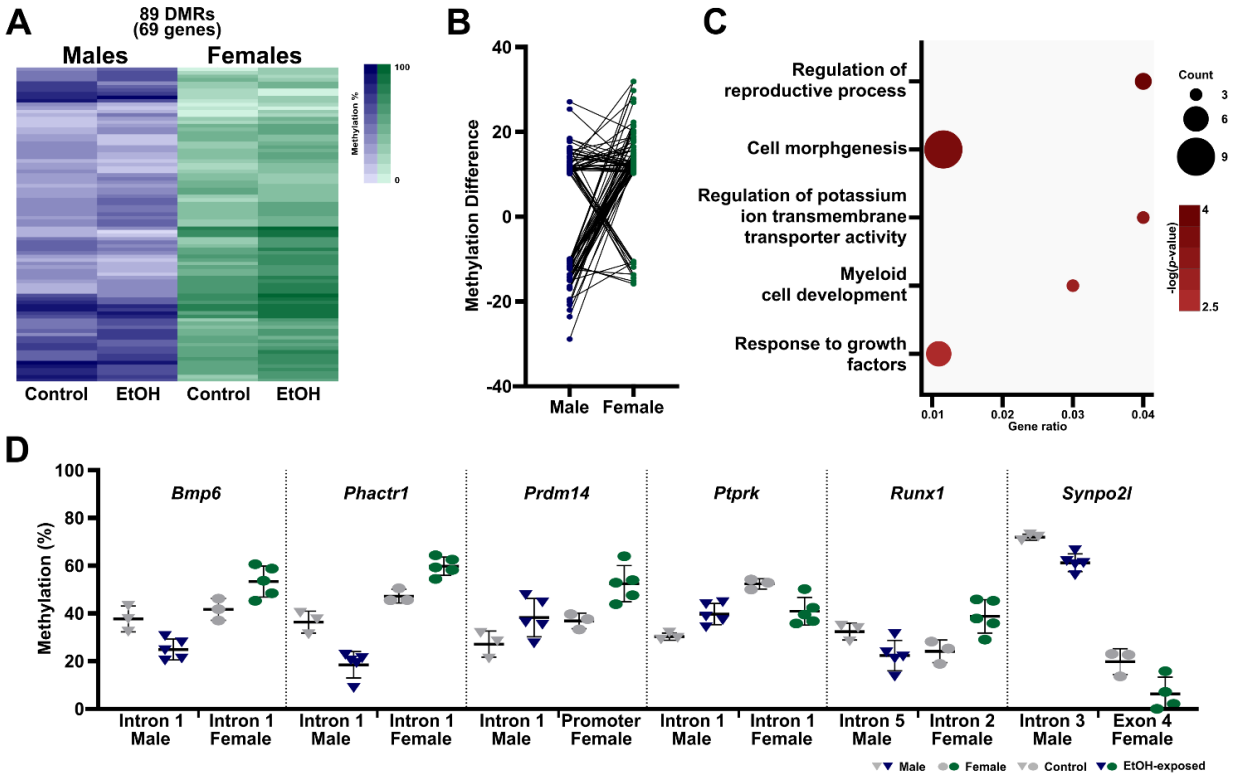

Figure supp 5: Changes in different regions of the same genes across sexes in ethanol-exposed placentas.

A) Heatmaps showing CpG methylation levels of different DMRs, in the same genes, for male (blue) or female (green) placentas. **B)** Methylation differences in males and females. Each

connected dot represents a DMR in a shared gene. **C)** Functional enrichment analysis showing top enriched pathways for common affected genes from male and female genic DMRs (n=69 unique gene) based on Metascape analysis for pathways and p value. **D)** Graph showing the CpG methylation levels in control and ethanol-exposed male (left dots; grey/blue) and female (right dots; grey/green) placentas for DMRs located in genes related to top enriched pathways as described by Metascape enrichment analysis in **BC)**. Data are represented as mean ± standard deviation (SD).

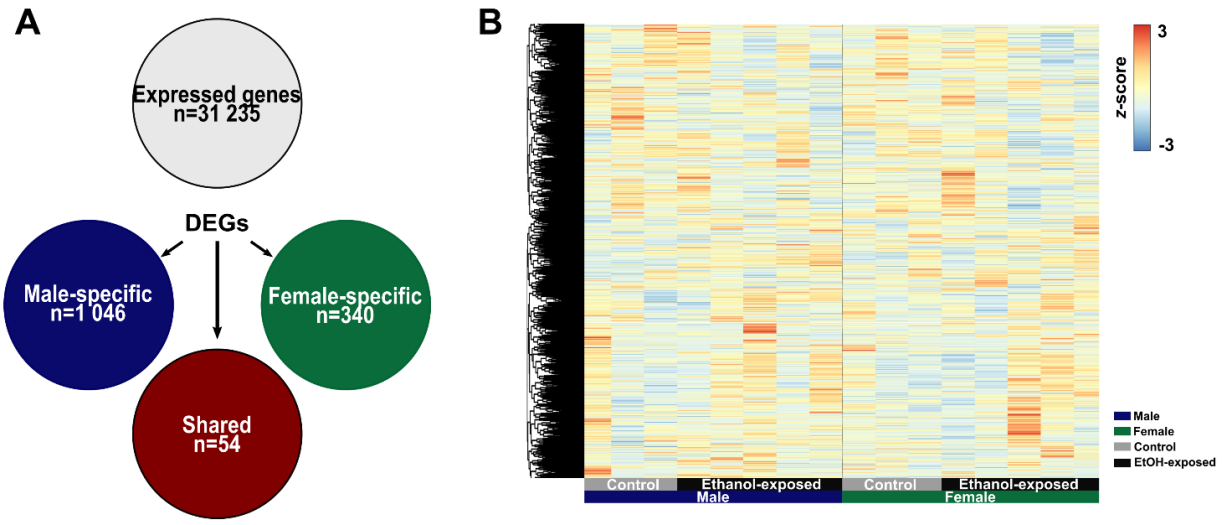

Figure supp 6: Establishing gene expression profiles in E18.5 placentas exposed to alcohol

A) Schematic design of sex-related differential transcriptomic analysis in male (Ctrl n = 3, EtOH n = 5) and female (Ctrl n = 3, EtOH n =5) E18.5 placentas. Identification of all expressed genes in both sexes (n = 31 235), male-specific differentially expressed genes (DEGs) (n= 1 046), female-specific DEGs (n = 340) and shared DEGs (n = 54) (see "Methods" section for details). **B)** Heatmap showing gene expression level (z score) of all analyzed genes (n= 31 235) for individual male and female control and ethanol-exposed placenta samples. No clustering applied.

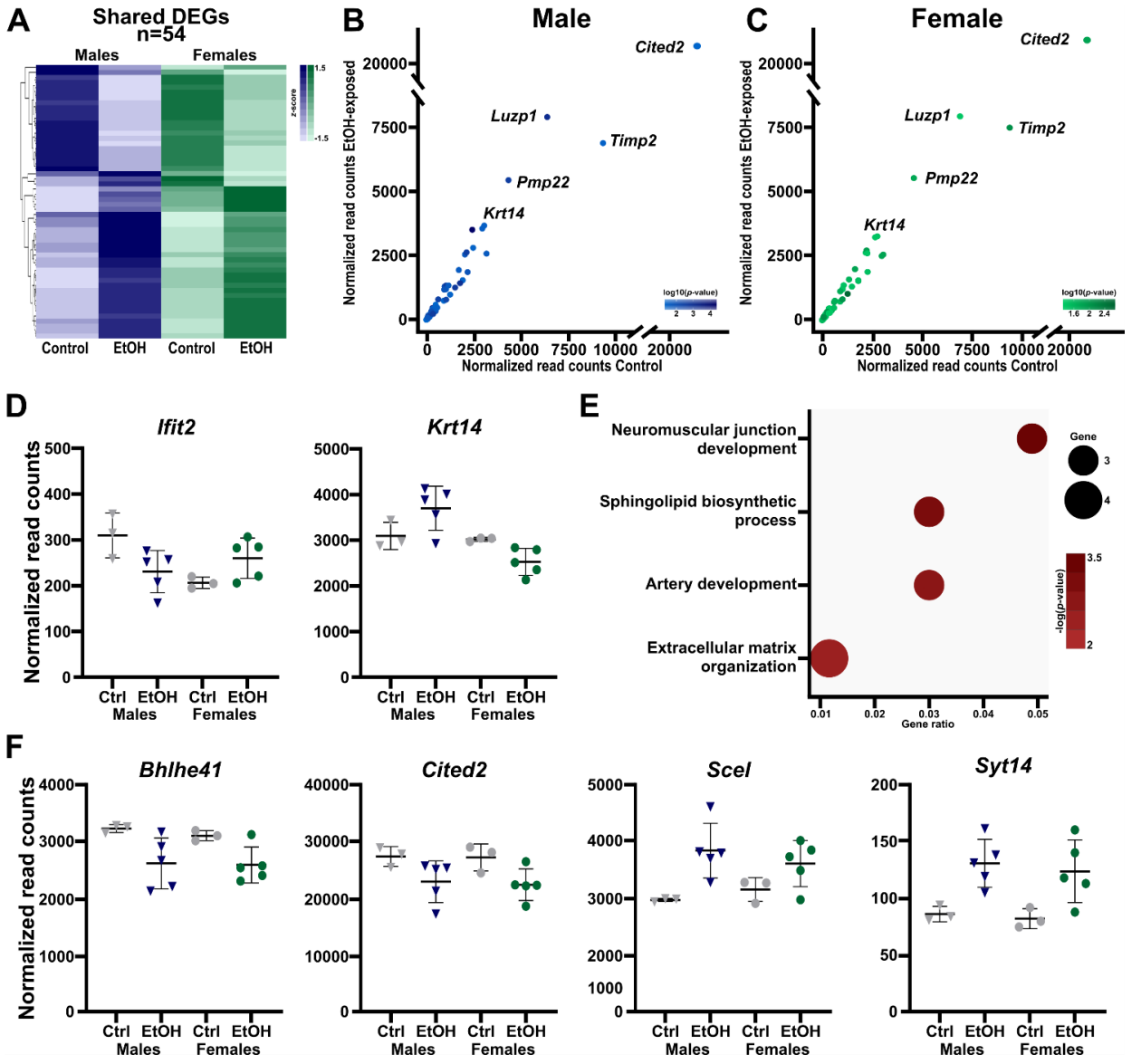

Figure Supp 7: Genes altered in both male and female ethanol-exposed placenta present similar changes

A) Heatmaps showing expression level (*z*-score) of common differentially expressed genes between male (blue; left) and female (green; right) placentas (n=54) following ethanol exposure. **B)** and **C)** Scatterplot showing normalized read counts of the 54 common DEG in control placentas (*X* axis) and ethanol-exposed placentas (*Y* axis) in males (blue; left) and females (green; right). **D)** Representation (normalized read counts) of 2 of the 4 genes with opposite alteration in expression in male and female ethanol-exposed placentas. Data are represented as mean ± standard deviation (SD). **E)** Functional enrichment analysis showing top enriched pathways for common DEGs (n=54)

based on Metascape analysis for pathways and p-value. **F)** Representation (normalized read counts) of genes with altered expression in male and female ethanol-exposed placentas. Data are represented as mean ± standard deviation (SD).

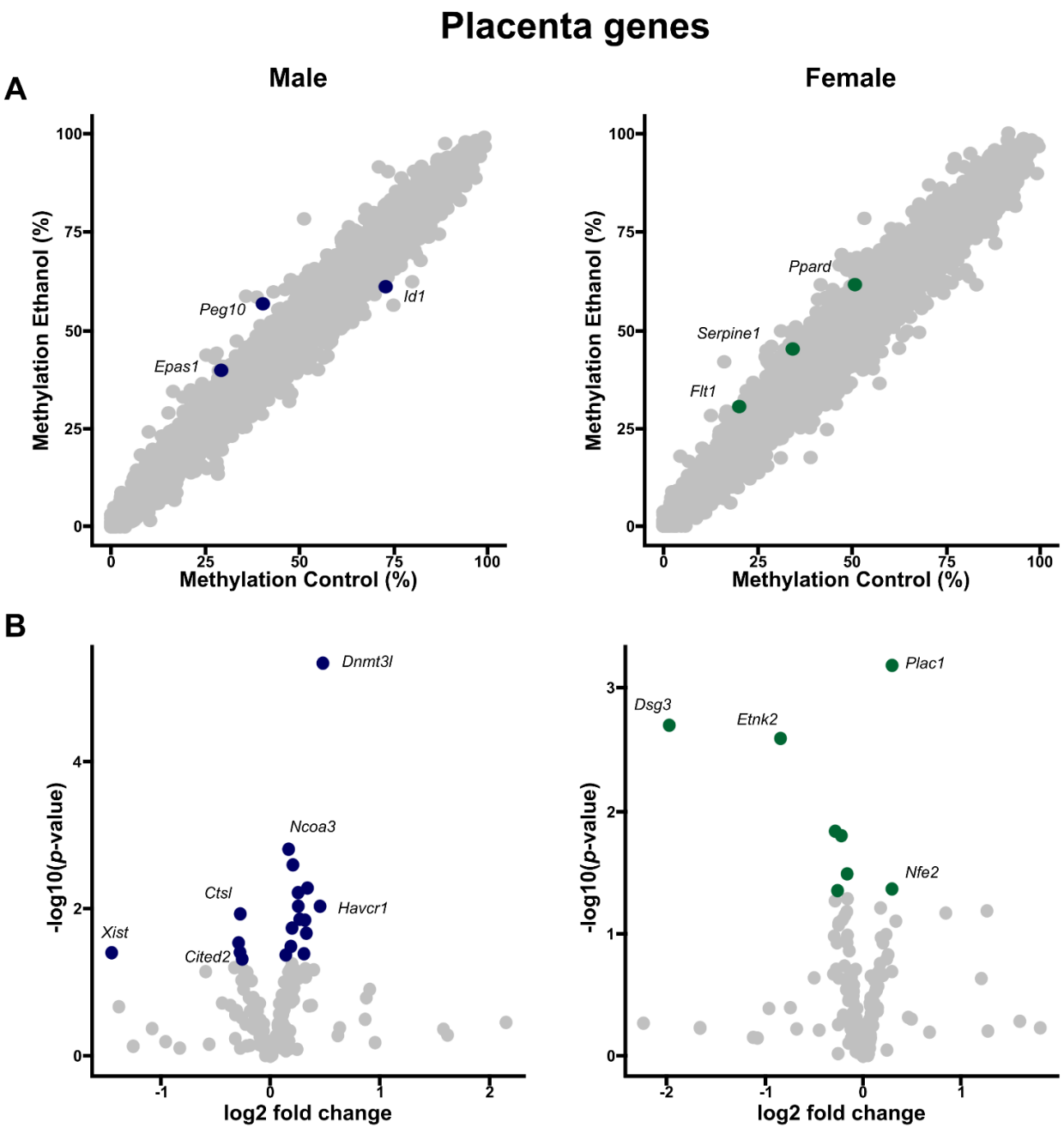

Figure Supp 8: Early preimplantation alcohol exposure alters epigenetic profiles in a minority of genes important for placenta development.

A) Scatterplot representing the tiles located in placenta developmental genes in control and ethanol-exposed placentas in males (left) and females (right). Blue (male) and green (female) dots represent the tiles with a methylation change of at least 10% in ethanol-exposed compared to control placentas (males n=3; females n=3). **B)** Differential expression analyses of placenta developmental genes between control and ethanol-exposed male (left) and female (right) placentas. Blue (male) and green (female) dots represent the genes that are significantly changed (p-value <0.05) in ethanol-exposed placentas (males n=19; females n=8) compared to controls.

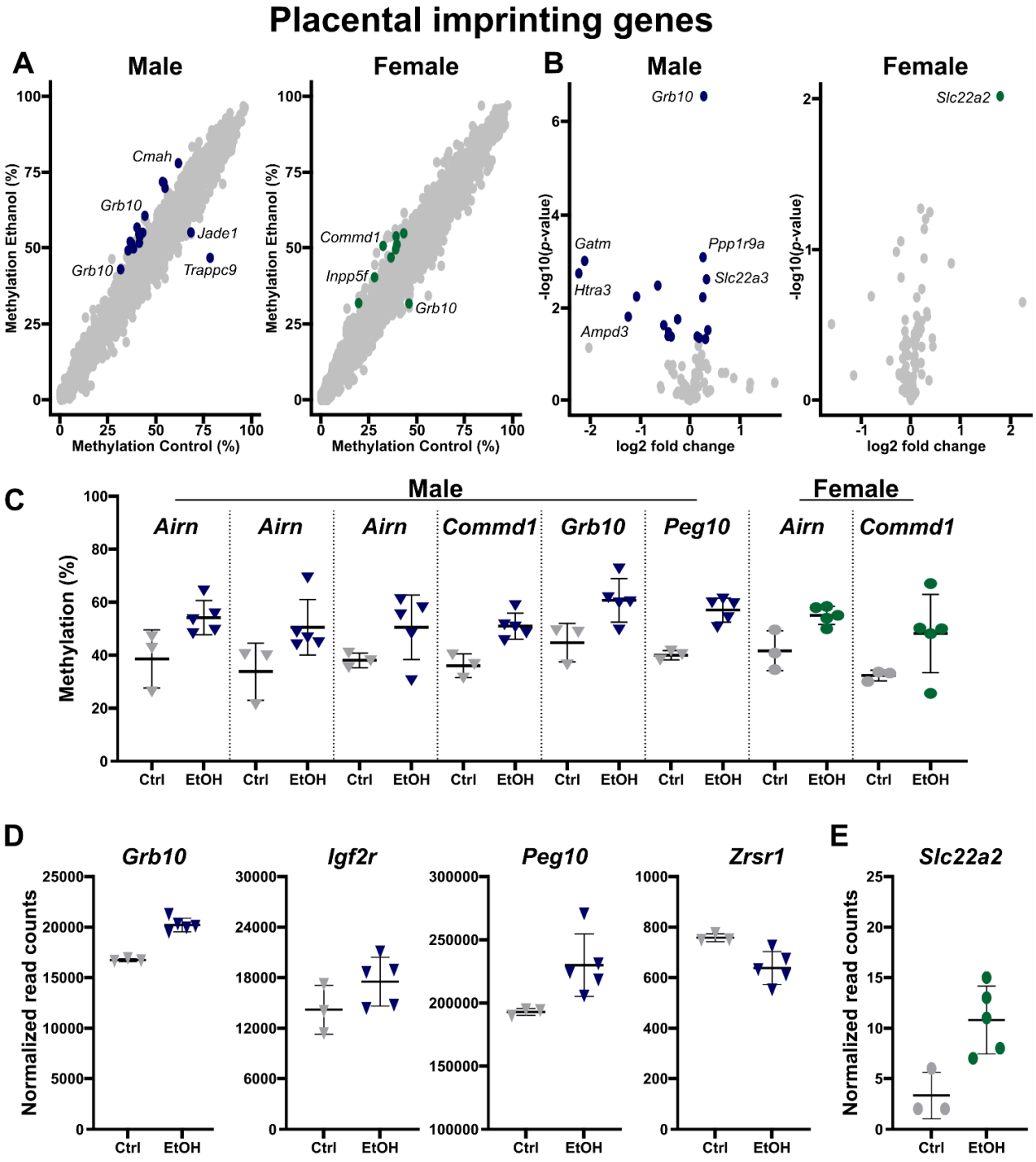

Figure Supp9: Early preimplantation alcohol exposure alters epigenetic profiles of placenta imprinting genes in late-gestation mouse placentas.

A) Scatterplot representing the tiles located in placenta imprinting genes in control and ethanol-exposed male (left) and female (right) placentas. Blue (male) and green (female) dots represent the tiles with a methylation change of at least 10% in ethanol-exposed placentas (males n=17 ; females

n=8) compared to controls. **B)** Differential expression analysis of placenta imprinting genes between control and ethanol-exposed male (left) and female (right) placentas. Blue (male) and green (female) dots represent the genes that are significantly changed (p-value <0.05) in ethanol-exposed placentas (males n=18 ; females n=1) compared to controls. **C)** Graph showing the CpG methylation levels in control and ethanol-exposed male (left; grey/blue) and female (right; grey/green) placentas for DMRs located in placenta imprinting genes. Data are represented as mean ± standard deviation (SD). **D)** Representation (normalized read counts) of placenta imprinting genes with altered expression in male (blue) ethanol-exposed placentas compared to controls. **E)** Representation (normalized read counts) of placenta imprinting gene with altered expression in female (green) ethanol-exposed placentas compared to controls. Data are represented as mean ± standard deviation (SD).

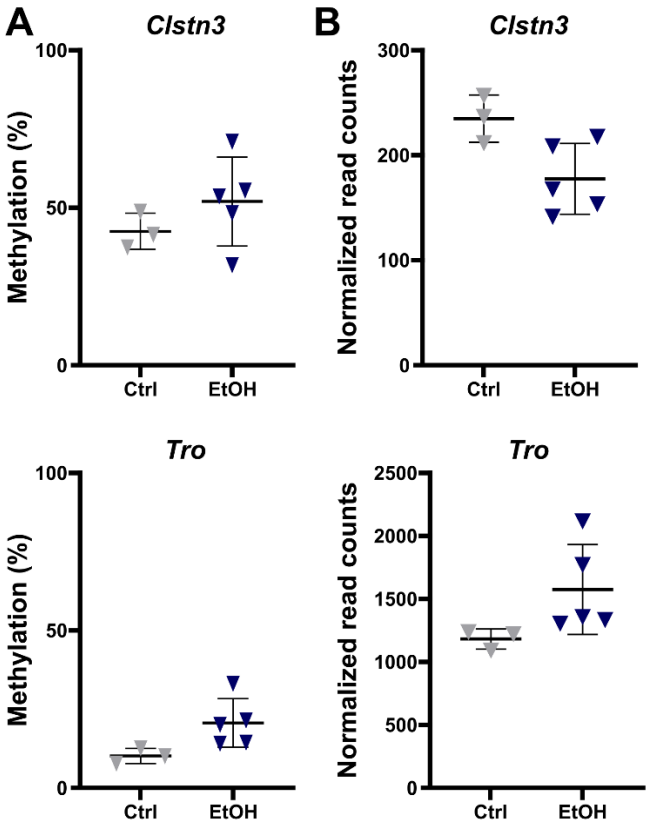

Figure Supp 10: Genes related to growth and presenting DNA methylation alteration in male and female ethanol-exposed placentas only show gene expression alteration in male ethanol-exposed placenta

A) Graph showing the CpG methylation level in control and ethanol-exposed male placentas for DMRs located in *Clstn3* (top) and *Tro* (bottom). **B)** Representation (normalized read counts) of the DEGs *Clsnt3* (top) and *Tro* (bottom) in control and ethanol-exposed male placentas. All data are represented as mean ± standard deviation (SD). n = 3-5.

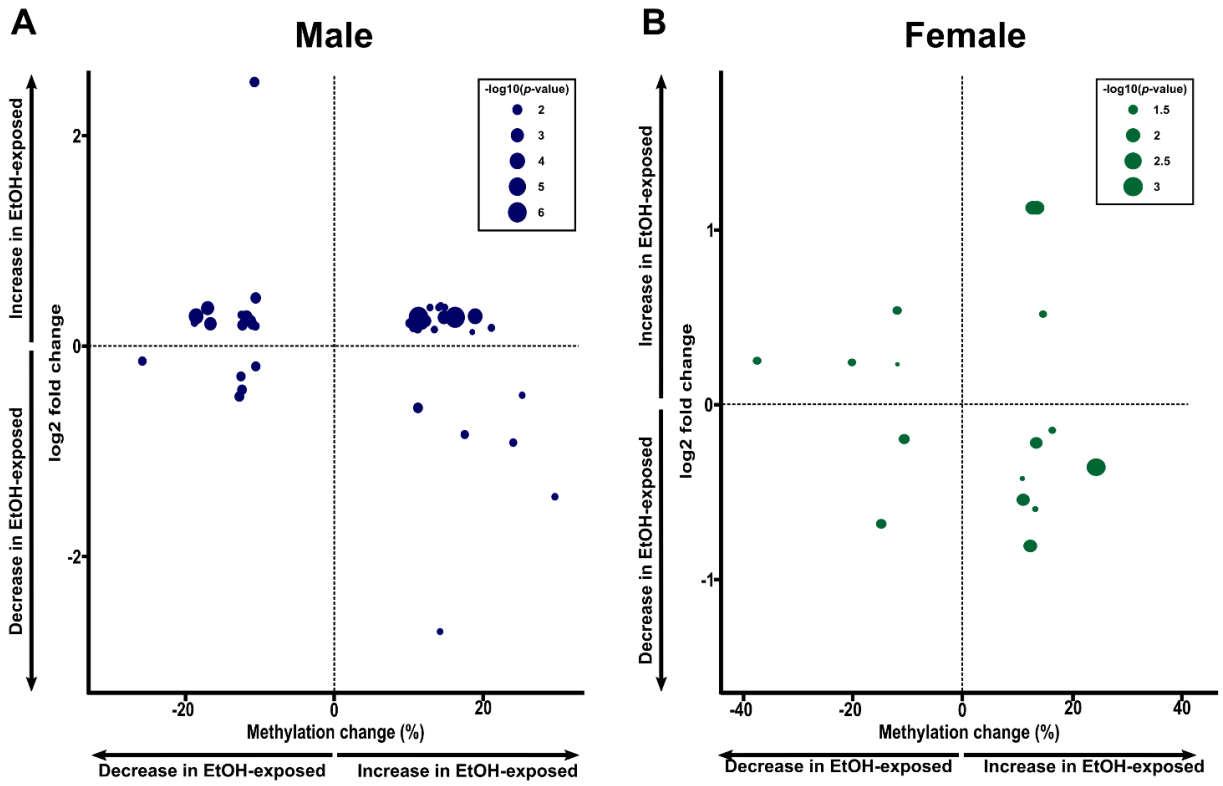

Figure supp 11: Differential expression is not directly linked to differential DNA methylation in late-gestation placentas following early preimplantation alcohol exposure

A) and **B)** Scatterplot showing DNA methylation differences between control and ethanol-exposed (X axis) and changes in gene expression (log2 fold change; Y axis) for regions presenting both DNA methylation and gene expression alterations between control and ethanol-exposed placentas in males (A) and females (B)

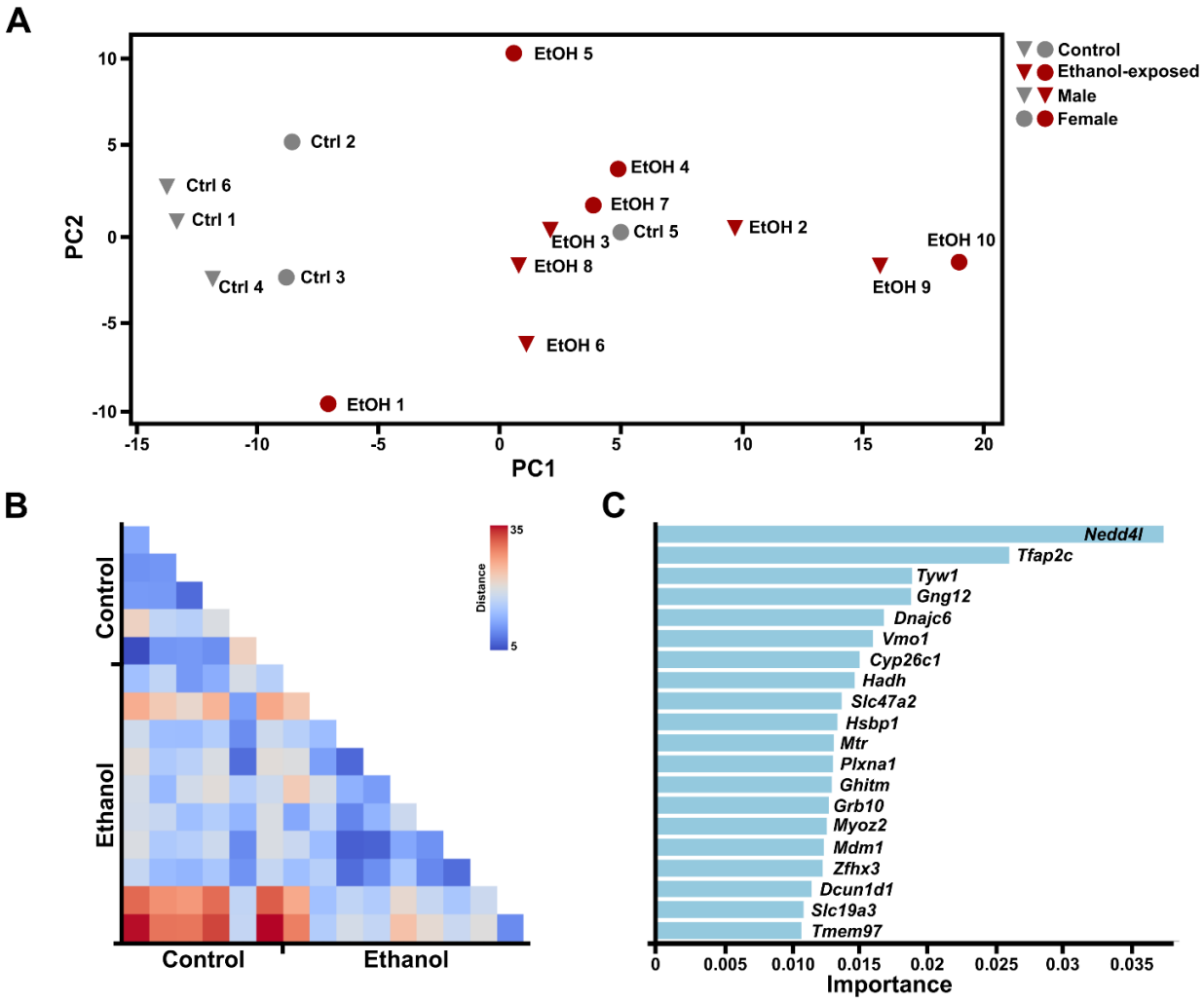

Figure Supp 12: Transcriptomic signature of preimplantation alcohol exposure does not allow for a good sample condition identification

A) Principal component analysis showing the clustering of control and ethanol-exposed samples based on their CpG methylation levels in the 20 genes (DEGs) identified as possible transcriptomic biomarkers. **B)** Heatmap of Eucledian distance of each control and ethanol-sample based on their CpG methylation level in the 20 genes identified as best transcriptomic biomarkers. **C)** Feature importance plot of each gene identified as biomarker based on LASSO analysis.

Supplementary tables

Table S1 : Male and female-specific DMRs located in imprinting genes

Male-specific DMRs in imprinting gene					
Condition	**Gene Name**	**Tile ID**	**Methylation change (%)**	**Annotation**	**In ICR?**
Decrease in EtOH-exposed	*Trappc9*	chr15.72945601.72945700	-31,79	Intron	No
Decrease in EtOH-exposed	*Phf17*	chr3.41556301.41556400	-13,38	Intron	No
Increase in EtOH-exposed	*Peg13*	chr15.72810001.72810100	10,24	Non-coding	Yes
Increase in EtOH-exposed	*Grb10*	chr11.12025901.12026000	11,29	Intron	Yes
Increase in EtOH-exposed	*Peg13*	chr15.72809901.72810000	11,39	Non-coding	Yes
Increase in EtOH-exposed	*H13*	chr2.152670801.152670900	11,83	Intron	No
Increase in EtOH-exposed	*Airn*	chr17.12741901.12742000	11,94	Intron	Yes
Increase in EtOH-exposed	*Kcnq1ot1*	chr7.143295601.143295700	13,34	Non-coding	Yes
Increase in EtOH-exposed	*Airn*	chr17.12741801.12741900	13,60	Intron	Yes
Increase in EtOH-exposed	*Airn*	chr17.12741701.12741800	14,11	Intron	Yes
Increase in EtOH-exposed	*Nap1l5*	chr6.58906901.58907000	14,84	Exon	Yes
Increase in EtOH-exposed	*Commd1*	chr11.22973201.22973300	15,38	Promoter-TSS	Yes
Increase in EtOH-exposed	*Cmah*	chr13.24468301.24468400	15,96	Intron	No
Increase in EtOH-exposed	*Grb10*	chr11.12035301.12035400	16,20	Intron	No
Increase in EtOH-exposed	*Peg10*	chr6.4748601.4748700	16,47	Intron	Yes
Increase in EtOH-exposed	*Nap1l5*	chr6.58907001.58907100	17,25	Promoter-TSS	Yes
Increase in EtOH-exposed	*Nap1l5*	chr6.58907101.58907200	18,13	Promoter-TSS	Yes
Female-specific DMRs in imprinting gene					
Condition	**Gene Name**	**Tile ID**	**Methylation change (%)**	**Annotation**	**In ICR?**
Decrease in EtOH-exposed	*Grb10*	chr11.12025501.12025600	-13,78	Intron	Yes
Increase in EtOH-exposed	*Art5*	chr7.102095201.102095300	10,68	Non-coding	No
Increase in EtOH-exposed	*Plagl1*	chr10.13090701.13090800	10,95	Promoter-TSS	Yes
Increase in EtOH-exposed	*H13*	chr2.152670901.152671000	11,87	Intron	No
Increase in EtOH-exposed	*Airn*	chr17.12742201.12742300	12,03	Intron	Yes
Increase in EtOH-exposed	*Pde10a*	chr17.8909701.8909800	12,48	Intron	No
Increase in EtOH-exposed	*Inpp5f*	chr7.128690801.128690900	12,72	Intron	No
Increase in EtOH-exposed	*Peg3*	chr7.6729401.6729500	14,97	Intron	Yes
Increase in EtOH-exposed	*Commd1*	chr11.22973101.22973200	18,60	Promoter-TSS	Yes

Table S2 : Male and female-specific DEGs located in imprinting genes

Male-specific DEGs in imprinting gene			
Condition	**Gene Name**	**Log2FoldChange**	***p*-value**
Decrease in EtOH-exposed	*Htra3*	-2,220	0,002
Decrease in EtOH-exposed	*Gatm*	-2,103	0,001
Decrease in EtOH-exposed	*Ampd3*	-1,234	0,016
Decrease in EtOH-exposed	*Dcn*	-1,068	0,006
Decrease in EtOH-exposed	*Qpct*	-0,645	0,003
Decrease in EtOH-exposed	*Rasgrf1*	-0,525	0,024
Decrease in EtOH-exposed	*Ano1*	-0,437	0,041
Decrease in EtOH-exposed	*Tnfrsf23*	-0,430	0,034
Decrease in EtOH-exposed	*Osbpl5*	-0,377	0,042
Decrease in EtOH-exposed	*Zrsr1*	-0,248	0,018
Increase in EtOH-exposed	*Gab1*	0,142	0,042
Increase in EtOH-exposed	*Ube3a*	0,183	0,045
Increase in EtOH-exposed	*Peg10*	0,254	0,006
Increase in EtOH-exposed	*Ppp1r9a*	0,258	0,001
Increase in EtOH-exposed	*Grb10*	0,273	0,000
Increase in EtOH-exposed	*Igf2r*	0,307	0,048
Increase in EtOH-exposed	*Slc22a3*	0,327	0,002
Increase in EtOH-exposed	*Cobl*	0,354	0,031
Female-specific DEGs in imprinting gene			
Condition	**Gene Name**	**Log2FoldChange**	***p*-value**
Increase in EtOH-exposed	Slc22a2	1,792	0,010

Chapitre 5 – Persistent molecular and behavioral changes in mice exposed to alcohol during early preimplantation

Mise en contexte et contribution de l'étudiant

Ce dernier chapitre est constitué de résultats qui feront partie d'un article dont quelques expériences sont toujours en cours. Nous nous intéressons cette fois-ci à l'impact à plus long-terme de l'exposition prénatale à l'alcool pendant la préimplantation sur le cerveau antérieur (*forebrain*) en fin de gestation, mais aussi sur les fonctions cognitives des souris. Nous avons donc effectué du Methyl-Seq Capture et du mRNA-seq sur des cerveaux antérieurs au stade embryonnaire E18.5 et réalisé une série de tests comportementaux sur des souris issues de notre modèle à l'âge correspondant environ à l'adolescence, soit P35 à P55. Cet article inclura aussi des résultats toujours en cours d'analyse en lien avec les interneurones GABAergiques (voir la section *Perspectives* de la discussion générale de ma thèse au Chapitre 6). Ce chapitre rapporte seulement les sections Méthodes et Résultats, qui seront discutés dans la discussion générale de ma thèse (Chapitre 6).

Contribution :

J'ai effectué les expériences avec les souris, la récolte et dissection d'embryons avec l'aide de Mélanie Breton-Larrivée. J'ai réalisé les expériences de méthylation (Methyl-Seq) et l'extraction d'ARN pour les librairies de mRNA-seq réalisé par la plateforme de Génome Québec. L'ensemble des données brutes a été analysé par Alexandra Langford-Avelar et j'ai ensuite réalisé les analyses sous-jacentes avec l'aide d'Anthony Lemieux. J'ai effectué les tests comportementaux sur les souris sous la supervision de Dr Elsa Rossignol. J'ai généré l'ensemble des graphiques et figures et fait l'assemblage final. J'ai écrit le manuscrit sous la supervision du Dr McGraw.

Persistent molecular and behavioral changes in mice exposed to alcohol during early preimplantation.

Lisa-Marie Legault[1,2], Mélanie Breton-Larrivée[1,2], Anthony Lemieux[1], Alexandra Langford-Avelar[1,2], Elsa Rossignol[1,3,4], Serge McGraw[1,2,4,#]

[1]CHU Ste-Justine Research Center, Montréal, Canada

[2]Department of Biochemistry and Molecular Medicine, Université de Montréal, Montréal, Canada

[3]Department of Neurosciences, Université de Montréal, Montréal, Canada

[4]Department of Pediatrics, Université de Montréal, Montréal, Canada

[5]Department of Obstetrics and Gynecology, Université de Montréal, Montréal, Canada

[#]Corresponding author : Serge McGraw : serge.mcgraw@umontreal.ca

ABSTRACT

Prenatal alcohol exposure is known to alter proper embryonic development, leading to Fetal Alcohol Spectrum Development (FASD). We previously demonstrated that prenatal alcohol exposure during early development, in the preimplantation period, can induce morphological defects and epigenetic errors in the late-gestation embryo. Yet, it remains unknown how such an early exposure to alcohol can affect the epigenetic and transcriptomic landscapes of the late-gestation forebrain., and the long-term impacts on cognitive functions are still unexplored. To address this, we used our established mouse model of preimplantation alcohol exposure and investigated DNA methylation and gene expression on forebrains of E18.5 ethanol-exposed and control embryos. Using Methyl-Seq Capture technology, we identified 625 differentially methylated regions (DMRs) exclusive to male forebrains, 359 DMRs exclusive to female forebrains and 58 DMRs shared between both sexes' forebrains. Using mRNA-seq to establish gene expression profiles following alcohol exposure, we uncovered 337 differentially expressed genes (DEGs) in male forebrains, 681 DEGs in female forebrains and 37 DEGs shared between both sexes. Our analyses show that up to 45% of the affected DMRs and DEGs are linked to genes that are involved in pathways related to brain development or function. Behavioral assays of adolescent mice showed alterations of sociability and short-term memory in ethanol-exposed compared to controls, with some altered functions being sex-specific. Together, our analyses show that prenatal alcohol exposure during early preimplantation development alters DNA methylation and gene expression profiles of the developing forebrain, resulting in altered cognitive functions later in life.

INTRODUCTION

So far, the long-term impacts on brain development and cognitive function of a single binge-like alcohol exposure during the preimplantation period remain unexplored. To overcome this caveat, we used our established mouse model of early prenatal alcohol exposure to study the impact of such a harmful environment during early development on DNA methylation and on the transcriptomic landscapes of the forebrain at late gestation. In addition, we also evaluated basic cognitive functions such as anxiety, repetitive behavior, sociability, and short-term memory in mice, following preimplantation alcohol exposure.

METHOD

Preimplantation alcohol exposure mouse model and tissue collection

All animal work was approved by the CHU Ste-Justine Research Center *Comité Institutionnel de Bonnes Pratiques Animales en Recherche* (CIBPAR) under the guidance of the Canadian Council on Animal Care (CCAC). Animals were housed in a 12 h light/dark cycle with unrestricted access to food and water. 8 weeks old C57BL/6 female mice were mated with same age C57BL/6 males (Charles River laboratories). Pregnancy at day 0.5 (E0.5) was confirmed by the presence of visible copulatory plug the following morning and pregnant females were separated from the males. As previously described, to model preimplantation binge-like alcohol exposure, pregnant females at embryonic day E2.5 (8-cell stage) were injected with 2 doses of 2.5g/kg of 50% ethanol, while control group received an equivalent volume of saline at 2h intervals (1). Pregnant females had limited handling during gestation. At E18.5, pregnant females were euthanized, and embryos were collected. Forebrains were isolated, flash frozen in liquid nitrogen and kept at -80°C. The sex of each embryo was determined by qPCR, probing for the *Ddx3* gene in digested DNA obtained from the tail of each embryo.

DNA/RNA extraction and library preparation

A total of 6 control forebrains (3 males and 3 females from 3 different litters) and 10 ethanol-exposed forebrains (5 males and 5 females from 5 different litters) were randomly selected from normal looking embryos. Forebrains were homogenized to powder in liquid nitrogen, and an equivalent amount of powder from each sample was used to extract DNA using QIAamp DNA

Micro kit (Qiagen #56304) and RNA using RNeasy Mini kit (Qiagen #74004), following manufacturer's protocols. Extracted DNA and RNA were quantified using QuBit fluorimeter apparatus with the Broad range DNA assay kit (ThermoFisher #Q32853) or the High Sensitivity RNA assay kit (ThermoFisher #Q32852).

1ug of DNA was used to produce methyl-seq libraries using the SureSelectXT Methyl-Seq Target Enrichment System with the mouse enrichment panel (Agilent #G9651B and #5191-6704) following manufacturer's recommendations. After final amplification with indexation, libraries were quantified using QuBit fluorimeter with the High Sensitivity DNA assay kit (ThermoFisher #Q32854) and quality was assessed by BioAnalyzer before paired-end sequencing on Illumina HiSeq 4000 PE100 at the Genome Quebec core facility. Each library generated between 81M and 99M reads.

500ng of high-quality RNA was used to produce mRNA-seq libraries using NEBNext mRNA stranded library kit by the Genome Quebec core facility, followed by paired-end sequencing on NovaSeq6000 S4. Between 28M and 47M reads were obtained for each sequenced library.

Bioinformatics analyses

Methyl-Seq sequencing data were analyzed using the GenPipes Methyl-Seq pipeline (v3.3.0) (2). Briefly, reads were aligned to the mouse reference genome (mm10) and methylation calls were obtained with Bismark (v0.18.1) (3). Differentially methylated regions (DMRs) were obtained with the R package MethylKit (version 1.8.1) (4) employing the Benjamini–Hochberg false discovery rate (FDR) procedure, with fixed parameters such as 100 bp stepwise tiling windows, a difference of DNA methylation level between conditions of at least 10% and a threshold of $q < 0.01$. DNA methylation levels were calculated as the average methylation of all CpGs within a tile for all the samples within a condition (minimum 3 samples/condition/sex ≥10X sequencing depth). Custom Perl scripts were used to calculate the number of CpGs per tile and the bisulfite conversion rate (> 96%) (1).

Homer (version 4.10.1) (5) was used for the annotation of analyzed tiles with the mouse mm10 reference genome. We used Metascape (6) online tool to perform gene ontology enrichment analyses by inputing differentially methylated tiles located in genic regions. CpG islands

coordinates were obtained from the UCSC table browser database (mm10 genome) and CpG content tracks were created, namely CpG shores and CpG shelves, by extending 0-2 kb and 2-4 kb, respectively, from the CpG islands coordinates, as described previously (1, 7, 8). All statistical analyses were performed using R (version 3.5.0) or GraphPad Prism (version 9.5.0).Post-sequencing bioinformatics analysis of mRNA-seq data was done using GenPipes RNA-Seq pipeline (v4.1.2) (2) including tools such as Trimmomatic (v0.36) (9), STAR (v2.5.3) (10) and BWA (v0.7.12) (11) and using the mouse mm10 genome as reference. Gene counts matrix and differentially expressed genes (DEGs) were obtained using the R package DESeq2 (v1.24.0) (12) with significant genes having a *p*-value <0.05.

Behavioral testing

All behavioral experiments were conducted by comparing aged-matched controls and ethanol exposed animals at P35 and P55, at a similar daytime period, in the dark and with appropriate acclimatation time before each test. Assays were conducted under video-tracking using the SMART tracking system (Harvard Apparatus), except for the marble burying task that was quantified manually.

All mice performed the four tasks sequentially from P35 onwards: Open field (P35-P36), Three-chamber maze assays (P41-P43), Novel object recognition assay (P47-P49), Marble burying task (P54-55). 70% ethanol was used to clean the apparatus between mice.

The open field test was conducted in a standard 45cm x 45cm walled arena. Mice were placed in the center and their behavior and movements were tracked for 10 minutes. Time spent in the central (45% of the total area) and peripheral zones, the distance travelled in each zone and the number of entries in the central zone were quantified by the software.

The three-chamber maze was composed of a rectangular (70cm x 45cm) arena separated in three equally sized zones with transparent walls and doors allowing the mice to freely circulate between zones. After being positioned in the central chamber, the mice were allowed to explore all empty chambers during a acclimation period of 5 minutes. After that period, a unfamiliar mouse (Stranger 1; S1) of the same sex and similar age was put inside a wire cage and placed in one of the side chambers. An empty cage was added in the opposite side chamber. Mice were allowed to freely explore all three chambers for 10 minutes under video tracking. Sociability was assessed by

quantifying the interaction time of the tested mice with Stranger 1 and the empty cage. Finally, a second unfamiliar mouse (Stranger 2; S2) of the same sex and similar age was placed in the previously empty wire cage. Mice were allowed to freely explore all three chambers for another 10 minutes under video tracking. Social novelty was assessed by quantifying the interaction time of the tested mice with Stranger 2 and Stranger 1.

The novel object recognition was conducted in the same arena as the open field test with visual symbols on the side wall. Mice were first placed in the arena for 5 minutes of acclimation to explore the empty area. Two similar objects (3cm round cap) were placed in the arena and mice were placed in the center of the field and let 10 minutes for exploration. Mice were removed for 5 minutes and placed again in the arena in which one of the objects was displaced to the opposite corner for 10 minutes of exploration under video tracking. Spatial memory and the recognition of the moved object was assessed by quantifying the interaction time with the displaced object and the unmoved object, with calculation of the discrimination index, defined as ($D_{index} = [(T_{displaced} - T_{unmoved})/(T_{displaced} - T_{unmoved})]$. After spatial memory assay, mice were removed for 5 minutes, and placed again in the field where the unmoved object was changed for a novel unfamiliar object (2cm x 4cm rectangular box). Mice were allowed to explore for 10 minutes under video tracking. Memory and recognition of a novel object was assessed by quantifying the interaction time with the novel object and the unchanged object, with calculation of the discrimination index, defined as ($D_{index} = [(T_{novel} - T_{unchanged})/(T_{novel} - T_{unchanged})]$.

The marble burying task was performed in a standard housing cage with 5cm depth of bedding. 20 similar marbles were placed on the bedding, in five equal rows of four marbles each. Mice were placed in the cage for 10 minutes. After that time, the number of completely buried (more than 75% of the marble covered in bedding), partially buried (25-75% of the marble covered in bedding) or unburied beads (less than 25% of the marble covered in bedding) was immediately assessed for each marble.

RESULTS

DNA methylation alterations in late-gestation forebrains following preimplantation alcohol exposure

To assess the long-term developmental impact of preimplantation alcohol exposure in the forebrain of late-gestation embryos, we established comprehensive genome-wide DNA methylation profiles. We randomly selected 6 normal non-exposed forebrains (3 males and 3 females) as controls and 10 ethanol-exposed forebrains (5 males and 5 females), all of which displayed typical morphometric measurements (weight and height) (13) and lacked visible morphological issues.

Our previous work using this preimplantation alcohol exposure model revealed significant sex-specific differences in DNA methylation profiles in forebrains of ethanol-exposed mice at mid-gestation. Therefore, we specifically examined sex-specific DNA methylation differences of forebrains at E18.5 in this current study. To do this, we compared the average DNA methylation levels in 100 bp non-overlapping segments (tiles) between control and ethanol-exposed male and female forebrains. Our analyses identified 187 761 tiles with sufficient coverage (10x) in both male and female forebrains, which were used to identify sex-specific and shared DNA methylation differences following early preimplantation alcohol exposure (Figure S1A-B).

When we first examined the distribution of these 187 761 tiles based on their DNA methylation levels in both control and ethanol-exposed forebrains, we observed subtle shifts. In males, the only significant shift occurred in the 90-100% methylation range, with a noticeable decrease in the number of tiles for ethanol-exposed samples (Figure S1C). In females, significant changes were observed in various methylation ranges (0-10%, 10-20%, 30-40%, 50-60%, 60-70%, 70-80%) in the ethanol-exposed forebrains (Figure S1C). Among the 187 761 tiles, we identified 625 differentially methylated regions (DMRs; 10% methylation difference) that were exclusively altered in males, 359 DMRs exclusively altered in females, and 58 shared DMRs that showed alterations in both sexes in response to preimplantation alcohol exposure (Figure S1A).

Sex-specific DNA methylation alterations in late-gestation forebrains following preimplantation alcohol exposure

To better understand the sex-specific effects of early prenatal alcohol exposure on DNA methylation profiles in late-gestation forebrains, we examined DMRs that were unique to males or females. Among the 625 male-specific DMRs, we noticed both increases (n=274; 44%) and decreases (n=351; 56%) in methylation levels in ethanol-exposed forebrains compared to controls (Figure 1A; Table 1). Most of these DMRs showed methylation changes within the 10-15% range (78% of both increased and decreased DMRs; Figure 1B). The proportion of DMRs with a methylation change of 20% or more was similar in both decreased- and increased-DMRs (4% and 3%, respectively; Figure 1B). In E18.5 female forebrains, the majority (n=287; 80%) of the 359 DMRs displayed an increase in methylation levels following preimplantation ethanol exposure (Figure 1C; Table 1). Of these increased-DMRs, 78% showed a methylation change of 10-15% (Figure 1D). Although overall less frequent, DMRs showing a decrease in methylation in ethanol-exposed forebrains (n=72; 20%; Figure 1C) exhibited greater methylation changes in the 15-20%, 20-25% and 30% or more ranges than the decreased-DMRs (Figure 1D).

When attributed to the different genomic annotations, the distribution of these sex specific DMRs was found to be similar between male and female forebrains, most of them being in intergenic regions (males 44%, females 47%), introns (males 43%, females 38%), and promoter regions (males 9%, females 8%; Figure 1E-F). Male DMRs showed a comparable average methylation level in control and ethanol-exposed forebrains, in line with the minor DNA methylation changes observed (Figure 1E). Contrarily, female DMRs displayed a broader difference in methylation levels between control and ethanol-exposed forebrains across various annotations. This was particularly notable for DMRs (control vs ethanol-exposed) located in promoters (37% vs 46%), exons (43% vs 50%), introns (49% vs 58%), transcription termination sites (TTS; 45% vs 59%), and 3' untranslated regions (UTR; 61% vs. 71%; Figure 1F). Among others, we observed DMRs located in intragenic regions of noticeable genes such as *Acot12* (acetyl- and acyl-CoA metabolism), *Poli* (response to UV), *Wdr76* (DNA damage checkpoint) and *Zfp637* (regulation of transcription) in males and *Dnajc5* (regulation of synaptic vesicle cycle), *Hdac9* (histone H4-K16 deacetylation), *Nav3* (regulation of microtubule polymerization) and *Nmrk1* (pyridine nucleotide biosynthetic process) in females.

We next performed gene ontology enrichment analysis to explore the potential biological significance associated with regions presenting altered methylation levels. Among the 625 male

DMRs, 351 were found within genic regions, representing 334 unique genes. These genes were enriched in pathways associated to: Regulation of synaptic vesicle exocytosis, Regulation of membrane potential, Regulation of sister chromatid cohesion, Hematopoiesis, and Formation of the primary germ layer (Figure 1I). In female forebrains, 190 out of the 359 DMRs were located in genic regions, contributing to a list of 153 unique genes. Associated enrichment pathways included: Regulation of peptide-cysteine S-nitrosylation, Cytoskeleton-dependent intracellular transport, Neuron projection morphogenesis, Regulation of cardiac muscle hypertrophy, and Neuromuscular process (Figure 1J).

Together our findings reveal that early preimplantation alcohol exposure alters DNA methylation profiles in the forebrain that can still be observed at late gestational stages. Moreover, the sex-specific DMRs and associated pathways shed light on how prenatal alcohol exposure during early development influences the developing brain in a sex-specific manner.

Preimplantation alcohol exposure leads to DNA methylation alterations in genes associated to embryonic development in males and females

Although we clearly see sex-specific DNA methylation differences, we also observed 58 shared DMRs across male and female ethanol-exposed forebrains. Of those, 27 DMRs showed increased DNA methylation levels in ethanol-exposed samples, while the remaining 31 DMRs displayed decreased DNA methylation levels in response to ethanol exposure in both sexes (Figure S2A; Table 2). Half of these shared DMRs are located in intergenic regions, while the others are found in introns and promoter-associated regions (Figure S2B), their methylation levels and patterns consistent between both sexes within the same condition for specific genomic annotations (Figure S2B). Gene ontology analysis of the 29 intragenic DMRs revealed a significant enrichment in the pathway associated to *in utero* embryonic development with differences in key genes such as *Eif2s2*, *Rbbp8*, *Syvn1*, and *Tgfbr2*. Our results suggest that these regions with altered DNA methylation in both male and female, may negatively impact the proper embryonic growth and contribute to the phenotype (e.g. growth restriction) associated with preimplantation alcohol exposure.

Preimplantation alcohol exposure causes sex-specific gene expression changes in forebrain at late-gestation stage

To further investigate the molecular effects of a preimplantation alcohol exposure on late gestation forebrains at late-gestation, we next sought to define the impact of alcohol on the transcriptomic profiles. We first established gene expression profiles using mRNA-seq and performed a sex-specific analysis. We found that 23 167 genes were transcribed in all samples of both sexes (normalized read counts >1; Figure S3A-B), with significant changes (p<0.05) in gene expression exclusive to male (337 DEGs) and female (681 DEGs) samples, as well as changes shared in both sexes (37 DEGs) (Figure S3A-B) in response to alcohol exposure.

Of the 337 DEGs identified in male ethanol-exposed forebrains, 146 showed decreased expression and 191 showed increased expression (Figure 2A-B; Table 3). Gene ontology enrichment analysis associated with these DEGs uncovered that the pathways affected were mainly related to: Purine nucleoside transmembrane transport, Elastic fiber assembly, Regulation of glomerular, Cell junction assembly and Metabolism of angiotensinogen to angiotensins (Figure 2C). Examples of dysregulated genes related to these pathways (*Slc29a2*, *Myh11*, *Rhoc*) are shown in Figure 2D. Ethanol-exposed female forebrains presented a higher number of DEGs (n=681), of which 325 showed a decreased level of expression and 356 showed an increased level of expression (Figure 2E-F; Table 3). Gene ontology analysis revealed enrichment in the pathways related to: Regulation of system process, Behavior, Regulation of developmental growth, Head development and Neuron projection development (Figure 2G). Examples of dysregulated genes (*Bmpr2*, *Dll1, Edn3*) are shown in Figure 2H.

Preimplantation alcohol exposure affects expression of genes involved in synaptic transmission and learning in forebrains at late gestational stage

Of the 23 167 expressed genes, only 37 DEGs were shared in both male and female ethanol-exposed forebrains (Figure S4A) (Table 4). The majority of these DEGs (89%) presented similar alterations in both male and female ethanol-exposed forebrains, with 19 showing decreased expression levels and 14 showing increased expression levels. Only 4 DEGs (*Slc4a9, Insm5, Lhx5, Usp2*) showed opposite levels (increased or decreased) between males and females. (Figure S4B).

Despite the limited number of shared DEGs, gene ontology analysis revealed significant enrichment in pathways associated to: Modulation of chemical synaptic transmission, Smooth muscle contraction, Cell morphogenesis involved in differentiation, Extracellular matrix organization and Associative learning (Figure S4C), implicating noteworthy genes such as *Gnal*,

Actg2, *Robo1*, *Eln* and *Tnr*. These findings revealed that a limited number of genes with altered gene expression level in both male and female ethanol-exposed forebrains present a strong enrichment in pathways related to brain function.

A link between sex-specific DNA methylation differences and gene expression changes following preimplantation alcohol exposure

Our results provide strong support of sex-specific DNA methylation and gene expression alterations in E18.5 forebrains following an early embryonic alcohol exposure. To determine the associations between these alterations, we compared the datasets (DEGs with corresponding intragenic DMRs). In males, 5 genes showed both DEGs and DMRs (all in intronic regions) (Figure S5A). Genes impacted in males included *Il13ra1* (cytokine-mediated signaling pathway), *Nrn1* (synaptic transmission) and *Trpm6* (ion channel transport; Figure S5B). In females, 7 genes revealed DEGs and DMRs, and included *Cdkl5* (regulation of axon extension), *Gnal* (dopamine receptor signaling pathway) and *Robo2* (chemotaxis; Figure S5C-D). All of female specific DMRs were located in introns, except for the DMR in *Cdkl5*, that is in its promoter. These results reveal that there is a poor correlation between dysregulation of DNA methylation and altered gene expression profiles at E18.5 following alcohol exposure.

Preimplantation alcohol exposure affects DNA methylation and expression of genes related to brain development and function

Given the enrichment of DMRs and DEGs in pathways related to various brain associated pathways (Figure 1I-J; 2G; S4C), we extended our gene ontology analysis by extracting all individual intragenic DMRs and DEGs related to brain development, brain organization and brain functions. In the methylation datasets, 10% (n=34) of male specific DMRs and 15% (n=28) of female specific DMRs were associated to pathways related to brain development or function. These regions encompassed genes such as *Blc11b*, *Dclk2*, *Glra3*, *Raph1* or *Slc4a8* in males and *Atxn1*, *Gbx2*, *Npas3*, *Ppp1r9a* or *Ptprd* in females (Figure 3 A-D; Table S1). None of the 29 shared DMRs were linked to brain associated pathways.

Similarly, when we looked at the entire set of DEGs, we found that 15% (n=49) of male-specific DEGs and 13% (n=86) of female-specific DEGs were related to brain associated pathways (Figure 4A-C; Table S1). The associated genes included *Cdh8*, *Chodl*, *Gas6* and *Lhx6* in males,

and *Gabrb2*, *Pou2f2*, *Syt4* and *Tekt2* in females. Interestingly, 46% (n=17) of shared DEGs were related to brain development, organization or functions (Figure 4E), and included *Grm3*, *Nrn1*, *Robo1* and *Usp2* (Figure 4F; Table S1). Network enrichment analysis containing these selected male- and female-specific DMRs and DEGs revealed their tight association with pathways related to brain development and functions (Figure S6A-B).

These findings showed a substantial representation of genes related to brain associated pathways among regions exhibiting altered DNA methylation or gene expression in late-gestation forebrains following preimplantation alcohol exposure. Although most molecular alterations are sex-specific, they encompass pathways and processes that are commonly affected in both sexes, suggesting potential long-term alterations on brain function in both sexes.

Preimplantation alcohol exposure does not impact locomotion, anxiety or repetitive behavior in mice

To investigate whether alcohol exposure prior to implantation affects future cognitive abilities, we conducted behavioral tests on adolescent mice (from postnatal days 35 to 55). We first evaluated their overall movement ability and anxiety levels using an open field test (Figure S7A; left panel). After allowing the mice to freely explore the area for 10 minutes while being video tracked, we found no sign of increased anxiety in either male or female mice that had been exposed to ethanol. Both groups had similar behaviors in terms of time spent in the central and the peripheral zones, number of entries into the central zone, and distance covered in both the central and peripheral zones (Figure S7B-G). Likewise, the total distance traveled in the arena did not differ between the two groups (Figure S7D;G).

To further confirm that ethanol exposure did not affect anxiety-related behavior, we tested repetitive behavior using the marble burying task (Figure S7A; right panel). We gave the mice 10 minutes of free time in a cage containing 20 marbles on a thick bedding layer, and then counted how many marbles were completely, partially, or not buried. In both male and female mice that were exposed to ethanol, their behavior mirrored that of the control mice, with similar numbers of marbles buried in each category (Figure S7H-I).

These two tests confirmed that preimplantation alcohol exposure does not increase anxiety or repetitive behavior, as well as movement ability, in adolescent mice.

Preimplantation alcohol exposure alters sociability and short-term memory in mice

To assess the long-term effect of preimplantation alcohol exposure on complex cognitive functions, we evaluated social behavior using the three-chamber maze test. We first tested the general sociability of mice by comparing the time spent interacting with a cage containing an unfamiliar mouse (Stranger 1; S1) versus an empty cage. Being curious and social animals by nature, mice typically spend more time interacting with a cage containing a stranger mouse than an empty one, as seen in our control male and female mice during 10-minute exploration period (Figure 5B-C). However, both male and female ethanol-exposed mice displayed a lack of sociability, spending similar time interacting with Stranger 1 and with the empty cage (Figure 5B-C). When comparing the discrimination ratio of interaction time, we observed a significant decrease in both male and female ethanol-exposed compared to the respective control group (Figure 5 D-E), confirming the alteration in normal sociability behavior.

We then evaluated the impact of preimplantation alcohol exposure on social novelty by comparing the interaction time of the mice with the cage with the previous stranger mouse (Stranger 1; S1) to a cage with a new unfamiliar mouse (Stranger 2; S2). Mice typically spend more time interacting with the new unfamiliar mouse du to preference for social novelty during a 10-minute exploration period. Although not significant, we observed a similar trend in both male and female control mice with more time of interaction with Stranger 2 (Figure 5F-G). Male ethanol-exposed mice showed a strong preference for social novelty, spending significantly more time interacting with Stranger 2 than Stranger 1, with a similar discrimination ratio as the control mice (Figure 5H). However, this preference for social novelty was not observed in female ethanol-exposed mice, who showed similar interaction time with both stranger mice and a near-significant (p=0.0537) decrease in the discrimination ratio (Figure 5I).

Finally, we assessed spatial learning and short time memory using a Novel Object Recognition task (Figure 5J). After a conditioning period with two identical objects and a five-minute waiting period outside of the arena, one object was moved to evaluate the recognition of a new location. After 10 minutes of free exploration, the discrimination index was calculated based on the interaction time with the moved and unmoved objects. Both male and female ethanol-exposed mice had a significantly decreased ratio, indicating impaired spatial learning (Figure 5K-

L). For short-term memory assessment, the mice were kept outside the arena for five minutes, during which the unmoved object was replaced with a completely different one. The discrimination ratio was calculated based on the interaction time with the changed object and the unchanged object during the 10-minute exploration. Male ethanol-exposed mice showed a significant decrease of their discrimination ratio, implying impaired short-term memory (Figure 5M). In female ethanol-exposed mice, we didn't observe a significant decrease in the discrimination ratio, although one mouse seemed more affected than the rest of the group (Figure 5N).

These results indicate that preimplantation alcohol exposure has shared effects between males and females on long-term cognitive functions, such as sociability and spatial learning. Other observed cognitive alterations are sex-specific, with female ethanol-exposed mice presenting impairments in social novelty skills, while males have decreased recognition of novel objects. These results emphasize the lasting negative effects of early preimplantation alcohol exposure on brain development and function.

Tables

Table 1 : Top 10 decrease and increase DMRs in male and female forebrains

Male-specific DMRs			
Condition	**Gene Name**	**Methylation change (%)**	**Annotation**
Decrease in EtOH	*Zfc3h1*	-35,22	Intron
Decrease in EtOH	*Arl6*	-31,59	Intron
Decrease in EtOH	*(Cox7c)*	-24,49	Intergenic
Decrease in EtOH	*Gm15787*	-23,20	Promoter-TSS
Decrease in EtOH	*(Ndufaf1)*	-22,63	Intergenic
Decrease in EtOH	*(Mir101c)*	-22,40	Intergenic
Decrease in EtOH	*Cfap54*	-21,83	Intron
Decrease in EtOH	*Anks1*	-21,15	Intron
Decrease in EtOH	*Nrg2*	-20,90	Intron
Decrease in EtOH	*(Smarca5-ps)*	-20,69	Intergenic
Increase in EtOH	*(Col6a4)*	24,44	Intergenic
Increase in EtOH	*Slain1*	24,13	Intron
Increase in EtOH	*(A1bg)*	23,57	Intergenic
Increase in EtOH	*(1700122O11Rik)*	22,82	Intergenic

Increase in EtOH	*Wdr76*	21,90	Intron
Increase in EtOH	*Hps3*	21,78	Promoter-TSS
Increase in EtOH	*(Lamc2)*	21,58	Intergenic
Increase in EtOH	*Acot12*	21,09	Intron
Increase in EtOH	*Adipor2*	20,32	Intron
Increase in EtOH	*(Il1f10)*	19,60	Intergenic
Female-specific DMRs			
Condition	**Gene Name**	**Methylation change (%)**	**Annotation**
Decrease in EtOH	*(Zfp369)*	-49,64	Intergenic
Decrease in EtOH	*(Zfp369)*	-32,26	Intergenic
Decrease in EtOH	*Crtap*	-31,47	Intron
Decrease in EtOH	*Hdac9*	-25,03	Intron
Decrease in EtOH	*Nos1ap*	-24,57	Intron
Decrease in EtOH	*(Zfp369)*	-24,41	Intergenic
Decrease in EtOH	*(Rpap3)*	-24,18	Intergenic
Decrease in EtOH	*(Gcm1)*	-22,02	Intergenic
Decrease in EtOH	*Pkhd1l1*	-21,59	Intron
Decrease in EtOH	*Dscam*	-21,39	Exon
Increase in EtOH	*(Duox2)*	39,66	Intergenic
Increase in EtOH	*(Fam107a)*	31,65	Intergenic
Increase in EtOH	*Pla2g12a*	30,92	Intron
Increase in EtOH	*(Plek2)*	30,87	Intergenic
Increase in EtOH	*Dnajc5*	28,64	Intron
Increase in EtOH	*Brd7*	28,11	Promoter-TSS
Increase in EtOH	*(Ldhal6b)*	27,20	Intergenic
Increase in EtOH	*(Suds3)*	25,66	Intergenic
Increase in EtOH	*(Bmp8b)*	25,63	Intergenic
Increase in EtOH	*1700001L05Rik*	24,92	Promoter-TSS

Table 2 : Top 10 decrease and increase shared DMRs in forebrains

Shared top DMRs					
Condition - Male	**Gene Name**	**Methylation change (%) - Male**	**Condition - Female**	**Methylation change (%) - Female**	**Annotation**
Decrease in EtOH	*(Pex2)*	-26,24	Decrease in EtOH	-34,79	Intergenic
Decrease in EtOH	*Tmem171*	-25,97	Decrease in EtOH	-12,90	Intron
Decrease in EtOH	*(Fam214a)*	-25,83	Decrease in EtOH	-37,87	Intergenic

Decrease in EtOH	*Cd40lg*	-18,95	Decrease in EtOH	-22,44	Intron
Decrease in EtOH	*(Hk2)*	-18,61	Decrease in EtOH	-17,15	Intergenic
Decrease in EtOH	*Treml4*	-16,59	Decrease in EtOH	-13,10	3' UTR
Decrease in EtOH	*(Rpap3)*	-14,98	Decrease in EtOH	-15,00	Intergenic
Decrease in EtOH	*Ccdc13*	-14,60	Decrease in EtOH	-22,01	Promoter-TSS
Decrease in EtOH	*Pitrm1*	-14,34	Decrease in EtOH	-14,57	Intergenic
Decrease in EtOH	*Tgfbr2*	-13,61	Decrease in EtOH	-10,59	3' UTR
Increase in EtOH	*(Wisp3)*	28,27	Increase in EtOH	19,97	Intergenic
Increase in EtOH	*Matn3*	23,18	Increase in EtOH	27,88	Intron
Increase in EtOH	*(Cntn1)*	20,84	Increase in EtOH	16,84	Intergenic
Increase in EtOH	*(Gm21190)*	20,78	Increase in EtOH	25,40	Intergenic
Increase in EtOH	*Stac*	19,20	Increase in EtOH	17,20	Intron
Increase in EtOH	*(Gm14496)*	18,58	Increase in EtOH	19,20	Intergenic
Increase in EtOH	*Zkscan8*	17,27	Increase in EtOH	14,82	Intron
Increase in EtOH	*Smarcad1*	15,89	Increase in EtOH	20,80	Promoter-TSS
Increase in EtOH	*Syvn1*	15,86	Increase in EtOH	16,67	Promoter-TSS

Table 3 : Top 10 decrease and increase DEGs in male and female forebrains

Male-specific DEGs			
Condition	**Gene Name**	**log2 fold change**	***p*-value**
Decrease in EtOH	*Skor2*	-4,79	0,00108
Decrease in EtOH	*Gsc*	-4,35	0,01315
Decrease in EtOH	*Pou2f3*	-3,91	0,00884
Decrease in EtOH	*A630031M04Rik*	-3,45	0,03980
Decrease in EtOH	*Hmx3*	-3,38	0,00003
Decrease in EtOH	*Atp6v1e2*	-3,09	0,04556
Decrease in EtOH	*Slc4a9*	-2,64	0,04045
Decrease in EtOH	*Stk31*	-2,41	0,03792
Decrease in EtOH	*Ces1d*	-2,23	0,00869
Decrease in EtOH	*Gm10075*	-2,16	0,04547
Increase in EtOH	*Muc15*	4,42	0,01669
Increase in EtOH	*Gm11448*	4,14	0,00490
Increase in EtOH	*Ifitm5*	4,10	0,00774
Increase in EtOH	*Gm13189*	4,02	0,01518
Increase in EtOH	*Awat2*	3,94	0,00532

Increase in EtOH	*Gm13293*	3,91	0,02481
Increase in EtOH	*SNORA79*	3,67	0,02725
Increase in EtOH	*Itih5l-ps*	3,61	0,04142
Increase in EtOH	*Gm15749*	3,60	0,04930
Increase in EtOH	*Aqp3*	3,59	0,00466
Female-specific DEGs			
Condition	**Gene Name**	**log2 fold change**	***p*-value**
Decrease in EtOH	*Gh*	-4,43	0,0207
Decrease in EtOH	*Gm13529*	-3,86	0,0421
Decrease in EtOH	*Gm9174*	-3,10	0,0364
Decrease in EtOH	*Avpr1b*	-2,91	0,0209
Decrease in EtOH	*Gm20512*	-2,76	0,0492
Decrease in EtOH	*Gm9009*	-2,69	0,0205
Decrease in EtOH	*Gm17055*	-2,17	0,0457
Decrease in EtOH	*Vip*	-2,12	0,0244
Decrease in EtOH	*Gm3222*	-2,08	0,0208
Decrease in EtOH	*Gm12791*	-1,69	0,0135
Increase in EtOH	*Nkx2-4*	7,18	0,0016
Increase in EtOH	*Rbp3*	7,03	0,0466
Increase in EtOH	*Irx5*	6,68	0,0003
Increase in EtOH	*Foxa1*	6,60	0,0238
Increase in EtOH	*Vgll2*	6,10	0,0169
Increase in EtOH	*Hcrt*	5,64	0,0070
Increase in EtOH	*Rax*	5,38	0,0202
Increase in EtOH	*Pmch*	5,23	0,0271
Increase in EtOH	*Irx6*	4,82	0,0250
Increase in EtOH	*Pitx2*	4,73	0,0188

Table 4 : Top 10 decrease and increase shared DEGs in forebrains

Shared top DEGs						
Condition - Male	**Gene Name**	**log2 fold change - Male**	***p*-value - Male**	**Condition - Female**	**log2 fold change - Female**	***p*-value - Female**
Decrease in EtOH	*Actg2*	-0,82	0,032913	Decrease in EtOH	-0,96	0,026
Decrease in EtOH	*Eln*	-0,61	0,000001	Decrease in EtOH	-0,31	0,031
Decrease in EtOH	*Oma1*	-0,31	0,035172	Decrease in EtOH	-0,31	0,007
Decrease in EtOH	*Tnr*	-0,27	0,023040	Decrease in EtOH	-0,29	0,021
Decrease in EtOH	*Nrip1*	-0,25	0,044961	Decrease in EtOH	-0,25	0,005

Decrease in EtOH	*Gucy1a3*	-0,23	0,009631	Decrease in EtOH	-0,31	0,003
Decrease in EtOH	*Gucy1b3*	-0,23	0,001901	Decrease in EtOH	-0,25	0,003
Decrease in EtOH	*Lhx5*	-0,41	0,006532	Increase in EtOH	0,39	0,024
Decrease in EtOH	*Insm2*	-0,55	0,038867	Increase in EtOH	0,67	0,044
Decrease in EtOH	*Slc4a9*	-2,64	0,040453	Increase in EtOH	3,42	0,020
Increase in EtOH	*Usp2*	0,24	0,021609	Decrease in EtOH	-0,21	0,037
Increase in EtOH	*4933436C 20Rik*	0,98	0,038350	Increase in EtOH	1,15	0,028
Increase in EtOH	*Mir3072*	0,80	0,010884	Increase in EtOH	0,80	0,020
Increase in EtOH	*Gm15538*	0,66	0,042469	Increase in EtOH	0,84	0,021
Increase in EtOH	*Gm14286*	0,56	0,004047	Increase in EtOH	0,59	0,006
Increase in EtOH	*A3galt2*	0,54	0,046016	Increase in EtOH	0,54	0,014
Increase in EtOH	*Nts*	0,42	0,009930	Increase in EtOH	0,36	0,024
Increase in EtOH	*Dnahc7b*	0,41	0,049719	Increase in EtOH	0,30	0,033
Increase in EtOH	*Zmynd15*	0,39	0,024606	Increase in EtOH	0,37	0,034
Increase in EtOH	*Nrn1*	0,31	0,013514	Increase in EtOH	0,33	0,002

Figures and legends

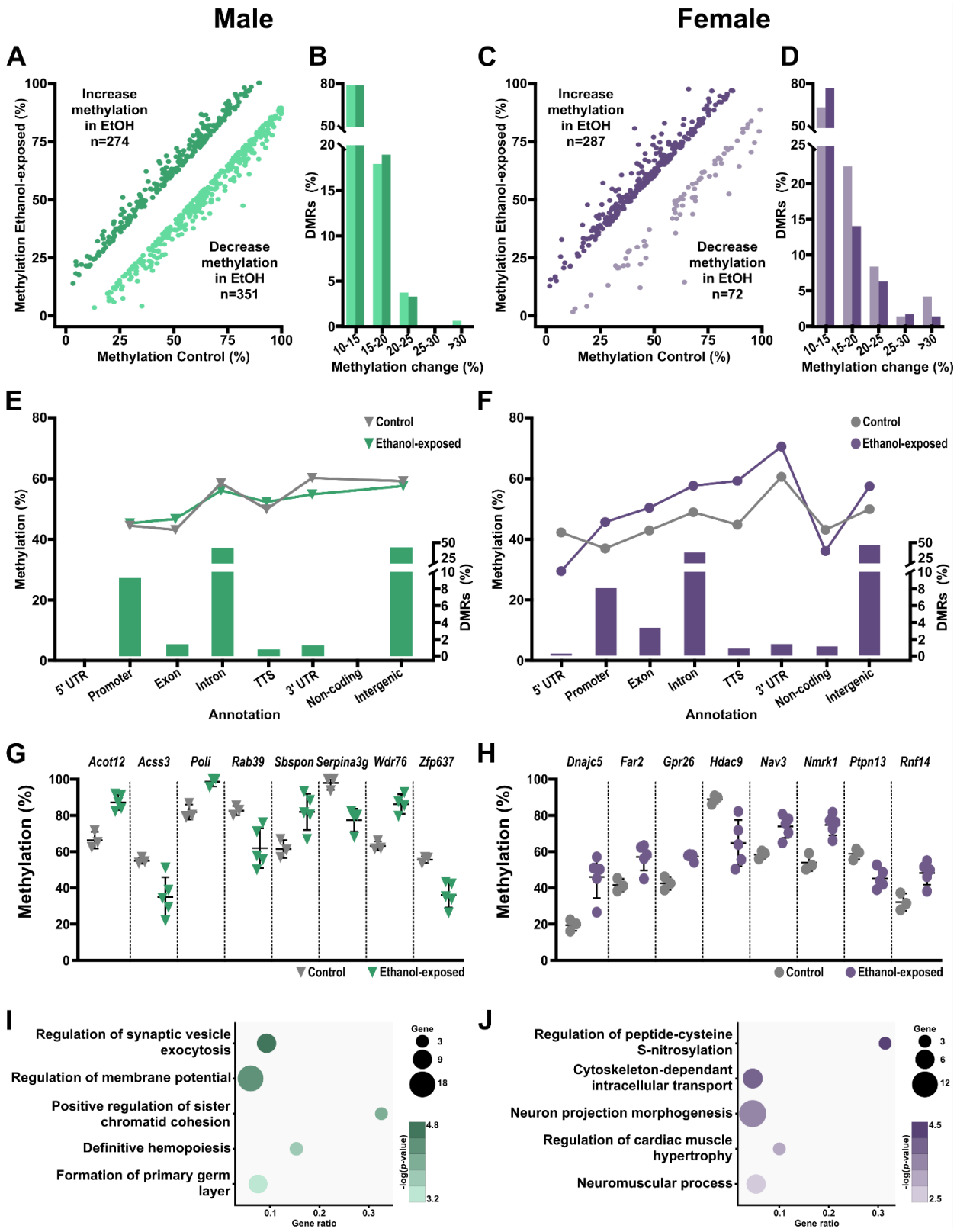

Figure 1: Early prenatal alcohol exposure induces sex-specific DNA methylation dysregulations in the forebrain

A) Scatterplot representing the DMRs between control and EtOH-exposed male forebrains. Green dots represent tiles with a methylation change of at least 10% in EtOH-exposed compared to control forebrains (n=625). **B)** Proportion of DMRs (n=625) associated with the changes in CpG methylation levels between control and EtOH-exposed male forebrains. **C)** Scatterplot representing the DMRs between control and EtOH-exposed female forebrains. Purple dots represent tiles with a methylation change of at least 10% in EtOH-exposed compared to control forebrains (n=359). **D)** Proportion of DMRs (n=359) associated with the changes in CpG methylation levels between control and EtOH-exposed female forebrains. **E)** and **F)** CpG methylation levels in control and ethanol-exposed male (**E**; grey/green) and female (**F**; grey/purple) forebrains based on DMR annotation (left *Y*-axis) and DMR distribution across genomic annotation (right *Y*-axis). **G)** and **H)** CpG methylation levels in control and ethanol-exposed male (**G**; grey/green) and female (**H**; grey/purple) forebrains for top changed DMRs. **I)** and **J)** Functional enrichment analysis showing top enriched pathways for male DMRs (**I**; n=351 unique gene DMRs; left, blue) and female DMRs (**J**; n=190 unique gene DMRs; right, green) based on Metascape analysis for pathways and *p*-value.

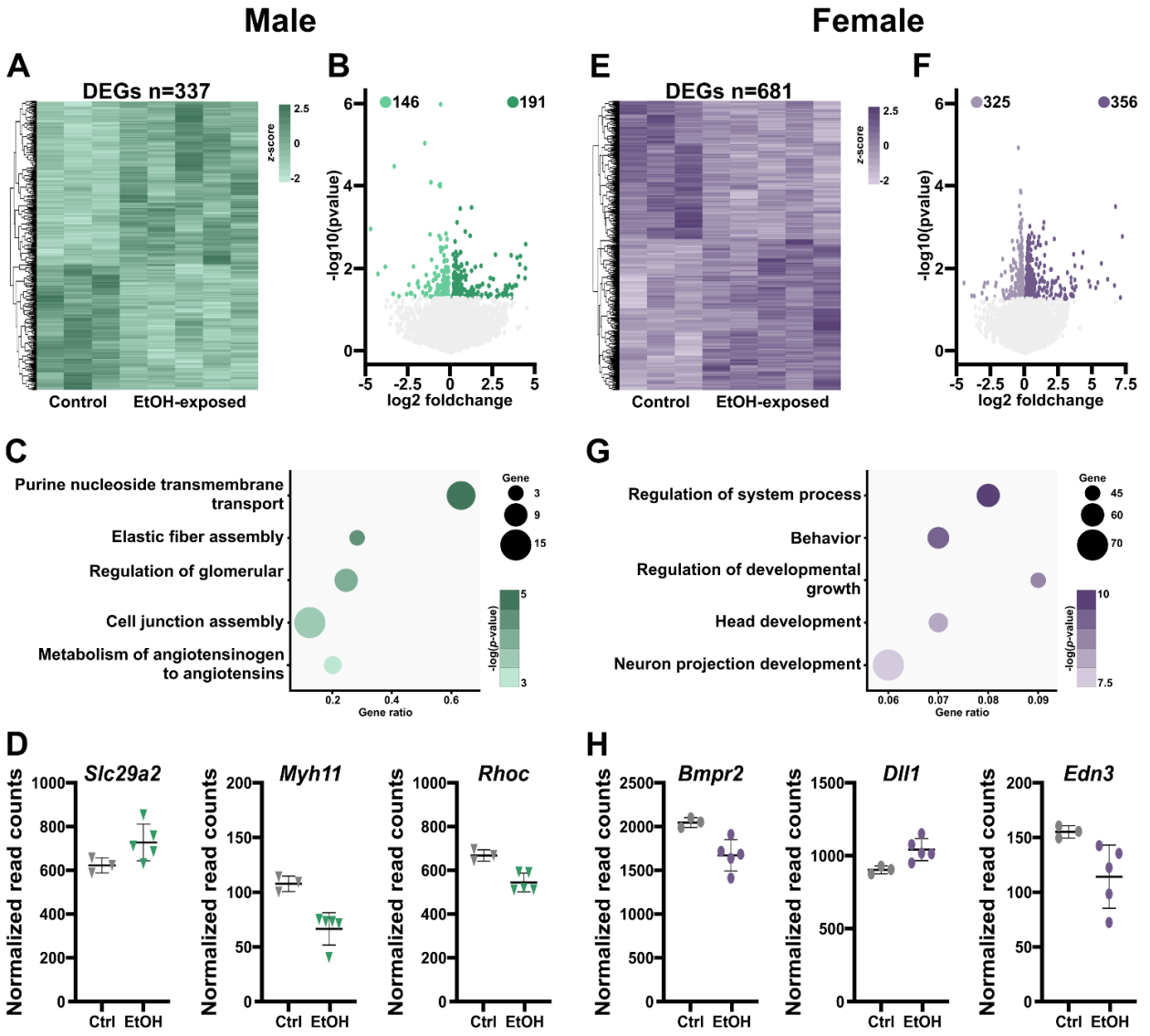

Figure 2: Early preimplantation alcohol exposure induces sex-specific transcriptomic changes in late-gestation forebrains

A) Heatmaps showing gene expression levels (*z*-score) of the 337 differentially expressed genes between control and EtOH-exposed forebrains in males. **B)** Differential expression analyses between control and EtOH-exposed forebrains in males. Colored dots represent statistically significant differentially expressed genes (DEGs) ($p<0.05$; n =337). **C)** Functional enrichment analysis showing top enriched pathways for male DEGs (n=337) based on Metascape analysis for pathways and *p*-value. **D)** Representation (normalized read counts) of genes with altered expression in male ethanol-exposed forebrains. **E)** Heatmaps showing gene expression levels (*z*-score) of the 681 differentially expressed genes between control and EtOH-exposed forebrains in females. **F)** Differential expression analyses between control and EtOH-exposed forebrains in females. Colored dots represent statistically significant differentially expressed genes ($p<0.05$; n =681). and **G)** Functional enrichment analysis showing top enriched pathways for female DEGs (n=681) based

on Metascape analysis for pathways **H)** Representation (normalized read counts) of genes with altered expression in female ethanol-exposed forebrains.

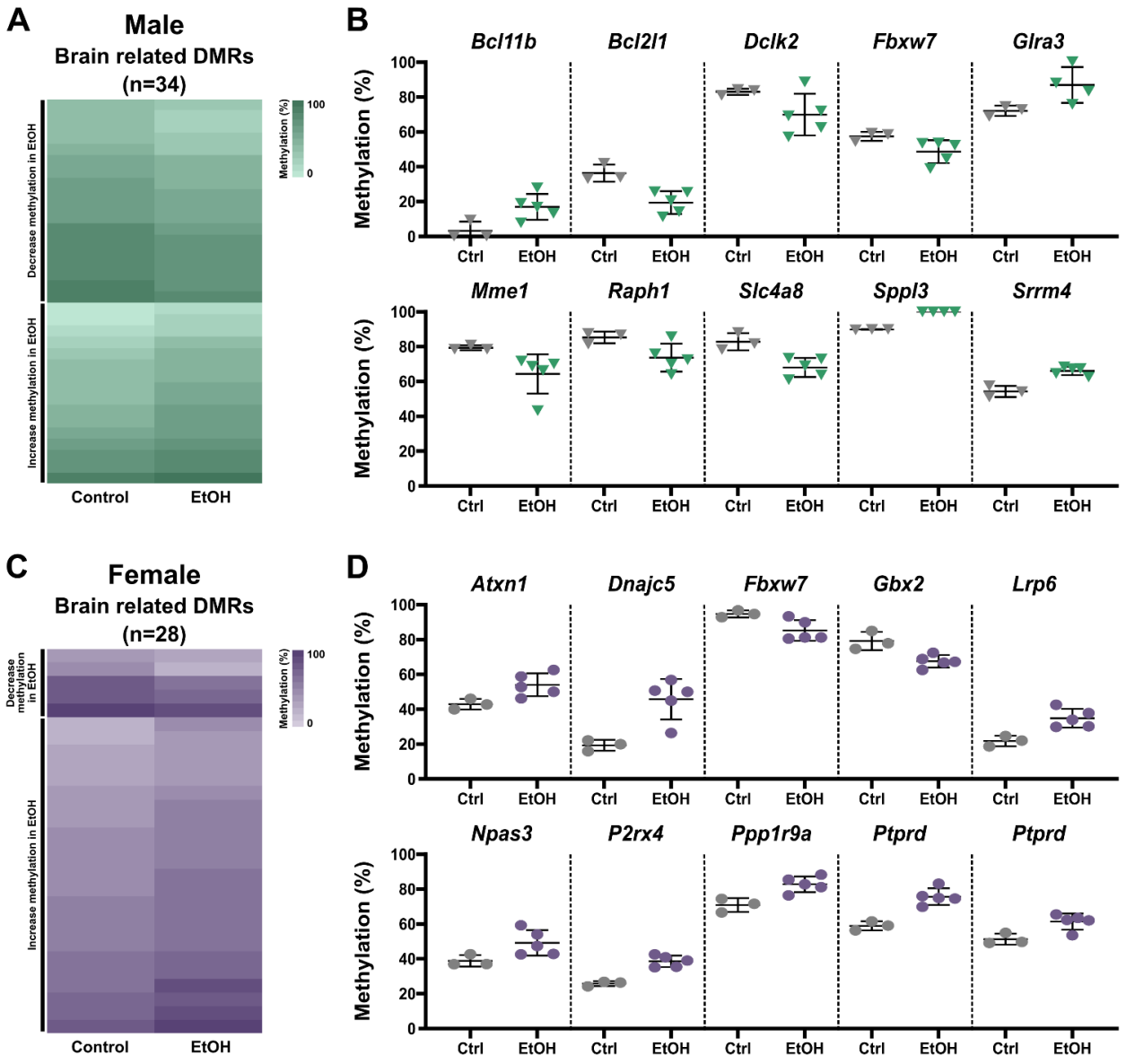

Figure 3: Sex-specific DNA methylation alterations in regions related to brain development and functions following preimplantation alcohol exposure

A) and **C)** Heatmaps showing CpG methylation levels in regions of genes related to brain development or function in males (A; n= 34 DMRs) and females (C; n= 28 DMRs). **B)** and **D)** CpG methylation levels in male (B) and female (D) control and ethanol-exposed forebrains for DMRs located in genes related to brain development or function.

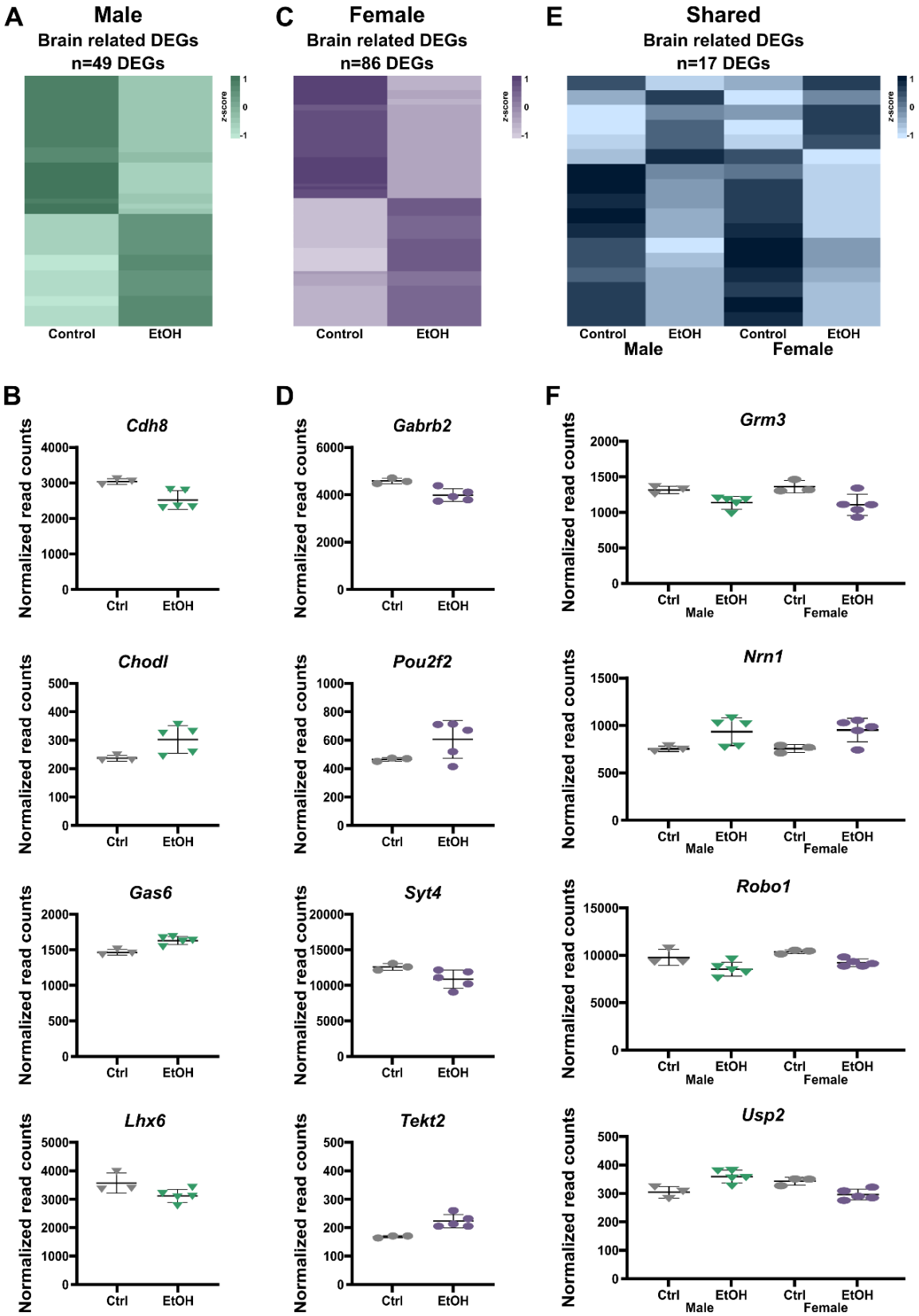
A
Male
Brain related DEGs
n=49 DEGs
z-score
1
0
-1
Control
EtOH
C
Female
Brain related DEGs
n=86 DEGs
z-score
1
0
-1
Control
EtOH
E
Shared
Brain related DEGs
n=17 DEGs
z-score
1
0
-1
Control
EtOH
Control
EtOH
Male
Female
B
D
F
Cdh8
Gabrb2
Grm3
Chodl
Pou2f2
Nrn1
Gas6
Syt4
Robo1
Lhx6
Tekt2
Usp2
Normalized read counts
Ctrl
EtOH
Male
Female

Figure 4: Sex-specific and shared expression dysregulation in genes related to brain development and functions following preimplantation alcohol exposure

A); **C)** and **E)** Heatmaps showing gene expression levels (*z*-score) in DEGs related to brain development and functions that are specific to males (A; n=49), to females (C; n=86) and shared between both sexes (E; n=17). **B)**; **D)** and **F)** Representation (normalized read counts) of DEGs related to brain development or function specific to males (B), females (D) or shared (F).

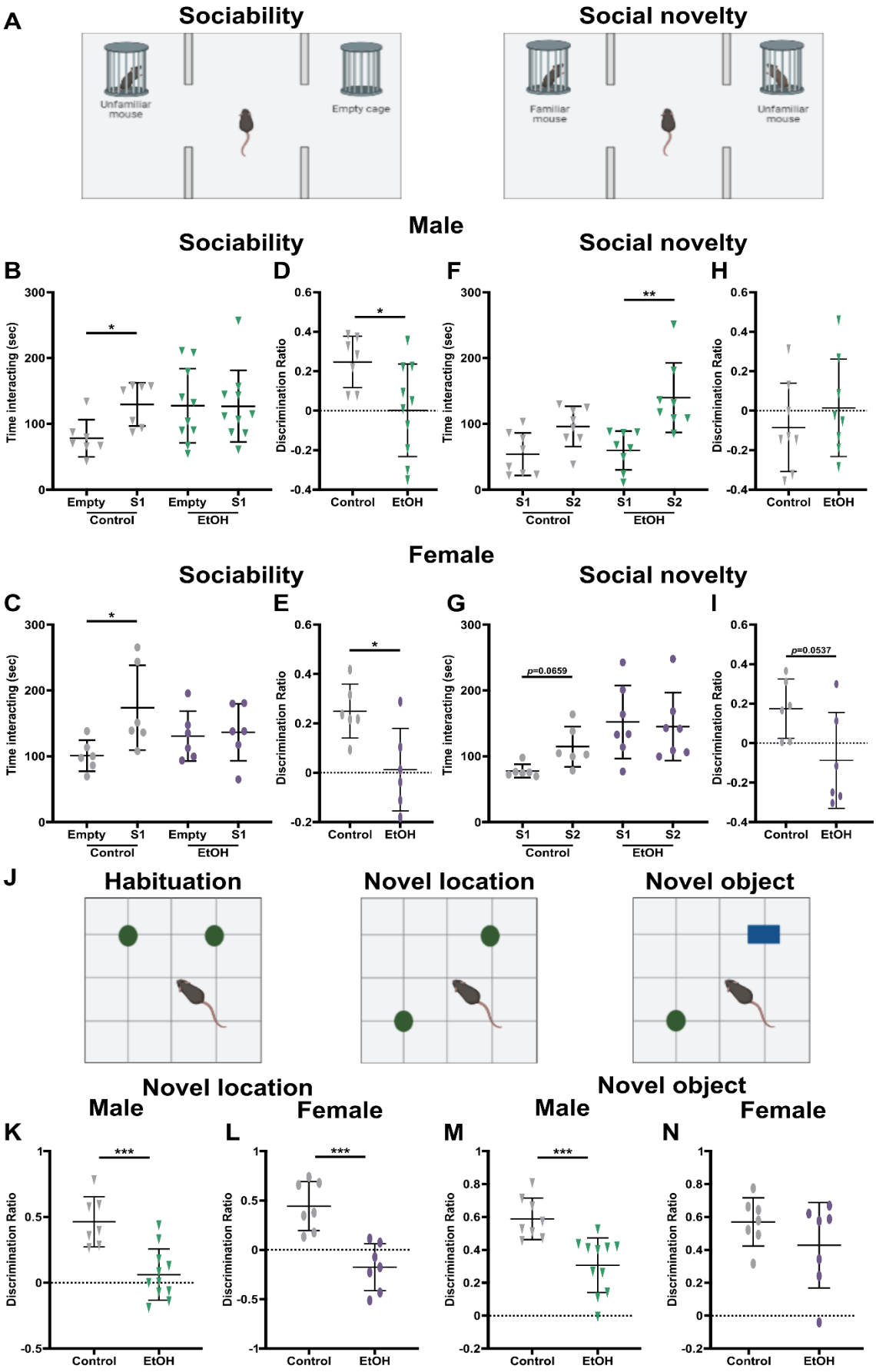
A
Sociability
Unfamiliar mouse
Empty cage
Social novelty
Familiar mouse
Unfamiliar mouse
Male
Sociability
Social novelty
B
D
F
H
Time interacting (sec)
Discrimination Ratio
Empty
S1
Control
EtOH
S2
Female
C
E
G
I
p=0.0659
p=0.0537
J
Habituation
Novel location
Novel object
Novel location
Male
Female
Novel object
K
L
M
N

Figure 5: Sex-specific changes in social abilities and short-term memory following preimplantation alcohol exposure

A) Schematic of the three-chamber maze assay to evaluate sociability and social novelty. **B)** and **C)** Interacting time of control and ethanol-exposed male (B) and female (C) mice with the empty cage and an unfamiliar mouse (Stranger 1; S1). **D)** and **E)** Discrimination ratio of the time of interaction with the novel mouse compared to empty cage for male (D) and female (E) mice. **F)** and **G)** Interacting time for control and ethanol-exposed male (B) and female (C) mice with the familiar mouse (Stranger 1; S1) and a novel unfamiliar mouse (Stranger 2; S2). **H)** and **I)** Discrimination ratio of the time of interaction with the novel mouse compared to the known mouse for male (H) and female (I) mice. **J)** Schematic of the novel object recognition assay to evaluate for short term memory. **K)** and **L)** Discrimination ratio of the time of interaction with the displaced object compared to the object at the initial location for male (K) and female (L) mice. **M)** and **N)** Discrimination ratio of the time of interaction with the novel object compared to the unchanged object for male (M) and female (N) mice.

Supplementary figures and legends

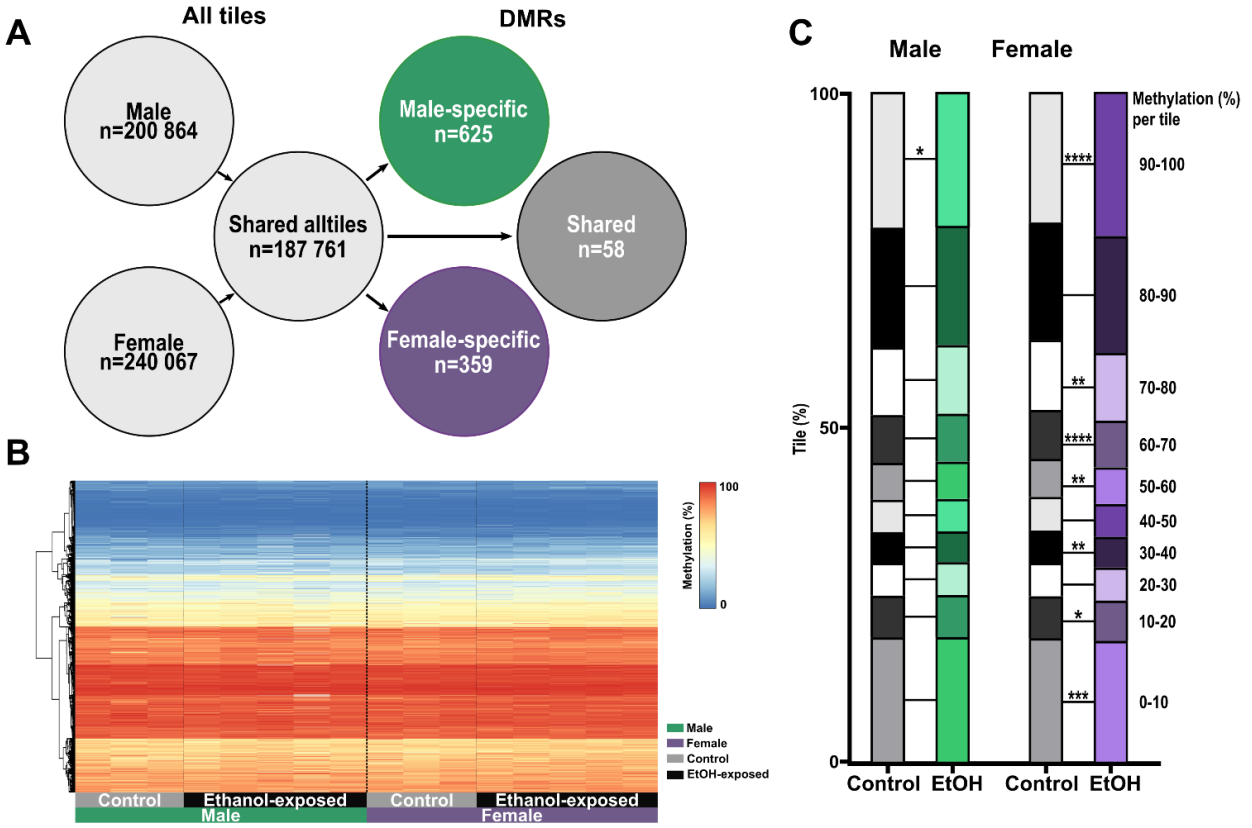

Figure Supp 1: Establishing DNA methylation profiles in E18.5 forebrains following preimplantation alcohol exposure

A) Schematic design of sex-related genome-wide CpG methylation analysis in male (Ctrl n = 3, EtOH n = 5) and female (Ctrl n = 3, EtOH n =5) E18.5 forebrains. Identification of all-tiles associated with either male samples (n = 200 864), female samples (n = 240 067), or shared between male and female samples (n = 187 761), as well as male-specific (n = 625), female-specific (n = 359) and common (n = 58) DMRs (see "Methods" section for details). **B)** Heatmap showing DNA methylation levels for a random subset of tiles (~5% of 187 761 total tiles; 100b, coverage >10X) for individual male and female control and EtOH-exposed forebrain samples. No column clustering applied. **C)** Tiles distribution across ranges of DNA methylation levels in male and female control and EtOH-exposed forebrains (shared tiles; n = 751 083). ****p < 0.0001, ***p < 0.001, **p < 0.01, *p < 0.05; two-proportions z-test test.

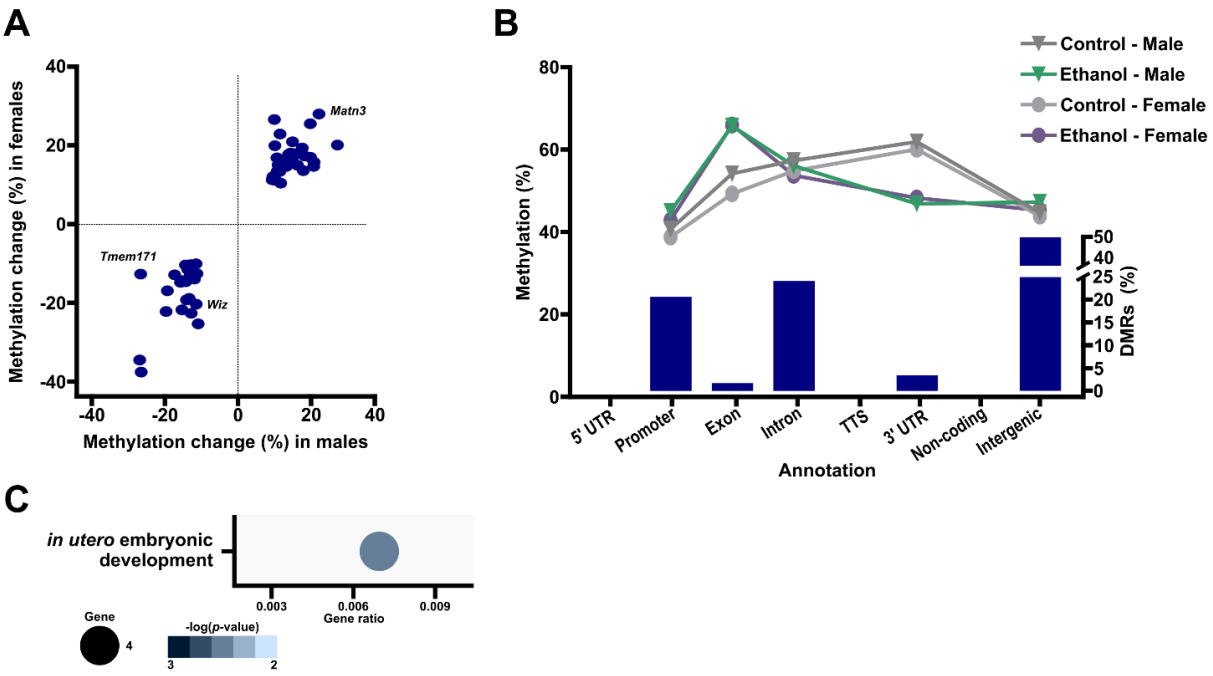

Figure supp 2 : DNA methylation alterations shared between male and female forebrains following preimplantation alcohol exposure are involved in embryonic development.

A) Scatterplot representing the percentage of CpG methylation changes of the 58 shared DMRs in male (*X* axis) and female (*Y* axis) forebrains. **B)** CpG methylation levels in control and ethanol-exposed male (**E**; dark grey/green) and female (**F**; light grey/purple) based on shared DMRs annotation (left *Y*-axis) and DMRs distribution across genomic annotation (right *Y*-axis). **C)** Functional enrichment analysis showing top enriched pathways for shared DMRs (n=29 unique gene DMRs) based on Metascape analysis for pathways and *p*-value.

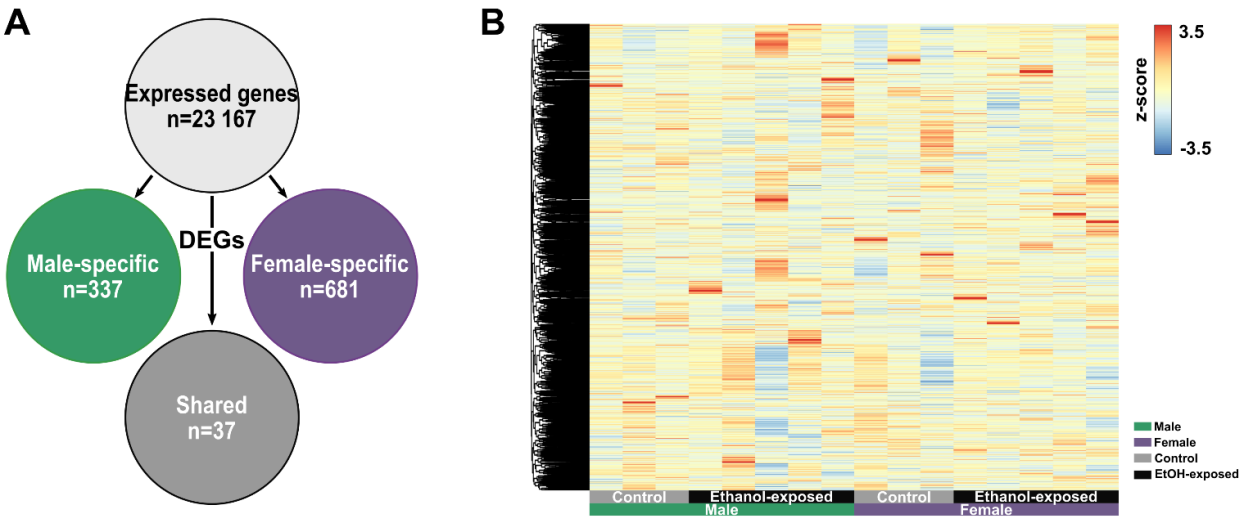

Figure supp 3: Establishing gene expression profiles in E18.5 forebrains following preimplantation alcohol exposure

A) Schematic design of sex-related differential transcriptomic analysis in male (Ctrl n = 3, EtOH n = 5) and female (Ctrl n = 3, EtOH n =5) E18.5 forebrains. Identification of all expressed genes in both sexes (n = 23 167), male-specific differentially expressed genes (DEGs) (n= 337), female-specific DEGs (n = 681) and shared DEGs (n = 37) (see "Methods" section for details). **B)** Heatmap showing gene expression levels (*z* score) of all analyzed genes (n= 23 167) for individual male and female control and EtOH-exposed forebrains. No column clustering applied.

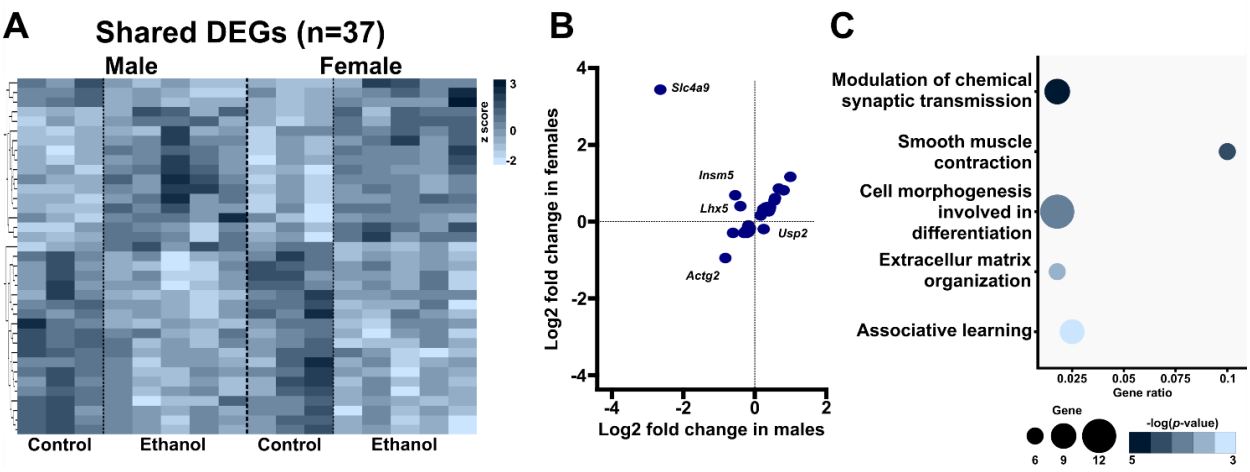

Figure Supp 4: Shared DEGs in late gestation forebrains are enriched in pathways related so synaptic transmission and learning

A) Heatmaps showing gene expression levels (*z*-score) of the 37 differentially expressed genes between control and EtOH-exposed forebrains in males and females. **B)** Scatterplot representing the changes in expression (log2 fold change) of the 37 shared DEGs in males (*X*-axis) and females (*Y*-axis). **C)** Functional enrichment analysis showing top enriched pathways for shared DEGs (n=37) based on Metascape analysis for pathways and *p*-value.

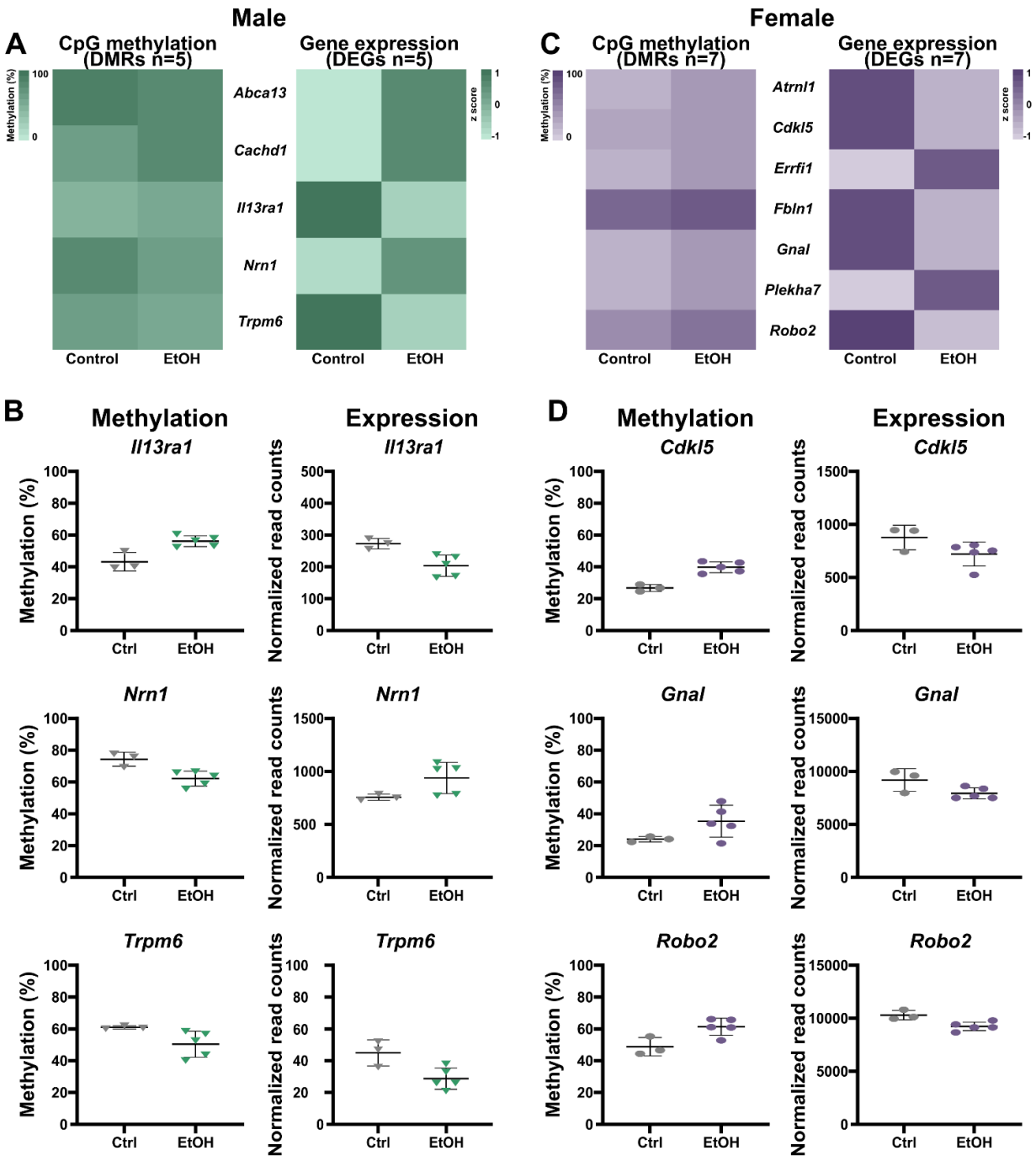

Figure Supp 5: Sex-specific regions showing DNA methylation alterations and gene expression changes following preimplantation alcohol exposure

A) and **C)** Heatmaps showing CpG methylation levels (left heatmap) and gene expression levels (*z*-score; right heatmap) in genic regions presenting both DNA methylation (DMRs) and gene expression alterations (DEGs) between control and EtOH-exposed forebrains in males (A; n= 5 DMRs and DEGs) or females (C; n= 7 DMRs and DEGs). **B)** and **D)** Representation (normalized read counts) of DMRs and DEGs in male (B) and female (D) forebrains.

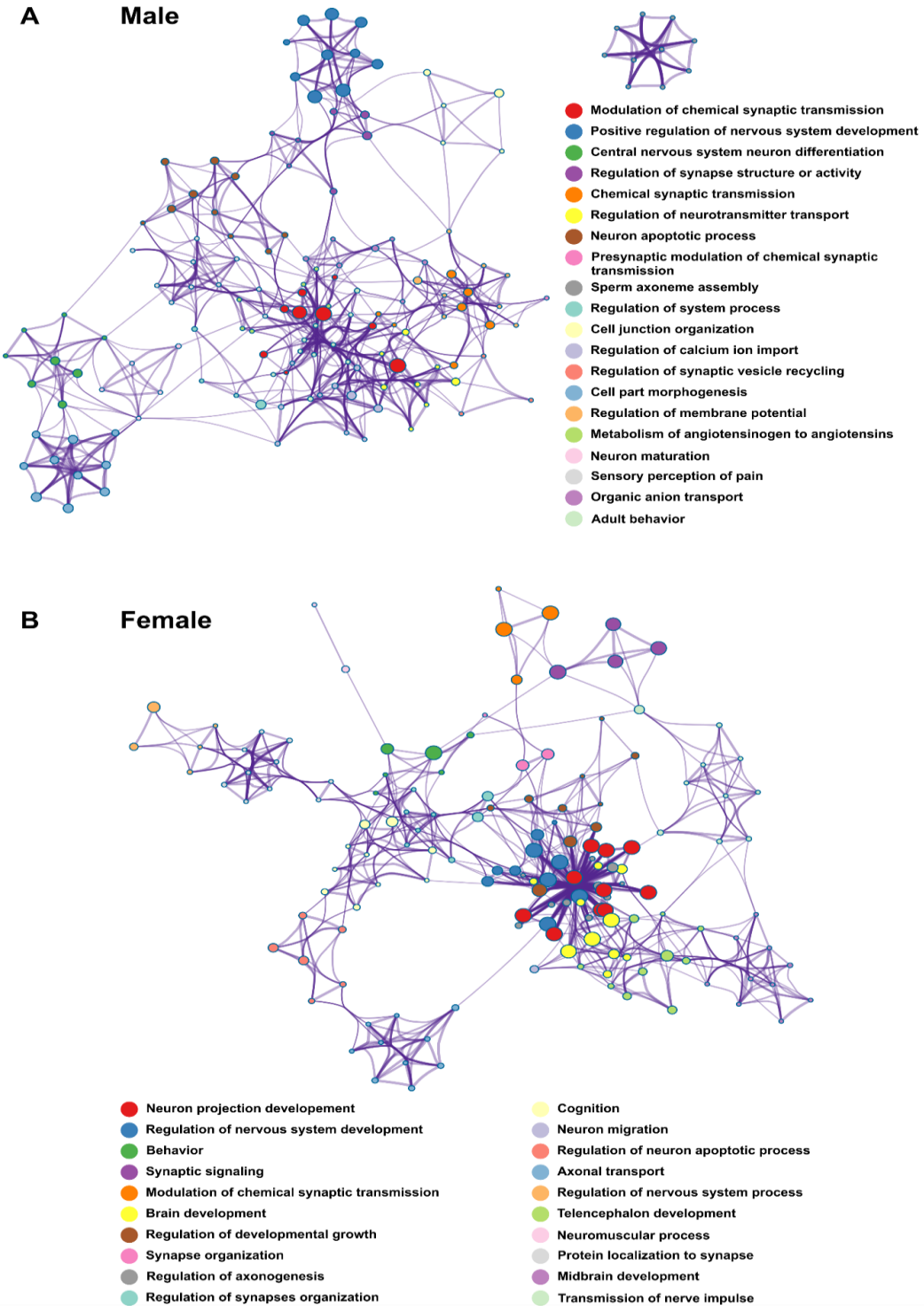

Figure Supp 6: DMRs and DEGs located in genes related to brain development and function network closely together

A) and **B)** Network enrichment analysis of the 34 DMRs and 49 DEGs in male (A) and the 28 DMRs and 86 DEGs in female (B) forebrains related to brain development and function.

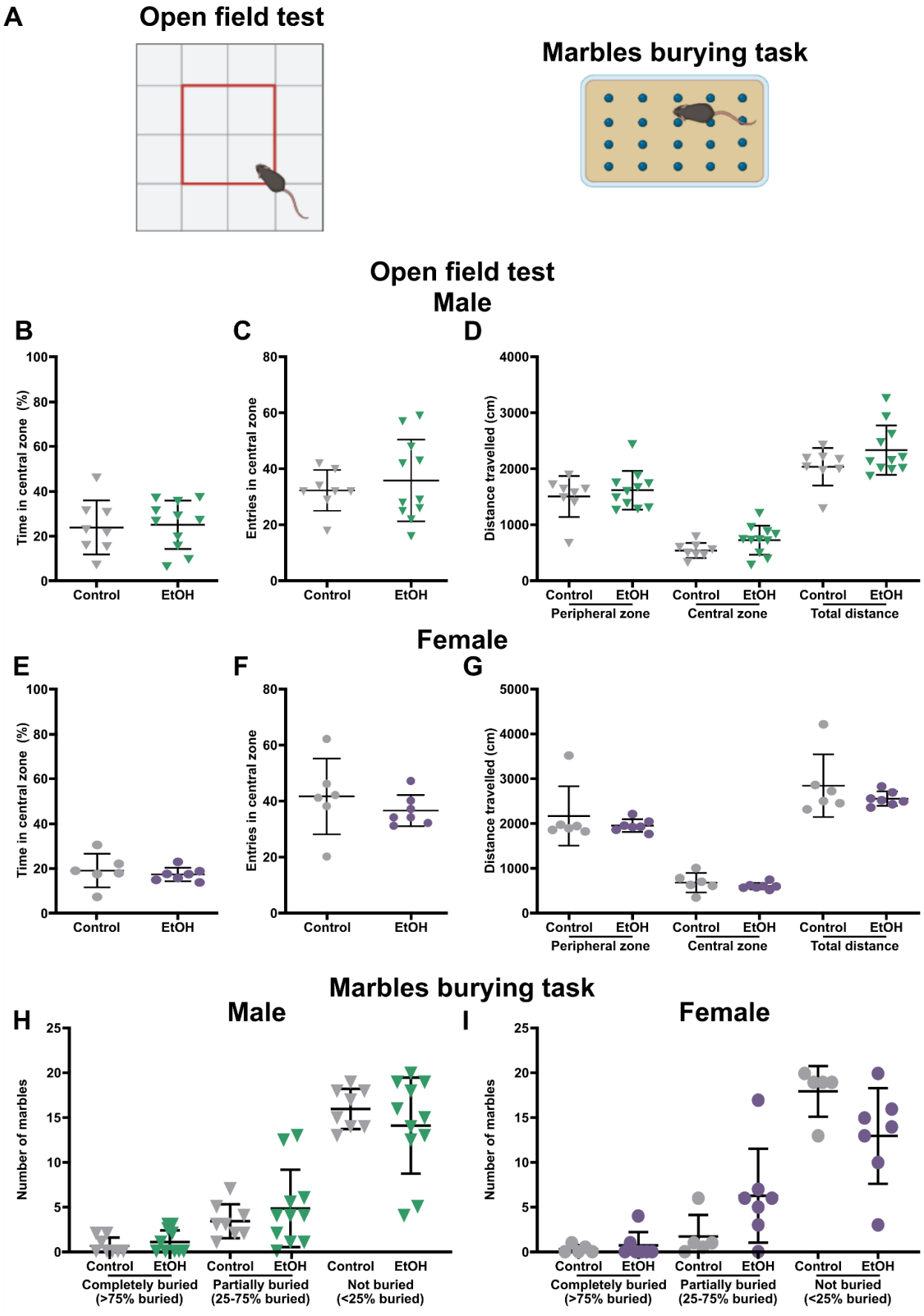
A
Open field test
Marbles burying task
Open field test
Male
B
C
D
Time in central zone (%)
Entries in central zone
Distance travelled (cm)
Control
EtOH
Peripheral zone
Central zone
Total distance
Female
E
F
G
Marbles burying task
Male
H
Female
I
Number of marbles
Completely buried (>75% buried)
Partially buried (25-75% buried)
Not buried (<25% buried)

Figure Supp 7: Preimplantation alcohol exposure does not increase anxiety nor repetitive behavior in young adult mice

A) Schematic of the open field test (left) and marble burying task (right). **B)** and **C)** percentage of time spent in the central zone for male (B) and female (C) control and ethanol-exposed mice. **D)** and **E)** Number of entries in the central zone for male (D) and female (E) control and ethanol-exposed mice. **F)** and **G)** Distance travelled in the peripheral and central zones and total distance travelled by male (F) and female (G) control and ethanol-exposed mice. **H)** and **I)** Number of marbles completely, partially, or not buried in male (H) and female (I) control and ethanol-exposed mice.

Supplementary tables

Table S1 : List of brain related genes in DMRs and DEGs

Brain related male-specific DMRs gene						
Abca13	*Cask*	*Fbxo31*	*Lmo4*	*Pawr*	*Rassf10*	*Slc4a8*
Anks1	*Chrna5*	*Fbxw7*	*Mmd*	*Pfn2*	*Rnf220*	*Sppl3*
Bcl11a	*Dclk1*	*Glra3*	*Mme*	*Prepl*	*Scyl3*	*Spry1*
Bcl11b	*Dclk2*	*Gpr1*	*Mns1*	*Ptn*	*Shroom3*	*Srrm4*
Bcl2l1	*Ddx21*	*Hsbp1*	*Nrn1*	*Raph1*	*Slc35a1*	
Brain related female-specific DMRs gene						
Ap3b1	*Cdkl5*	*Gbx2*	*Lrrn3*	*Nrcam*	*Ppp1r9a*	*Robo2*
Ap3s2	*Dnajc5*	*Hsbp1*	*Mmp24*	*Oxr1*	*Ppp3cb*	*Scgn*
Atxn1	*Dscam*	*Kalrn*	*Neurod6*	*P2rx4*	*Ptprd* (2)	*Trak2*
Btbd10	*Fbxw7*	*Lrp6*	*Npas3*	*Pmp22*	*Rims2*	
Brain related male-specific DEGs						
Abca13	*Ccdc135*	*Crtac1*	*Grid2*	*Lingo4*	*Prtn3*	*Slc7a10*
Ace	*Ccdc147*	*Dnm3*	*Gsc*	*Nr4a2*	*Shisa7*	*Sulf2*
Ace2	*Cdh8*	*Dscam*	*Hmx3*	*Ntrk1*	*Shisa9*	*Tfap2a*
Adnp	*Chodl*	*Gas6*	*Htr2c*	*Obsl1*	*Slc10a4*	*Tnfrsf1b*
Aph1c	*Chrm2*	*Gja1*	*Icam5*	*Otp*	*Slc17a7*	*Trh*
C1ql2	*Cpne6*	*Gnrh1*	*Irf8*	*Pcdh17*	*Slc24a2*	*Ttll5*
Cap2	*Crh*	*Gprin3*	*Lhx6*	*Pnoc*	*Slc29a1*	*Xrcc4*
Brain related female-specific DEGs						
Adora2a	*Col4a5*	*Filip1*	*Lhx4*	*Nhlh2*	*Radil*	*Tbr1*
Alcam	*Cpeb1*	*Foxb1*	*Lrrtm2*	*Notch3*	*Robo2*	*Tead3*
Aph1b	*Cpne9*	*Fzd3*	*Mag*	*Nptxr*	*Scrib*	*Tekt2*
Arhgap22	*Dbx1*	*Gabrb2*	*Map2k7*	*Npy1r*	*Sema3a*	*Tnfrsf21*
Bcl11b	*Dcx*	*Gpc6*	*Mdga2*	*Ntng1*	*Sema3d*	*Tpgs1*
Bmpr1a	*Dlg2*	*Gpm6a*	*Mlh3*	*Ntrk2*	*Sema3e*	*Uba6*
Cdc40	*Dmpk*	*Grm5*	*Mpp4*	*Penk*	*Sema5b*	*Usp9x*
Cdkl5	*En1*	*Hif1a*	*Mtap2*	*Pitx2*	*Sox21*	*Vgf*
Chrna4	*Fam107a*	*Homer3*	*Musk*	*Pls3*	*Stac3*	
Chrna6	*Fgf12*	*Insm1*	*Nefh*	*Pmch*	*Synpo*	
Clcn1	*Fgfr1*	*Irx5*	*Nefl*	*Pou2f2*	*Synpr*	
Cmah	*Fgfr3*	*Irx6*	*Neto2*	*Pou4f1*	*Syt17*	
Cmtm8	*Fig4*	*Lhx3*	*Neurod4*	*Prickle2*	*Syt4*	
Brain related shared DEGs						
Cbln4	*Flrt2*	*Grm3*	*Lhx5*	*Nrn1*	*Tnr*	
Cxcl12	*Foxp1*	*Gucy1a3*	*Lrrc4c*	*Nts*	*Usp2*	
Dnahc7b	*Gnal*	*Gucy1b3*	*Neto1*	*Robo1*		

REFERENCES

1. Legault LM, Doiron K, Breton-Larrivée M, Langford-Avelar A, Lemieux A, Caron M, et al. Pre-implantation alcohol exposure induces lasting sex-specific DNA methylation programming errors in the developing forebrain. Clinical epigenetics. 2021;13(1):164.
2. Bourgey M, Dali R, Eveleigh R, Chen KC, Letourneau L, Fillon J, et al. GenPipes: an open-source framework for distributed and scalable genomic analyses. GigaScience. 2019;8(6).
3. Krueger F, Andrews SR. Bismark: a flexible aligner and methylation caller for Bisulfite-Seq applications. Bioinformatics (Oxford, England). 2011;27(11):1571-2.
4. Akalin A, Kormaksson M, Li S, Garrett-Bakelman FE, Figueroa ME, Melnick A, et al. methylKit: a comprehensive R package for the analysis of genome-wide DNA methylation profiles. Genome biology. 2012;13(10):R87.
5. Heinz S, Benner C, Spann N, Bertolino E, Lin YC, Laslo P, et al. Simple combinations of lineage-determining transcription factors prime cis-regulatory elements required for macrophage and B cell identities. Molecular cell. 2010;38(4):576-89.
6. Zhou Y, Zhou B, Pache L, Chang M, Khodabakhshi AH, Tanaseichuk O, et al. Metascape provides a biologist-oriented resource for the analysis of systems-level datasets. Nature communications. 2019;10(1):1523.
7. Legault LM, Doiron K, Lemieux A, Caron M, Chan D, Lopes FL, et al. Developmental genome-wide DNA methylation asymmetry between mouse placenta and embryo. Epigenetics. 2020;15(8):800-15.
8. Karolchik D, Hinrichs AS, Furey TS, Roskin KM, Sugnet CW, Haussler D, et al. The UCSC Table Browser data retrieval tool. Nucleic acids research. 2004;32(Database issue):D493-6.
9. Bolger AM, Lohse M, Usadel B. Trimmomatic: a flexible trimmer for Illumina sequence data. Bioinformatics (Oxford, England). 2014;30(15):2114-20.
10. Dobin A, Davis CA, Schlesinger F, Drenkow J, Zaleski C, Jha S, et al. STAR: ultrafast universal RNA-seq aligner. Bioinformatics (Oxford, England). 2013;29(1):15-21.
11. Li H, Durbin R. Fast and accurate short read alignment with Burrows-Wheeler transform. Bioinformatics (Oxford, England). 2009;25(14):1754-60.
12. Love MI, Huber W, Anders S. Moderated estimation of fold change and dispersion for RNA-seq data with DESeq2. Genome biology. 2014;15(12):550.
13. Legault LM, Breton-Larrivée M, Filion-Bienvenue F, Lemieux A, Langford-Avelar A, McGraw S. Early preimplantation binge alcohol exposure induces sex-specific changes in DNA methylation and gene expression in the mouse placenta. JCI Insight. To be submitted.

Chapitre 6 – Discussion et conclusion

L'impact négatif à long terme d'une exposition préimplantatoire à l'alcool.

Ma thèse en bref!

Encore aujourd'hui, la consommation d'alcool par la femme enceinte est parfois banalisée, particulièrement en tout début de grossesse. Puisque l'embryon n'est pas encore physiquement implanté au cours de la première semaine de la grossesse, même plusieurs professionnels de la santé entretiennent le dogme que la consommation d'alcool pendant cette période est sans danger pour le bébé. Loin de vouloir stigmatiser les femmes enceintes, il faut plutôt promouvoir la prévention et éduquer la population aux risques associés à la consommation prénatale à l'alcool, même en tout début de grossesse.

Au cours de cette thèse, j'ai étudié les impacts d'une exposition prénatale à l'alcool pendant la préimplantation sur le développement embryonnaire ainsi que le paysage épigénétique et transcriptomique du cerveau embryonnaire et du placenta. J'ai aussi étudié les impacts fonctionnels à long terme sur certaines fonctions cognitives.

Tout d'abord, nous avons démontré qu'une exposition prénatale à l'alcool pendant la préimplantation augmente de façon significative la présence d'anomalies morphologiques chez les embryons à mi-gestation. Alors que plusieurs études ont démontré qu'une exposition prénatale à l'alcool au cours du premier trimestre de grossesse était plus susceptible d'entrainer des anomalies cranio-faciales (163), l'apport de la préimplantation dans ces défauts est méconnu. Bien que les anomalies détectées étaient variées, nous avons retrouvé une prépondérance de retard de croissance et d'anomalies de la structure du cerveau, ce qui est similaire à ce qui est observé dans plusieurs modèles d'exposition en début de grossesse (1er trimestre) ou chronique (163). Certains retards de croissance semblent d'ailleurs perdurer au cours de la gestation, particulièrement chez les embryons mâles exposés à l'alcool qui présentent globalement une réduction du poids fœtal en fin de gestation.

Au cours de ce projet, nous avons aussi montré que l'exposition à l'alcool pendant la préimplantation induit des changements des profils de méthylation d'ADN et d'expression génique dans le cerveau antérieur de l'embryon à mi-gestation, en fin de gestation de même que dans les placentas en fin de gestation. Lors des analyses d'ontologie génique des gènes différentiellement méthylés dans le cerveau antérieur aux deux stades développementaux ou des gènes différentiellement exprimés dans le cerveau antérieur en fin de gestation, nous avons trouvé un enrichissement relié à plusieurs voies métaboliques ou biologiques en lien avec le développement de l'embryon, le développement du cerveau, les fonctions cérébrales ou le comportement, rappelant le spectre de phénotypes associés au TSAF, dont les troubles neurodéveloppementaux.

Finalement, nous avons démontré que notre modèle d'exposition à l'alcool cause des altérations cognitives à plus long terme chez les souris adolescentes qui ont été exposées pendant la préimplantation. Certaines altérations cognitives, comme une baisse de la sociabilité ou un trouble de mémoire, ont déjà été observées lors d'exposition prénatale à l'alcool de type chronique, tout au long de la grossesse ou strictement pendant le premier trimestre. Par exemple, une étude datant de 1997 a démontré une baisse de la sociabilité autant chez les rats mâles que femelles à la suite d'une exposition de type *binge*, avec une haute concentration d'alcool, mais tout au long du premier trimestre (164). Au niveau de la mémoire et de la reconnaissance spatiale, un modèle d'alcool chronique avec une dose modérée d'alcool au cours du premier trimestre a observé des altérations de ces fonctions en utilisant le test du *Morris Water Maze* (165). Bien que d'autres études aillent aussi observer des dérèglements de la sociabilité, de la mémoire ou même de l'anxiété, les résultats sont variables selon le temps d'exposition, la concentration d'alcool à laquelle les souris sont exposées et l'âge à laquelle le test comportemental est effectué (166). Les trouvailles dans la littérature décrivent tout de même avec précision le spectre de symptômes en lien avec une exposition prénatale à l'alcool. Nous sommes néanmoins les premiers à prouver qu'une exposition unique à l'alcool pendant la préimplantation peut entraîner des conséquences néfastes sur le développement cognitif, notamment au niveau de la sociabilité et de la mémoire, qui sont observables à un stade murin comparable à l'adolescence chez l'humain.

Notre modèle d'exposition prénatale à l'alcool est unique et permet d'étudier spécifiquement une consommation d'alcool maternelle en tout début de grossesse, avant même que la femme sache avec certitude qu'elle est enceinte. Contrairement aux modèles d'exposition de

type chronique, c'est-à-dire à plusieurs moments dans la grossesse ou tout au long de celle-ci, une exposition unique évite d'avoir une multitude d'impacts causés par l'exposition à différents stades développementaux. Notre modèle permet donc de caractériser précisément les conséquences reliées seulement à l'exposition prénatale à l'alcool au stade 8-cellules, un stade développemental particulièrement vulnérable. Il s'agit d'une preuve que l'environnement maternelle, dès les premiers jours de la grossesse, est crucial pour le développement embryonnaire et la santé du bébé à long terme. Ainsi, il faut arrêter d'entretenir la croyance qu'une consommation maternelle d'alcool en début de grossesse est sans danger pour le bébé. Au cours de ma thèse, j'ai démontré que ce dogme est faux et qu'une exposition prénatale à l'alcool pendant la préimplantation peut entraîner des conséquences néfastes sur le développement embryonnaire et même sur les fonctions cognitives à long terme.

Induction de perturbations spécifiques au sexe à la suite d'une exposition préimplantatoire à l'alcool

Un des constats majeurs lors de l'analyse des différentes expériences en lien avec mon projet était la prépondérance constante d'altérations spécifiques à chacun des sexes chez les échantillons exposés à l'alcool lors de la préimplantation. En effet, que ce soit dans le cerveau (Chapitres 3 et 5) ou dans le placenta (Chapitre 4), dans les altérations de la méthylation d'ADN ou d'expression génique, ou même dans les changements comportementaux à long terme, une proportion significative des dérégulations que nous avons observées était unique à chacun des sexes et la proportion de dérégulations communes aux mâles et aux femelles était étonnamment limitée.

Étant donné que notre exposition se fait en tout début de grossesse, au stade embryonnaire 8-cellules, il est difficile, à première vue, de comprendre l'abondance de ces résultats spécifiques au sexe que nous obtenons. Il est toutefois clair que le développement embryonnaire s'adapte de façon divergente entre les mâles et les femelles à une exposition prénatale à l'alcool faite au stade 8-cellules et que le patron des modifications épigénétiques et transcriptomiques peut être transmis différemment à travers la différentiation en types cellulaires subséquemment. Il est aussi important de prendre en compte le fait qu'au moment de l'exposition, l'inactivation du chromosome X chez les femelles n'est pas encore complétée, entrainant d'importantes différences au niveau transcriptionnelles des gènes associés au chromosome X, et de certains gènes autosomaux qui peuvent être régulés par ces derniers (167-169). D'ailleurs, un modèle exposant des embryons

préimplantatoires en culture à des corps cétoniques a démontré des altérations spécifiques au sexe dans les profils transcriptomiques du foie, du placenta et du cerveau des embryons au jour E14.5 après leur implantation dans une souris porteuse, incluant des dérégulations importantes dans des gènes du chromosome X et des gènes impliqués dans la modification de la chromatine (i.e. *Hdac2*, *Foxo3*, *Kat7*, etc.) (170).

Récemment, nous avons évalué les différences épigénétiques et transcriptomiques intrinsèques présentes entre les mâles et les femelles dans les placentas contrôles en fin de gestation. Dans cet article (voir Annexe 2), nous avons découvert 358 gènes autosomaux différentiellement exprimés entre les mâles et les femelles dans les placentas au jour embryonnaire 18.5 et 9 gènes différentiellement exprimés situés sur le chromosome X. Au niveau de la méthylation d'ADN, nous avons caractériser 1 705 régions différentiellement méthylées (DMRs) localisées sur des chromosomes autosomaux et 3 756 DMRs sur le chromosome X. Dans cet article, nous avons aussi démontré que certains DMRs identifiés au stade E18.5 étaient déjà présents à mi-gestation, soit au stade embryonnaire E10.5. Des études chez l'humain, la souris et le bovin ont aussi démontré des différences au niveau de l'expression de certains gènes situés sur des chromosomes autosomaux entre les mâles et les femelles à plusieurs stades de la préimplantation, incluant le stade 8-cellules (171-173). Par exemple, chez le bovin au stade blastocyste, ils ont montré qu'environ le tier des gènes différentiellement exprimés entre les mâles et les femelles étaient autosomaux, soit une proportion similaire aux différences de méthylation que nous observons dans le placenta de souris en fin de gestation (172). Ces études ont aussi permis d'illustrer que certaines différences entre les mâles et les femelles sont conservées pendant le développement embryonnaire alors que d'autres sont plutôt dynamiques. Ces données ont aussi permis d'établir que les différences biologiques entre les deux sexes sont aussi présentes chez plusieurs espèces de mammifères.

Une autre particularité du stade 8-cellules, est l'isoforme de DNMT1 DNMT1o, spécifiquement actif à ce stade afin de maintenir les profils de méthylation sur les gènes à empreinte et d'autres régions spécifiques du génome (30, 73). Cette fonction est maintenue par l'isoforme DNMT1s aux autres stades du développement préimplantatoire. Environ à mi-gestation (E9.5), les placentas d'embryons issus de femelles knock-out pour DNMT1o (*Dnmt1*$^{\Delta 1o/\Delta 1o}$) présentent des altérations au niveau morphologique et au niveau de la méthylation d'ADN, principalement une

perte de méthylation, principalement sur le chromosome X, par rapport au placenta des souris contrôles. Toutefois, chez les embryons femelles, les défauts morphologiques étaient plus fréquents et plus prononcés. Au niveau moléculaire, les pertes de méthylation d'ADN dans les placentas *Dnmt1*$^{\Delta 1o/\Delta 1o}$ en comparaison avec les contrôles étaient aussi plus fréquentes chez les femelles (73). Cette étude démontre, la vulnérabilité du paysage épigénétique au stade 8-cellules, mais surtout que l'adaptation se fait de façon asymétrique entre les embryons mâles et femelles pour une portion du génome.

Plusieurs autres articles utilisant des modèles d'exposition ou de perturbations en début de grossesse, principalement l'impact du stress et de la diète maternelle en début de grossesse ou encore l'effet de certaines conditions de culture en lien avec la fécondation *in vitro* ont aussi démontré des impacts spécifiques au sexe au cours du développement et à long terme sur la vie du futur bébé. Ces différences incluent la survie embryonnaire, la sévérité des phénotypes, des troubles neurodéveloppementaux, le poids embryonnaire et des troubles métaboliques (174-177). À travers leurs résultats, l'ensemble de ces études a aussi démontré que certaines des conséquences observées en lien avec une perturbation en début de grossesse étaient spécifiques au sexe, la réponse étant hétérogène d'un modèle d'exposition à l'autre.

Chez l'humain, les différences spécifiques au sexe ont longtemps été ignorées dans les études épidémiologiques, incluant celles sur l'exposition prénatale à l'alcool. Malgré la très grande variété de symptômes possibles, la prévalence de ceux-ci chez les filles ou les garçons n'était jamais départagée. Récemment, le réseau de recherche canadien sur le TSAF (CanFASD) a publié un article où une méta-analyse de plus de 2 500 patients a permis de démontrer que certains phénotypes ou certaines conséquences du TSAF sont plus prévalentes chez un sexe ou l'autre (178). Le patron d'exposition de l'ensemble des patients analysés n'était pas déterminé, ce qui fait que ce facteur n'était pas pris en compte. Malgré l'hétérogénéité dans le type d'exposition à l'alcool, les différences spécifiques au sexe sont bien démarquées et certains de leurs résultats sont particulièrement pertinents pour nous puisqu'ils nous permettent de mettre nos résultats en parallèle avec leur rétrospective. En accord avec les études démontrant plus de susceptibilité à l'environnement maternel chez les mâles, ils ont d'abord observé que légèrement plus de garçons (58%) que de filles (42%) étaient atteint d'un TSAF dans l'ensemble des cohortes étudiées (178). Similairement à nos observations chez les embryons à mi-gestation, aucune différence de retards

de croissance entre les mâles et les femelles n'a été observé. De façon intéressante, ils ont montré une plus grande prévalence pour certains troubles neurodéveloppementaux chez les garçons que chez les filles, dont des troubles de l'attention, de l'adaptation ou de la mémoire (178). Rappelons que nos études comportementales démontrent une diminution de la mémoire de reconnaissance d'un nouvel objet seulement chez nos souris mâles. La méta-analyse de CanFASD démontre toutefois plus d'anxiété, de dépression et de trouble de l'humeur chez les femelles (178). Bien que lors de nos tests de comportement nous n'ayons observé aucune augmentation de l'anxiété, les femelles démontraient une baisse pour la nouveauté sociale qui, à long terme chez l'humain, peut être reliée à de l'isolement et, possiblement, à la dépression (179). Globalement, leurs résultats démontrent une plus grande prévalence de plusieurs phénotypes directement reliés au cerveau (comme les troubles neurodéveloppementaux) chez les mâles (178). Plusieurs études rétrospectives sur l'exposition prénatale à la nicotine via la cigarette traditionnelle ou la cigarette électronique ont aussi trouvé une plus grande prévalence chez les garçons pour plusieurs problèmes neurodéveloppementaux, dont les troubles d'attention et les troubles d'hyperactivité (180-182). Plus de tests comportementaux seraient nécessaire afin d'évaluer complètement le portrait cognitif de nos souris avec notre modèle d'exposition à l'alcool pendant la préimplantation et définir plus précisément les différences spécifiques au sexe à long terme.

Contribution du placenta dans les phénotypes moléculaires et morphologiques associés à une exposition prénatale à l'alcool.

Le placenta joue un rôle majeur dans le développement embryonnaire et son intégrité peut influencer de façon permanente le déroulement de la grossesse. Le placenta est dérivé des cellules du trophectoderme et est donc un organe d'origine embryonnaire. Ce dernier est rarement étudié dans les modèles d'exposition prénatale à l'alcool et l'impact d'une exposition sur son développement et sur ses profils moléculaires est peu connu. Mes résultats démontrent qu'une exposition à l'alcool au stade 8-cellules affecte les profils de méthylation d'ADN et transcriptomiques du placenta en fin de gestation, sans toutefois démontrer des signes majeurs de perturbations de sa morphologie.

De façon intéressante, nous observons une baisse significative du poids embryonnaire à E18.5 chez les embryons mâles exposés à l'alcool pendant la préimplantation alors que nous n'observons aucun changement chez les embryons femelles. Nous observons aussi un nombre plus

élevé de gènes dérégulés dans les placentas mâles à la suite de notre exposition à l'alcool, bien que les placentas femelles présentent un plus grand nombre de région différentiellement méthylées. L'ensemble de ces changements moléculaires ont le potentiel de moduler le fonctionnement placentaire. Bien que nous n'observions pas de changement drastique dans la morphologie des placentas exposés à l'alcool, nous notons tout de même des changements de méthylation et d'expression génique du gène *Slc16a3*, qui code pour la protéine MCT4, chez les mâles. Cette protéine, avec MCT1, une autre protéine transmembranaire de la même famille, jouent un rôle crucial dans l'organisation trophoblastique du placenta et dans son pouvoir de vascularisation. Récemment, un groupe de recherche a démontré une structure placentaire altérée, via une désorganisation des protéines MCT4 et MCT1, ainsi qu'une baisse du poids fœtal dans un modèle de souris étudiant la voie de signalisation mTOR lors d'un apport insuffisant en nutriment (183). Une diminution de l'expression du gène *Slc16a3* a aussi été observé dans des placentas humains exposés à l'acide valproïque, un traitement contre l'épilepsie (184). Cette exposition est bien connue pour augmenter le risque de retard intellectuel et de malformations fœtales, incluant de retard de croissance intra-utérin (185-188). De façon similaire, il est possible que notre exposition prénatale à l'alcool au stade 8-cellules entraine des dérégulations moléculaires dans les cellules placentaires, générant un environ intra-utérin sous-optimal. L'adaptation variable entre les sexes pourrait entrainer des changements plus importants dans les structures trophoblastiques des placentas des embryons mâles, causés par des perturbations moléculaires du gène *Slc16a3,* et entrainant une réduction du poids fœtal des embryons mâles. Les retards de croissance pourraient donc être directement causés par des altérations moléculaires du placenta dans certains cas de TSAF chez les enfants. Chez l'humain, il est connu que les grossesses d'un embryon mâle sont plus sujet à certaines pathologies comme la prééclampsie ou le retard de croissance intra-utérin (189-195). Le mécanisme exact reste, à ce jour, inconnu. Cependant, une des hypothèses largement acceptée stipule que les embryons mâles semblent se développer plus rapidement, requérant donc beaucoup de nutriments et d'oxygène devant être fournis par la mère via le placenta. Lorsque l'environnement intra-utérin devient sous-optimal, les embryons mâles ne sont pas en mesure d'adapter leur développement comme le fait un embryon femelle, afin de mieux gérer les changements de l'environnement ou la baisse dans la disponibilité de certains éléments essentiels, entrainant le développement d'une pathologie de la grossesse (195, 196). L'exposition à l'alcool pendant la préimplantation a le potentiel d'engendrer des erreurs épigénétiques et

transcriptomiques dans les cellules qui seront perpétuées à travers le développement placentaire et altérant son fonctionnement optimal et donc le développement de l'embryon.

Il est aussi intéressant de mentionner que l'impact de l'exposition à l'alcool sur le développement d'un retard de croissance n'est qu'en partie mitigé lorsque nous supplémentons la diète maternelle avec différents donneurs de groupement méthyle, comme l'acide folique et la choline. En effet, notre groupe de recherche s'est intéressé à savoir si une diète préventive, enrichie en donneur de groupements méthyles, débutée avant la grossesse et poursuivie tout au long de celle-ci pouvait diminuer la présence de certains défauts morphologiques et altérations moléculaires. Alors que les anomalies du développement du cerveau et de l'œil sont presque totalement absentes chez les embryons exposés à l'alcool mais dont la mère consomme la diète enrichie, nous observons seulement une baisse partielle de la proportion d'embryons présentant un retard de croissance entre les embryons exposés à l'alcool avec ou sans la diète supplémentée (197). Des études moléculaires approfondies du placenta avec ce modèle permettront aussi de mieux évaluer l'impact direct de cet organe sur le développement de l'embryon lors d'une exposition prénatale à l'alcool pendant la préimplantation. Toutefois, la persistance de ce phénotype démontre bien l'immense impact négatif qu'une exposition à l'alcool en tout début de grossesse peut avoir sur le développement embryonnaire, même lorsqu'une supplémentation est ajoutée dans la diète dans le but de contrecarrer l'effet de l'alcool sur l'épigénome.

Outre son impact direct sur le développement embryonnaire, les dérégulations moléculaires du placenta observés à la suite d'une exposition prénatale à l'alcool pendant la préimplantation peuvent aussi stimuler de façon indirecte le développement d'autres phénotypes couramment associés au TSAF comme les troubles neurodéveloppementaux. Nous avons d'ailleurs observé dans nos DMRs intragéniques associés aux placentas mâles exposés à l'alcool un enrichissement dans la voie ontologique associé à la transmission synaptique. Récemment, une étude s'intéressant aux impacts d'une exposition au cannabis avant et pendant toute la gestation a aussi étudié les placentas en fin de gestation (198). Leur étude a permis de trouver de nombreux CpG différentiellement méthylés dans les placentas, dont plusieurs changements spécifiques au sexe. Lors de leur propre analyse d'ontologie génique, ils ont trouvé de nombreux enrichissement dans plusieurs voies relié au développement ou au fonctionnement du système nerveux, incluant les synapses (198). Lorsque nous recoupons notre liste de DMRs avec leurs résultats, nous trouvons

que plusieurs de nos DMRs impliqués dans la transmission synaptique sont aussi situés dans des gènes avec des CpGs différentiellement méthylés dans les placentas mâles dans leur étude sur le cannabis, tel *Celf4*, *Dgki*, *Dgkz*, *Fyn*, *Gnai2*, *Igf1r*, *Lrrk2* et *Shank2* (198). Bien que le type d'exposition et la fréquence d'exposition soit différente, il est intéressant de remarquer que certaines régions soient altérées dans les deux cas. Plus encore, il peut sembler étonnant que ces régions différentiellement exprimées se retrouvent dans le placenta, mais soient en lien avec le fonctionnement du cerveau. D'ailleurs, dans son étude, Laufer et *al*. ont démontré que plusieurs DMRs retrouvés dans les placentas étaient aussi altérés dans les cerveaux des embryons correspondants (198). Cette étude est un exemple concret de l'importance de l'axe placenta-cerveau pendant le développement embryonnaire ainsi que du lien entre le méthylome du placenta et du cerveau. Il sera intéressant d'évaluer aussi le lien entre les dérégulations de méthylation d'ADN et transcriptomique du placenta et du cerveau et si certaines altérations sont conservées entre les tissus dans notre modèle d'exposition à l'alcool pendant la préimplantation.

Finalement, en plus de leur impact sur le développement de phénotypes reliés au TSAF, les changements moléculaires dans les placentas exposés à l'alcool pendant la préimplantation et persistants jusqu'en fin de gestation pourrait aussi être utile d'un point de vue clinique afin de développer un outil de diagnostic moléculaire pour le TSAF. Présentement, le diagnostic basé sur plusieurs évaluations provenant d'une équipe multidisciplinaire est subjectif et ne permet pas d'identifier tous les cas de TSAF. L'absence d'outil moléculaire probants est un problème très souvent mis en lumière.

Pour notre projet, nous avons émis l'hypothèse que les profils de méthylation d'ADN ou ceux transcriptomiques pourraient être utilisés pour identifier de façon efficace les embryons exposés à l'alcool provenant de notre modèle précis d'exposition pendant la préimplantation. Grâce aux données de méthylation d'ADN, nous avons été en mesure d'utiliser un algorithme basé sur l'intelligence artificielle et l'apprentissage automatique (*machine learning*) afin d'établir une signature moléculaire pouvant éventuellement servir de biomarqueurs lors d'une exposition prénatale à l'alcool au stade 8-cellules. Basé sur nos données, ce profil moléculaire constitué de 24 régions du génome présentant des altérations de méthylation d'ADN (DMRs) permet, en effet, de séparer de façon précise les placentas contrôles et les placentas exposés à l'alcool, sexe confondu. Étonnamment, le même type d'analyse impliquant notre approche d'apprentissage automatiqueen

utilisant les données transcriptomiques ne permet pas une discrimination aussi nette des différents placentas. Notre petit nombre d'échantillons constitue assurément une limite à la méthode et l'augmentation du nombre d'échantillons pourrait éventuellement permettre d'établir une meilleure signature transcriptomique. Cette limite démontre bien que le développement d'un outil diagnostic moléculaire est complexe et requiert beaucoup de précision, même à l'intérieur d'un modèle unique d'exposition.

Dans les dernières années, deux groupes de recherche distincts au Canada ont tenté de faire une percée clinique en étudiant les profils de méthylation d'ADN d'enfants atteint du TSAF dans les cellules épithéliales buccales et identifiant certains profils divergents permettant de discriminer ces enfants d'une population contrôle (158-160). Bien que prometteur, ces études comportent cependant quelques lacunes qui empêchent de déployer cette technique à grande échelle. D'abord, chacune de ces études incluait un nombre relativement limité de sujets (entre 6 et 100), d'âges variés, dont le diagnostic de TSAF avait été confirmé, mais présentant des symptômes mixtes. Le type d'exposition prénatale à l'alcool (les moments dans la grossesse où l'enfant a été exposé, la fréquence de l'exposition, la dose et la concentration d'alcool atteint dans le sang) était aussi très hétérogène dans la population. Comme mentionné précédemment, l'intensité des phénotypes et les structures principalement affectées par l'alcool varient en fonction du patron d'exposition et modulent donc les impacts épigénétiques possible à plus long terme. Cette variabilité diminue assurément la puissance statistique pour définir une signature épigénétique, un peu comme s'ils recherchaient une signature commune à plusieurs maladies distinctes. L'épigénome étant énormément variable d'un type cellulaire à l'autre, l'utilisation de cellules épithéliales n'est pas représentative des changements épigénétiques réels initiés pendant le développement embryonnaire, ni des changements qui pourraient avoir eu lieu dans un organe spécifique ou même le cerveau. Contrairement à une mutation génétique se retrouvant dans le génome de tous les types cellulaires de tous les organes, une altération épigénétique peut n'être présente que dans un type cellulaire bien précis. Malgré leurs résultats intéressants, à ce jour, aucun essai clinique public au Canada n'est poursuivi dans le but de développer un outil de dépistage moléculaire utilisant les profils de méthylation d'ADN des cellules épithéliales buccales.

Le placenta pourrait être une excellente option comme outil de dépistage puisque, peu importe le type d'exposition, il sera directement ou indirectement aussi exposé à l'alcool. Bien que

l'impact d'une exposition à l'alcool après la formation du placenta sur ses profils épigénétiques et transcriptomiques soient méconnus, nous pouvons assumer que l'exposition direct entrainerait aussi des dérégulations à long terme, comme il fut déjà observé dans la littérature avec d'autres types d'exposition. Parmi ces études, un modèle murin d'exposition prénatal au dexaméthasone (utilisé dans certains types de cancer) après l'implantation lors des dernières étapes de remodelage du placenta (E7.5 à E9.5) démontrent des changements transcriptomiques, spécifique au sexe, aux jours embryonnaires E11.5 et E18.5 (199). Plus encore, des changements morphologiques de la vascularisation du placenta ont été observés chez des souris exposées de façon intermittente à la chaleur entre les jours embryonnaires E15.5 et E17.5, soit après le remodelage du placenta (200), démontrant bien le caractère modulable du placenta même après sa maturation. L'importance de l'axe placenta-cerveau doit aussi être considérée. Comme démontré par Laufer et *al*. lors de son étude sur l'exposition au cannabis (198), les dérégulations du méthylome du placenta peuvent aussi, dans une certaine mesure, être un miroir des altérations du méthylome du cerveau.

Pour notre étude, nous avons démontré, à petite échelle, avec notre modèle de souris que la signature épigénétique de placenta serait une excellente candidate pour la détection du TSAF dès la naissance. L'analyse de nombreux placentas, provenant d'enfant ayant un patron d'exposition connu, permettrait de mettre en place une charte de certaines altérations épigénétiques ou transcriptomiques présentes selon le modèle d'exposition et, ultimement, le déploiement de l'utilisation du placenta comme outil de dépistage moléculaire novateur pour le TSAF et ce dès la naissance. Ce processus requerrait évidemment beaucoup de temps, de recherche et de collaboration entre les différentes équipes de cliniciens et de chercheurs, mais, à long terme, cette découverte permettrait d'améliorer considérablement la vie des enfants atteints du TSAF et d'alléger cet enjeu de santé publique. Éventuellement, cette approche pourrait s'appliquer à plusieurs autres expositions néfastes, telles les drogues ou les métaux lourds afin d'améliorer le suivi des enfants exposés et d'offrir un support adapté.

Limitations et perspectives

Étudier la méthylation d'ADN à grande échelle

La méthylation d'ADN est une modification épigénétique largement étudié dans divers contextes, allant de son rôle dans le développement embryonnaire à ses profils distincts dans les tumeurs cancéreuses. Lorsque j'ai débuté mon doctorat, mon intérêt était de déterminer les profils

de méthylation à travers le génome. Cependant, les approches de génome entier (*Whole Genome Bisulfite Sequencing* - WGBS) étaient très dispendieuses, et trop complexes à analyser (*e.g.*, espace et puissance de calcul) à cette époque. D'autres techniques par pyroséquençage (*PyroMark*, Qiagen) ne permettaient de cibler qu'une région à la fois du génome. Afin de choisir l'approche idéale, nous avons considéré divers facteurs dont le type de régions couvertes, la reproductibilité, la quantité de matériel génomique de départ nécessaire, le temps de préparation des librairies et les coûts associés autant à la préparation des échantillons qu'à leur séquençage. Basé sur ces considérations, notre choix s'est arrêté sur le *Reduced Representation Bisulfite Sequencing* (RRBS), une technique nous permettant d'acquérir les niveaux de méthylation sur environ 1.5 millions de CpGs répartis à travers le génome, qui nécessite que de petites quantités d'ADN génomique (moins de 500ng) de départ, et qui ne requérant que 20 à 30 millions de lecture en couverture de séquence (PE100-150).

Même si le premier protocole de RRBS a été originalement publié en 2011 (201) et était utilisé depuis 2008 par le laboratoire du chercheur ayant développé la technique (202), il demeurait long et fastidieux. À l'époque, aucun kit commercial n'était disponible. J'ai donc optimisé le protocole existant afin d'être capable de préparer des librairies de plusieurs échantillons en multiplex, prête à séquencer, en moins de 2 jours de travail et à un coût d'environ 25$ par réaction. De plus, notre protocole permet de réduire la quantité de duplicats PCR générés lors de l'amplification des librairies en suivant la réaction d'amplification via fluorescence par PCR quantitatif (qPCR). La présence élevée de duplicats PCR dans les résultats de séquençage n'est pas souhaitable puisque qu'ils engendrent des biais dans les analyses bio-informatiques. Notre approche minimise leurs présences comparativement à la méthode classique en limitant au maximum le nombre de cycles d'amplification. Contrairement à certaines approches plus ciblées, comme les micropuces d'ADN spécifiquement conçues pour l'humain ou la souris, le rRRBS peut aussi être utilisé pour étudier la méthylation d'ADN sur de nombreuses autres espèces, comme le rat ou même le poisson zèbre.

Pour la suite du projet, nous souhaitions étudier plus en profondeur les dérèglements de la méthylation d'ADN causé par notre exposition prénatale à l'alcool. Malgré les excellents résultats obtenus à l'aide de notre méthode de rRRBS, la couverture génomique restait tout de même limitée et nous avons ainsi choisi d'opter pour une autre technique, le Methyl-Seq (Capture) de la

compagnie Agilent. Cette méthode est basée sur l'enrichissement de régions à partir d'un panel commercial conçu spécifiquement pour le génome murin. Permettant pour sa part d'établir les profils de méthylation sur environ 3.2 millions de CpG (vs 1.5M pour le RRBS), son protocole requiert cependant une plus grande quantité d'ADN, raison pour laquelle son utilisation avec des tissus embryonnaire à mi-gestation était incompatible. Concrètement, cette technique nous a permis d'augmenter d'environ 4-10 fois le nombre de régions de 100pb (tuile) étudié et d'ainsi élargir considérablement la caractérisation des dérégulations reliées à notre exposition prénatale à l'alcool pendant la préimplantation. Malgré le changement de techniques, les analyses bio-informatiques restaient similaires et partiellement compatibles avec le RRBS, ce qui nous a permis de faire certains recoupements entre différents jeux de donnés, comme lorsque nous avons étudié les différences dans les profils de méthylation d'ADN entre les placentas mâles et femelles (voir Annexe 2).

Avec l'avènement de technologies de séquençage toujours plus puissantes et le prix en décroissance, le séquençage du méthylome entier (environ ~28-29 millions de CpGs chez l'humain et ~19 millions chez la souris (203-205)) est de plus en plus populaire et tant à prendre le dessus sur les techniques ne donnant qu'une vue partielle des profils de méthylation à travers le génome. Une autre amélioration dans les techniques existantes est le changement de la conversion d'ADN avec le bisulfite de sodium au profit d'une conversion enzymatique à l'aide de TET2 et APOBEC. En plus de diminuer la dégradation d'ADN reliée au traitement au bisulfite de sodium, la conversion enzymatique permet la détection et la discrimination entre la présence de méthylation d'ADN (5-mC) et d'hydroxyméthylation d'ADN (5-hmC) (206). Cet état intermédiaire entre l'absence et la présence de la méthylation est reconnu pour jouer un rôle important dans la régulation de certains processus développementaux tels la pluripotence ou le développement neuronal et représenterait environ 20% des cytosines modifiées du génome (207-209). Étudier les dérégulations associées précisément à chacune des marques nous donneraient donc assurément des informations supplémentaires dans le but de mieux comprendre les mécanismes reliés aux conséquences de notre exposition prénatale à l'alcool pendant la préimplantation.

Les techniques permettant d'étudier la méthylation d'ADN sont donc en constante évolution, toujours dans le but de les rendre plus rapides, plus fiables et nécessitant moins d'ADN. Malheureusement, une limitation majeure des différents résultats présentés dans ma thèse est la

spécificité de chaque technique disponible au moment de réaliser les différentes expériences. En effet, les résultats et conclusions basés sur les études de la méthylation d'ADN sont biaisés par la technique utilisée puisqu'autant le RRBS que le Methyl-Seq Capture ne couvrent par tous les CpGs du génome. Nous sommes donc seulement en mesure d'étudier ce qui est couvert par la méthode utilisée. Certains changements de méthylation d'ADN causés par l'exposition prénatale à l'alcool pendant la préimplantation restent donc méconnus tout simplement en raison de l'absence de couverture. Une approche couvrant l'entièreté du génome (comme le WGBS) par cellule-unique (*single-cell*) aurait permis de définir avec plus de précision les dérèglements épigénétiques et possiblement mieux comprendre les mécanismes sous-jacents à ces altérations. Plus encore, cela nous aurait aussi permis de suivre l'évolution des changements à travers le développement embryonnaire (en comparant le cerveau antérieur à E10.5 et E18.5 par exemple) et en limitant les contraintes reliées à la méthode ou à la qualité du séquençage.

L'origine des dérégulations

Un autre aspect que nous n'avons pas abordé encore dans mon projet de doctorat et qui pourrait possiblement nous aider dans l'établissement d'un mécanisme serait de caractériser les profils de méthylation d'ADN et d'expression génique dès les premières divisions après l'exposition à l'alcool pendant la préimplantation. En effet, toujours grâce à l'émergence des techniques requérant une faible quantité de matériel de départ (*low-input*), établir les profils de méthylation d'ADN ou transcriptomique sur un embryon 16-cellules ou blastocyste par exemple est maintenant possible. En générant les profils moléculaires à différents stades avant l'implantation et tout juste après celle-ci, nous pourrions établir une chronologie de l'évolution des dérèglements, autant pour la méthylation que pour le transcriptome. À partir de ces résultats, nous pourrions déterminer si l'impact original se produit d'abord au niveau de méthylation d'ADN, du transcriptome ou même dans les profils de modifications des histones qui engendreraient ensuite des modifications sur les profils de méthylation d'ADN et transcriptomique.

Étudier les impacts dès l'exposition prénatale à l'alcool au stade 8-cellules nous permettrait aussi de répondre à certaines questions spécifiquement en lien avec notre modèle. D'abord, les différences spécifiques au sexe dans les dérégulations à la suite de l'exposition à l'alcool sont-elles autant présentes dès le départ ou émergent-elles au cours du développement et à quel stade? Ensuite, allons-nous observer un ralentissement du cycle cellulaire sur les embryons exposés à

l'alcool? Nous observions, en effet, que certains embryons présentaient un retard de croissance à mi-gestation, alors qu'en fin de gestation, seulement les embryons mâles présentaient une baisse globale du poids fœtale en comparaison avec les embryons contrôles. Si nous observions un ralentissement du cycle cellulaire, serait-ce sur tous les embryons ou seulement une minorité d'entre eux, possiblement ceux qui présenteraient un retard de croissance plus tard dans le développement? À partir du stade du blastocyste, nous pourrions déterminer les dérégulations des cellules embryonnaires et extra-embryonnaires dès la séparation des cellules de la masse interne et celles du trophectoderme. Il serait aussi intéressant de voir quel est l'impact de l'ajout de notre diète préventive tout juste après l'exposition à l'alcool. Est-ce qu'une partie des dérégulations épigénétiques serait évitée dès les premiers moment de l'exposition par la présence de la supplémentation en donneur de groupement méthyle ou l'effet positif observé sur la morphologie des embryons en fin de gestation émergent plus tard pendant le développement embryonnaire?

Une meilleure compréhension des dérèglements épigénétiques initiaux causés par l'exposition prénatale à l'alcool au stade 8-cellules en complément aux altérations observées plus tard pendant la gestation pourrait aussi permettre le développement de méthodes alternatives pour restaurer le paysage épigénétique normal de l'embryon. L'avènement de technologies permettant l'édition de l'épigénome, tel le CRISPR-dCas9 (210) pouvant être utilisé *in vivo,* pourrait éventuellement nous permettre de viser certaines régions bien spécifiques de l'épigénome et de rétablir les niveaux normaux de méthylation d'ADN de ces régions à la suite de l'exposition à l'alcool. À plus long terme, il sera intéressant de déterminer si cela permet ainsi d'éviter le développement de conséquences à long terme comme les changements comportementaux et de mieux définir le lien direct entre les perturbations épigénétique et le développement neurocognitif.

L'effet de l'hétérogénéité cellulaire et pistes de solution

Une des grandes difficultés dans les modèles étudiant les effets et conséquences d'une exposition prénatale à l'alcool sur la progéniture est le potentiel de l'alcool à agir sur tous les types cellulaires. Lors d'une exposition plus tard dans la gestation, plusieurs recherches ont permis de déterminer les atteintes majeures en fonction des processus développementaux en cours lors de l'exposition, particulièrement au cerveau, basée sur les principales étapes du neurodéveloppement. Lors d'une exposition pendant la préimplantation, les dérégulations épigénétiques ont littéralement le potentiel d'être transmise dans tous les types cellulaires lors des divisions subséquentes et des

différenciations en plusieurs sous-types cellulaires, en plus de pouvoir elles aussi engendrer d'autres altérations épigénétiques ou transcriptomiques, tel un effet boule de neige.

En caractérisant les dérégulations dans le cerveau embryonnaire et le placenta plus tard pendant la gestation, nous étudions une population mixte de types cellulaires dans l'organe d'intérêt, sans être en mesure d'identifier si un ou plusieurs types seraient plus particulièrement affectés que d'autres. Assumant que les erreurs épigénétiques engendrés au stade 8-cellules par notre exposition à l'alcool sont transmises aux cellules filles de façon asymétrique et hétéroclite dans les différents embryons, il est tout à fait justifié de supposer que différents types cellulaires pourraient être plus ou moins affectés dans les différents échantillons en fonction de comment les erreurs ont progressé dans le développement de chaque embryon. L'hétérogénéité cellulaire provenant du fait que nous utilisons un tissu complet pourrait en partie expliquer la variabilité inter-échantillons que nous observons et potentiellement certaines différences spécifiques au sexe. Pour la suite du projet, il serait donc intéressant de prendre en compte cette contrainte et de l'adresser grâce à des techniques supplémentaires.

Plusieurs avenues sont possibles afin de corriger cette lacune. D'abord, il serait possible d'effectuer une analyse de déconvolution, particulièrement à partir de nos données transcriptomiques. La déconvolution est une méthode bio-informatique s'appuyant sur des données publiées de types cellule-unique (*single-cell*). Pour l'expression des gènes, les techniques de cellule-unique permettent d'établir précisément le profil transcriptomique de chaque type cellulaire et ainsi d'établir une signature transcriptomique propre à chacun. Lors d'une analyse de déconvolution, différents outils bio-informatique comprenant plusieurs algorithmes mathématiques utilisent la matrice des différentes signatures en y comparant nos données dites « *bulk* », c'est-à-dire comprenant une hétérogénéité cellulaire, et en y estimant la proportion de chaque type cellulaire basée sur les profils d'expression. Cette méthode dite « basée sur une matrice référence » requiert donc des données de bonne qualité, obtenues à partir d'échantillons du même âge et idéalement du même sexe. Bien qu'elle soit plus courante au niveau transcriptomique, il est aussi possible de faire des analyses de déconvolution à l'aide de données de méthylation d'ADN. Les données de cellule-unique pour cette modification sont, en revanche, plus rares et il peut donc être plus complexe d'obtenir une matrice de référence de qualité. Le tissu de départ constitue aussi une limitation en soit pour la même raison. Des données de cellule-unique pour le cerveau à

différents stades embryonnaires et post-nataux sont disponibles publiquement. Des données du même type pour le placenta sont cependant beaucoup plus rares et il peut donc devenir difficile d'effectuer des analyses de déconvolution fiables sur ce tissu. Par des analyses de déconvolution, il serait donc possible d'identifier si un type cellulaire est sous ou sur-représenté dans les échantillons exposés à l'alcool par rapport à la distribution dans les contrôles. Nous pourrions donc savoir si le développement ou la différenciation d'un type cellulaire semble être particulièrement inhibé ou stimulé par les dérégulations épigénétiques causées par notre exposition à l'alcool pendant la préimplantation. Il serait toutefois impossible d'identifier si des changements épigénétiques ou transcriptomiques sont plus proéminents dans ce type cellulaire.

Une première façon d'adresser cela serait d'effectuer à notre tour des librairies de type cellule-unique afin d'établir les signatures épigénétiques et transcriptomiques propre à notre modèle. Cela permettrait de déterminer les dérégulations uniques à chacun des types cellulaires du tissu d'intérêt sur l'ensemble de ceux-ci. D'un point de vue technique, la dissociation parfaite de tissus complexes, comme le cerveau et le placenta, demande des réactifs et des appareils précis et, surtout, une optimisation impeccable de la technique afin d'être certain d'avoir une population de cellules complètement dissociées et proportionnellement représentatives de la population totale du tissu étudié. Ceci est crucial afin d'obtenir des résultats de qualité et reproductibles. Une limitation majeure des approches cellules-uniques réside aussi dans le fait qu'il est pour l'instant impossible de séquencer tous les CpGs d'une même cellule, limitant alors l'étendue des résultats et des analyses possibles.

Alternativement, il serait aussi possible de cibler un type cellulaire précis basé sur les résultats précédents ou sur certaines données de la littérature. En utilisant un modèle génétique marquant un type cellulaire par fluorescence ou via un marquage subséquent à l'aide d'un anticorps suite à la dissociation cellulaire, un tri par cytométrie en flux permet d'isoler les cellules d'intérêt et d'effectuer les librairies par la suite. Cette approche est d'ailleurs utilisée pour notre projet, en ce moment, afin d'isoler un type cellulaire précis du cerveau (*i.e.*, les interneurones GABAergiques issues du MGE) discuté à la section suivante. Cependant, puisque nous isolons un type cellulaire à la fois, cette approche requièrent un plus grand nombre de librairies si nous souhaitons étudier plus d'un type cellulaire, ce qui multiplie aussi les analyses bio-informatiques subséquentes.

Impact d'une exposition prénatale à l'alcool pendant la préimplantation sur les interneurones GABAergiques du cortex

Lors des analyses dans les cerveaux antérieurs à mi-gestation et en fin de gestation, nous avons découvert que certains gènes cruciaux pour la migration et la maturation des interneurones GABAergiques, tels *Dlx1*, *Dlx2*, *Lhx6*, *Tbr1*, *Arx* et *Sox6* présentaient des dérégulations de méthylation d'ADN ou d'expression génique (162). Ces six gènes sont directement impliqués dans la cascade d'activation et de migration des interneurones GABAergiques émergeant de l'éminence ganglionnaire médiale (MGE) en direction du cortex (211, 212). Un déficit des interneurones GABAergiques dans le cortex induit plusieurs phénotypes neurocognitifs dont plusieurs peuvent aussi être retrouvés chez les enfants atteints du TSAF, comme des déficits d'attention ou des troubles socio-cognitifs (211, 213). Portée par cette observation, nous avons décidé de porter une attention particulière à ce type cellulaire dans une portion subséquente du projet. En collaboration avec un autre laboratoire situé au centre de recherche du CHU Ste-Justine, l'équipe de Dre Elsa Rossignol, nous avons implémenté notre modèle d'exposition prénatale à l'alcool pendant la préimplantation à un de leur modèle génétique, soit *Nkx2.1*^{Cre} *x RCE*^{eGFP}. *Nkx2.1* étant le premier acteur dans la cascade d'activation des interneurones GABAergiques, ce modèle nous permet de marquer par fluorescence les interneurones dès le début de leur prolifération et migration depuis le MGE dans les embryons issus du croisement des deux génotypes. À l'aide de ce modèle, il est possible de suivre la migration des interneurones dans le cortex à différents stades embryonnaires afin de déterminer s'il semble y avoir un retard migratoire ou de quantifier les interneurones afin de déterminer si leur prolifération est affectée dans notre modèle d'exposition à l'alcool. Plus encore, ce modèle nous permet aussi d'isoler facilement par FACS les interneurones et d'établir les profils de méthylation d'ADN et transcriptomiques spécifiquement sur ce type de cellulaire.

Alors que nous sommes toujours en attente des résultats de séquençage des librairies de *Whole Genome Bisulfite Sequencing* (E15.5) et des librairies de RNA-Seq (E13.5; E15.5; E18.5), j'ai, pour l'instant, démontré un retard dans la migration et dans la densité d'interneurones GABAergiques chez les embryons E15.5 exposés à l'alcool (résultats non-montrés). Nous poursuivons aussi les analyses histologiques sur des embryons à d'autres stades embryonnaires (E13.5 et E18.5) de même qu'avec des cerveaux post-nataux (P21) afin de déterminer l'évolution dans les atteintes des interneurones GABAergiques. L'ensemble de ces résultats seront combinés

aux résultats présentés au chapitre 5 afin d'établir un portait complet de l'impact de l'exposition prénatale à l'alcool pendant la préimplantation avec une attention toute particulièrement aux interneurones GABAergiques. Ces futurs résultats nous aideront aussi assurément à comprendre les mécanismes derrière certains troubles neurodéveloppementaux retrouvés chez les enfants atteints du TSAF.

Bien que ce ne soit pas une analyse du cerveau entier par une approche de type cellule-unique, cette avenue nous permet tout de même d'isoler avec précision un type cellulaire et de déterminer avec spécificité les altérations épigénétiques et transcriptomiques causées par notre modèle d'exposition à l'alcool et ainsi de réduire l'hétérogénéité des différents types cellulaires.

Conclusion

En conclusion, j'ai démontré, au cours de ma thèse, qu'une exposition prénatale à l'alcool induit des altérations épigénétiques et transcriptomiques du cerveau embryonnaire et du placenta, en plus de causer des dérégulations cognitives à long termede la sociabilité et de la mémoire. Nos résultats démontrent, pour la toute première fois, le caractère nocif d'une exposition à l'alcool unique en tout début de grossesse, au moment où l'embryon n'est même pas encore implanté et où la femme ne sait pas qu'elle est enceinte. Plus encore, nous avons démontré que les profils de méthylation altérés dans le placenta pourraient éventuellement permettre d'établir une signature épigénétique particulière afin d'identifier dès la naissance les enfants exposés à l'alcool pendant la gestation. L'ensemble de ces résultats se doivent aussi d'être relayé aux professionnels de la santé ainsi qu'à la population générale dans le but de mieux sensibiliser les femmes aux risques associés à la consommation prénatale d'alcool en tout début de grossesse. La suite de nos travaux permettra de déterminer avec plus de précision les mécanismes épigénétiques derrière les altérations démontrées lors de cette thèse et une meilleure compréhension des phénotypes reliés au TSAF.

Références bibliographiques

1. Canovas S, Ross PJ. Epigenetics in preimplantation mammalian development. Theriogenology. 2016;86(1):69-79.
2. Kundakovic M, Gudsnuk K, Franks B, Madrid J, Miller RL, Perera FP, et al. Sex-specific epigenetic disruption and behavioral changes following low-dose in utero bisphenol A exposure. Proceedings of the National Academy of Sciences of the United States of America. 2013;110(24):9956-61.
3. Pagé-Larivière F, Tremblay A, Campagna C, Rodriguez MJ, Sirard MA. Low concentrations of bromodichloromethane induce a toxicogenomic response in porcine embryos in vitro. Reproductive toxicology (Elmsford, NY). 2016;66:44-55.
4. Wang J, Cao M, Yang M, Lin Y, Che L, Fang Z, et al. Intra-uterine undernutrition amplifies age-associated glucose intolerance in pigs via altered DNA methylation at muscle GLUT4 promoter. The British journal of nutrition. 2016;116(3):390-401.
5. Laufer BI, Mantha K, Kleiber ML, Diehl EJ, Addison SM, Singh SM. Long-lasting alterations to DNA methylation and ncRNAs could underlie the effects of fetal alcohol exposure in mice. Disease models & mechanisms. 2013;6(4):977-92.
6. Gutherz OR, Deyssenroth M, Li Q, Hao K, Jacobson JL, Chen J, et al. Potential roles of imprinted genes in the teratogenic effects of alcohol on the placenta, somatic growth, and the developing brain. Experimental neurology. 2022;347:113919.
7. Lussier AA, Bodnar TS, Weinberg J. Intersection of Epigenetic and Immune Alterations: Implications for Fetal Alcohol Spectrum Disorder and Mental Health. Frontiers in neuroscience. 2021;15:788630.
8. Auclair G, Guibert S, Bender A, Weber M. Ontogeny of CpG island methylation and specificity of DNMT3 methyltransferases during embryonic development in the mouse. Genome biology. 2014;15(12):545.
9. Pinney SE. Mammalian Non-CpG Methylation: Stem Cells and Beyond. Biology. 2014;3(4):739-51.
10. Jones PL, Veenstra GJ, Wade PA, Vermaak D, Kass SU, Landsberger N, et al. Methylated DNA and MeCP2 recruit histone deacetylase to repress transcription. Nature genetics. 1998;19(2):187-91.
11. Keshet I, Lieman-Hurwitz J, Cedar H. DNA methylation affects the formation of active chromatin. Cell. 1986;44(4):535-43.
12. Lande-Diner L, Zhang J, Ben-Porath I, Amariglio N, Keshet I, Hecht M, et al. Role of DNA methylation in stable gene repression. The Journal of biological chemistry. 2007;282(16):12194-200.
13. Ehrlich M, Lacey M. DNA methylation and differentiation: silencing, upregulation and modulation of gene expression. Epigenomics. 2013;5(5):553-68.
14. Hahn MA, Wu X, Li AX, Hahn T, Pfeifer GP. Relationship between gene body DNA methylation and intragenic H3K9me3 and H3K36me3 chromatin marks. PloS one. 2011;6(4):e18844.
15. Jones PA. Functions of DNA methylation: islands, start sites, gene bodies and beyond. Nature reviews Genetics. 2012;13(7):484-92.

16. Gregory TR. Synergy between sequence and size in large-scale genomics. Nature reviews Genetics. 2005;6(9):699-708.
17. Padeken J, Zeller P, Gasser SM. Repeat DNA in genome organization and stability. Current opinion in genetics & development. 2015;31:12-9.
18. Nishibuchi G, Déjardin J. The molecular basis of the organization of repetitive DNA-containing constitutive heterochromatin in mammals. Chromosome research : an international journal on the molecular, supramolecular and evolutionary aspects of chromosome biology. 2017;25(1):77-87.
19. Babaian A, Mager DL. Endogenous retroviral promoter exaptation in human cancer. Mobile DNA. 2016;7:24.
20. Argaw-Denboba A, Balestrieri E, Serafino A, Cipriani C, Bucci I, Sorrentino R, et al. HERV-K activation is strictly required to sustain CD133+ melanoma cells with stemness features. Journal of experimental & clinical cancer research : CR. 2017;36(1):20.
21. Coskran TM, Jiang Z, Klaunig JE, Mager DL, Obert L, Robertson A, et al. Induction of endogenous retroelements as a potential mechanism for mouse-specific drug-induced carcinogenicity. PloS one. 2017;12(5):e0176768.
22. Robertson KD. DNA methylation and chromatin - unraveling the tangled web. Oncogene. 2002;21(35):5361-79.
23. Okano M, Bell DW, Haber DA, Li E. DNA methyltransferases Dnmt3a and Dnmt3b are essential for de novo methylation and mammalian development. Cell. 1999;99(3):247-57.
24. Bourc'his D, Xu GL, Lin CS, Bollman B, Bestor TH. Dnmt3L and the establishment of maternal genomic imprints. Science (New York, NY). 2001;294(5551):2536-9.
25. Andrews S, Krueger C, Mellado-Lopez M, Hemberger M, Dean W, Perez-Garcia V, et al. Mechanisms and function of de novo DNA methylation in placental development reveals an essential role for DNMT3B. Nature communications. 2023;14(1):371.
26. Yagi M, Kabata M, Tanaka A, Ukai T, Ohta S, Nakabayashi K, et al. Identification of distinct loci for de novo DNA methylation by DNMT3A and DNMT3B during mammalian development. Nature communications. 2020;11(1):3199.
27. Golbabapour S, Majid NA, Hassandarvish P, Hajrezaie M, Abdulla MA, Hadi AH. Gene silencing and Polycomb group proteins: an overview of their structure, mechanisms and phylogenetics. Omics : a journal of integrative biology. 2013;17(6):283-96.
28. Turek-Plewa J, Jagodziński PP. The role of mammalian DNA methyltransferases in the regulation of gene expression. Cellular & molecular biology letters. 2005;10(4):631-47.
29. Mayer W, Niveleau A, Walter J, Fundele R, Haaf T. Demethylation of the zygotic paternal genome. Nature. 2000;403(6769):501-2.
30. McGraw S, Zhang JX, Farag M, Chan D, Caron M, Konermann C, et al. Transient DNMT1 suppression reveals hidden heritable marks in the genome. Nucleic acids research. 2015;43(3):1485-97.
31. Ross PJ, Canovas S. Mechanisms of epigenetic remodelling during preimplantation development. Reproduction, fertility, and development. 2016;28(1-2):25-40.
32. Kobayashi H, Sakurai T, Imai M, Takahashi N, Fukuda A, Yayoi O, et al. Contribution of intragenic DNA methylation in mouse gametic DNA methylomes to establish oocyte-specific heritable marks. PLoS genetics. 2012;8(1):e1002440.
33. Butler MG. Imprinting disorders in humans: a review. Current opinion in pediatrics. 2020;32(6):719-29.
34. Edwards CA, Ferguson-Smith AC. Mechanisms regulating imprinted genes in clusters. Current opinion in cell biology. 2007;19(3):281-9.

35. Ishida M, Moore GE. The role of imprinted genes in humans. Molecular aspects of medicine. 2013;34(4):826-40.
36. Wilkins JF, Úbeda F, Van Cleve J. The evolving landscape of imprinted genes in humans and mice: Conflict among alleles, genes, tissues, and kin. BioEssays : news and reviews in molecular, cellular and developmental biology. 2016;38(5):482-9.
37. Lei H, Oh SP, Okano M, Jüttermann R, Goss KA, Jaenisch R, et al. De novo DNA cytosine methyltransferase activities in mouse embryonic stem cells. Development (Cambridge, England). 1996;122(10):3195-205.
38. Sharif J, Muto M, Takebayashi S, Suetake I, Iwamatsu A, Endo TA, et al. The SRA protein Np95 mediates epigenetic inheritance by recruiting Dnmt1 to methylated DNA. Nature. 2007;450(7171):908-12.
39. Yamaguchi TP, Bradley A, McMahon AP, Jones S. A Wnt5a pathway underlies outgrowth of multiple structures in the vertebrate embryo. Development (Cambridge, England). 1999;126(6):1211-23.
40. Andre P, Song H, Kim W, Kispert A, Yang Y. Wnt5a and Wnt11 regulate mammalian anterior-posterior axis elongation. Development (Cambridge, England). 2015;142(8):1516-27.
41. Yang DH, Yoon JY, Lee SH, Bryja V, Andersson ER, Arenas E, et al. Wnt5a is required for endothelial differentiation of embryonic stem cells and vascularization via pathways involving both Wnt/beta-catenin and protein kinase Calpha. Circulation research. 2009;104(3):372-9.
42. Zhao Y, Flandin P, Long JE, Cuesta MD, Westphal H, Rubenstein JL. Distinct molecular pathways for development of telencephalic interneuron subtypes revealed through analysis of Lhx6 mutants. The Journal of comparative neurology. 2008;510(1):79-99.
43. Liodis P, Denaxa M, Grigoriou M, Akufo-Addo C, Yanagawa Y, Pachnis V. Lhx6 activity is required for the normal migration and specification of cortical interneuron subtypes. The Journal of neuroscience : the official journal of the Society for Neuroscience. 2007;27(12):3078-89.
44. Tahiliani M, Koh KP, Shen Y, Pastor WA, Bandukwala H, Brudno Y, et al. Conversion of 5-methylcytosine to 5-hydroxymethylcytosine in mammalian DNA by MLL partner TET1. Science (New York, NY). 2009;324(5929):930-5.
45. Ponnaluri VK, Maciejewski JP, Mukherji M. A mechanistic overview of TET-mediated 5-methylcytosine oxidation. Biochemical and biophysical research communications. 2013;436(2):115-20.
46. Yin X, Hu L, Xu Y. Structure and Function of TET Enzymes. Advances in experimental medicine and biology. 2022;1389:239-67.
47. Donaghay M, Lessey BA. Uterine receptivity: alterations associated with benign gynecological disease. Seminars in reproductive medicine. 2007;25(6):461-75.
48. Yoshinaga K. A sequence of events in the uterus prior to implantation in the mouse. Journal of assisted reproduction and genetics. 2013;30(8):1017-22.
49. Feuer S, Rinaudo P. Preimplantation stress and development. Birth defects research Part C, Embryo today : reviews. 2012;96(4):299-314.
50. Fisher DA. The unique endocrine milieu of the fetus. The Journal of clinical investigation. 1986;78(3):603-11.
51. Graham E, Moss J, Burton N, Roochun Y, Armit C, Richardson L, et al. The atlas of mouse development eHistology resource. Development (Cambridge, England). 2015;142(11):1909-11.

52. Ducibella T, Ukena T, Karnovsky M, Anderson E. Changes in cell surface and cortical cytoplasmic organization during early embryogenesis in the preimplantation mouse embryo. The Journal of cell biology. 1977;74(1):153-67.
53. Handyside AH. Distribution of antibody- and lectin-binding sites on dissociated blastomeres from mouse morulae: evidence for polarization at compaction. Journal of embryology and experimental morphology. 1980;60:99-116.
54. Reeve WJ, Ziomek CA. Distribution of microvilli on dissociated blastomeres from mouse embryos: evidence for surface polarization at compaction. Journal of embryology and experimental morphology. 1981;62:339-50.
55. Pratt HP, Ziomek CA, Reeve WJ, Johnson MH. Compaction of the mouse embryo: an analysis of its components. Journal of embryology and experimental morphology. 1982;70:113-32.
56. Watkins AJ, Lucas ES, Fleming TP. Impact of the periconceptional environment on the programming of adult disease. Journal of developmental origins of health and disease. 2010;1(2):87-95.
57. Fleming TP, Johnson MH. From egg to epithelium. Annual review of cell biology. 1988;4:459-85.
58. Stephenson RO, Rossant J, Tam PP. Intercellular interactions, position, and polarity in establishing blastocyst cell lineages and embryonic axes. Cold Spring Harbor perspectives in biology. 2012;4(11).
59. Messerschmidt DM, Knowles BB, Solter D. DNA methylation dynamics during epigenetic reprogramming in the germline and preimplantation embryos. Genes & development. 2014;28(8):812-28.
60. Guo F, Li X, Liang D, Li T, Zhu P, Guo H, et al. Active and passive demethylation of male and female pronuclear DNA in the mammalian zygote. Cell stem cell. 2014;15(4):447-59.
61. Reik W, Dean W, Walter J. Epigenetic reprogramming in mammalian development. Science (New York, NY). 2001;293(5532):1089-93.
62. Legault LM, Bertrand-Lehouillier V, McGraw S. Pre-implantation alcohol exposure and developmental programming of FASD: an epigenetic perspective. Biochemistry and cell biology = Biochimie et biologie cellulaire. 2018;96(2):117-30.
63. Seisenberger S, Peat JR, Hore TA, Santos F, Dean W, Reik W. Reprogramming DNA methylation in the mammalian life cycle: building and breaking epigenetic barriers. Philosophical transactions of the Royal Society of London Series B, Biological sciences. 2013;368(1609):20110330.
64. Guo H, Zhu P, Yan L, Li R, Hu B, Lian Y, et al. The DNA methylation landscape of human early embryos. Nature. 2014;511(7511):606-10.
65. Wossidlo M, Nakamura T, Lepikhov K, Marques CJ, Zakhartchenko V, Boiani M, et al. 5-Hydroxymethylcytosine in the mammalian zygote is linked with epigenetic reprogramming. Nature communications. 2011;2:241.
66. Shen L, Inoue A, He J, Liu Y, Lu F, Zhang Y. Tet3 and DNA replication mediate demethylation of both the maternal and paternal genomes in mouse zygotes. Cell stem cell. 2014;15(4):459-71.
67. Nakamura T, Liu YJ, Nakashima H, Umehara H, Inoue K, Matoba S, et al. PGC7 binds histone H3K9me2 to protect against conversion of 5mC to 5hmC in early embryos. Nature. 2012;486(7403):415-9.
68. Trasler JM. Gamete imprinting: setting epigenetic patterns for the next generation. Reproduction, fertility, and development. 2006;18(1-2):63-9.

69. Hirasawa R, Chiba H, Kaneda M, Tajima S, Li E, Jaenisch R, et al. Maternal and zygotic Dnmt1 are necessary and sufficient for the maintenance of DNA methylation imprints during preimplantation development. Genes & development. 2008;22(12):1607-16.
70. Toppings M, Castro C, Mills PH, Reinhart B, Schatten G, Ahrens ET, et al. Profound phenotypic variation among mice deficient in the maintenance of genomic imprints. Human reproduction (Oxford, England). 2008;23(4):807-18.
71. Howell CY, Bestor TH, Ding F, Latham KE, Mertineit C, Trasler JM, et al. Genomic imprinting disrupted by a maternal effect mutation in the Dnmt1 gene. Cell. 2001;104(6):829-38.
72. Cirio MC, Martel J, Mann M, Toppings M, Bartolomei M, Trasler J, et al. DNA methyltransferase 1o functions during preimplantation development to preclude a profound level of epigenetic variation. Developmental biology. 2008;324(1):139-50.
73. McGraw S, Oakes CC, Martel J, Cirio MC, de Zeeuw P, Mak W, et al. Loss of DNMT1o disrupts imprinted X chromosome inactivation and accentuates placental defects in females. PLoS genetics. 2013;9(11):e1003873.
74. Whidden L, Martel J, Rahimi S, Chaillet JR, Chan D, Trasler JM. Compromised oocyte quality and assisted reproduction contribute to sex-specific effects on offspring outcomes and epigenetic patterning. Human molecular genetics. 2016;25(21):4649-60.
75. Robinson WP, Price EM. The human placental methylome. Cold Spring Harbor perspectives in medicine. 2015;5(5):a023044.
76. Legault LM, Doiron K, Lemieux A, Caron M, Chan D, Lopes FL, et al. Developmental genome-wide DNA methylation asymmetry between mouse placenta and embryo. Epigenetics. 2020;15(8):800-15.
77. Hemberger M, Hanna CW, Dean W. Mechanisms of early placental development in mouse and humans. Nature reviews Genetics. 2020;21(1):27-43.
78. Latos PA, Hemberger M. From the stem of the placental tree: trophoblast stem cells and their progeny. Development (Cambridge, England). 2016;143(20):3650-60.
79. Simmons DG, Natale DR, Begay V, Hughes M, Leutz A, Cross JC. Early patterning of the chorion leads to the trilaminar trophoblast cell structure in the placental labyrinth. Development (Cambridge, England). 2008;135(12):2083-91.
80. Simmons DG, Fortier AL, Cross JC. Diverse subtypes and developmental origins of trophoblast giant cells in the mouse placenta. Developmental biology. 2007;304(2):567-78.
81. Hales CN, Barker DJ. Type 2 (non-insulin-dependent) diabetes mellitus: the thrifty phenotype hypothesis. Diabetologia. 1992;35(7):595-601.
82. Hausburg MA, Dekrey GK, Salmen JJ, Palic MR, Gardiner CS. Effects of paraquat on development of preimplantation embryos in vivo and in vitro. Reproductive toxicology (Elmsford, NY). 2005;20(2):239-46.
83. Wilson RD, O'Connor DL. Guideline No. 427: Folic Acid and Multivitamin Supplementation for Prevention of Folic Acid-Sensitive Congenital Anomalies. Journal of obstetrics and gynaecology Canada : JOGC = Journal d'obstetrique et gynecologie du Canada : JOGC. 2022;44(6):707-19.e1.
84. Antony AC. In utero physiology: role of folic acid in nutrient delivery and fetal development. The American journal of clinical nutrition. 2007;85(2):598s-603s.
85. Bodnar LM, Tang G, Ness RB, Harger G, Roberts JM. Periconceptional multivitamin use reduces the risk of preeclampsia. American journal of epidemiology. 2006;164(5):470-7.
86. Botto LD, Lisi A, Robert-Gnansia E, Erickson JD, Vollset SE, Mastroiacovo P, et al. International retrospective cohort study of neural tube defects in relation to folic acid

recommendations: are the recommendations working? BMJ (Clinical research ed). 2005;330(7491):571.
87. Czeizel AE, Tímár L, Sárközi A. Dose-dependent effect of folic acid on the prevention of orofacial clefts. Pediatrics. 1999;104(6):e66.
88. De Wals P, Tairou F, Van Allen MI, Uh SH, Lowry RB, Sibbald B, et al. Reduction in neural-tube defects after folic acid fortification in Canada. The New England journal of medicine. 2007;357(2):135-42.
89. Wen SW, Chen XK, Rodger M, White RR, Yang Q, Smith GN, et al. Folic acid supplementation in early second trimester and the risk of preeclampsia. American journal of obstetrics and gynecology. 2008;198(1):45.e1-7.
90. Ojeda DA, Hutton O, Hopkins R, Cagampang F, Smyth NR, Fleming TP, et al. Preimplantation or gestation/lactation high-fat diet alters adult offspring metabolism and neurogenesis. Brain communications. 2023;5(2):fcad093.
91. Li T, Vu TH, Ulaner GA, Littman E, Ling JQ, Chen HL, et al. IVF results in de novo DNA methylation and histone methylation at an Igf2-H19 imprinting epigenetic switch. Molecular human reproduction. 2005;11(9):631-40.
92. Suzuki J, Jr., Therrien J, Filion F, Lefebvre R, Goff AK, Smith LC. In vitro culture and somatic cell nuclear transfer affect imprinting of SNRPN gene in pre- and post-implantation stages of development in cattle. BMC developmental biology. 2009;9:9.
93. Smith LC, Therrien J, Filion F, Bressan F, Meirelles FV. Epigenetic consequences of artificial reproductive technologies to the bovine imprinted genes SNRPN, H19/IGF2, and IGF2R. Frontiers in genetics. 2015;6:58.
94. Smith LC, Suzuki J, Jr., Goff AK, Filion F, Therrien J, Murphy BD, et al. Developmental and epigenetic anomalies in cloned cattle. Reproduction in domestic animals = Zuchthygiene. 2012;47 Suppl 4:107-14.
95. Lazaraviciute G, Kauser M, Bhattacharya S, Haggarty P, Bhattacharya S. A systematic review and meta-analysis of DNA methylation levels and imprinting disorders in children conceived by IVF/ICSI compared with children conceived spontaneously. Human reproduction update. 2015;21(4):555-7.
96. Vermeiden JP, Bernardus RE. Are imprinting disorders more prevalent after human in vitro fertilization or intracytoplasmic sperm injection? Fertility and sterility. 2013;99(3):642-51.
97. El Hajj N, Haertle L, Dittrich M, Denk S, Lehnen H, Hahn T, et al. DNA methylation signatures in cord blood of ICSI children. Human reproduction (Oxford, England). 2017;32(8):1761-9.
98. Ghosh J, Coutifaris C, Sapienza C, Mainigi M. Global DNA methylation levels are altered by modifiable clinical manipulations in assisted reproductive technologies. Clinical epigenetics. 2017;9:14.
99. Miller MW. Limited ethanol exposure selectively alters the proliferation of precursor cells in the cerebral cortex. Alcoholism, clinical and experimental research. 1996;20(1):139-43.
100. Cui SJ, Tewari M, Schneider T, Rubin R. Ethanol promotes cell death by inhibition of the insulin-like growth factor I receptor. Alcoholism, clinical and experimental research. 1997;21(6):1121-7.
101. Zhang FX, Rubin R, Rooney TA. Ethanol induces apoptosis in cerebellar granule neurons by inhibiting insulin-like growth factor 1 signaling. Journal of neurochemistry. 1998;71(1):196-204.
102. Varela-Rey M, Woodhoo A, Martinez-Chantar ML, Mato JM, Lu SC. Alcohol, DNA methylation, and cancer. Alcohol research : current reviews. 2013;35(1):25-35.

103. Muggli E, Matthews H, Penington A, Claes P, O'Leary C, Forster D, et al. Association Between Prenatal Alcohol Exposure and Craniofacial Shape of Children at 12 Months of Age. JAMA pediatrics. 2017;171(8):771-80.
104. Feldman HS, Jones KL, Lindsay S, Slymen D, Klonoff-Cohen H, Kao K, et al. Prenatal alcohol exposure patterns and alcohol-related birth defects and growth deficiencies: a prospective study. Alcoholism, clinical and experimental research. 2012;36(4):670-6.
105. Larkby CA, Goldschmidt L, Hanusa BH, Day NL. Prenatal alcohol exposure is associated with conduct disorder in adolescence: findings from a birth cohort. Journal of the American Academy of Child and Adolescent Psychiatry. 2011;50(3):262-71.
106. Alati R, Davey Smith G, Lewis SJ, Sayal K, Draper ES, Golding J, et al. Effect of prenatal alcohol exposure on childhood academic outcomes: contrasting maternal and paternal associations in the ALSPAC study. PloS one. 2013;8(10):e74844.
107. Popova S, Charness ME, Burd L, Crawford A, Hoyme HE, Mukherjee RAS, et al. Fetal alcohol spectrum disorders. Nature reviews Disease primers. 2023;9(1):11.
108. Lange S, Probst C, Gmel G, Rehm J, Burd L, Popova S. Global Prevalence of Fetal Alcohol Spectrum Disorder Among Children and Youth: A Systematic Review and Meta-analysis. JAMA pediatrics. 2017;171(10):948-56.
109. Popova S, Lange S, Poznyak V, Chudley AE, Shield KD, Reynolds JN, et al. Population-based prevalence of fetal alcohol spectrum disorder in Canada. BMC public health. 2019;19(1):845.
110. Graves L, Carson G, Poole N, Patel T, Bigalky J, Green CR, et al. Guideline No. 405: Screening and Counselling for Alcohol Consumption During Pregnancy. Journal of obstetrics and gynaecology Canada : JOGC = Journal d'obstetrique et gynecologie du Canada : JOGC. 2020;42(9):1158-73.e1.
111. WHO Guidelines Approved by the Guidelines Review Committee. Guidelines for the Identification and Management of Substance Use and Substance Use Disorders in Pregnancy. Geneva: World Health Organization

112. Conigrave KM, Ali RL, Armstrong R, Chikritzhs TN, d'Abbs P, Harris MF, et al. Revision of the Australian guidelines to reduce health risks from drinking alcohol. The Medical journal of Australia. 2021;215(11):518-24.
113. General US, Carmona VARH. A 2005 message to women from the US Surgeon General: Advisory on alcohol use in pregnancy. Centers for Disease Control and Prevention. 2005.
114. Clarren SK, Smith DW. The fetal alcohol syndrome. The New England journal of medicine. 1978;298(19):1063-7.
115. Astley SJ, Clarren SK. A case definition and photographic screening tool for the facial phenotype of fetal alcohol syndrome. The Journal of pediatrics. 1996;129(1):33-41.
116. May PA, Hasken JM, Baete A, Russo J, Elliott AJ, Kalberg WO, et al. Fetal Alcohol Spectrum Disorders in a Midwestern City: Child Characteristics, Maternal Risk Traits, and Prevalence. Alcoholism, clinical and experimental research. 2020;44(4):919-38.
117. Chudley AE, Conry J, Cook JL, Loock C, Rosales T, LeBlanc N. Fetal alcohol spectrum disorder: Canadian guidelines for diagnosis. CMAJ : Canadian Medical Association journal = journal de l'Association medicale canadienne. 2005;172(5 Suppl):S1-s21.
118. Mattson SN, Riley EP, Gramling L, Delis DC, Jones KL. Neuropsychological comparison of alcohol-exposed children with or without physical features of fetal alcohol syndrome. Neuropsychology. 1998;12(1):146-53.

119. Popova S, Lange S, Probst C, Gmel G, Rehm J. Estimation of national, regional, and global prevalence of alcohol use during pregnancy and fetal alcohol syndrome: a systematic review and meta-analysis. The Lancet Global health. 2017;5(3):e290-e9.
120. Astley SJ. Validation of the fetal alcohol spectrum disorder (FASD) 4-Digit Diagnostic Code. Journal of population therapeutics and clinical pharmacology = Journal de la therapeutique des populations et de la pharmacologie clinique. 2013;20(3):e416-67.
121. Astley SJ, Bledsoe JM, Davies JK, Thorne JC. Comparison of the FASD 4-Digit Code and Hoyme et al. 2016 FASD diagnostic guidelines. Advances in pediatric research. 2017;4(3).
122. Cook JL, Green CR, Lilley CM, Anderson SM, Baldwin ME, Chudley AE, et al. Fetal alcohol spectrum disorder: a guideline for diagnosis across the lifespan. CMAJ : Canadian Medical Association journal = journal de l'Association medicale canadienne. 2016;188(3):191-7.
123. Cassidy SB, Allanson JE. Management of genetic syndromes: John Wiley & Sons; 2010.
124. Garro AJ, McBeth DL, Lima V, Lieber CS. Ethanol consumption inhibits fetal DNA methylation in mice: implications for the fetal alcohol syndrome. Alcoholism, clinical and experimental research. 1991;15(3):395-8.
125. Hamid A, Wani NA, Rana S, Vaiphei K, Mahmood A, Kaur J. Down-regulation of reduced folate carrier may result in folate malabsorption across intestinal brush border membrane during experimental alcoholism. The FEBS journal. 2007;274(24):6317-28.
126. Meethal SV, Hogan KJ, Mayanil CS, Iskandar BJ. Folate and epigenetic mechanisms in neural tube development and defects. Child's nervous system : ChNS : official journal of the International Society for Pediatric Neurosurgery. 2013;29(9):1427-33.
127. Black MM. Effects of vitamin B12 and folate deficiency on brain development in children. Food and nutrition bulletin. 2008;29(2 Suppl):S126-31.
128. Barak AJ, Beckenhauer HC, Tuma DJ. Betaine effects on hepatic methionine metabolism elicited by short-term ethanol feeding. Alcohol (Fayetteville, NY). 1996;13(5):483-6.
129. Perkins A, Lehmann C, Lawrence RC, Kelly SJ. Alcohol exposure during development: Impact on the epigenome. International journal of developmental neuroscience : the official journal of the International Society for Developmental Neuroscience. 2013;31(6):391-7.
130. Singh RP, Shiue K, Schomberg D, Zhou FC. Cellular epigenetic modifications of neural stem cell differentiation. Cell transplantation. 2009;18(10):1197-211.
131. Haycock PC. Fetal alcohol spectrum disorders: the epigenetic perspective. Biology of reproduction. 2009;81(4):607-17.
132. Haycock PC, Ramsay M. Exposure of mouse embryos to ethanol during preimplantation development: effect on DNA methylation in the h19 imprinting control region. Biology of reproduction. 2009;81(4):618-27.
133. Hicks SD, Middleton FA, Miller MW. Ethanol-induced methylation of cell cycle genes in neural stem cells. Journal of neurochemistry. 2010;114(6):1767-80.
134. Zhou FC, Balaraman Y, Teng M, Liu Y, Singh RP, Nephew KP. Alcohol alters DNA methylation patterns and inhibits neural stem cell differentiation. Alcoholism, clinical and experimental research. 2011;35(4):735-46.
135. Veazey KJ, Carnahan MN, Muller D, Miranda RC, Golding MC. Alcohol-induced epigenetic alterations to developmentally crucial genes regulating neural stemness and differentiation. Alcoholism, clinical and experimental research. 2013;37(7):1111-22.
136. Judson MC, Bergman MY, Campbell DB, Eagleson KL, Levitt P. Dynamic gene and protein expression patterns of the autism-associated met receptor tyrosine kinase in the developing mouse forebrain. The Journal of comparative neurology. 2009;513(5):511-31.

137. Ikonomidou C, Bittigau P, Ishimaru MJ, Wozniak DF, Koch C, Genz K, et al. Ethanol-induced apoptotic neurodegeneration and fetal alcohol syndrome. Science (New York, NY). 2000;287(5455):1056-60.
138. Sulik KK. Fetal alcohol spectrum disorder: pathogenesis and mechanisms. Handbook of clinical neurology. 2014;125:463-75.
139. Sulik KK, Johnston MC, Webb MA. Fetal alcohol syndrome: embryogenesis in a mouse model. Science (New York, NY). 1981;214(4523):936-8.
140. Jarmasz JS, Basalah DA, Chudley AE, Del Bigio MR. Human Brain Abnormalities Associated With Prenatal Alcohol Exposure and Fetal Alcohol Spectrum Disorder. Journal of neuropathology and experimental neurology. 2017;76(9):813-33.
141. Leach RE, Stachecki JJ, Armant DR. Development of in vitro fertilized mouse embryos exposed to ethanol during the preimplantation period: accelerated embryogenesis at subtoxic levels. Teratology. 1993;47(1):57-64.
142. Stachecki JJ, Yelian FD, Schultz JF, Leach RE, Armant DR. Blastocyst cavitation is accelerated by ethanol- or ionophore-induced elevation of intracellular calcium. Biology of reproduction. 1994;50(1):1-9.
143. Kowalczyk CL, Stachecki JJ, Schultz JF, Leach RE, Armant DR. Effects of alcohols on murine preimplantation development: relationship to relative membrane disordering potency. Alcoholism, clinical and experimental research. 1996;20(3):566-71.
144. Macaulay AD, Hamilton CK, Bartlewski PM, King WA. The effects of substituting glassware for plasticware and the use of an ethanol vector on oocyte maturation in vitro. Veterinary medicine international. 2012;2012:914715.
145. Avery B, Greve T. Effects of ethanol and dimethylsulphoxide on nuclear and cytoplasmic maturation of bovine cumulus-oocyte complexes. Molecular reproduction and development. 2000;55(4):438-45.
146. Kleiber ML, Mantha K, Stringer RL, Singh SM. Neurodevelopmental alcohol exposure elicits long-term changes to gene expression that alter distinct molecular pathways dependent on timing of exposure. Journal of neurodevelopmental disorders. 2013;5(1):6.
147. Padmanabhan R, Hameed MS. Effects of acute doses of ethanol administered at pre-implantation stages on fetal development in the mouse. Drug and alcohol dependence. 1988;22(1-2):91-100.
148. Pierce DR, West JR. Blood alcohol concentration: a critical factor for producing fetal alcohol effects. Alcohol (Fayetteville, NY). 1986;3(4):269-72.
149. Popova S, Lange S, Probst C, Gmel G, Rehm J. Global prevalence of alcohol use and binge drinking during pregnancy, and fetal alcohol spectrum disorder. Biochemistry and cell biology = Biochimie et biologie cellulaire. 2018;96(2):237-40.
150. Lange S, Probst C, Rehm J, Popova S. Prevalence of binge drinking during pregnancy by country and World Health Organization region: Systematic review and meta-analysis. Reproductive toxicology (Elmsford, NY). 2017;73:214-21.
151. Checiu M, Sandor S. The effect of ethanol upon early development in mice and rats. IX. Late effect of acute preimplantation intoxication in mice. Morphologie et embryologie. 1986;32(1):5-11.
152. Cole LA. New discoveries on the biology and detection of human chorionic gonadotropin. Reproductive Biology and Endocrinology. 2009;7(1):1-37.
153. Sedgh G, Singh S, Hussain R. Intended and unintended pregnancies worldwide in 2012 and recent trends. Studies in family planning. 2014;45(3):301-14.

154. Organization WH. Global status report on alcohol and health 2018: World Health Organization; 2019.
155. Dwyer-Lindgren L, Flaxman AD, Ng M, Hansen GM, Murray CJ, Mokdad AH. Drinking Patterns in US Counties From 2002 to 2012. American journal of public health. 2015;105(6):1120-7.
156. Wilsnack SC, Wilsnack RW, Kantor LW. Focus on: women and the costs of alcohol use. Alcohol research : current reviews. 2013;35(2):219-28.
157. Tan CH, Denny CH, Cheal NE, Sniezek JE, Kanny D. Alcohol use and binge drinking among women of childbearing age - United States, 2011-2013. MMWR Morbidity and mortality weekly report. 2015;64(37):1042-6.
158. Laufer BI, Kapalanga J, Castellani CA, Diehl EJ, Yan L, Singh SM. Associative DNA methylation changes in children with prenatal alcohol exposure. Epigenomics. 2015;7(8):1259-74.
159. Portales-Casamar E, Lussier AA, Jones MJ, MacIsaac JL, Edgar RD, Mah SM, et al. DNA methylation signature of human fetal alcohol spectrum disorder. Epigenetics & chromatin. 2016;9:25.
160. Lussier AA, Morin AM, MacIsaac JL, Salmon J, Weinberg J, Reynolds JN, et al. DNA methylation as a predictor of fetal alcohol spectrum disorder. Clinical epigenetics. 2018;10:5.
161. Legault LM, Chan D, McGraw S. Rapid Multiplexed Reduced Representation Bisulfite Sequencing Library Prep (rRRBS). Bio-protocol. 2019;9(4):e3171.
162. Legault LM, Doiron K, Breton-Larrivée M, Langford-Avelar A, Lemieux A, Caron M, et al. Pre-implantation alcohol exposure induces lasting sex-specific DNA methylation programming errors in the developing forebrain. Clinical epigenetics. 2021;13(1):164.
163. Wozniak JR, Riley EP, Charness ME. Clinical presentation, diagnosis, and management of fetal alcohol spectrum disorder. The Lancet Neurology. 2019;18(8):760-70.
164. Kelly SJ, Tran TD. Alcohol exposure during development alters social recognition and social communication in rats. Neurotoxicology and teratology. 1997;19(5):383-9.
165. Sanchez Vega MC, Chong S, Burne TH. Early gestational exposure to moderate concentrations of ethanol alters adult behaviour in C57BL/6J mice. Behavioural brain research. 2013;252:326-33.
166. Marquardt K, Brigman JL. The impact of prenatal alcohol exposure on social, cognitive and affective behavioral domains: Insights from rodent models. Alcohol (Fayetteville, NY). 2016;51:1-15.
167. Sugawara O, Takagi N, Sasaki M. Correlation between X-chromosome inactivation and cell differentiation in female preimplantation mouse embryos. Cytogenetics and cell genetics. 1985;39(3):210-9.
168. Goto T, Monk M. Regulation of X-chromosome inactivation in development in mice and humans. Microbiology and molecular biology reviews : MMBR. 1998;62(2):362-78.
169. Patrat C, Okamoto I, Diabangouaya P, Vialon V, Le Baccon P, Chow J, et al. Dynamic changes in paternal X-chromosome activity during imprinted X-chromosome inactivation in mice. Proceedings of the National Academy of Sciences of the United States of America. 2009;106(13):5198-203.
170. Whatley EG, Truong TT, Harvey AJ, Gardner DK. Preimplantation embryo exposure to ketone bodies exerts sex-specific effects on mouse fetal and placental transcriptomes. Reproductive BioMedicine Online. 2023:103320.

171. Lowe R, Gemma C, Rakyan VK, Holland ML. Sexually dimorphic gene expression emerges with embryonic genome activation and is dynamic throughout development. BMC genomics. 2015;16(1):295.
172. Bermejo-Alvarez P, Rizos D, Rath D, Lonergan P, Gutierrez-Adan A. Sex determines the expression level of one third of the actively expressed genes in bovine blastocysts. Proceedings of the National Academy of Sciences of the United States of America. 2010;107(8):3394-9.
173. Richardson V, Zhang K, Engel N, Kulathinal RJ. Comparative developmental genomics of sex-biased gene expression in early embryogenesis across mammals. bioRxiv. 2022:2022.03.17.484606.
174. Fleming TP, Watkins AJ, Sun C, Velazquez MA, Smyth NR, Eckert JJ. Do little embryos make big decisions? How maternal dietary protein restriction can permanently change an embryo's potential, affecting adult health. Reproduction, fertility, and development. 2015;27(4):684-92.
175. Feuer SK, Donjacour A, Simbulan RK, Lin W, Liu X, Maltepe E, et al. Sexually dimorphic effect of in vitro fertilization (IVF) on adult mouse fat and liver metabolomes. Endocrinology. 2014;155(11):4554-67.
176. Fernández-Gonzalez R, Moreira P, Bilbao A, Jiménez A, Pérez-Crespo M, Ramírez MA, et al. Long-term effect of in vitro culture of mouse embryos with serum on mRNA expression of imprinting genes, development, and behavior. Proceedings of the National Academy of Sciences of the United States of America. 2004;101(16):5880-5.
177. Tan K, Wang Z, Zhang Z, An L, Tian J. IVF affects embryonic development in a sex-biased manner in mice. Reproduction (Cambridge, England). 2016;151(4):443-53.
178. Flannigan K, Poole N, Cook J, Unsworth K. Sex-related differences among individuals assessed for fetal alcohol spectrum disorder in Canada. Alcohol (Hoboken, NJ). 2023;47(3):613-23.
179. Elmer T, Stadtfeld C. Depressive symptoms are associated with social isolation in face-to-face interaction networks. Scientific reports. 2020;10(1):1444.
180. Willoughby M, Greenberg M, Blair C, Stifter C, Group FLI. Neurobehavioral consequences of prenatal exposure to smoking at 6 to 8 months of age. Infancy. 2007;12(3):273-301.
181. Rodriguez A, Bohlin G. Are maternal smoking and stress during pregnancy related to ADHD symptoms in children? Journal of child psychology and psychiatry, and allied disciplines. 2005;46(3):246-54.
182. Hutchinson J, Pickett KE, Green J, Wakschlag LS. Smoking in pregnancy and disruptive behaviour in 3-year-old boys and girls: an analysis of the UK Millennium Cohort Study. Journal of epidemiology and community health. 2010;64(1):82-8.
183. Shao X, Cao G, Chen D, Liu J, Yu B, Liu M, et al. Placental trophoblast syncytialization potentiates macropinocytosis via mTOR signaling to adapt to reduced amino acid supply. Proceedings of the National Academy of Sciences of the United States of America. 2021;118(3).
184. Jinno N, Furugen A, Kurosawa Y, Kanno Y, Narumi K, Kobayashi M, et al. Effects of single and repetitive valproic acid administration on the gene expression of placental transporters in pregnant rats: An analysis by gestational period. Reproductive toxicology (Elmsford, NY). 2020;96:47-56.
185. Saeed M, Saleem U, Anwar F, Ahmad B, Anwar A. Inhibition of Valproic Acid-Induced Prenatal Developmental Abnormalities with Antioxidants in Rats. ACS omega. 2020;5(10):4953-61.

186. Meador KJ, Baker GA, Browning N, Clayton-Smith J, Combs-Cantrell DT, Cohen M, et al. Cognitive function at 3 years of age after fetal exposure to antiepileptic drugs. New England journal of medicine. 2009;360(16):1597-605.
187. Meador K, Reynolds MW, Crean S, Fahrbach K, Probst C. Pregnancy outcomes in women with epilepsy: a systematic review and meta-analysis of published pregnancy registries and cohorts. Epilepsy research. 2008;81(1):1-13.
188. Jentink J, Loane MA, Dolk H, Barisic I, Garne E, Morris JK, et al. Valproic acid monotherapy in pregnancy and major congenital malformations. The New England journal of medicine. 2010;362(23):2185-93.
189. Di Renzo GC, Rosati A, Sarti RD, Cruciani L, Cutuli AM. Does fetal sex affect pregnancy outcome? Gender medicine. 2007;4(1):19-30.
190. Eriksson JG, Kajantie E, Osmond C, Thornburg K, Barker DJ. Boys live dangerously in the womb. American journal of human biology : the official journal of the Human Biology Council. 2010;22(3):330-5.
191. Ingemarsson I. Gender aspects of preterm birth. BJOG : an international journal of obstetrics and gynaecology. 2003;110 Suppl 20:34-8.
192. Murji A, Proctor LK, Paterson AD, Chitayat D, Weksberg R, Kingdom J. Male sex bias in placental dysfunction. American journal of medical genetics Part A. 2012;158a(4):779-83.
193. Al-Qaraghouli M, Fang YMV. Effect of Fetal Sex on Maternal and Obstetric Outcomes. Frontiers in pediatrics. 2017;5:144.
194. Christians JK, Ahmadzadeh-Seddeighi S, Bilal A, Bogdanovic A, Ho R, Leung EV, et al. Sex differences in the effects of prematurity and/or low birthweight on neurodevelopmental outcomes: systematic review and meta-analyses. Biology of sex differences. 2023;14(1):47.
195. Christians JK, Chow NA. Are there sex differences in fetal growth strategies and in the long-term effects of pregnancy complications on cognitive functioning? Journal of developmental origins of health and disease. 2022;13(6):766-78.
196. Meakin AS, Cuffe JSM, Darby JRT, Morrison JL, Clifton VL. Let's Talk about Placental Sex, Baby: Understanding Mechanisms That Drive Female- and Male-Specific Fetal Growth and Developmental Outcomes. International journal of molecular sciences. 2021;22(12).
197. Breton-Larrivée M, Elder E, Legault LM, Langford-Avelar A, MacFarlane AJ, McGraw S. Mitigating the detrimental developmental impact of early fetal alcohol exposure using a maternal methyl donor-enriched diet. FASEB journal : official publication of the Federation of American Societies for Experimental Biology. 2023;37(4):e22829.
198. Laufer BI, Neier K, Valenzuela AE, Yasui DH, Schmidt RJ, Lein PJ, et al. Placenta and fetal brain share a neurodevelopmental disorder DNA methylation profile in a mouse model of prenatal PCB exposure. Cell reports. 2022;38(9):110442.
199. Lee JY, Yun HJ, Kim CY, Cho YW, Lee Y, Kim MH. Prenatal exposure to dexamethasone in the mouse induces sex-specific differences in placental gene expression. Development, growth & differentiation. 2017;59(6):515-25.
200. Olivier K, Reinders LA, Clarke MW, Crew RC, Pereira G, Maloney SK, et al. Maternal, Placental, and Fetal Responses to Intermittent Heat Exposure During Late Gestation in Mice. Reproductive sciences (Thousand Oaks, Calif). 2021;28(2):416-25.
201. Gu H, Smith ZD, Bock C, Boyle P, Gnirke A, Meissner A. Preparation of reduced representation bisulfite sequencing libraries for genome-scale DNA methylation profiling. Nature protocols. 2011;6(4):468-81.

202. Meissner A, Mikkelsen TS, Gu H, Wernig M, Hanna J, Sivachenko A, et al. Genome-scale DNA methylation maps of pluripotent and differentiated cells. Nature. 2008;454(7205):766-70.
203. Fouse SD, Nagarajan RO, Costello JF. Genome-scale DNA methylation analysis. Epigenomics. 2010;2(1):105-17.
204. Lövkvist C, Dodd IB, Sneppen K, Haerter JO. DNA methylation in human epigenomes depends on local topology of CpG sites. Nucleic acids research. 2016;44(11):5123-32.
205. Grimm SA, Shimbo T, Takaku M, Thomas JW, Auerbach S, Bennett BD, et al. DNA methylation in mice is influenced by genetics as well as sex and life experience. Nature communications. 2019;10(1):305.
206. Vaisvila R, Ponnaluri VKC, Sun Z, Langhorst BW, Saleh L, Guan S, et al. Enzymatic methyl sequencing detects DNA methylation at single-base resolution from picograms of DNA. Genome research. 2021;31(7):1280-9.
207. Yu M, Hon GC, Szulwach KE, Song CX, Zhang L, Kim A, et al. Base-resolution analysis of 5-hydroxymethylcytosine in the mammalian genome. Cell. 2012;149(6):1368-80.
208. Shi DQ, Ali I, Tang J, Yang WC. New Insights into 5hmC DNA Modification: Generation, Distribution and Function. Frontiers in genetics. 2017;8:100.
209. He B, Zhang C, Zhang X, Fan Y, Zeng H, Liu J, et al. Tissue-specific 5-hydroxymethylcytosine landscape of the human genome. Nature communications. 2021;12(1):4249.
210. Brocken DJW, Tark-Dame M, Dame RT. dCas9: A Versatile Tool for Epigenome Editing. Current issues in molecular biology. 2018;26:15-32.
211. Chattopadhyaya B, Cristo GD. GABAergic circuit dysfunctions in neurodevelopmental disorders. Frontiers in psychiatry. 2012;3:51.
212. Lim L, Mi D, Llorca A, Marín O. Development and Functional Diversification of Cortical Interneurons. Neuron. 2018;100(2):294-313.
213. Stolp HB, Fleiss B, Arai Y, Supramaniam V, Vontell R, Birtles S, et al. Interneuron Development Is Disrupted in Preterm Brains With Diffuse White Matter Injury: Observations in Mouse and Human. Frontiers in physiology. 2019;10:955.

Annexe 1 - Developmental Genome-Wide DNA Methylation Asymmetry Between Mouse Placenta and Embryo

En parallèle à mon projet principal, j'ai étudié les différences existantes entre les profils de méthylation d'ADN de l'embryon et de son placenta à mi-gestation (E10.5). Cet article a été publié en 2020 dans la revue *Epigenetics* doi: 10.1080/15592294.2020.172292. (76)

Le matériel supplémentaire est disponible sur le site du journal https://www.tandfonline.com/doi/full/10.1080/15592294.2020.1722922

Developmental Genome-Wide DNA Methylation Asymmetry Between Mouse Placenta and Embryo

Legault LM[1,2], Doiron K[1], Lemieux A[1,2], Caron M[1,3], Chan D[3], Lopes FL[4], Bourque G[5,6,7], Sinnett D[1,8], McGraw S[1,2,9,#].

[1]Research Center of the CHU Sainte-Justine, Montreal, Canada.
[2]Department of Biochemistry and Molecular Medicine, Université de Montréal, Montreal, Canada.
[3]Research Institute of the McGill University Health Centre, Montreal, Quebec, Canada
[4]São Paulo State University (Unesp), School of Veterinary Medicine, Aracatuba, Brazil
[5]Department of Human Genetics, McGill University, Montreal, Quebec, Canada
[6]McGill University and Genome Quebec Innovation Centre, Montreal, Quebec, Canada
[7]Canadian Center for Computational Genomics, Montreal, Quebec, Canada
[8]Department of Pediatrics, Université de Montréal, Montreal, Canada.
[9]Department of Obstetrics and Gynecology, Université de Montréal, Montreal, Canada.

[#]Corresponding author: serge.mcgraw@umontreal.ca

Running title: Embryonic & Placental DNAme Asymmetry

Summary statement: The kinetics of asymmetric DNA methylation acquisition of embryo-placenta differentially methylated regions is not a stepwise process occurring in embryonic and extraembryonic lineages, but a prompt progression in the early post-implanted conceptus.

ABSTRACT

In early embryos, DNA methylation is remodelled to initiate the developmental program but for mostly unknown reasons, methylation marks are acquired unequally between embryonic and placental cells. To better understand this, we generated high-resolution DNA methylation maps of mouse mid-gestation (E10.5) embryo and placenta. We uncovered specific subtypes of differentially methylated regions (DMRs) that contribute directly to the developmental asymmetry existing between mid-gestation embryonic and placental DNA methylation patterns. We show that the asymmetry occurs rapidly during the acquisition of marks in the post-implanted conceptus (E3.5-E6.5), and that these patterns are long-lasting across subtypes of DMRs throughout prenatal development and in somatic tissues. We reveal that at the peri-implantation stages, the *de novo* methyltransferase activity of DNMT3B is the main driver of methylation marks on asymmetric DMRs, and that DNMT3B can largely compensate for lack of DNMT3A in the epiblast and extraembryonic ectoderm, whereas DNMT3A can only partially compensate in the absence of DNMT3B. However, as development progresses and as DNMT3A becomes the principal *de novo* methyltransferase, the compensatory DNA methylation mechanism of DNMT3B on DMRs becomes less effective.

INTRODUCTION

Throughout the eutherian mammalian gestation, the placenta plays an essential role in mediating maternal–embryonic exchanges of gas, nutrients and waste, and also provides the developing embryo with a protective layer against adverse environmental exposures and the maternal immune system (Rossant & Cross, 2001). These unique placental functions are orchestrated by several distinct trophoblast cell subtypes organized in separate layers (Cross, 2000). The initial steps of lineage specialization of both placental and embryonic cells occur promptly following fertilization during the first few embryonic cleavages as DNA methylation marks are being reprogrammed (Morgan, Santos, Green, Dean, & Reik, 2005).

DNA methylation is an epigenetic mechanism that is critical in the determination of lineage-specific differentiation and development, and is mainly recognized for its involvement in processes such as transcriptional repression, genomic imprinting and X-inactivation (Bestor, 2000). DNA methylation marks are mediated by the action of DNA methyltransferases (DNMTs). Establishment of new or de novo DNA methylation patterns required for cell lineage determination during development is mediated by DNMT3A and DNMT3B, with cofactor DNMT3L, (Li, 2002; Okano, Bell, Haber, & Li, 1999), whereas DNMT1 maintains heritable DNA methylation patterns during cellular divisions (Lei et al., 1996; Leonhardt, Page, Weier, & Bestor, 1992). These enzymes are critical, as deletion of *Dnmt3b* or *Dnmt1* is embryonic lethal, while Dnmt3a-deficient offspring die shortly after birth (Li, Bestor, & Jaenisch, 1992; Okano et al., 1999). During gametogenesis, the acquisition of genome-wide and allele-specific methylation patterns (i.e. genomic imprinting) in both oocytes and sperm is essentially due to the activity of DNMT3A (Kaneda et al., 2004; Kato et al., 2007). Following fertilization, a reprogramming wave removes most methylation signatures across the genome, except for imprinted regions, some types of repeat sequences, as well as imprinted-like sequences, to trigger the developmental program (Hirasawa et al., 2008; Howell et al., 2001; McGraw et al., 2015). Then, during the peri-implantation process, DNA methylation profiles are re-acquired in a sex-, cell- and tissue-specific manner across most parts of the genome by the combined action of DNMT3A and DNMT3B. In the early stages of the de novo methylation wave (E4.5-E7.5), the expression of *Dnmt3b* is more robust than *Dnmt3a* in the epiblast and embryonic-derived cells (Auclair, Guibert, Bender, & Weber, 2014; Smith et al., 2017; Watanabe, Suetake, Tada, & Tajima, 2002), with the relative expression of *Dnmt3b* and *Dnmt3a* being considerably reduced in the extraembryonic ectoderm (ExE) and trophoblast lineages (Senner,

Krueger, Oxley, Andrews, & Hemberger, 2012; Smith et al., 2017). This discrepancy in *Dnmt3a* and *Dnmt3b* expression levels coincides with the initiation of divergent DNA methylation acquisition between the trophoblast and the inner cell mass of the blastocyst (Fulka, Mrazek, Tepla, & Fulka, 2004; Guo et al., 2014; Monk, 1987; Nakanishi et al., 2012; Oda, Oxley, Dean, & Reik, 2013; Santos, Hendrich, Reik, & Dean, 2002; Smith et al., 2014), a difference that becomes extremely apparent by E6.5, as the epiblast has acquired most of its global DNA methylation compared to the lower-methylation state of the ExE (Auclair et al., 2014; Smith et al., 2017; Zhang et al., 2018). This divergence is a common feature across mammalian placenta, as a heterogeneous and lower-methylation state compared to somatic tissues and other cell types is constantly observed (Chatterjee et al., 2016; Decato et al., 2017, Lopez-Tello, Sferruzzi-Perri, Smith, & Dean, 2017; Schroeder et al., 2013; Schroeder et al., 2015; Smith et al., 2017).

Although the functional role of reduced methylation levels observed across the placental genome is still not fully understood, studies suggest that it may activate transposable elements that are typically silenced in other tissues (Chuong, 2013). DNA methylation plays an important role in suppressing retrotransposons in mammalian cells, for which the activity has been associated with genomic instability and disease development (Church et al., 2009; Slotkin & Martienssen, 2007). Following the de novo methylation wave, in embryonic-derived cells from the inner cell mass, transposable elements acquire higher levels of DNA methylation causing transcriptional silencing, whereas in the trophectoderm-derived cells that will form the placenta, these transposable elements are maintained in a relaxed methylation state and preferentially expressed (Okahara et al., 2004; Price et al., 2012; Warren et al., 2015). The low-methylation levels on these elements contributed to the evolution and diversification of the placenta function through the regulation of gene expression by providing placenta-specific enhancers, cryptic promoters and other cis-regulatory elements (Cohen et al., 2011; Emera & Wagner, 2012; Haig, 2012; Macaulay, Weeks, Andrews, & Morison, 2011; Mi et al., 2000; Xie et al., 2013).

Despite the evident distinction between embryonic and placental DNA methylation levels, it remains unclear how, when and where methylation levels are acquired unequally across these genomes. To better understand the developmental dynamics of epigenetic asymmetry that exists between embryo and placenta, we first generated high-resolution maps of DNA methylation marks using Reduced Representation Bisulfite Sequencing (RRBS) at mid-gestation, when the mouse placenta is first considered mature (E10.5), to identify embryo-placenta differentially methylated

regions (DMRs). Then, using publicly available DNA methylation data sets and computational analyses, we defined how various categories of DMRs are established in early stages and maintained throughout development. In addition, we outlined the contribution of *Dnmt3a* and *Dnmt3b* in the acquisition and maintenance of embryonic and extraembryonic specific DMR patterns.

METHODS

Animals and Sample Collection

Female C57BL/6N (8-10 week-old) were purchased from Harlan Sprague-Dawley Laboratories (Indianapolis, IN) and were mated with male C57BL/6N (4 months of age). Following natural mating, embryos and placental tissues were collected at E10.5 (presence of vaginal plug at E0.5). Maternal decidua was removed from placentas. Samples were frozen immediately in liquid nitrogen and stored at -80 °C until analyzed.

DNA Methylation Analyses

RRBS libraries were generated as published protocols (Boyle et al., 2012; Gu et al., 2011) with our specifications (Legault, Chan, & McGraw, 2019; Magnus et al., 2014; McGraw et al., 2015). 500 ng of extracted DNA (Qiagen) from placenta (male n=2, female n=2) and embryo (male n=2, female n=2) samples was *MspI* digested, adaptor ligated and PCR amplified (multiplex). Multiplexed samples were pooled and 100 bp paired-end sequenced (HiSeq-2000, Illumina). The data analyses were done according to the pipeline established at the McGill Epigenomics Mapping and Data Coordinating Centers (Magnus et al., 2014; McGraw et al., 2015) that include BSMAP and methylKit. Specific parameters were chosen including 100 bp step-wise tiling windows, containing a minimum of 2 CpGs per tile and a minimum 15× CpG coverage of each tile per sample. The methylation level of a 100-bp tile was the result of all CpG C/T read counts within the tile after coverage normalization between samples, and the methylation level reported for a sample on autosomal chromosomes was the average methylation level across all individual replicates. Significant DNA methylation changes were designated as $\pm \geq 20\%$ average differences between groups of replicates and a q-value < 0.01 using the logistic regression function of methylKit (Akalin et al., 2012). Direct comparisons between DNA methylation averages were done using Wilcoxon-Mann-Whitney test in R. Gene ontology (GO) terms and pathway analyses for RefSeqs associated to promoter-TSS were conducted using Metascape gene annotation and analysis resource (Zhou et al., 2019).

Sequencing Data

Publicly available DNA methylation datasets (Auclair et al., 2014; Decato et al., 2017; Hon et al., 2013; Smith et al., 2014; Smith et al., 2017; Whidden et al., 2016) (see Table S5 for description) were analyzed using a custom script to intersect single CpG site methylation calls from these datasets within defined 100bp tiles associated to the embryo-placenta DMR categories and calculated resulting DNA methylation average per tile.

RESULTS

Increased Fluctuation in Genome-Wide DNA Methylation Levels in Placental Cells

To identify the overall epigenetic asymmetry that exists between placental and embryonic genomes during mouse in utero development, we first established genome-wide DNA methylation profiles using RRBS (Legault et al., 2019; Magnus et al., 2014; McGraw et al., 2015) of embryos and their corresponding placentas at mid-gestation (E10.5), the developmental stage at which the mouse placenta is considered mature (Cross, Werb, & Fisher, 1994). Using this approach, we quantified the DNA methylation profiles of ~1.8 million CpG sites in each sample (embryo n=4, placenta n=4). We found that the accumulation of CpG methylation was very distinct between the placenta and the embryo. In the placenta, we detected a greater proportion of CpGs in the 0-50% methylation range and a lower proportion of CpGs in the 80-100% methylation range (Figure 1A). Although we observed that a large proportion of CpGs within the examined regions had no methylation marks in both the embryo and the placenta, interestingly, most CpGs with partial methylation (20-50%) in placenta showed high methylation levels (>80%) in embryos (Figure 1B). The divergence in global DNA methylation profiles conferred a high degree of clustering between both tissue types (Figure S1). These results are consistent with previous studies indicating lower levels of overall DNA methylation in extraembryonic tissues (Price et al., 2012; Schroeder et al., 2013; Smith et al., 2017), reviewed in (Robinson & Price, 2015).

To further investigate the dynamics of DNA methylation between placental and embryonic genomes and enable direct comparison of precise regions, we segmented the genome of autosomal chromosomes into 100bp non-overlapping genomic windows (*tiles*; see methods section). After removal of sex chromosomes, we identified 245 048 unique sequenced tiles (referred to as All-tiles) containing 896 820 common CpGs between all placenta and embryo samples and with a minimum of 15x sequencing depth. We observed a strong reduction in the fraction of highly methylated tiles (80-100%) in the placenta compared to the embryo (Figure 1C), which correlated

with a sharp increase in the number of placenta tiles in the 0-20%, 20-40% and 40-60% methylation range. Globally, we found that the average DNA methylation level across all placental tiles was significantly lower compared to all embryo tiles (27% vs 45%, $p<0.0001$) (Figure 1C). This overall epigenetic disparity in embryo and placenta DNA methylation levels was especially noticeable when we mapped the methylation mean of All-tiles with respect to regions surrounding the transcription start sites (TSS) (Figure 1D). When we focused on a specific chromosome section (e.g., chr 7, 35Mb) (Figure 1E), we observed that genomic segments with high DNA methylation levels in embryos had predominantly lower levels in placenta. We also observed that gene or CpG island (CGI) poor regions had consistently high methylation levels in embryos and lower methylation levels in the placenta. Together, these results indicate that the mid-gestation placenta has very distinctive global DNA methylation levels compared to the embryo, and that this lower level of global DNA methylation across the placental genome is due to a significant lower number of highly methylated (≥80%) genomic regions. We can also conclude that despite the cellular heterogeneity in E10.5 placental and embryonic tissues, the vast majority of the conceptus possesses specific genomic regions with either low (0-20%) or high (80-100%) levels of methylation. However, the placenta genome presents an increased number of regions having a broader distribution of DNA methylation (20-80%), revealing a greater diversity in methylation levels across placental cell types compared to embryonic cell types.

Embryonic and Placental DNA Methylation Divergences across Genomic Features

To explain the developmentally divergent methylated states between the mouse embryo and the placenta, we next sought to precisely determine the genomic features revealing DNA methylation differences. We defined differentially methylated regions (DMRs) as 100bp genomic segments showing a significant difference of methylation levels between embryonic and placental samples with an absolute mean methylation difference of 20% or higher (McGraw et al., 2015; Piche et al., 2019; Shaffer et al., 2015). Using these conditions, we screened the 245 048 unique tiles common between all samples and identified 110 240 DMRs (~45% of All-tiles; Supplementary Table 1) with tissue- and/or developmental-specific DNA methylation variations between the embryo and the placenta (Figure2A; random subset of 20,000 DMRs shown). Consistent with our findings (Figure 1), the majority (96.8%; n=106 712) of DMRs had lower DNA methylation in the placenta (referred to as Hypo-DMRs) and only a small proportion (3.2%; n=3

528) showed increased methylation levels (referred to as Hyper-DMRs) compared to the embryo (Figure S2). For Hypo-DMRs, tiles mainly overlapped (96%; n=102 982) with intergenic, intron, exon and promoter-TSS regions (Figure S2). For each of the genomic feature categories of Hypo-DMRs, the average DNA methylation levels in the placenta were essentially half of those present in the embryo (Figure 2B). As for DMRs with higher methylation levels in the placenta (Hyper-DMRs), we noticed that the vast majority of these tiles (83%; n=2 929) had low methylation levels in the embryo (<20%) (Figure 2A-B). Most of Hyper-DMRs overlapped intergenic, intron, exon and promoter-TSS regions (93%; n=3 272, Figure S2). Illustrative examples of DNA methylation differences between the placenta and embryo are shown in Figure 2D. Syna (Syncytin A), implicated in the formation of a syncytium during placenta morphogenesis (Mi et al., 2000), showed overall lower methylation levels in the placenta when compared to the embryo (Figure 2D, smoothed representation (Hansen, Langmead, & Irizarry, 2012)). Similar observations were made in the gene body of *Atf6b* (*Activating Transcription Factor 6 Beta*), a gene implicated in the transcriptional downregulation of *Pgf* (*Placental Growth Factor*) in response to endoplasmic reticulum stress in pathological placentas (Mizuuchi et al., 2016). As for *Mir219a-2* and *Mir219b*, brain-specific non-coding microRNAs, they showed higher methylation in the placenta (Figure 2D). Another example of placenta Hyper-DMRs is *Sox6* (*SRY-Box 6*), which is implicated in the terminal differentiation of muscle (Figure 2D) (Kamachi & Kondoh, 2013). Gene ontology enrichment analyses showed that promoter-associated Hypo-DMRs (n=1 152 unique promoters) were strongly associated to germline functions and reproduction (*e.g.*, male and female gamete generation, reproduction, piRNA metabolic process, meiotic cell cycle, germ cell development) (Figure 2C). As for promoter-associated Hyper-DMRs (n=182 unique promoters), top biological processes were mostly associated with developmental and differentiation processes (*e.g.*, regionalization, embryo development, pattern specification process, skeletal system, head development) (Figure 2C). Fittingly, the biological functions were completely divergent between Hypo- and Hyper-DMRs. Altogether, these results denote that Hypo- and Hyper-DMRs are present across genomic features between mid-gestation embryo and placenta, and that these DNA methylation divergences are implicated in promoting/repressing specific processes during embryonic and placental development.

Presence of Distinctive DMR Categories between Mid-Gestation Embryo and Placenta

Amongst DMRs, our analyses also suggest the presence of particular DMR categories based on their level of DNA methylation in the embryo and placenta (Figure 2A). By defining subsets of DMRs and establishing their dynamic properties between tissues, we might better understand the genome-wide asymmetry in DNA methylation levels observed between the embryo and the placenta. To do so, we first clustered DMR-associated tiles in 6 different categories based on their range of low, mid and high methylation level (Low; <20%, Mid; ≥20 to <80%, High; ≥80%) in the embryo and the placenta, and followed the DMR category transitions between both tissues. We observed that DMRs with High-levels of methylation in the embryo overlapped with a large proportion of DMRs that showed Mid-levels of methylation in the placenta (Figure 3A,B; High-Mid n=72 715), whereas only a fraction corresponded to DMRs with Low-levels of methylation in the placenta (Figure 3A,B; High-Low n=1 889). As for DMRs with Mid-levels of methylation in embryo, the largest part remained in that same Mid-levels category in the placenta (Figure 3A; Mid-Mid n=23 640). Nonetheless, a portion of these embryonic Mid-levels DMRs were directed to DMRs with either Low- (Figure 3A; Mid-Low n=9 055) or High- (Figure 3A; Mid-High n= 21) levels of methylation in the placenta. Finally, DMRs with Low-levels of methylation in the embryo all showed Mid-levels of methylation in the placenta (Figure 3A; Low-Mid n=2 920). Thus, when we subdivide our DMRs into distinctive categories, we uncover that embryonic cells possess a large proportion of DMRs of High-level (≥80%) of DNA methylation, which remain potentially static in embryonic tissues, whereas the vast majority of these DMRs have lower and wide-range DNA methylation levels within placental tissue.

Specific Genomic Features Associated with DMR Categories

We next aimed to determine if the genomic distribution of embryo-placenta DMR categories was associated with distinct genomic features. First, by classifying by genomic annotations, we observed that DMRs with reduced methylation levels in the placenta (High-Mid, High-Low, Mid-Low) were prevailingly found in intergenic regions (>50% of tiles) (Figure 3C), whereas DMR categories with equivalent (Mid-Mid) or greater methylation level (Mid-High, Low-Mid) in the placenta were more frequent in genic associated regions (>50% of tiles). However, divergence between DMR categories was observed when we performed ontology analyses on promoter regions (Figure S3), as each DMR subtype clearly showed distinct biological functions. Since we know that in placenta, activation of retrotransposon-derived genes is interrelated with

low DNA methylation levels (Cohen et al., 2011; Macaulay et al., 2011; Reiss, Zhang, & Mager, 2007), we next assessed how DMR categories overlapped with major types of retrotransposons (LINE; long interspersed nuclear elements, SINE; short interspersed nuclear element, and LTR; long terminal repeats). Out of the DMR categories, those with High-levels of methylation in the embryo and either Mid- or Low-levels in the placenta (High-Mid and High-Low) showed the most enriched overlap with retrotransposons, with 92% and 96% respectively (Figure 3D). DMR categories associated with higher level of methylation in the placenta (Mid-High and Low-Mid) showed the least overlap with retrotransposons, especially the Low-Mid subtype. This highlights that during the *de novo* acquisition of DNA methylation patterns, DMRs with High-levels of methylation in the embryo and lower levels in the placenta are almost exclusively within retrotransposons-associated sequences, whereas DMRs with Low-levels of methylation in the embryo and higher DNA methylation in the placenta are preferentially outside retrotransposons-associated sequences. Finally, we investigated the proximity of the DMR categories in regards to CpG rich (CpG islands; CGI), neighbouring (shore; < 2kb away from CGIs, shelf; 2-4kb away from CGIs) and distant (open sea; > 4kb away from CGIs) regions (Figure 3E). We observed that most DMR categories are depleted from CGIs and are mostly found in open sea regions. In contrast, ~60% of tiles in Low-Mid DMRs overlapped with CGI, shores and shelves, revealing that the acquisition of *de novo* methylation for these genomic fragments in the extraembryonic lineage preferentially targets sequences inside or surrounding CGIs.

Altogether, these results indicate that the asymmetry within DMR categories, based on their methylation levels in the embryo and the placenta, can be associated to specific biological functions and genomic-derived features (e.g., CpG, retrotransposon contents). This is particularly apparent for DMRs with High-levels in the embryo (High-Mid, High-Low) and those with higher methylation levels in the placenta (Low-Mid).

DMR Categories are Established During the De Novo Methylation Wave and Maintained Throughout Development

To gain insights into the kinetics of lineage-specific DMR establishment between mid-gestation embryo and placenta, as well as their status during development, we assessed the levels of methylation associated with tiles for each DMR category as a function of their developmental stage. Publicly available sequencing data (Smith et al., 2014; Whidden et al., 2016) were analyzed

using our custom script to generate 100bp tiles, and the DNA methylation levels for each tile were calculated. In E3.5 blastocysts, when the mouse genome is mostly depleted from DNA methylation marks, we observed low global DNA methylation levels (average <20%) for all DMR subtypes, with similar median levels between the committed cells of the inner cell mass (ICM) and trophectoderm lineages (Figure 4). DNA methylation levels tended to be higher in the trophectoderm for regions falling in the Mid-High DMRs, although measurements are based on very few DMRs for this specific category (n=21, Figure 3B, Mid-High). Since global DNA methylation is re-acquired in the next few subsequent developmental stages, we then asked whether the contrast in DNA methylation levels associated with the various DMR categories at mid-gestation would already be present between E6.5 epiblast and extraembryonic ectoderm (ExE) cell lineages, layers that are mostly composed of homogeneous and undifferentiated cell populations. For all DMR categories, DNA methylation levels in the E6.5 epiblast and ExE already showed similar pattern trends to those observed in the E10.5 embryo and placenta (Figure 4, Table S2). Interestingly, for all DMR categories we observed higher DNA methylation levels in E6.5 ExE compared to E10.5 placenta (Figure 4, Table S2; Mid-High DMRs: $p=0.0021$, other DMRs: $p<0.0001$). Although we observe a ~10% higher DNA methylation mean difference for all common tiles between E6.5 ExE and E10.5 Placenta (35.66% vs 25.79%, $p<0.0001$; n=188 098) (Fig S5A), there is less than 1% difference in DNA methylation levels between all common tiles (n=200 581) from the E6.5 Epi and E10.5 embryo (43.2% vs 43.65%; $p<0.0001$). Furthermore, ~24% of tiles have ≥20% methylation in the E6.5 ExE vs the E10.5 Placenta (70.22% vs 37.49%; $p<0.0001$; n=45 967), whereas ~5.5% of tiles have ≥20% methylation in the E6.5 epiblast vs the E10.5 embryo (77.80% vs 43.87%; $p<0.0001$; n=11 183) (Fig S5B). In the subsequent developmental stages (E10.5, E11.5, E15 and E18) DNA methylation profiles associated with each DMR category stabilized and persisted in the placental cells. For categories of DMRs, their individual profiles in the E6.5 epiblast closely matched those observed in the E10.5 embryo and persisted across time points (E6.5, E10.5, E11.5). Although no public DNA methylation data were available for whole embryos at later stages, when we overlapped tiles associated with E10.5 DMR categories with data from differentiated tissues of adult mice, the global DNA methylation profiles closely matched those for the majority of DMR categories (High-Mid, High-Low, Mid-Mid and Mid-Low) (Figure 4, Figure S4). We conclude that the various DMR categories observed at E10.5 are established during the embryonic and extraembryonic lineage-specification processes occurring during the

peri-implantation wave of *de novo* methylation, and that these DNA methylation landscapes are widely retained throughout embryo and placenta development. Furthermore, for most DMR categories, the DNA methylation levels observed in developing embryos are long-lasting and conserved throughout somatic cell differentiation.

Dnmt3a- or Dnmt3b-Deficiency Alters Proper Establishment of DMR-Associated Patterns

Since the combined activity of DNMT3A and DNMT3B is essential for proper establishment of DNA methylation profiles and normal development, we next sought to define the contribution of each enzyme in the *de novo* establishment of DNA methylation in subtypes of DMRs in embryonic and extraembryonic cell lineages. To do so, we used DNA methylation data from publicly available datasets (whole genome bisulfite sequencing and RRBS) at E6.5 (epiblast and ExE) (Smith et al., 2017) and E8.5 (embryo) (Auclair et al., 2014) with inactive forms of *Dnmt3a* and *Dnmt3b*. First, when we overlapped our All-tiles subset, we observed a substantial reduction ($p<0.0001$) in average DNA methylation in absence of DNMT3A (37.81%) or DNMT3B (31.48%) in the E6.5 epiblast compared to wild-type (44.81%), whereas in the E6.5 ExE such a comparable loss was only associated with a *Dnmt3b*-deficiency (wt: 34.38% vs *Dnmt3b*$^{-/-}$: 19.33%, $p<0.0001$) (Figure S5). Similarly, in the E8.5 embryo, a significant reduction in average DNA methylation level was measured with lack of *Dnmt3a* or *Dnmt3b* expression compared to wild-type (wt: 47.5%; *Dnmt3a*$^{-/-}$: 43.6%; *Dnmt3b*$^{-/-}$: 34%, $p<0.0001$) (Figure S5). For most DMR subtypes, absence of DNMT3A caused modest, although significant ($p<0.0001$), or no reduction on overall DNA methylation levels in E6.5 epiblast and ExE (Figure 5A, Table S3). In comparison, *Dnmt3b*-depletion led to a substantial and significant loss of average methylation levels in all DMR categories in the E6.5 epiblast and ExE (Mid-High DMRs: $p<0.05$, other DMRs: $p<0.0001$) (Figure 5A, Table S3). In most DMR categories (High-Mid, Mid-Mid, Mid-Low, Low-Mid), the loss of *Dnmt3b* yielded a larger DNA methylation mean difference in the ExE compared to the epiblast at E6.5 (Table S3). For example, in the epiblast High-Mid DMRs, a compensatory mechanism provided high levels of methylation (wt: 84.13% vs *Dnmt3b*$^{-/-}$: 71.6%; $p <0.0001$), whereas this compensatory mechanism was ineffective in the E6.5 ExE (wt: 60.7% vs *Dnmt3b*$^{-/-}$: 36.28%; $p <0.0001$). When we focused on promoter-TSS for each DMR categories, we observed again that loss of methylation for these regulatory regions was principally associated with *Dnmt3b*-deficiency (Figure 5B). The promoter-TSS regions associated with High-Mid DMRs retained relatively high

methylation levels for either *Dnmt3a*$^{-/-}$ or *Dnmt3b*$^{-/-}$ epiblast samples, demonstrating a robust and compensatory *de novo* methylation mechanism. To further underline the impact of DNMT3A or DNMT3B on the *de novo* methylation of DMRs, we measured methylation levels for DMRs selected from our gene enrichment analyses (*Fgb*, *P2rx7*, *Pcyt2*, *Etnppl*, *Ralgds*, *Lrp5*) and other genomic segments covered by multiple tiles (*Cxxc1*, *Fcgrt*, *Lamp5*, *Mbd1*, *Lphn1*, *Pick1*, *Irf1*) (Figure S6 & S7) in *Dnmt3a*- or *Dnmt3b*-deficient epiblast and ExE. In line with our global observations, for most DMR-associated tiles, a *Dnmt3b*-deficiency in E6.5 epiblast or ExE caused a more severe loss of methylation compared to lack of *Dnmt3a.* However, for some regions in the E6.5 epiblast (e.g., *Pick1*, *Irf1*), *Dnmt3a*$^{-/-}$ methylation levels were lower to those of *Dnmt3b*$^{-/-}$. Overall, we show that of DNMT3A and DNMT3B participate in the establishment of the asymmetric methylation patterns associated with the various DMR categories in both embryonic and extraembryonic cells, with DNMT3B being the principal contributor in both cell lineages during the *de novo* reprogramming wave as it can compensate almost entirely for the absence of DNMT3A.

Decline in Compensatory DNA Methylation Mechanisms in Response to Dnmt3a- or Dnmt3b-Deficiency.

As embryonic development progresses from E6.5 to E8.5, our data suggest that lack of DNMT3A or DNMT3B further impedes the proper establishment and maintenance of DNA methylation levels of specific DMRs, evoking that absence of either enzymatic activity causes an additive and extended effect (Figure 5A-B). To further define the robustness in compensatory mechanism between DNMT3A or DNMT3B in the establishment and maintenance of DNA methylation on DMRs categories, we focused on High-Mid promoter-TSS- associated DMRs as they have the highest DNA methylation levels and require the most *de novo* methyltransferase activity. Methylation differences of ≥20% between wild-type and *Dnmt3a*- or *Dnmt3b*-deficient samples were considered as regions showing substantial lack of compensation. In agreement with our results (Figure 5A-B), we observed that at E6.5, DNMT3B can compensate almost entirely for DNMT3A loss by maintaining methylation levels on most promoters-TSS associated tiles in the epiblast (410/437 = 93.8%) and ExE (558/602 = 92.7%), whereas DNMT3A can only partially alleviate the lack of DNMT3B in the epiblast (315/410 = 78.6%) and ExE (244/524 = 46.6%) (Figure 6A-B). As embryonic cell lineages development evolves between E6.5 and E8.5, global

methylation levels increase on promoter-TSS of High-Mid DMRs. However, at E8.5, we detected a sharp decline in the number of promoter-TSS of High-Mid DMRs showing compensation (i.e., <20% difference) in *Dnmt3a*- (524/627 = 80.9%) and *Dnmt3b*- (256/622 = 41.2%) deficient embryos compared to wild-type (Figure 6B). This is further highlighted when we focus on a subgroup of 314 promoter-TSS associated tiles overlapping all of 9 data sets (Figure 6C), including gene promoters (e.g., *Asz1, Catsper1, Ccdc42, Dmrtb1, Piwil2, Rpl10l, Sox30, Sycp1, Tnp1, Ttll1, Zfn42*) related to our top enriched biological functions (i.e., piRNA, gamete generation and germ cells, meiotic nuclear division). Although E8.5 *Dnmt3a*- or *Dnmt3b*-deficient ExE data was not available, our data suggest that greater compensation failure would also be observed in this tissue. Thus, specific High-Mid promoter-TSS- associated DMRs need the combined action of DNMT3A and DNMT3B to both establish and maintain proper asymmetric levels during early development as compensatory DNA methylation mechanisms fail to overcome a DNMT3A or DNMT3B shortage during the E6.5 to E8.5 transition.

DISCUSSION

With recent breakthroughs in high-throughput sequencing, we now have a better understanding of the dynamic of DNA methylation erasure occurring in early cleavage stage embryos following fertilization. However, the discrepancies in acquisition of genome-wide DNA methylation patterns in early post-implantation embryonic and extraembryonic cell lineages remain to be methodically delineated. To address this issue and further our understanding of the DNA methylation asymmetry that guides the developmental trajectory of embryonic and extraembryonic cell lineages, we established genome-wide DNA methylation profiles of mouse embryo and placenta at mid-gestation, and analyzed various publicly available developmental stage specific embryo and placenta DNA methylation datasets. Using this strategy, we uncovered that 45% of the genomic regions analyzed differ in DNA methylation status (≥20%) between mid-gestation embryo and placenta, and that these DMRs can be further divided into categories based on their levels of DNA methylation (Low; <20%, Mid; ≥20 to <80%, High; ≥80%) in the embryo and placenta. We show that the embryo and placenta acquire specific DMR categories during the early stage of the *de novo* DNA methylation wave, and that these DMRs persist throughout prenatal development, as well as into somatic adult tissues. Furthermore, we show that *Dnmt3b* primarily drives the divergence in DNA methylation levels associated with these specific DMRs and that *de novo*

methyltransferase activity of *Dnmt3b* can almost entirely compensate for lack of *Dnmt3a* in the asymmetric establishment of embryonic and placental DMRs, but that *Dnmt3a* can only partially compensate the absence of *Dnmt3b*. However, with developmental progression, this compensatory DNA methylation mechanism becomes less effective.

Our results indicate that the kinetics of DNA methylation acquisition leading to specific embryo-placenta DMR categories is not a stepwise process occurring throughout cell fate decisions and patterning of embryonic and extraembryonic lineages, but a prompt progression in the early post-implanted conceptus. These results are in line with studies reflecting that the initiation of asymmetric DNA methylation levels begins within the trophoblast and the inner cell mass of the blastocyst (Santos et al., 2002), and becomes highly evident by the time the epiblast acquires its initial global DNA methylation patterns at E6.5 during the de novo reprogramming wave (Auclair et al. 2014, Smith et al. 2017). Our results show that the acquisition period between E4.5 and E6.5 is particularly key to establishing asymmetric DNA methylation patterns associated with mid-gestation embryo-placenta DMR classes, and that these DMR associated-patterns are long-lasting across stages of prenatal development. Since we studied cell populations derived from embryonic and placental tissues, we cannot dismiss the prevalence of cell-to-cell heterogeneity in the acquisition kinetics of specific DMR patterns. Despite this concern, our results indicate that embryonic cells have a large body of DMRs with High-levels (≥80%) and Low-levels (<20%) of methylation that remain static across development, as well as in somatic cell types (High-Mid & High-Low DMRs), whereas compared to the embryo, the placental DMRs have overall lower methylation levels and are more broadly distributed amongst methylation levels, which has also been shown in other studies where genome-wide DNA methylation profiles of placental cells were compared to other tissues and specific cell types (Schroeder et al., 2013; Chatterjee et al., 2016; Smith et al., 2017). Lower methylation levels in the placenta have been associated with reduced *de novo* methyltransferase activity in the ExE during the *de novo* reprogramming wave (Fulka et al., 2004; Santos et al., 2002). Nevertheless, we observe methylation level peaks for all DMR categories within the ExE at E6.5 before levels stabilize at E10.5. As of now, the implication of these methylation level peaks on future regulation mechanisms and methylation profiles is unknown. Moreover, it remains to be determined whether global reduction in DNA methylation marks on DMRs between the E6.5 and E10.5 extraembryonic cell lineages is stochastic or targeted, and whether it occurs through passive or active mechanisms. In addition, since analyses combine

datasets from divergent mouse strains, we cannot exclude that particular DNA methylation differences could be genetically driven.

We also observed an enrichment of retrotransposons (i.e., LINE, SINE, LTR) in DMRs especially in those with High-levels of methylation in the embryo and lower-levels in the placenta, whereas DMRs with Low-levels of methylation in the embryo and higher levels in the placenta are preferentially outside retrotransposons-associated sequences. Earlier findings of Chapman et al. (Chapman, Forrester, Sanford, Hastie, & Rossant, 1984) rev ealed that repeat regions in the placenta appear to lack tight control of their methylation patterns, perhaps indicating that maintaining methylation, and therefore repression of these elements for genome stability and integrity, is not critical given the relatively short lifespan of this organ. However, we do observe Mid-range methylation levels (20-80%) in the placenta for a substantial portion of DMRs that are associated with retrotransposons, revealing that specific genomic regions associated with repetitive elements do need tight regulation in extraembryonic cell lineages for proper development. These results are in line with findings exposing that the deletion of genome-defense gene *Tex19.1* leads to the de-repression of LINE1 and compromises placental development, suggesting that disparities between retrotransposon suppression and genome-defense mechanisms might contribute to placenta dysfunction and disease (Reichmann et al., 2013).

DNMT3A and DNMT3B are required to establish proper methylation profiles on the embryonic genome during the *de novo* reprogramming wave, as both methyltransferase enzymes have redundant, but also specific functions. However, the activity of DNMT3B is the main contributor in the acquisition of profiles in epiblast cells, and especially commands methylation on CGIs associated with developmental genes (Auclair et al., 2014). Auclair et *al*. highlighted that in the absence of DNMT3B, DNMT3A was not able to counterbalance, leading to the loss of promoter-CGI methylation and gain of expression of germline genes (e.g., *Sycp1*, *Sycp2*, *Mael*, *Rpl10l*, *Dmrtb1*) in somatic cells of the embryo. Here, we show that the promoter of these germline genes, associated with meiotic and piRNA processes as well as other genes with similar biological functions, are highly enriched in High-Mid DMRs. We also show that with the absence *Dnmt3b*, the methylation loss on most DMR categories is more pronounced in the E6.5 ExE than in the E6.5 Epi, revealing that the compensatory mechanism by DNMTA is less efficient in the ExE. Globally, we show that DNMT3B is much more potent at compensating than DNMT3A in both the epiblast and ExE for all DMR categories, indicating that DNMT3B is the main *de novo* enzyme driving

asymmetric DNA methylation patterns between the embryo and placenta. Although compensatory mechanisms have been observed in *Dnmt3a* or *Dnmt3b*-depleted conceptuses, we still do not fully understand the process as *Dnmt3a* and *Dnmt3b* have cell lineage specific expression during the peri-implantation developmental period. As development progresses, we observed that the compensation mechanism in *Dnmt3a* or *Dnmt3b*-deficient embryos remains apparent at E8.5 on most DMR categories, but is less effective as the methylation gaps increase compared to wild-type. This correlates with a developmental period where DNMT3A is now the main *de novo* methyltransferase enzyme in both the embryo and placenta (Okano et al., 1999; Watanabe et al., 2002), and with a compensatory activity of DNMT3A being less effective. This suggests that DNMT3B activity is critical to ensure proper establishment of DNA methylation asymmetry between the embryonic and extraembryonic cell lineages during the *de novo* reprogramming wave, but that DNMT3A is required during the developmental progression to safeguard methylation levels on DMR categories.

CONCLUSION

We demonstrate that asymmetry between embryo and placenta DNA methylation patterns occurs rapidly during *de novo* acquisition of methylation marks in the early post-implanted conceptus, and that these patterns are long-lasting across subtypes of DMRs. We also reveal that at the peri-implantation stages, *de novo* methyltransferase activity of DNMT3B is the main provider of asymmetric methylation marks on DMRs, and that it largely compensates the lack of DNMT3A in the epiblast and ExE. However, as development progresses, DNMT3A becomes the principal *de novo* methyltransferase by mid-gestation, and DNMT3B methyltransferase activity is less effective at promoting compensation. These results further underline why embryos developing without DNMT3B have severe DNA methylation defects and die at mid-gestation, whereas those without DNMT3A only die postnatally. Further investigation is required to determine the molecular mechanisms controlling the precise *de novo* acquisition of long-lasting methylation marks on specific DMR subtypes in the embryonic and extraembryonic cell lineages, and how errors in this process could lead to abnormal development and diseases.

ACKNOWLEDGMENTS

We thank the McGraw lab for critical comments and suggestions, as well as Elizabeth Maurice-Elder for editing.

COMPETING INTERESTS

No competing interests declared

FUNDING

This work was supported by a research grant from the Natural Sciences and Engineering Research Council of Canada. We acknowledge the Fonds de Recherche du Québec en Santé (L.M.L), l'Institut de Valorisation des Données (A.L), and the Réseau Québécois en Reproduction and Fonds de recherche du Québec – Nature et technologies (K.D) for salary awards.

DATA AVAILABILITY

The data from this study have been submitted to the Gene Expression Omnibus (#GSE95610).

Table S1. Annotation and DNA methylation values associated with DMRs.

Table S2. DNA methylation levels for DMR categorises across development (Figure 4), and Statistics associated with Figure 4.

Table S3. DNA methylation levels for DMR categories in various *Dnmt* knockout mouse models (Figure 5A), Statistics associated with Figure 5A, and Absence of *Dnmt3b* causes a larger loss of DNA methylation in the ExE vs the epiblast (Figure 5A).

Table S4. Number of 100bp tiles in each category of public data that overlap with Embryo-Placenta DMRs (related to Figure 4; 5A; S4; S5).

Table S5. Description of publically available datasets used in the various analyses.

REFERENCES

Akalin, A., Kormaksson, M., Li, S., Garrett-Bakelman, F. E., Figueroa, M. E., Melnick, A., & Mason, C. E. (2012). methylKit: a comprehensive R package for the analysis of genome-wide DNA methylation profiles. *Genome Biol*, 13(10), R87. doi:10.1186/gb-2012-13-10-r87

Auclair, G., Guibert, S., Bender, A., & Weber, M. (2014). Ontogeny of CpG island methylation and specificity of DNMT3 methyltransferases during embryonic development in the mouse. *Genome Biol*, 15(12), 545. doi:10.1186/s13059-014-0545-5

Bestor, T. H. (2000). The DNA methyltransferases of mammals. *Hum Mol Genet*, 9(16), 2395-2402.

Boyle, P., Clement, K., Gu, H., Smith, Z. D., Ziller, M., Fostel, J. L., . . . Meissner, A. (2012). Gel-free multiplexed reduced representation bisulfite sequencing for large-scale DNA methylation profiling. *Genome Biol*, 13(10), R92. doi:10.1186/gb-2012-13-10-r92

Chapman, V., Forrester, L., Sanford, J., Hastie, N., & Rossant, J. (1984). Cell lineage-specific undermethylation of mouse repetitive DNA. *Nature*, 307(5948), 284-286.

Chatterjee, A., Macaulay, E. C., Rodger, E. J., Stockwell, P. A., Parry, M. F., Roberts, H. E., . . . Morison, I. M. (2016). Placental Hypomethylation Is More Pronounced in Genomic Loci Devoid of Retroelements. *G3 (Bethesda)*, 6(7), 1911-1921. doi:10.1534/g3.116.030379

Chuong, E. B. (2013). Retroviruses facilitate the rapid evolution of the mammalian placenta. *Bioessays*, 35(10), 853-861. doi:10.1002/bies.201300059

Church, D. M., Goodstadt, L., Hillier, L. W., Zody, M. C., Goldstein, S., She, X., . . . Mouse Genome Sequencing, C. (2009). Lineage-specific biology revealed by a finished genome assembly of the mouse. *PLoS Biol*, 7(5), e1000112. doi:10.1371/journal.pbio.1000112

Cohen, C. J., Rebollo, R., Babovic, S., Dai, E. L., Robinson, W. P., & Mager, D. L. (2011). Placenta-specific expression of the interleukin-2 (IL-2) receptor beta subunit from an endogenous retroviral promoter. *J Biol Chem*, 286(41), 35543-35552. doi:10.1074/jbc.M111.227637

Cross, J. C. (2000). Genetic insights into trophoblast differentiation and placental morphogenesis. *Semin Cell Dev Biol*, 11(2), 105-113. doi:10.1006/scdb.2000.0156

Cross, J. C., Werb, Z., & Fisher, S. J. (1994). Implantation and the placenta: key pieces of the development puzzle. *Science*, 266(5190), 1508-1518. doi:10.1126/science.7985020

Decato, B. E., Lopez-Tello, J., Sferruzzi-Perri, A. N., Smith, A. D., & Dean, M. D. (2017). DNA Methylation Divergence and Tissue Specialization in the Developing Mouse Placenta. *Mol Biol Evol*, 34(7), 1702-1712. doi:10.1093/molbev/msx112

Emera, D., & Wagner, G. P. (2012). Transposable element recruitments in the mammalian placenta: impacts and mechanisms. *Brief Funct Genomics*, 11(4), 267-276. doi:10.1093/bfgp/els013

Fulka, H., Mrazek, M., Tepla, O., & Fulka, J., Jr. (2004). DNA methylation pattern in human zygotes and developing embryos. *Reproduction*, 128(6), 703-708. doi:10.1530/rep.1.00217

Gu, H., Smith, Z. D., Bock, C., Boyle, P., Gnirke, A., & Meissner, A. (2011). Preparation of reduced representation bisulfite sequencing libraries for genome-scale DNA methylation profiling. *Nat Protoc*, 6(4), 468-481. doi:10.1038/nprot.2010.190

Guo, H., Zhu, P., Yan, L., Li, R., Hu, B., Lian, Y., . . . Qiao, J. (2014). The DNA methylation landscape of human early embryos. *Nature*, 511(7511), 606-610. doi:10.1038/nature13544

Haig, D. (2012). Retroviruses and the placenta. *Curr Biol*, 22(15), R609-613. doi:10.1016/j.cub.2012.06.002

Hansen, K. D., Langmead, B., & Irizarry, R. A. (2012). BSmooth: from whole genome bisulfite sequencing reads to differentially methylated regions. *Genome Biol*, 13(10), R83. doi:10.1186/gb-2012-13-10-r83

Hirasawa, R., Chiba, H., Kaneda, M., Tajima, S., Li, E., Jaenisch, R., & Sasaki, H. (2008). Maternal and zygotic Dnmt1 are necessary and sufficient for the maintenance of DNA methylation

imprints during preimplantation development. *Genes Dev*, 22(12), 1607-1616. doi:10.1101/gad.1667008

Hon, G. C., Rajagopal, N., Shen, Y., McCleary, D. F., Yue, F., Dang, M. D., & Ren, B. (2013). Epigenetic memory at embryonic enhancers identified in DNA methylation maps from adult mouse tissues. *Nat Genet*, 45(10), 1198-1206. doi:10.1038/ng.2746

Howell, C. Y., Bestor, T. H., Ding, F., Latham, K. E., Mertineit, C., Trasler, J. M., & Chaillet, J. R. (2001). Genomic imprinting disrupted by a maternal effect mutation in the Dnmt1 gene. *Cell*, 104(6), 829-838.

Kamachi, Y., & Kondoh, H. (2013). Sox proteins: regulators of cell fate specification and differentiation. *Development*, 140(20), 4129-4144. doi:10.1242/dev.091793

Kaneda, M., Okano, M., Hata, K., Sado, T., Tsujimoto, N., Li, E., & Sasaki, H. (2004). Essential role for de novo DNA methyltransferase *Dnmt3a* in paternal and maternal imprinting. *Nature*, 429(6994), 900-903. doi:10.1038/nature02633

Kato, Y., Kaneda, M., Hata, K., Kumaki, K., Hisano, M., Kohara, Y., . . . Sasaki, H. (2007). Role of the Dnmt3 family in de novo methylation of imprinted and repetitive sequences during male germ cell development in the mouse. *Hum Mol Genet*, 16(19), 2272-2280. doi:10.1093/hmg/ddm179

Legault, L.-M., Chan, D., & McGraw, S. (2019). Rapid Multiplexed Reduced Representation Bisulfite Sequencing Library Prep (rRRBS). *BIO-PROTOCOL*, 9(4).

Lei, H., Oh, S. P., Okano, M., Juttermann, R., Goss, K. A., Jaenisch, R., & Li, E. (1996). De novo DNA cytosine methyltransferase activities in mouse embryonic stem cells. *Development*, 122(10), 3195-3205.

Leonhardt, H., Page, A. W., Weier, H. U., & Bestor, T. H. (1992). A targeting sequence directs DNA methyltransferase to sites of DNA replication in mammalian nuclei. *Cell*, 71(5), 865-873. doi:10.1016/0092-8674(92)90561-p

Li, E. (2002). Chromatin modification and epigenetic reprogramming in mammalian development. *Nat Rev Genet*, 3(9), 662-673. doi:10.1038/nrg887

Li, E., Bestor, T. H., & Jaenisch, R. (1992). Targeted mutation of the DNA methyltransferase gene results in embryonic lethality. *Cell*, 69(6), 915-926.

Lillycrop, K. A., & Burdge, G. C. (2011). Epigenetic changes in early life and future risk of obesity. *Int J Obes (Lond)*, 35(1), 72-83. doi:10.1038/ijo.2010.122

Macaulay, E. C., Weeks, R. J., Andrews, S., & Morison, I. M. (2011). Hypomethylation of functional retrotransposon-derived genes in the human placenta. *Mamm Genome*, 22(11-12), 722-735. doi:10.1007/s00335-011-9355-1

Magnus, N., Garnier, D., Meehan, B., McGraw, S., Lee, T. H., Caron, M., . . . Rak, J. (2014). Tissue factor expression provokes escape from tumor dormancy and leads to genomic alterations. *Proc Natl Acad Sci U S A*, 111(9), 3544-3549. doi:10.1073/pnas.1314118111

McGraw, S., Zhang, J. X., Farag, M., Chan, D., Caron, M., Konermann, C., . . . Trasler, J. M. (2015). Transient DNMT1 suppression reveals hidden heritable marks in the genome. *Nucleic Acids Res*. doi:10.1093/nar/gku1386

Mi, S., Lee, X., Li, X., Veldman, G. M., Finnerty, H., Racie, L., . . . McCoy, J. M. (2000). Syncytin is a captive retroviral envelope protein involved in human placental morphogenesis. *Nature*, 403(6771), 785-789. doi:10.1038/35001608

Mizuuchi, M., Cindrova-Davies, T., Olovsson, M., Charnock-Jones, D. S., Burton, G. J., & Yung, H. W. (2016). Placental endoplasmic reticulum stress negatively regulates transcription of placental growth factor via ATF4 and ATF6beta: implications for the pathophysiology of human pregnancy complications. *J Pathol*, 238(4), 550-561. doi:10.1002/path.4678

Monk, M. (1987). Genomic imprinting. Memories of mother and father. *Nature*, 328(6127), 203-204. doi:10.1038/328203a0

Morgan, H. D., Santos, F., Green, K., Dean, W., & Reik, W. (2005). Epigenetic reprogramming in mammals. *Hum Mol Genet*, 14 Spec No 1, R47-58. doi:10.1093/hmg/ddi114

Nakanishi, M. O., Hayakawa, K., Nakabayashi, K., Hata, K., Shiota, K., & Tanaka, S. (2012). Trophoblast-specific DNA methylation occurs after the segregation of the trophectoderm and inner cell mass in the mouse periimplantation embryo. *Epigenetics*, 7(2), 173-182. doi:10.4161/epi.7.2.18962

Nardelli, C., Iaffaldano, L., Ferrigno, M., Labruna, G., Maruotti, G. M., Quaglia, F., . . . Sacchetti, L. (2014). Characterization and predicted role of the microRNA expression profile in amnion from obese pregnant women. *Int J Obes (Lond)*, 38(3), 466-469. doi:10.1038/ijo.2013.121

Oda, M., Oxley, D., Dean, W., & Reik, W. (2013). Regulation of lineage specific DNA hypomethylation in mouse trophectoderm. *PLoS One*, 8(6), e68846. doi:10.1371/journal.pone.0068846

Okahara, G., Matsubara, S., Oda, T., Sugimoto, J., Jinno, Y., & Kanaya, F. (2004). Expression analyses of human endogenous retroviruses (HERVs): tissue-specific and developmental stage-dependent expression of HERVs. *Genomics*, 84(6), 982-990. doi:10.1016/j.ygeno.2004.09.004

Okano, M., Bell, D. W., Haber, D. A., & Li, E. (1999). DNA methyltransferases *Dnmt3a* and *Dnmt3b* are essential for de novo methylation and mammalian development. *Cell*, 99(3), 247-257.

Piche, J., Gosset, N., Legault, L. M., Pacis, A., Oneglia, A., Caron, M., . . . Andelfinger, G. (2019). Molecular Signature of CAID Syndrome: Noncanonical Roles of SGO1 in Regulation of TGF-beta Signaling and Epigenomics. *Cell Mol Gastroenterol Hepatol*, 7(2), 411-431. doi:10.1016/j.jcmgh.2018.10.011

Price, E. M., Cotton, A. M., Penaherrera, M. S., McFadden, D. E., Kobor, M. S., & Robinson, W. (2012). Different measures of "genome-wide" DNA methylation exhibit unique properties in placental and somatic tissues. *Epigenetics*, 7(6), 652-663. doi:10.4161/epi.20221

Reichmann, J., Reddington, J. P., Best, D., Read, D., Ollinger, R., Meehan, R. R., & Adams, I. R. (2013). The genome-defence gene Tex19.1 suppresses LINE-1 retrotransposons in the placenta and prevents intra-uterine growth retardation in mice. *Hum Mol Genet*, 22(9), 1791-1806. doi:10.1093/hmg/ddt029

Reiss, D., Zhang, Y., & Mager, D. L. (2007). Widely variable endogenous retroviral methylation levels in human placenta. Nucleic Acids Res, 35(14), 4743-4754. doi:10.1093/nar/gkm455

Robinson, W. P., & Price, E. M. (2015). The human placental methylome. *Cold Spring Harb Perspect Med*, 5(5), a023044. doi:10.1101/cshperspect.a023044

Rossant, J., & Cross, J. C. (2001). Placental development: lessons from mouse mutants. *Nat Rev Genet*, 2(7), 538-548. doi:10.1038/35080570

Santos, F., Hendrich, B., Reik, W., & Dean, W. (2002). Dynamic reprogramming of DNA methylation in the early mouse embryo. *Dev Biol*, 241(1), 172-182. doi:10.1006/dbio.2001.0501

Schroeder, D. I., Blair, J. D., Lott, P., Yu, H. O., Hong, D., Crary, F., . . . LaSalle, J. M. (2013). The human placenta methylome. *Proc Natl Acad Sci U S A*, 110(15), 6037-6042. doi:10.1073/pnas.1215145110

Schroeder, D. I., Jayashankar, K., Douglas, K. C., Thirkill, T. L., York, D., Dickinson, P. J., . . . LaSalle, J. M. (2015). Early Developmental and Evolutionary Origins of Gene Body DNA Methylation Patterns in Mammalian Placentas. *PLoS Genet*, 11(8), e1005442. doi:10.1371/journal.pgen.1005442

Senner, C. E., Krueger, F., Oxley, D., Andrews, S., & Hemberger, M. (2012). DNA methylation profiles define stem cell identity and reveal a tight embryonic-extraembryonic lineage boundary. *Stem Cells*, 30(12), 2732-2745. doi:10.1002/stem.1249

Shaffer, B., McGraw, S., Xiao, S. C., Chan, D., Trasler, J., & Chaillet, J. R. (2015). The dnmt1 intrinsically disordered domain regulates genomic methylation during development. *Genetics*, 199(2), 533-541. doi:10.1534/genetics.114.173609

Slotkin, R. K., & Martienssen, R. (2007). Transposable elements and the epigenetic regulation of the genome. *Nat Rev Genet*, 8(4), 272-285. doi:10.1038/nrg2072

Smith, Z. D., Chan, M. M., Humm, K. C., Karnik, R., Mekhoubad, S., Regev, A., . . . Meissner, A. (2014). DNA methylation dynamics of the human preimplantation embryo. *Nature*, 511(7511), 611-615. doi:10.1038/nature13581

Smith, Z. D., Shi, J., Gu, H., Donaghey, J., Clement, K., Cacchiarelli, D., . . . Meissner, A. (2017). Epigenetic restriction of extraembryonic lineages mirrors the somatic transition to cancer. *Nature*, 549(7673), 543-547. doi:10.1038/nature23891

Warren, I. A., Naville, M., Chalopin, D., Levin, P., Berger, C. S., Galiana, D., & Volff, J. N. (2015). Evolutionary impact of transposable elements on genomic diversity and lineage-specific innovation in vertebrates. *Chromosome Res*, 23(3), 505-531. doi:10.1007/s10577-015-9493-5

Watanabe, D., Suetake, I., Tada, T., & Tajima, S. (2002). Stage- and cell-specific expression of *Dnmt3a* and *Dnmt3b* during embryogenesis. *Mech Dev*, 118(1-2), 187-190.

Whidden, L., Martel, J., Rahimi, S., Richard Chaillet, J., Chan, D., & Trasler, J. M. (2016). Compromised oocyte quality and assisted reproduction contribute to sex-specific effects on offspring outcomes and epigenetic patterning. *Hum Mol Genet*. doi:10.1093/hmg/ddw293

Xie, M., Hong, C., Zhang, B., Lowdon, R. F., Xing, X., Li, D., . . . Wang, T. (2013). DNA hypomethylation within specific transposable element families associates with tissue-specific enhancer landscape. *Nat Genet*, 45(7), 836-841. doi:10.1038/ng.2649

Zhang, Y., Xiang, Y., Yin, Q., Du, Z., Peng, X., Wang, Q., . . . Xie, W. (2018). Dynamic epigenomic landscapes during early lineage specification in mouse embryos. *Nat Genet*, 50(1), 96-105. doi:10.1038/s41588-017-0003-x

Zhou, Y., Zhou, B., Pache, L., Chang, M., Khodabakhshi, A. H., Tanaseichuk, O., . . . Chanda, S. K. (2019). Metascape provides a biologist-oriented resource for the analysis of systems-level datasets. *Nat Commun*, 10(1), 1523. doi:10.1038/s41467-019-09234-6

Figures and legends

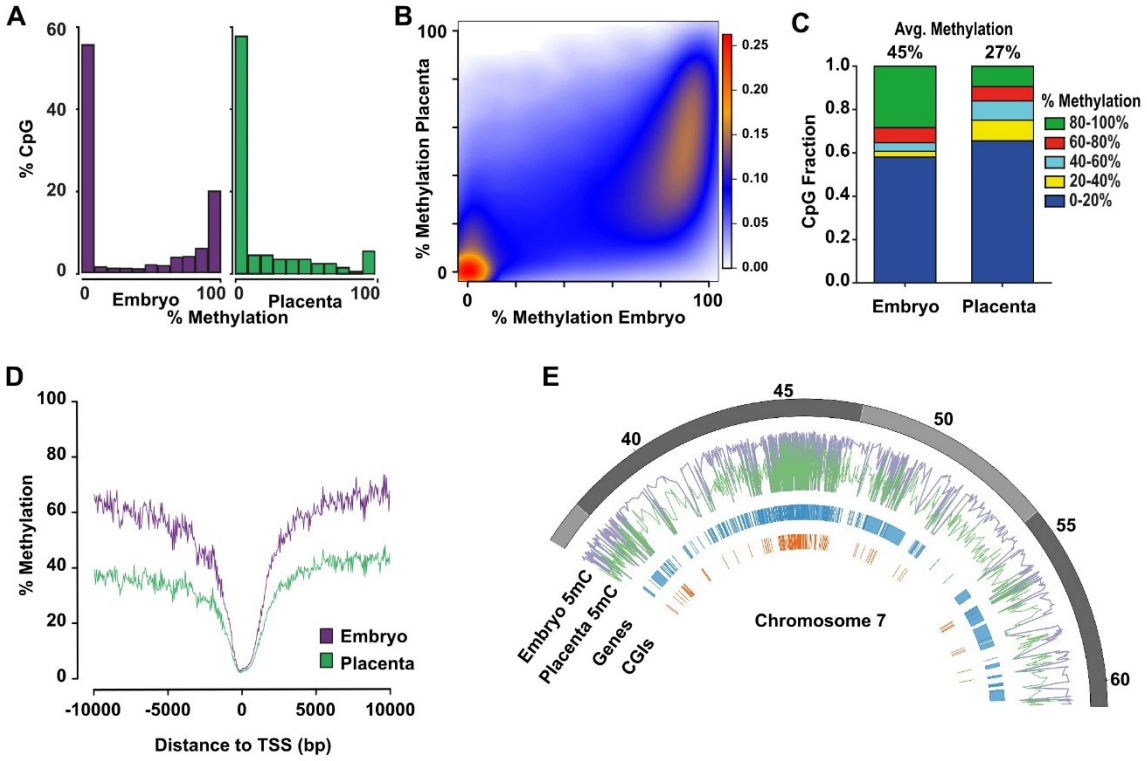

Figure 1. Distinctive patterns of genome-wide DNA methylation accumulation between E10.5 embryo and placenta. Analyses of genome-wide DNA methylation sequencing results for embryo (n=4) and placenta (n=4). **A)** Density histograms showing the distribution of CpG methylation levels for embryo (*purple*) and placenta (*green*). **B)** Pairwise comparison of CpG methylation between embryo and placenta. Density increases from blue to red. **C)** CpG fraction of 100 bp tiles within 0-20%, 20-40%, 40-60%, 60-80% and 80-100% ranges in embryo and placenta. Shown above bars, is the average CpG methylation for each unique tile represented in graph. **D)** DNA methylation means surrounding the transcription start site (TSS) for All-tiles in each experimental group. **E)** Circle plot showing methylation average of embryo (*purple*) and placenta (*green*) across a portion of chromosome 7.

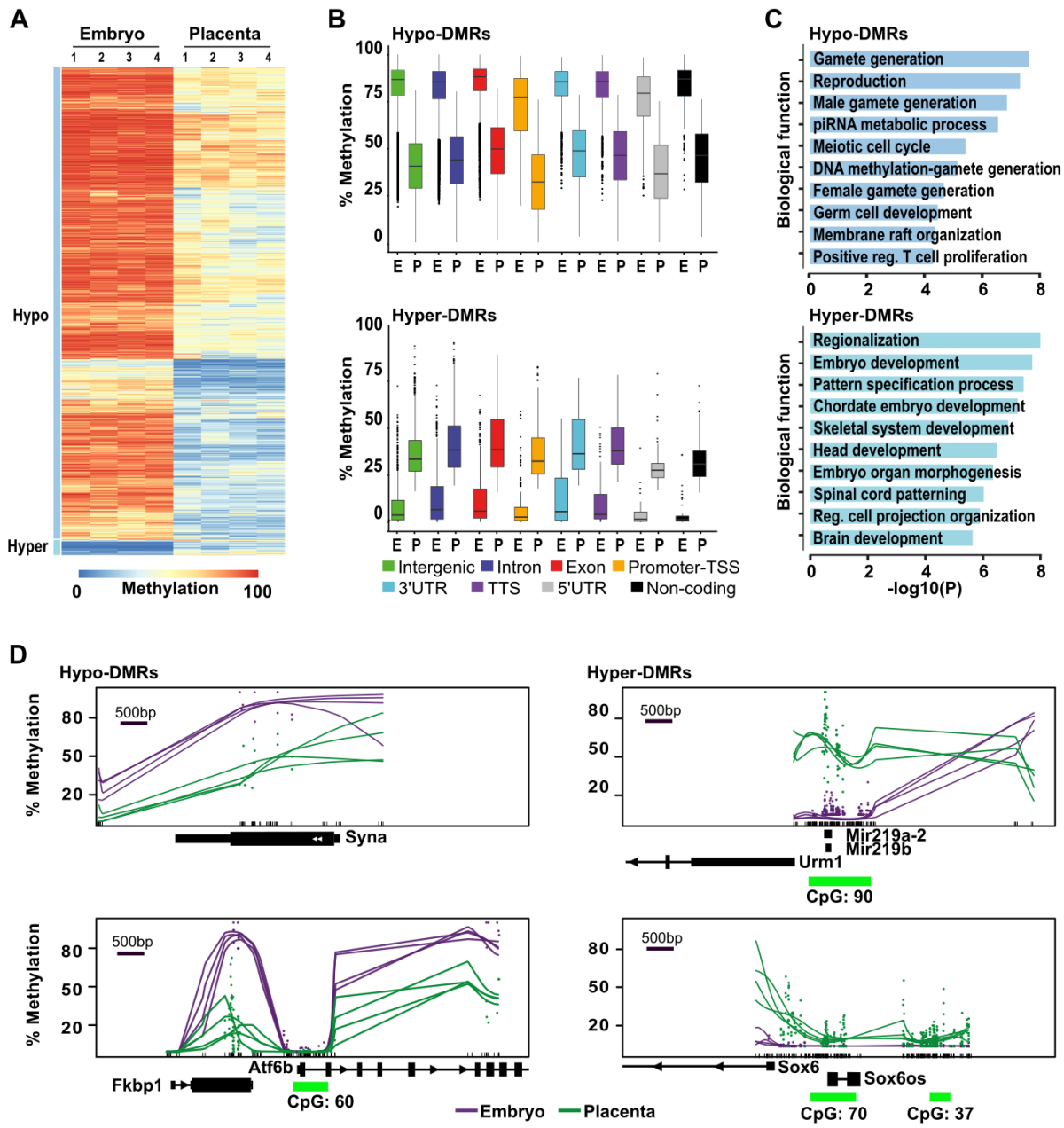

Figure 2. Genome-wide methylation asymmetry across genomic features between E10.5 embryo and placenta. Analyses of genome-wide DNA methylation sequencing results for embryo (n=4) and placenta (n=4) samples. **A)** Heatmap representation of DNA methylation levels for the 20 000 tiles with the most variable levels between embryo and placenta (DNA methylation variance >20% and $P<0.05$). **B)** Box-plots representing DNA methylation distribution in embryo and placenta for the different genomic annotation regions (intergenic, intron, exon, promoter-TSS, 3′UTR, TTS, 5'UTR and non-coding). **C)** Summary of biological functions associated with promoter regions in Hypo- and Hyper-DMRs (n=1 152 and n=182 unique promoters respectively). **D)** Examples of smoothed methylation profiles (*BSmooth* tool) in regions with lower methylation profiles (*Syna and Atf6b*) or higher methylation profiles (*Mir219a-2/Mir219b,* and *Sox6*) in placenta. Green dashes represent position of CpG islands.

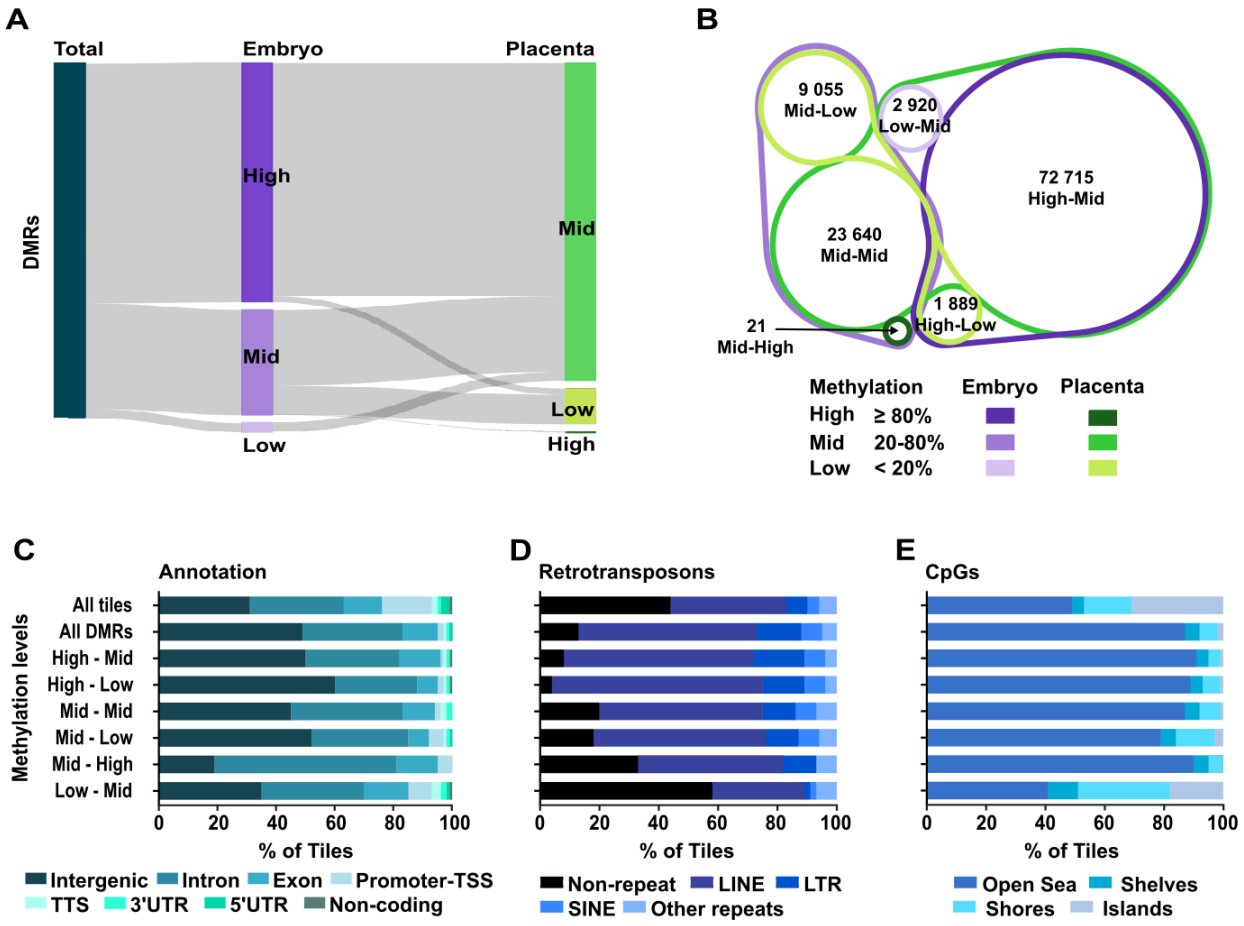

Figure 3. Distinct genomic features in DMRs based on their methylation status in E10.5 embryo and placenta. DMR analysis by methylation levels in embryo and placenta. **A)** Sankey diagram dividing DMRs by methylation levels in embryo (*purple*) and placenta (*green*) for the associated tiles. High : ≥80% methylation, Mid (intermediate) : ≥20% - <80% methylation , Low : <20% methylation. **B)** Venn diagram showing the proportion of tiles in the different DMR categories based on DNA methylation levels between embryo and placenta. **C), D)** and **E)** Analysis of All-tiles, all the DMRs, as well as the 6 different DMR categories based on levels of DNA methylation in embryo and placenta for : **C)** Genomic annotations, **D)** Main retrotransposons and **E)** Proximity of CpG rich regions. Neighboring CpG dense regions were defined as shore; up to 2kb away from CGIs, shelf; 2-4kb away from CGIs, and open sea; >4kb away from CGIs.

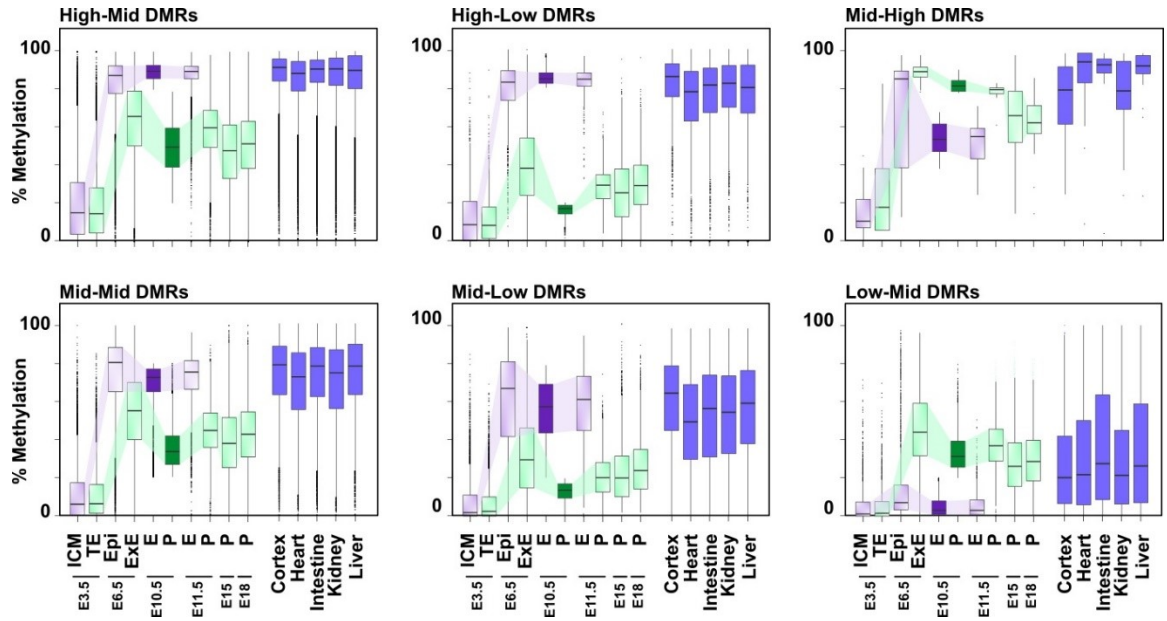

Figure 4. Dynamics of DNA methylation profiles associated with DMR categories and their evolution across embryo and placenta development. Box plots representing the DNA methylation distribution and median values for each DMR category in various developmental stages. Tiles associated with DMR categories at E10.5 were overlapped with previously published and publicly available data, and methylation levels were determined at each developmental stage (Smith et *al*. 2014, Whidden et *al*. 2016, Decato et al., 2017) or in adult somatic tissues (Hon et *al*. 2013). ICM: inner cell mass, TE: trophectoderm, Epi: epiblast, ExE: extraembryonic ectoderm, E: embryo, Pla: placenta. See Table S2 for median and mean methylation values, and Table S4 for number of overlapping tiles analysed.

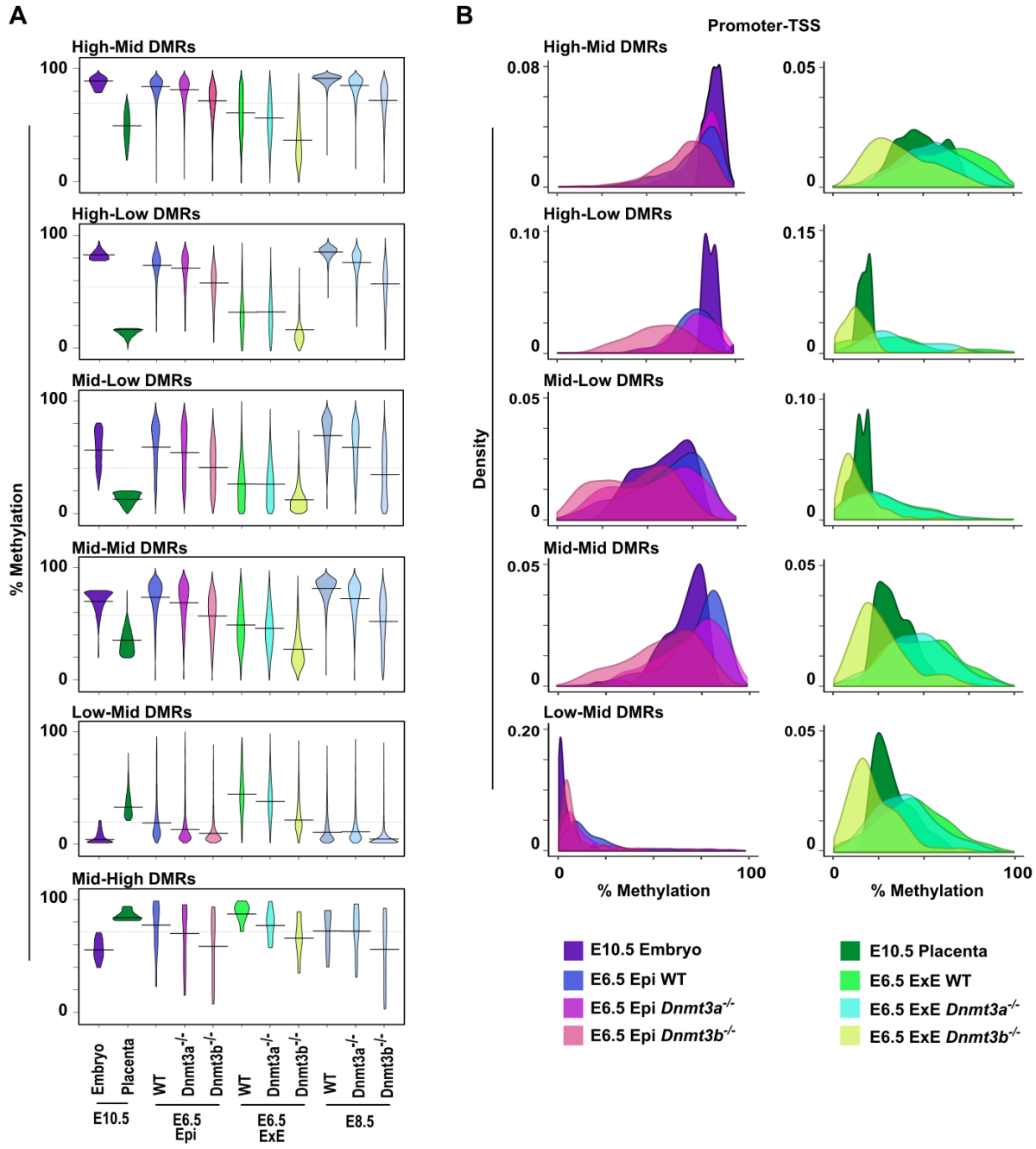

Figure 5. *Dnmt3a*- or *Dnmt3b*-deficiency alters proper establishment of DMR-associated patterns. A) Violin plots representing DNA methylation distribution and median values of tiles associated with the different DMR categories at E10.5, and their methylation levels in overlapping tiles of different tissues and genotypes at E6.5 (Smith et *al*. 2017) and E8.5 (Auclair et *al*. 2014). **B)** Density plots describing the mean methylation profiles of promoter-TSS associated tiles in each DMR category for E10.5 embryo and E6.5 epiblast (wt, *Dnmt3a*$^{-/-}$ and *Dnmt3b*$^{-/-}$) (left panel) and for E10.5 placenta and E6.5 extraembryonic ectoderm (wt, *Dnmt3a*$^{-/-}$ and *Dnmt3b*$^{-/-}$) (right panel). E: embryo, Epi: epiblast, ExE: extraembryonic ectoderm. See Table S3 for median and mean methylation values, and Table S4 for number of overlapping tiles analysed.

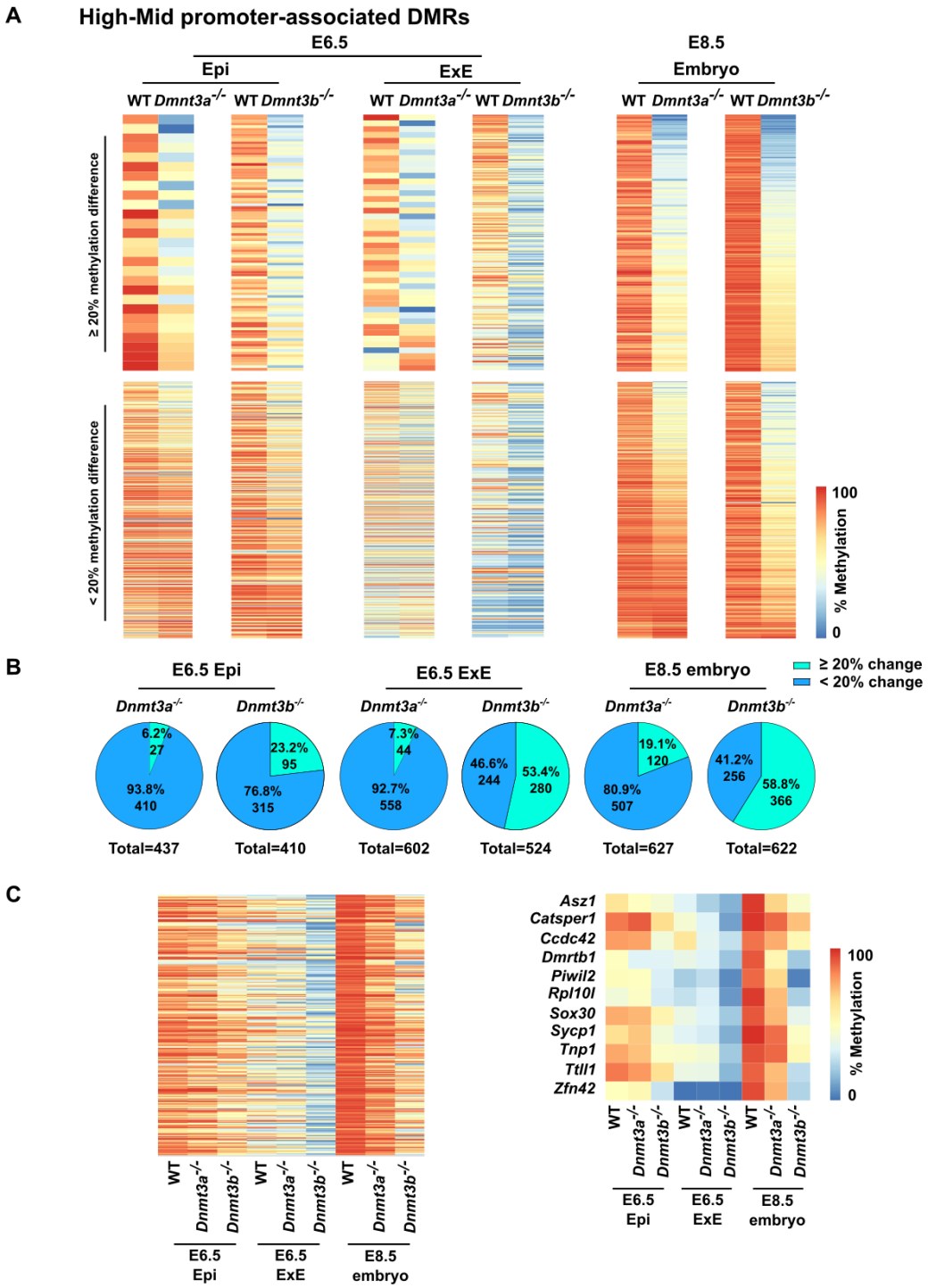

Figure 6. Developmental decline in compensatory DNA methylation mechanism in response to *Dnmt3a*- or *Dnmt3b*-deficiency at promoter-TSS associated with High-Mid DMRs. A) Heatmaps comparing the DNA methylation profiles of wt vs *Dnmt3a*$^{-/-}$ or wt vs *Dnmt3b*$^{-/-}$ for E6.5 epiblast, E6.5 extraembryonic ectoderm (Smith et *al*. 2017) or E8.5 embryo (Auclair et *al*. 2014) in 100bp tiles overlapping promoter-associated High-Mid DMRs that are highly methylated in the embryo (≥80%) and mildly methylated in the placenta (≥20 and <80%). Upper panel represents

regions with a difference of methylation of at least 20% between wt and *Dnmt3a*$^{-/-}$ or wt and *Dnmt3b*$^{-/-}$. Lower panel represents stable regions (lower than 20% difference in methylation). **B)** Pie charts representing promoter-associated High-Mid DMR numbers for each comparison in A). **C)** Heatmap of the methylation levels of tiles commonly represented in all 9 public data samples that overlap with promoters-associated High-Mid DMRs (n = 314 tiles) (left panel). Heatmap of the methylation level of gene associated with piRNA, gamete generation and germ cells or meiotic nuclear division that are covered in all 9 public datasets (right panel).

Supplemental figures and legends

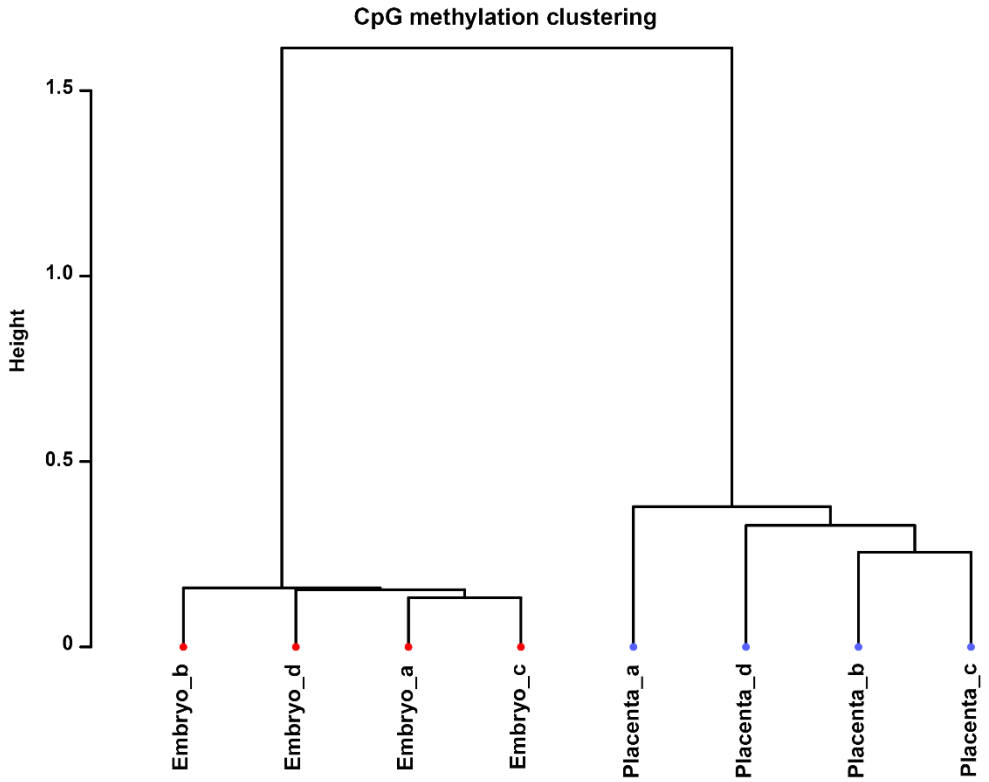

Figure S1. Hierarchical dendrogram showing clustering of E10.5 embryo and placenta samples according to genome-wide DNA methylation profiles. Samples a, c: females; Samples b, d: males.

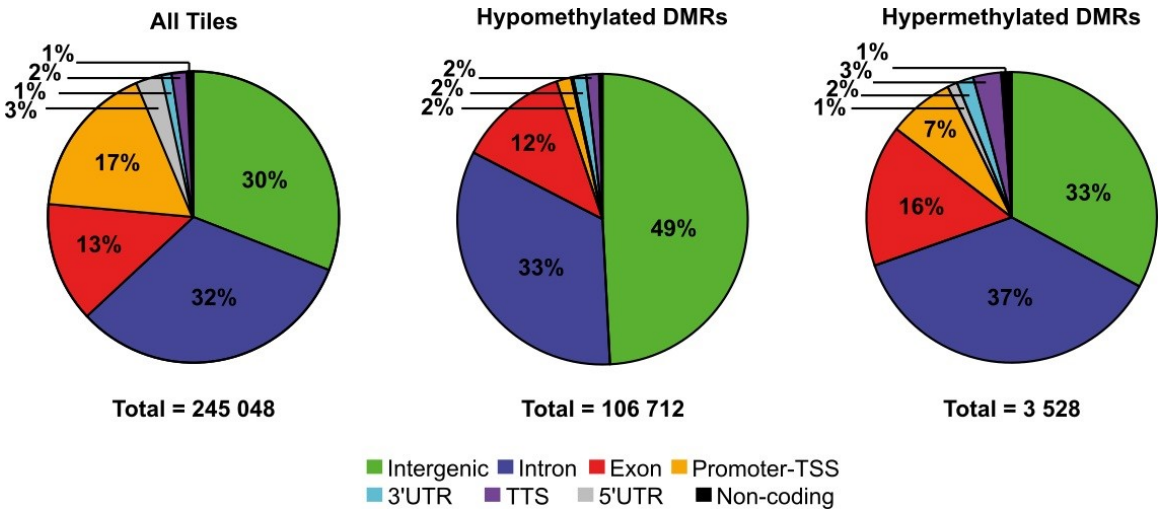

Figure S2. Pie charts representing genomic annotation of Hypo- and Hyper-DMRs found between E10.5 embryo and placenta. Proportion of all sequenced tiles (All-tiles; n=245 048) common to embryo and placenta, Hypo-DMRs (n=106 712) and Hyper-DMRs (n=3 528), found in intergenic and genic regions (exons, introns, promoters-TSS, 3′ and 5′ untranslated regions, and transcription termination sites, non-coding).

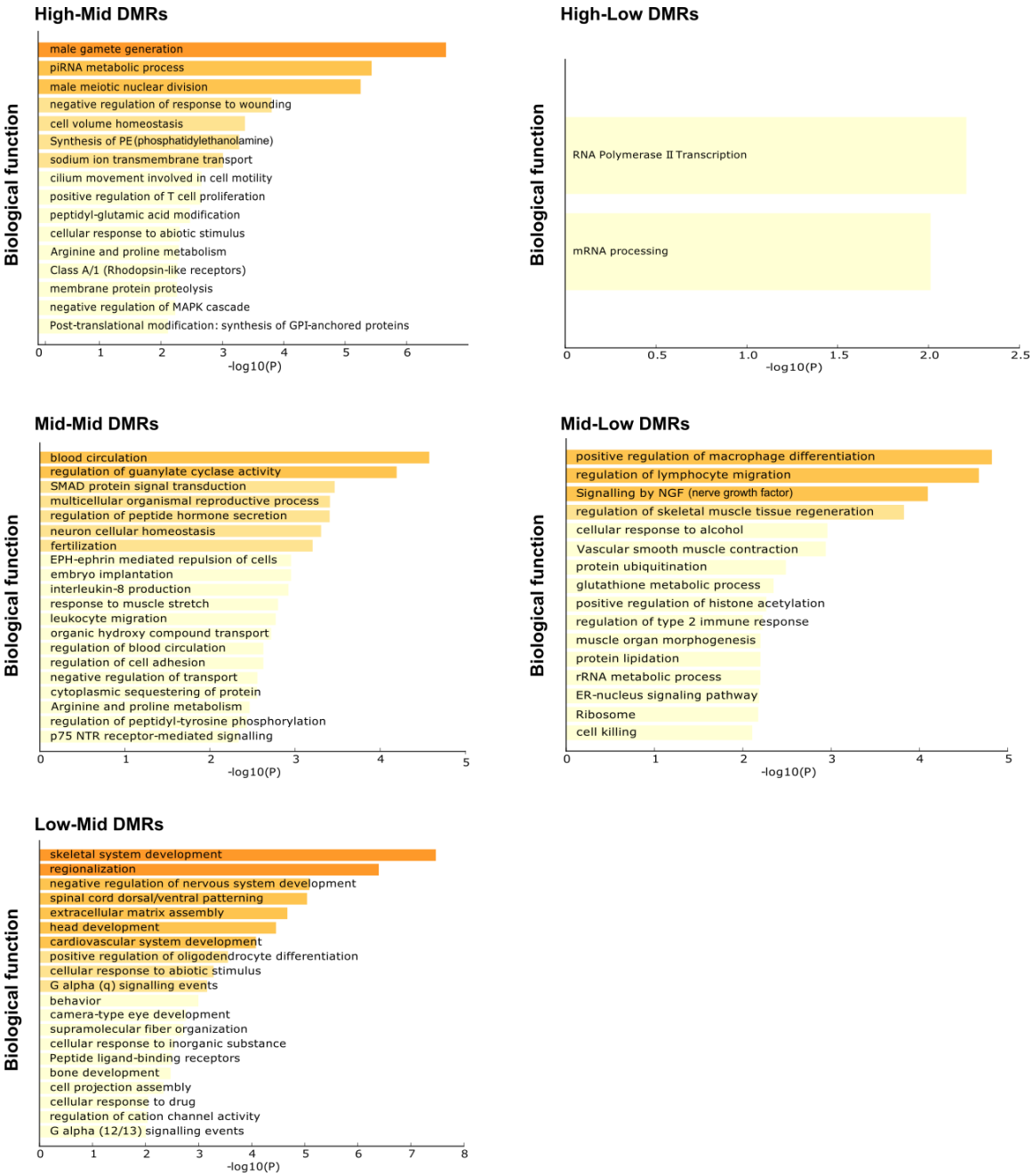

Figure S3. Summary of biological functions associated with E10.5 embryo-placenta DMRs subtypes. Number of tiles in promoter-TSS regions used as input for each methylation category: High-Low: 38; High-Mid: 749; Mid-Lo: 477; Mid-Mid: 509 and Low-Mid: 235. No enrichment in biological functions found for Mid-High: 1.

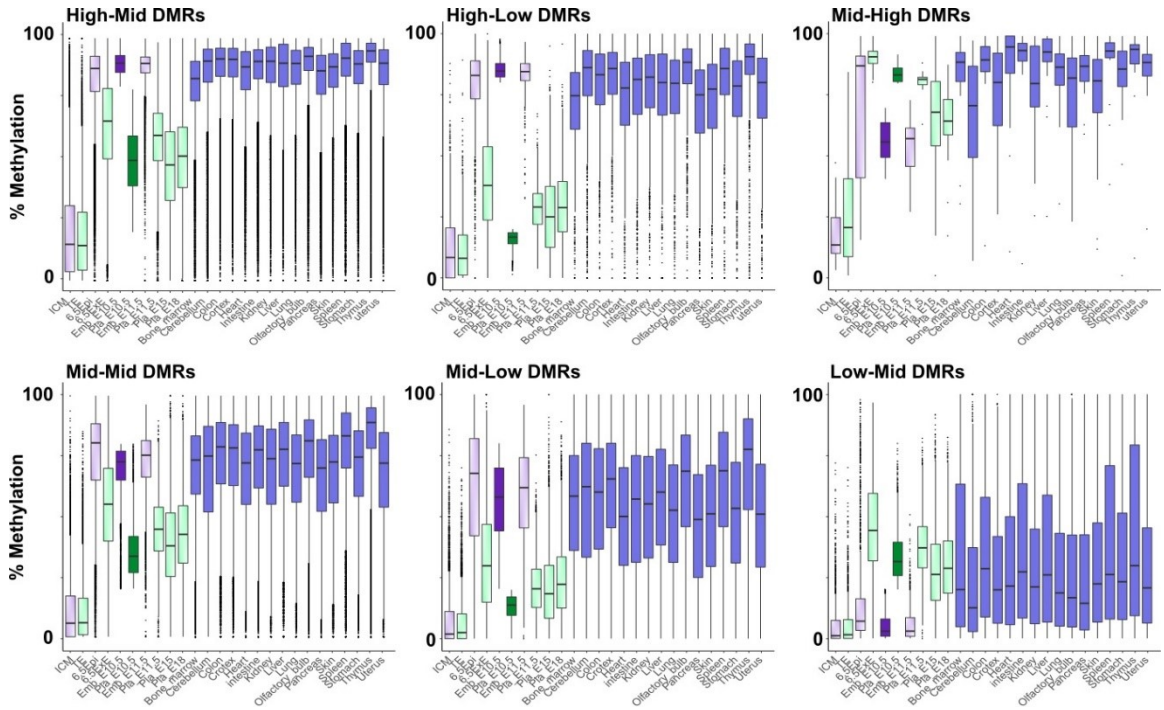

Figure S4. Dynamics of DMR regions during embryonic development and in adult tissues. Box-plots showing DNA methylation distribution and median values of overlapping DMRs to publicly available methylation data at different developmental stages and in different adult tissues (Smith et al., 2014, Whidden et al., 2016, Hon et al., 2013, Decato et al., 2017). ICM: inner cell mass, TE: trophectoderm, Epi: epiblast, ExE: extraembryonic ectoderm, Emb: embryo, Pla: placenta. See Table S2 for median and mean methylation values.

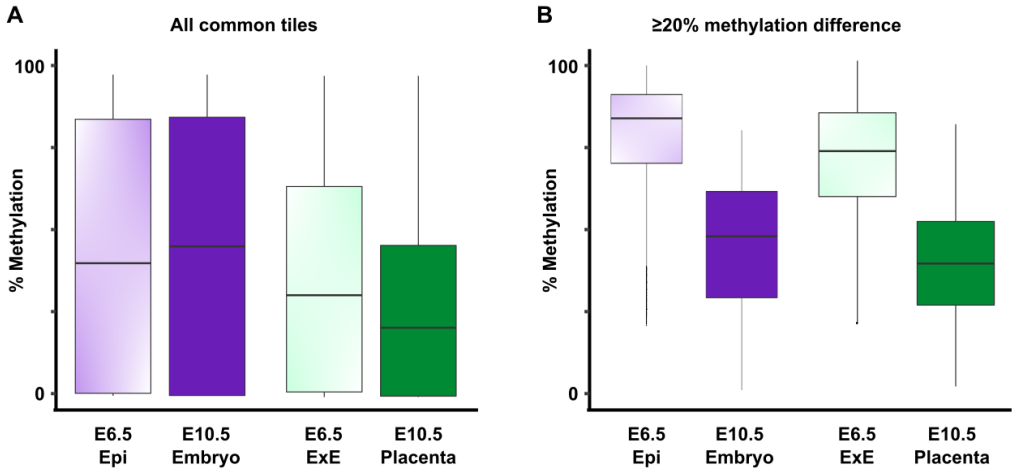

Figure S5. DNA methylation profiles at E6.5 and E10.5. A) Box plots representing the DNA methylation distribution and median values of overlapping common tiles between E6.5 ExE (Smith

et *al*. 2014) and E10.5 placenta (All-tiles), as well as E6.5 epiblast (Smith et *al*. 2014) and E10.5 embryo (All-tiles). E6.5 ExE vs E10.5 placenta; 35.66% vs 25.79%, p<0.0001; n=188 098 tiles, E6.5 epi vs E10.5 embryo; 43.2% vs 43.65%; p<0.0001; n=200 581 tiles. **B)** Box plots representing the DNA methylation distribution and median values of overlapping common tiles between E6.5 ExE (Smith et *al*. 2014) and E10.5 placenta (All-tiles) (70.22% vs 37.49%; p<0.0001; n=45 967), as well as E6.5 epiblast (Smith et *al*. 2014) and E10.5 embryo (All-tiles) (77.80% vs 43.87%; p<0.0001; n=11 183), having more than 20% higher DNA methylation at E6.5.

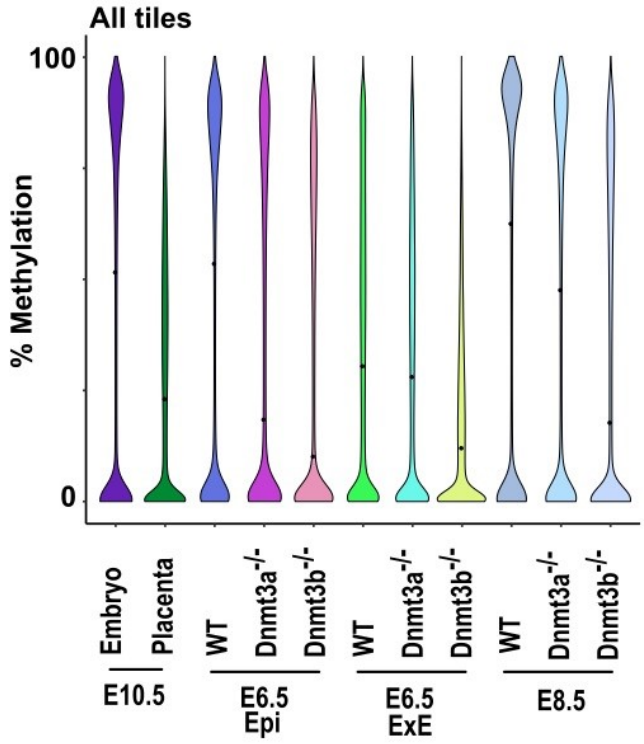

Figure S6. Global DNA methylation profiles in *Dnmt3a*$^{-/-}$ and *Dnmt3b*$^{-/-}$ samples. Violin plots showing DNA methylation distribution and median values of *Dnmt3a* or *Dnmt3b* knockout mice in E6.5 epiblast (Epi), E6.5 extraembryonic ectoderm (ExE) (Smith et *al*. 2017) and E8.5 embryos (Auclair et *al*. 2014) in 100bp tiles corresponding to the 245 048 analyzed tiles (All-tiles). Overlapping tiles (minimum 15x coverage) in each dataset: E6.5 Epi WT n=227 657 ; E6.5 Epi *Dnmt3a*$^{-/-}$ n=160 283 ; E6.5 Epi *Dnmt3b*$^{-/-}$ n=145 590 ; E6.5 ExE WT n=227 926 ; E6.5 ExE *Dnmt3a*$^{-/-}$ n=200 801 ; E6.5 ExE *Dnmt3b*$^{-/-}$ n=170 164 ; E8.5 embryo WT n=209 466 ; E8.5 embryo *Dnmt3a*$^{-/-}$ n=209 466 ; E8.5 embryo *Dnmt3b*$^{-/-}$ n=207 974. See Table S3 for median and mean methylation values.

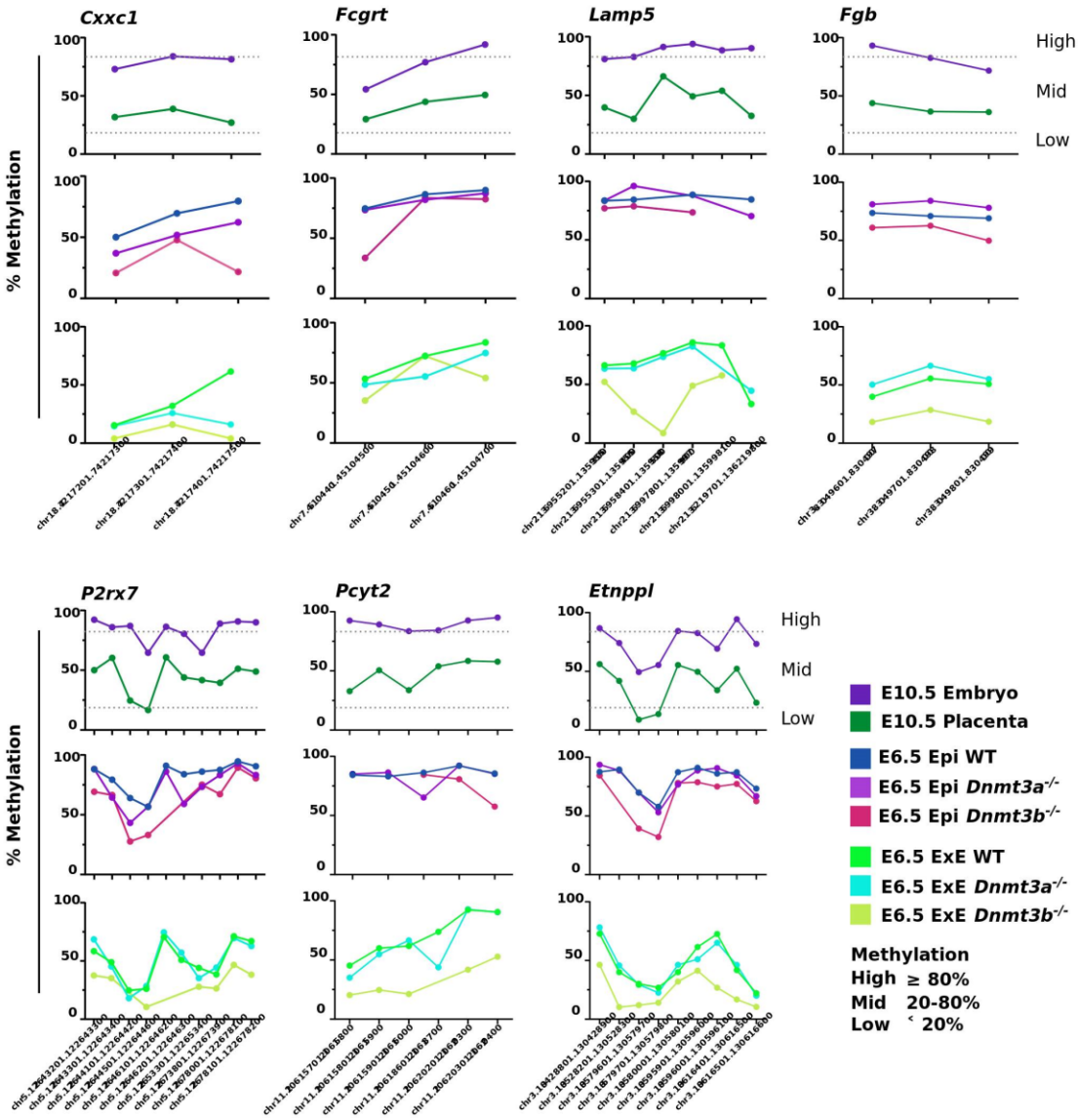

Figure S7. *Dnmt3a*- or *Dnmt3b*-deficiency alter proper establishment of DNA methylation associated with various DMR categories within gene promoter-TSS. DNA methylation average (%) per tile in *Dnmt3a*$^{-/-}$ and *Dnmt3b*$^{-/-}$ E6.5 epiblast and extraembryonic tissues (Smith et *al*. 2017) for E10.5 embryo-placenta associated DMRs. *Lrp5* (activation of *Wnt* signaling, important role in development processes); *Fgb* (encode for beta component of fibrinogen); *P2rx7* (ATP receptor); *Pcyt2* (role in the biosynthesis of phospholipid phosphatidylethanolamine); *Etnppl* (role in the biosynthesis of glycerophospholipid and metabolism); *Ralgds* (role in signaling processes).

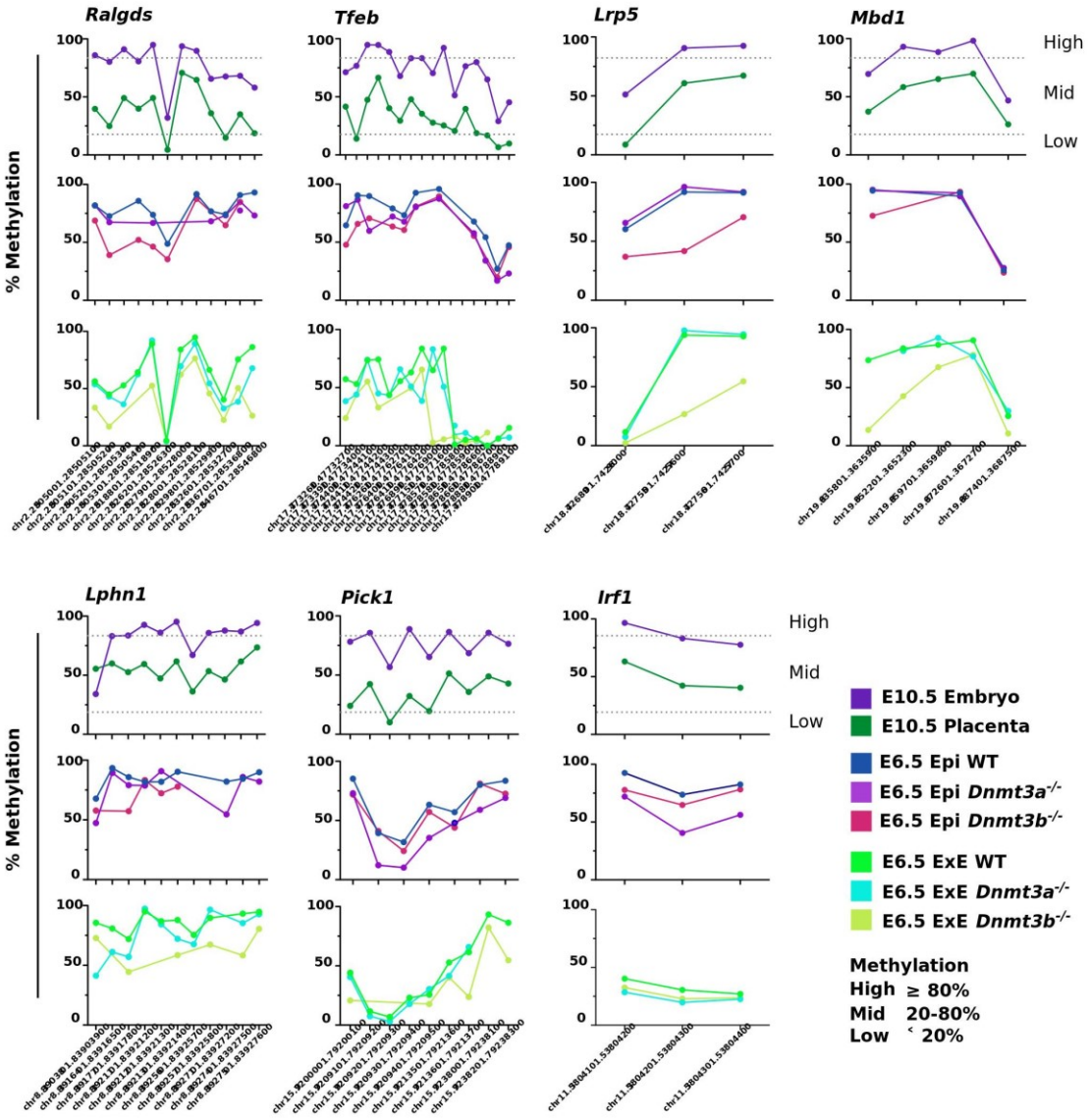

Figure S8. *Dnmt3a*- or *Dnmt3b*-deficiency alter proper establishment of DNA methylation associated with various DMR categories within genic regions. DNA methylation average (%) per tile in *Dnmt3a*$^{-/-}$ and *Dnmt3b*$^{-/-}$ E6.5 epiblast and extraembryonic tissues (Smith et *al*. 2017) for E10.5 embryo-placenta associated DMRs. *Cxxc1* (role in regulation of gene expression and development); *Fcgrt1* (transfers IgG from mother to fetus across the placenta); *Lamp5* (role in synaptic plasticity in some GABAergic neurons); *Mbd1* (transcriptional repressor); *Lphn1* (role in cell adhesion and signal transduction); *Pick1* (role in synaptic plasticity and regulation of astrocyte morphology); *Tfeb* (role in the regulation of lysosomal genes and autophagy); *Irf1* (regulation of cellular response, including *IFN* and *IFN*-inducible-genes).

Annexe 2 - Sex-specific differences in DNA methylation and gene expression in late-gestation mouse placentas

Toujours en complément de mon projet principal, je me suis aussi intéressée aux différences intrinsèques existantes entre les mâles et les femelles au niveau des profils de méthylation d'ADN et transcriptomiques dans les placentas de souris en fin de gestation (E18.5). Cet article est accepté dans le journal *Biology of Sex Differences*.

Sex-specific differences in DNA methylation and gene expression in late-gestation mouse placentas

Lisa-Marie Legault[1,2], Mélanie Breton-Larrivée[1,2], Alexandra Langford-Avelar[1,2], Anthony Lemieux[1], Serge McGraw[1,2,3].

[1]CHU Ste-Justine Research Center, 3175 Chemin de la Côte-Sainte-Catherine, Montréal, QC H3T 1C5, Canada

[2]Department of Biochemistry and Molecular Medicine, Université de Montréal, 2900 Boulevard Edouard-Montpetit, Montréal, QC H3T 1J4, Canada

[3]Department of Obstetrics and Gynecology, Université de Montréal, 2900 Boulevard Edouard-Montpetit, Montréal, QC H3T 1J4, Canada

Lisa-Marie Legault : lisa-marie.legault@umontreal.ca

Mélanie Breton-Larrivée : melanie.breton-larrivee@umontreal.ca

Alexandra Langford-Avelar : alexandra.langford.avelar@umontreal.ca

Anthony Lemieux : anthony.lemieux@umontreal.ca

Serge McGraw : serge.mcgraw@umontreal.ca (corresponding author)

Plain English summary

The placenta is a crucial organ for a healthy pregnancy and proper fetal development, and its functions are often studied in mice. The placenta stems from the developing embryo, and therefore shares its sex. Male fetuses have higher risks of pregnancy complications and neurodevelopmental disorders, and these risks are linked to placenta functions. However, how the placenta's sex influences the proteins it contains—and therefore, how it helps the fetus develop—remains largely unknown. We used cutting-edge techniques to systematically examine late-pregnancy mouse placentas, cataloging the genes being expressed (*i.e.*, sections of DNA used to make proteins) and the patterns of a specific DNA mark (called methylation) that controls gene expression. We identified several genes with important placental functions, such as protecting the fetus from viruses and responding to environmental changes, whose expression levels were sex-specific. We

also observed differences in DNA methylation between male and female placentas. Most DNA methylation differences were on the X-chromosomes associated with sex, and the majority had higher methylation levels in female placentas. Conversely, on other chromosomes, most DNA methylation differences were increased in male placentas. As methylation affects gene expression, we found links between the changes. Additionally, we found that some sex-specific differences in the placenta were already present earlier in pregnancy. Our findings provide important insights into the molecular differences between male and female mouse placentas during late pregnancy. Including sex-specific analyses in placenta studies will improve our understanding of how the placenta ensures the healthy development of male and female fetuses.

Abstract

Background: The placenta is vital for fetal development and its contributions to various developmental issues, such as pregnancy complications, fetal growth restriction, and maternal exposure, have been extensively studied in mice. Contrary to popular belief, the placenta forms mainly from fetal tissue; therefore, it has the same biological sex as the fetus it supports. However, while placental function is linked to increased risks of pregnancy complications and neurodevelopmental diseases in male offspring in particular, the sex-specific epigenetic (*e.g.*, DNA methylation) and transcriptomic features of the late-gestation mouse placenta remain largely unknown.

Methods: We collected male and female mouse placentas at late gestation (E18.5, n = 3/sex) and performed next-generation sequencing to identify genome-wide sex-specific differences in transcription and DNA methylation.

Results: Our sex-specific analysis revealed 358 differentially expressed genes (DEGs) on autosomes, which were associated with signaling pathways involved in transmembrane transport and the responses to viruses and external stimuli. X chromosome DEGs (n = 39) were associated with different pathways, including those regulating chromatin modification and small GTPase-mediated signal transduction. Sex-specific differentially methylated regions (DMRs) were more common on the X chromosomes (n = 3756) than on autosomes (n = 1705). Interestingly, while most X chromosome DMRs had higher DNA methylation levels in female placentas and tended to

be included in CpG dinucleotide-rich regions, 73% of autosomal DMRs had higher methylation levels in male placentas and were distant from CpG-rich regions. Several sex-specific DEGs were correlated with sex-specific DMRs. A subset of the sex-specific DMRs present in late-stage placentas were already established in mid-gestation (E10.5) placentas, while others were acquired later in placental development.

Conclusion: Our study provides comprehensive lists of sex-specific DEGs and DMRs that collectively cause profound differences in the DNA methylation and gene expression profiles of late-gestation mouse placentas. Our results demonstrate the importance of incorporating sex-specific analyses into epigenetic and transcription studies to enhance the accuracy and comprehensiveness of their conclusions and help address the significant knowledge gap regarding how sex differences influence placental function.

Highlights

- In the mouse placenta, sex-specific gene expression and DNA methylation profiles, enriched in various metabolic and developmental pathways, are observed for both X-linked and autosomal genes from mid-gestation onward.
- Regions with different DNA methylation are commonly found in CpG-rich areas on the X chromosomes and in CpG-poor regions on autosomes.
- A subset of the sex-specific DMRs observed in late-stage placentas were already established in mid-gestation placentas, whereas others were acquired during the later stages of placental development.
- Several sex-specific DNA methylation differences could be correlated with sex-specific differences in gene expression.
- The results highlight the importance of including sex-based analyses in epigenetic and transcriptional studies of the mouse placenta.

Keywords: Placenta, DNA methylation, gene expression, late pregnancy, mouse, sex-specific, development

BACKGROUND

Biological sex significantly impacts various aspects of life, ranging from cellular processes to the overall functioning of the organism. The placenta plays a critical role in allocating maternal-fetal resources, including oxygenation, nutrition, and metabolic exchanges between the mother and the fetus. It also acts as a protective barrier, responding to infection, stress, and other external factors to safeguard the developing fetus (1-3). The placenta comprises mainly tissue derived from early embryonic development and shares the same sex chromosomes as the embryo. However, it is commonly thought to be of maternal origin—and has been historically viewed as such, resulting in a lack of studies that consider the roles of the placenta's biological sex in their analyses.

Given its importance for fetal development, placental dysfunction and altered responses to external stressors can lead to numerous pregnancy complications, including preeclampsia, fetal growth restriction, gestational diabetes, and preterm birth (4, 5). Recent studies demonstrate that the placenta has sex-specific responses to certain stimuli or perturbations, which influence their impacts on the embryo (6-8). These findings align with existing evidence—primarily based on meta-analyses of human pregnancies—consistently indicating that male fetuses have higher susceptibility to pregnancy complications such as gestational diabetes, premature membrane rupture, preterm birth, and macrosomia (8-14). Males also exhibit a higher prevalence of neurodevelopmental disorders, including dyslexia and attention deficit hyperactivity disorder, which may be influenced by placental dysfunction and adaptations to diverse pregnancy conditions (6). Collectively, the evidence indicates that biological sex influences how the placenta functions and adapts to diverse pregnancy conditions; however, how sex-specific epigenetic and transcriptomic responses contribute to these increased risks to male fetuses remains unknown.

The critical roles of DNA methylation and gene expression in regulating development have been studied in detail in various biological systems (15-17). Significant differences in the methylation patterns and gene expression levels of an embryo and its placenta are established quickly after implantation (18, 19). Mouse embryos display sex-specific DNA methylation patterns, which can be differently altered following adverse maternal exposure (*e.g.* alcohol, environmental toxicant, drug) (20-23). While initially thought to occur primarily on sex chromosomes, sex-specific differences in DNA methylation and gene expression have been detected throughout the genome in various tissues and organs, including the human placenta (24-

29). Systematically investigating the DNA methylation and gene expression profiles of male and female mouse placentas will provide valuable insights into these sex-based variations in placental functions.

The mouse is a widely used model organism to study pregnancy outcomes and complications, because of its short gestation period and the ease of manipulating its genome (30). Historically, many studies often focused solely on male mice to exclude processes associated with X inactivation and hormonal differences in females. In other studies, male and female samples were not discriminated or even pooled when studying autosomally regulated processes, assuming them to be sex-independent. In addition, to mitigate the risk of significant sex biases, a common strategy in the -omics era has been to simply exclude sequences annotated to the X and Y chromosomes from the analyses. However, the mounting evidence that diseases and disorders of fetal origin due to adverse gestational conditions have sex-specific prevalence makes it crucial to carefully investigate how the placenta responds to various stimuli in both sexes.

In this study, we have systematically identified sex-specific DNA methylation and gene expression differences between male and female late-gestation mouse placentas. We uncovered numerous disparities in genes linked to important placental functions and embryonic development, including some on autosomal chromosomes. Our findings underscore the importance of including male and female samples and analyzing them independently, as biological sex results in important molecular differences that could profoundly impact a study's results.

METHODS

Mouse studies and tissue collection

All animal studies were approved by the CHU Ste-Justine Research Center *Comité Institutionnel de Bonnes Pratiques Animales en Recherche* under the guidance of the Canadian Council on Animal Care. Male and female C57BL/6 mice (Charles River Laboratories, Wilmington, MA, USA) were housed in a 12 h light/dark cycle with unlimited access to food and water and were mated at 8 weeks old. Females who had developed copulatory plugs by the next morning were considered pregnant with day 0.5 embryos (E0.5) and were separated from the males and housed together. The pregnant mice were euthanized at E18.5, and the placentas were dissected to remove maternal tissue, flash frozen in liquid nitrogen, and stored at -80°C until DNA and RNA extraction.

The sex of each placenta was determined by *Ddx3* qPCR using digested DNA from the corresponding embryo's tail (21).

DNA/RNA extraction and library preparation

We selected healthy looking placentas from three different litters (n = 3/sex) for DNA and RNA extraction. Whole placentas were homogenized to powder in liquid nitrogen. Samples were split in two, and the halves were used to extract genomic DNA with a QIAamp DNA Micro Kit (Qiagen, Hilden, Germany, #56304) and RNA using a RNeasy Mini Kit (Qiagen #74004), respectively, following the manufacturer's recommendations. Extracted DNA and RNA were quantified using a Qubit dsDNA BR (Broad Range) Assay Kit (Thermo Fisher Scientific, Waltham, MA, USA, #Q32853) and a High Sensitivity RNA assay kit (Thermo Fisher Scientific, #Q32852), respectively, on a Qubit 3.0 Fluorometer (Thermo Fisher Scientific #Q33217).

Mouse methyl capture sequencing (Methyl-Seq) libraries were generated using the SureSelect^{XT} Methyl-Seq Target Enrichment System (Agilent, Santa Clara, CA, USA, #G9651B) and the SureSelect^{XT} Mouse Methyl-Seq target enrichment panel (Agilent, #5191-6704) following the manufacturer's recommendations. Briefly, 1 µg of genomic DNA was used for library preparation. Target regions were enriched by biotinylated precipitation, followed by sodium bisulfite conversion and library amplification/indexing. Libraries were quantified using a Qubit dsDNA HS (High Sensitivity) Assay Kit (Thermo Fisher Scientific #Q32854) on a Qubit 3.0 Fluorometer. Library quality control was assessed using a BioAnalyzer (Agilent) followed by paired-end sequencing on a NovaSeq 6000 S4 sequencer at the Genome Québec core facility. We obtained 112–139M reads for the sequenced libraries.

Reduced Representation Bisulfite Sequencing libraries were performed based on the rapid RRBS protocol (rRRBS)(19, 21, 31-33). Briefly, 500 ng of DNA was digested with *Msp1* restriction enzyme and adapters were attached to DNA fragments. DNA was converted using sodium bisulfite treatment and amplification/indexation of libraries was performed. Libraries were quantified using QuBit fluorimeter apparel with the High Sensitivity DNA assay kit (ThermoFisher Scientific #Q32854). Quality of the libraries was assessed using BioAnalyzer following by paired-end sequencing was done on Illumina HiSeq 2500 at the Genome Québec core facility.

We generated mRNA-sequencing (mRNA-Seq) libraries using 500 ng of good-quality RNA (RIN >7and a NEBNext Ultra II Directional RNA Library Prep Kit (New England BioLabs, Ipswich, MA, USA, #E7760L) at the Genome Québec core facility and paired-end sequenced on a NovaSeq6000 S4 sequencer. We obtained 26–40M reads for the sequenced libraries.

Bioinformatics analyses

Post-sequencing bioinformatic analyses of mRNA-Seq data were performed using the GenPipes RNA-Seq pipeline (v4.1.2) (34) with alignment to the mouse GRCm38 genome (mm10). Differential gene expression analysis was performed with the R (v3.5.0) package DESeq2 (v1.24.0) (35) at a significance threshold of $p < 0.05$ with a normalized read count ≥ 1 in all replicates.

Methyl-Seq data were analyzed using the GenPipes Methyl-Seq pipeline (v3.3.0) (34) with reads aligned to the mouse GRCm38 reference genome, and methylation counts were obtained using Bismark (v0.18.1) (36). DMRs were identified with the R package MethylKit (version 1.8.1) (37) using the Benjamini-Hochberg false discovery rate procedure. Fixed parameters were used, including 100-bp stepwise tiling windows and a threshold of $q < 0.01$. Reported DNA methylation levels represent the average methylation levels of all CpG dinucleotides (CpGs) within a tile for all samples within a condition. The number of CpGs and bisulfite conversion rate (> 96%) of each tile were obtained using a custom Perl script (21).

Genome annotation of the tiles was performed using Homer (version 4.10.1) (38) and the mouse mm10 reference genome. Intragenic regions were defined as all annotations not in promoter or intergenic regions, such as 3’ UTR (untranslated regions), 5’ UTR, exons, introns, TTS (transcriptional termination site), non-coding regions. Gene ontology term enrichment analyses of differentially methylated tiles located in intragenic regions were performed in Metascape (metascape.org) (39). Repeats and CpG island coordinates for the mm10 genome were obtained from the UCSC Genome Browser (genome.ucsc.edu) (40). CpG shores and CpG shelves represent the regions within 0–2 kb and 2–4 kb of CpG islands, respectively, as previously described (19, 21). Statistical analyses were performed in R (v3.5.0) or GraphPad Prism (version 9.5.0; GraphPad Software, San Diego, CA, USA).

RESULTS

Late-gestation mouse placentas have sex-specific gene expression profiles

To reveal the molecular differences between male and female placentas during mouse development, we first conducted an in-depth gene expression analysis of six whole E18.5 placentas (n = 3/sex, from three different litters) using RNA-Seq. The expressed genes were divided into three groups based on their location on autosomal chromosomes, the X chromosomes, or the Y chromosome. We found that male placentas contained more transcribed autosomal genes than their female counterparts (26182 vs. 25758; Figure 1A). Female placentas had slightly more transcribed X chromosome genes than male placentas (1139 and 1129 in male and female placentas, respectively; Figure 1A). As expected, Y chromosome gene expression was observed exclusively in male placentas, with seven transcripts detected (Figure S1).

We identified 397 significantly differentially expressed genes (DEGs; $p < 0.05$) between male and female placentas. The majority (358) were located on autosomal chromosomes; of these, 145 were more highly expressed in male placentas and 213 were higher in female placentas (Figure 1B and C; Table 1). The X chromosomes contained 39 DEGs, with 37 and two upregulated in male and female placentas, respectively (Figure 1B and C; Table 2). Strikingly, many of the DEGs on autosomal chromosomes (43%) and X chromosomes (38%) had $|\log_2$ fold change$|$ values ≥ 0.5, indicating substantial differences in gene expression between male and female placentas from all shared chromosomes (Figure 1B). Most genes (99%) had < 10000 normalized read counts, and approximately 62% (n = 18277) had < 100 normalized read counts (Figure S2A–B). DEGs on autosomal or X chromosomes were not restricted to genes with lower normalized read counts but were distributed across the abundance spectrum, as observed for genes without sex-specific expression (Figure S2A–B). DEGs included *Gata6*, *Panct2*, *Prl2a1*, and *Prl7a1* on the autosomes and *Bcorl1*, *Kdm5c*, *Taf1,* and *Xist* on the X chromosomes (Figure 1D).

Gene ontology term enrichment analysis of autosomal DEGs with higher expression in male placentas revealed roles in regulating lactation (*Prl3d1*, *Prl2c2*), viral defense (*Apobec1*, *Ifi203*), and regulating responses to external stimuli (*C3ar1*, *Oprm1*; Figure 1E, left panel). In contrast, autosomal DEGs with higher expression in female placentas were enriched for roles in SLC-mediated transmembrane transport (*Slc22a1*, *Slc39a8*), tube morphogenesis (*Ackr3*, *Fgf18*), and gland development (*Cebpa*, *Ephb3*; Figure 1E, middle panel). X chromosome DEGs were notably enriched in genes encoding chromatin modifying enzymes (*Kdm5c*, *Xist*) and regulating small GTPase-mediated signal transduction (*Amot*, *Ogt*), actin cytoskeleton organization (*Arhgap6*,

Shroom2), non-coding RNA processing (*Suv39h1*, *Ftsj1*), and cellular macromolecule biosynthesis (*Alas2*, *Eif2s3x*; Figure 1E, right panel).

These results reveal significant transcriptomic differences between male and female late-gestation mouse placentas. Notably, these differences extend beyond genes located on the sex chromosomes, indicating comprehensive impacts on gene expression throughout the autosomal genome.

Late-gestation mouse placentas display sex-specific DNA methylation differences

To further investigate sex-specific molecular differences in late-gestation mouse placentas, we generated genome-wide DNA methylation profiles of the same six E18.5 placenta samples using Methyl-Seq. After applying thresholds (*e.g*., minimum two CpGs, 100-bp tiles, 10× coverage in all samples), we identified 756638 tiles covering 2.4 million CpGs (Figure S3). Although the global DNA methylation patterns on these tiles were generally similar between male and female placentas (Figure S3A), we observed higher mean methylation values in male placentas (38.3%) than in female placentas (37.6%; Figure S3B). This trend was maintained across all autosomes (38.4% vs. 37.7%); however, the X chromosomes exhibited higher mean methylation levels in female placentas (29.9%) than in male placentas (29.0%; Figure S3C). These differences caused notable shifts in the percentages of tiles in different methylation categories (*e.g.,* 0–10% to 90–100%) between both the autosomal and X chromosomes of male and female placentas (Figure S3D–E).

We next analyzed the tiles to identify sex-specific differentially methylated regions (DMRs; 100-bp tiles, > 10% increase or decrease, $q < 0.01$) in the genomes of male and female placentas. On autosomal chromosomes, we found 1705 DMRs (0.2% of the 745699 tiles) between male and female placentas (Figure 2A–C; Table S1). Of these, 73% ($n = 1251$) and 27% (n = 454) exhibited higher methylation levels in male and female placentas, respectively. Considerably more DMRs ($n = 3756$; 34% of 10939 tiles) were observed on the X chromosomes, with 66% ($n = 2491$) and 34% ($n = 1265$) displaying higher methylation levels in female and male placentas, respectively (Figure 2A–C; Table S1). Most autosomal (86%) and X chromosomal (72%) DMRs had 10–20% changes in their methylation levels between male and female placentas (Figure 2D). Only 2% of the autosomal DMRs and 4.5% of the X chromosomal DMRs had a > 30% change in methylation between the sexes.

X chromosome DMRs with higher methylation in female placentas had average methylation levels below 50% in both sexes, while DMRs with higher methylation in male placentas predominantly displayed > 50% methylation (Figure 2C). This distribution was not observed for autosomal DMRs (Figure 2C). Some example DMRs are shown in Figure S4A, including *Cflr2*, which is involved in cell proliferation and hematopoietic system development; *Bcl2l11*, which is implicated in apoptosis, *Morf4l2*, which is predicted to play a role in heterochromatin assembly, and *Xist*, a well-known X chromosome inactivation factor. The top 20 DMRs on autosomes and X chromosomes are listed in Tables 3 and 4, respectively. Most sex-specific DMRs were located in intronic and intergenic regions (76% and 56% on the autosomes and X chromosomes, respectively; Figure S4B). However, 26% of sex-specific DMRs on the X chromosomes were located in promoter regions. We also observed methylation level changes across various genomic features on both the autosomes and X chromosomes (*e.g.*, introns, promoters, transcriptional start sites (TTSs), 3′ and 5′ untranslated regions (UTRs), and intergenic regions; Figure S4C).

To examine the potential biological functions of these sex-specific DNA methylation differences, we performed gene ontology term enrichment analyses on all DMRs located in gene-associated features like promoters, introns, and exons. For autosomal DMRs with higher methylation levels in male placentas (n = 735; in 672 unique genes such as *Apk10, Ntrk2,* and *Pik3r1*), the top pathways were related to metabolic processes and signaling pathways (Figure 2E). Conversely, DMRs with higher levels in female placentas (n= 303; in 254 unique genes such as *Cvr2a*, *Emx2,* and *Pax2*), were linked to brain development, cell differentiation/specification, and morphogenesis (Figure 2E). X chromosome DMRs with higher methylation levels in male placentas (n = 693; in 232 unique genes such as *Mtmr1* and *Xlr4a*) were associated with metabolic processes, protein interactions, and synaptic localization (Figure 2E). X chromosome DMRs with higher methylation in female placentas (n = 2237; in 430 unique genes such as *Arx, Fgf13,* and *Hdac6)* were associated with protein deacetylation and regulating cell growth and macroautophagy. The DNA methylation levels of selected gene-associated DMRs are shown in Figure 2F.

Together, these analyses reveal significant sex-specific differences in DNA methylation profiles across the autosomes and X chromosomes of male and female E18.5 mouse placentas,

despite their similar overall methylation status. These changes occur in critical genes and could impact their regulation during mouse placenta development. This underscores the importance of considering sex-specific variations when studying placental methylation patterns.

Sex-specific DMRs are enriched in CpG islands on the X chromosome but are located away from them on autosomes

To investigate the genomic contexts of sex-specific DMRs in E18.5 placentas, we examined the annotations and CpG densities of autosomal and X chromosome DMRs. X chromosome DMRs had higher CpG enrichment per tile than autosome DMRs (4.8 vs. 3.4 CpGs per tile, $p < 0.0001$; Figure 3A). Of the autosomal DMRs, 3% (49 DMRs) contained > 10 CpGs per tile (maximum: 19 CpGs). X chromosome DMRs also contained up to 19 CpGs per tile; however, 11% (403 DMRs) contained > 10 CpGs. A significantly higher percentage of DMRs were present in high-density CpG islands (35%) and their immediate flanking regions (CpG shores; 33%) on X chromosomes than on autosomes (islands: 6%; shores 18%; $p < 2.2e^{-16}$; Figure 3B). Autosomal DMRs were enriched in regions away from CpG islands (open sea; autosomes: 69%; X chromosome: 29%; $p < 2.2e^{-16}$). The average DNA methylation levels in CpG island DMRs were higher in female placentas than in male placentas for both autosomal and X chromosomal DMRs (Figure 3C). However, in the CpG shelves, the average DMR methylation levels were higher in male placentas, averaging close to 50% methylation on both autosomes and X chromosomes.

Since CpG islands can function as TSSs and play key roles in regulating gene expression, we annotated the CpG island-associated DMRs to genomic features. We observed that 26% (n = 27) of autosomal DMRs and 33% (n = 435) of X chromosomal DMRs were in CpG islands within promoter regions (Figure 3D). The majority of CpG island DMRs (autosomes: 54%, n = 57; X chromosomes: 59%, n = 765) were located within genes (*i.e.*, in intragenic regions). For CpG island DMRs present in promoters, intragenic, and intergenic regions, DNA methylation levels were higher in female placentas compared to male placentas (Figure 3E), with the average methylation level being lower on the X chromosomes.

Overall, sex-specific DMRs were mainly found in CpG-poor regions on autosomes but in CpG-rich regions on the X chromosomes. However, the normally observed inverse correlation between DNA methylation and CpG density was not particularly obvious for DMRs located in

autosomal CpG-rich promoters compared to their counterparts on the X chromosomes, suggesting that the higher methylation levels play a regulatory role during development.

Associations between sex-specific DNA methylation and gene expression patterns in E18.5 mouse placentas

Our findings provide compelling evidence of sex-specific DNA methylation and gene expression levels in E18.5 placentas. To assess the associations between these variations, we compared the datasets. First, we annotated DMRs located in promoters or intragenic regions to unique genes. On autosomes, we identified 58 DMRs associated with 34 unique genes, while on the X chromosomes, 111 DMRs were linked to 18 genes. Next, we overlapped these DMR-associated genes with the identified DEGs (Figure 4A). This analysis identified 52 genes with 169 associated DMRs that displayed sex-specific differences in both DNA methylation and gene expression profiles. Of these, 34 (linked to 58 DMRs) were autosomal, while 18 (linked to 111 DMRs) were located on the X chromosomes.

We also examined the distributions of these DMRs, specifically whether they were present in promoters or other intragenic regions (Figure 4B). On autosomes, we observed direct correlations between sex-specific promoter DMRs and DEGs. For instance, genes like *Inpp5f*, *Shisa7, Gm7120, 4833420G17Rik*, and *Plxnd* displayed higher methylation levels in one sex and higher expression in the other (Figure 4B). However, this correlation was not observed for *Stk10* and *Elf3* (Figure 4B). On the X chromosomes, we observed this association only for *Xist*, which had higher methylation in male placentas and higher expression in female placentas. The remaining nine X chromosome promoter DMRs had higher methylation and gene expression levels in female placentas (Figure 4B). While the negative correlation between promoter DNA methylation and transcriptional expression is well documented (41, 42), the role of intragenic methylation is less clear. However, previous studies have shown positive associations between DNA methylation within intragenic regions and gene expression in various contexts (43-45). In our datasets, we identified 46 DEGs (29 on autosomes, 17 on X chromosomes) also displaying intragenic DMRs (Figure 4D–E). On autosomes, intragenic DMRs with higher DNA methylation levels in male or female placentas had both positive (male: *Tmem266*, *Apobec1*, *Pde10a;* female: *Ephb2*, *Hmgc2*, *Grb10*) and negative (male: *Plekha7*, *Carmll1*, *Zfp64*; female: *Cdk5rap1, 4833420G17Rik, Scd2*) correlations with gene expression. On the X chromosomes, intragenic DMRs with higher levels in

either male or female placentas were associated with DEGs with increased expression in female placentas. Example associations between promoter and intragenic DMRs and gene expression are shown in Figures 4F–4I.

Sex-specific DNA methylation and expression differences in genes essential for placental development

To assess the potential significance of sex-specific DMRs in placental development and function, we conducted an overlap analysis between all DMRs and a curated list of 205 published essential placental genes (Table S2). Of these, 192 genes had sufficient sequencing coverage for downstream analyses, representing 7360 tiles in promoter and intragenic regions after excluding intergenic regions (Figure S5A). There were 47 DMRs (12 autosomal, 35 X chromosomal) associated with 16 unique essential placental development genes (10 autosomal, 6 X chromosomal; Figure S5B–D). Among the autosomal DMRs, 11/12 displayed higher methylation levels in male placentas, while 26/35 X chromosome DRMs were more methylated in female placentas (Figure S5B, E). Functional gene ontology term enrichment analysis of the 16 essential placental genes containing the 47 sex-specific DMRs confirmed their pivotal roles in various processes related to placenta development and function (Figure S5F). Only 10/205 (~ 0.5%) of the essential placenta genes showed significant sex-specific expression differences (Figure S5G). *Serpine1* displayed higher expression in male placentas, while the rest (*Met*, *Pcld1*, *Ovol2*, *Havcr1*, *Etnk2*, *Gcm1*, *Dsg3*, and *Xist*) exhibited enhanced expression in female placentas. The higher expression of *Etnk2* (autosomal gene) and *Xist* (X chromosome gene) in female placentas also correlated with DMRs with higher methylation levels in male placentas.

Overall, our findings indicate that there are no substantial differences in the DNA methylation and gene expression patterns of crucial placental development genes between male and female placentas. This suggests that the underlying main control mechanisms driving placental development in late gestation are similar in both sexes. However, the presence of sex-specific variations in DNA methylation or transcription patterns implies potential differences in the regulation of some placental functions during late pregnancy.

Subsets of sex-specific DMRs emerge during early placental development

To define the timing of the sex-specific DMRs observed in late-gestation placentas, we compared the DNA methylation levels of mid-gestation (E10.5; *via* low-coverage reduced-representation bisulfite sequencing) and E18.5 placentas. The E10.5 placenta dataset contained 73 of the 1705 autosomal sex-specific DMRs identified at E18.5 and 583 of the 3756 E18.5 X chromosomal DMRs (Figure 5A–B). In E18.5 placentas, 19 autosomal DMRs exhibited higher methylation levels in male (n = 6) or female (n = 13) placentas, while at E10.5, methylation at these regions was consistently higher in female placentas (Figure 5B). For most autosomal regions, we observed increased overall DNA methylation levels at E18.5 compared to at E10.5 in all placentas, indicating a sex-independent developmental gain in DNA methylation (Figure 5B–C). One DMR, associated with *Vsx2*, displayed similar DNA methylation levels across all stages of development in both male and female placentas (Figure 5C). For other genes, (*Armc10*, *Grip1*, *Map7d1*), the DNA methylation levels at E10.5 and E18.5 closely matched only in female placentas. When we examined the 563 sex-specific X chromosome DMRs, 348 (62%) were significantly different between male and female E10.5 placentas (Figure 5A, D). These regions all displayed higher DNA methylation levels in female placentas at both E10.5 and E18.5. Smoothed plots depicting multiple DMRs in *Arx*, *Bcor*, *Gpc3*, and *Hs6st2* are shown in Figure 5E.

These findings suggest that as the maturing mouse placenta (E10.5) develops and becomes more complex, sex-specific DMRs arise. The presence of both consistent methylation levels across development and differential methylation patterns in specific genes highlights the intricate and selective nature of sex-specific epigenetic regulation in the placenta.

DISCUSSION

In this study, our objective was to identify sex-specific molecular differences in the gene expression and DNA methylation profiles of male and female late-gestation mouse placentas. Consistent with the intricacies of proper development and X chromosome inactivation, a significant proportion of the molecular changes occurred on the X chromosomes, which had particularly divergent sex-specific DNA methylation profiles and displayed sex-specific differences in gene expression. However, significant sex-specific epigenetic and transcriptomic differences were also observed on the autosomes. These data demonstrate that sex-specific differences are widespread in the mouse

placenta genome, and that simply excluding sex chromosome-derived sequencing data is an inadequate means of mitigating their effects in -omics studies.

On autosomes, female placentas had more DEGs with increased expression, while male placentas had more DMRs with increased methylation levels. These differences were associated with various biological functions, consistent with the mounting evidence of a mechanistic link between placental pathways and sex-specific growth differences and risks of pregnancy complications (6, 46, 47). Male placentas exhibited higher expression of genes associated with immune responses than female placentas, including DEGs involved in the responses to interferon α (*Ifit*, *Ifit2*), viruses (*Apobec1*, *Ifi203*), and other external stimuli (*C3ar1*, *Oprm1*). This suggests that male placentas exist in a state of heightened immune response compared to female placentas. Notably, the male fetal-placental unit is more sensitive to maternal inflammation than the female unit, and this sensitivity is particularly mediated *via* placental immune responses to infection (48). Studies have reported upregulated innate and adaptive immune responses in male placentas, including in cases of maternal SARS-CoV-2 infection (reviewed in (49)). Maternal infection during early pregnancy is a recognized prenatal risk factor for mental illness in the offspring, particularly in males (50, 51). A recent study examining the consequences of a high-fat diet during pregnancy, which creates a chronic inflammatory environment, highlighted the significant influence of sex in shaping distinct vulnerabilities and outcomes affecting the placenta, fetal brain, adult brain, and behavior (52). It remains uncertain whether the heightened immune sensitivity of the male fetal-placental unit confers potential advantages, such as protection against viral infections, or disadvantages, such as increased placental inflammation, higher risk of fetal growth restriction, or impaired placental function.

Genes with higher DNA methylation levels in male placentas were linked to metabolic processes and signaling pathways, while genes that were more highly methylated in female placentas were associated with brain development, cell differentiation/specification, and neuron morphogenesis. Sexual dimorphism contributes to slight variations in placental metabolism, which are believed to be adaptive responses triggered by the fetus to promote optimal growth and ensure healthy development. In a recent study using a mouse model (C57BL/6J mice, standard diet) similar to the one used here, Saoi *et al*. observed distinct metabolic differences between male and female E18.5 placentas. Specifically, the levels of intracellular metabolites related to fatty acid

oxidation and purine degradation were higher in female placentas than in male placentas. This is consistent with our expression data showing that fatty acid transporter proteins like SLC27A1—which are critical for nutrient transport in the placenta—are more highly expressed in female placentas. Interestingly, we observed sex-specific DMRs in neurodevelopmental genes, highlighting the connection between the placenta and the brain (the "placenta-brain axis") (52, 53). Various studies have reported associations between brain development and sex-specific DNA methylation differences in autosomal genes, with specific DNA methylation profiles related to both normal and complicated pregnancies. For instance, in a mouse model of neurodevelopmental disorder induced by exposure to polychlorinated biphenyls, Laufer *et al*. observed shared sex-specific DNA methylation alterations related to neurodevelopment and autism spectrum disorder that were shared by the fetal brain and placenta (54). In their study and in others, prenatal insults consistently impact male offspring more significantly than female offspring (6, 54, 55). Importantly, these studies provide evidence that placental DNA methylation profiles can predict brain DNA methylation profiles—and possibly the risk of neurodevelopmental disorders.

The sex-specific differences in DNA methylation levels we observed within the placenta were consistent with those observed in humans, in that male placentas typically exhibited higher methylation levels at DMRs than female placentas (24, 56). Interestingly, it is the opposite of what occurs in most somatic tissues, where sex-associated DMRs tend to be more highly methylated in females (57-61). Furthermore, we observed that some sex-specific differences in DNA methylation levels occurred as early as E10.5, suggesting that they emerge during early placental development. Notably, we also identified regions where methylation remains consistent within one sex across both time points, particularly in autosomal regions. This indicates that in certain regions, DNA methylation is stable in one sex throughout embryonic development but highly dynamic in the other. Our findings also align with sex-based differences observed in human placental DNA methylation profiles associated with gestational age (62). Further research will be required to fully comprehend the potential implications of these sex-specific differences on fetal development in both healthy and complicated pregnancies.

Despite the thousands of sex-specific DMRs observed on the X chromosomes, only a few dozen genes exhibited differential expression between male and female placentas. However, the increased expression of several X-linked chromatin-modifying enzymes and transcription factors

(*e.g.*, *Bcorl1*, *Jade3*, *Kdm5c*, *Kdm6a*, *Ogt*, *Suv39h1*, *Wnk3*, *Xist*, and *Zdhhc9*) in female placentas could profoundly influence their epigenetic landscape and contribute to the unique responses of male and female placentas to the maternal environment. While *Xist* is normally not expressed in male cells, other genes, such as *Ogt* (an O-linked N-acetylglucosamine (O-GlcNAc) transferase) and *Kdm5c* (a histone H3K4-specific demethylase) have been observed at higher baseline levels in female placentas due to their ability to escape X inactivation (63). In addition, OGT is selectively downregulated in male placentas from mothers with gestational diabetes (64), and mouse studies indicate that prenatal stress impacts OGT and O-GlcNAcylation levels more in males than in females (65). The finding that suboptimal environments can influence the expression of X-linked genes involved in key epigenetic regulatory processes reinforces the need to systematically acquire and analyze sex-specific measurements in transcriptomic and epigenetic placental studies, especially those investigating responses to adverse maternal environmental stimuli.

PERSPECTIVES AND SIGNIFICANCE

Although the specific functions of the placenta are associated with elevated risks of pregnancy complications and neurodevelopmental disorders, particularly in male offspring, the sex-specific epigenetic (such as DNA methylation) and transcriptomic characteristics of the late-gestation mouse placenta are mostly unexplored. Our study uncovers significant sex-specific differences in the DNA methylation and gene expression profiles of late-gestation mouse placentas, providing comprehensive lists of the affected regions and genes. Importantly, we observed changes not only on the X chromosome but also the autosomes, demonstrating the importance of accounting for sex differences and not assuming equivalency between males and females on non-sex chromosomes. These findings emphasize the importance of examining the impacts of sex-specificity in epigenetic and transcriptomic research, regardless of the species or developmental staged studied. Recognizing sex as a crucial biological variable will enhance our understanding of the intricate interplay between fetal sex, placental biology, and adverse maternal environmental stimuli, ultimately advancing our knowledge of reproductive health and improving pregnancy outcomes.

Declarations

The authors have no conflicts of interest to declare.

Ethics approval and consent to participate

All animal studies were approved by the CHU Ste-Justine Research Center *Comité Institutionnel de Bonnes Pratiques Animales en Recherche* under the guidance of the Canadian Council on Animal Care.

Consent for publication

Not applicable

Availability of data and materials

All datasets used will be publicly available via the Gene Expression Omnibus.

Competing interests

The authors declare no competing interests.

Funding

This work was supported by a research grant to SM from the Natural Sciences and Engineering Research Council of Canada. LML is supported by Canadian Institutes of Health Research scholarship. MBL is supported by a scholarship/fellowship from Fonds de Recherche du Québec - Santé (FRQS). ALA is supported by scholarships from Université de Montréal and Réseau Québécois en Reproduction. SM is supported by an FRQS-Junior 2 salary award.

Authors' contributions

LML and SM conceptualized the study. LML and MBL contributed to data acquisition. LML, ALA, AL, participated in data analysis. LML and SM wrote the manuscript. All authors read and approved the final manuscript.

Acknowledgements

We thank the McGraw lab for critical comments and suggestions, the staff of the Centre de Recherche du CHU Sainte-Justine animal facility for their assistance, and High-Fidelity Science Communications for editing the manuscript.

Table 1. Top DEGs on autosomal chromosomes ($p < 0.05$)

Gene symbol	Chromosome	Change in expression (log2 fold change)
Increased in male placentas		
Pcdhb8	18	-4.28
Oprm1	10	-4.21
Klk1b8	7	-4.13
Cyp4a29	4	-4.11
Acnat1	4	-2.71
Ctnna3	10	-2.66
Efcab1	16	-1.90
Aknaos	4	-1.80
Clrn3	7	-1.66
Ccdc172	19	-1.59
Dazl	17	-1.50
Cidec	6	-1.48
Ctse	1	-1.42
Sohlh2	3	-1.40
Ccl2	11	-1.24
Sycp1	3	-1.20
Cd48	1	-1.17
Cftr	6	-1.15
Rnf180	13	-1.03
Mnda	1	-0.96
Increased in female placentas		
Serpina1f	12	4.87
En1	1	4.19
Fezf1	6	3.64

Krt77	15	2.85
Dsc3	18	2.28
Hba-x	11	1.86
Them5	3	1.78
Slc22a1	17	1.77
Dsg3	18	1.67
Acsm3	7	1.27
Panct2	1	1.20
Slc51a	16	1.18
Mst1	9	1.12
Fgf18	11	1.12
Bnc1	7	1.11
Trpv3	11	1.07
Aspa	11	1.07
Sall3	18	0.98
Pramel6	2	0.97
Pramel6	2	0.97

Table 2. Top differentially expressed genes on the X chromosomes ($p < 0.05$)

Gene symbol	Change in expression (log2 fold change)
Increased in male placentas	
Gm16411	-1.72
AA414768	-0.47
Increased in female placentas	
Xist	5.73
Ripply1	1.04
Xkrx	0.97
Tmem255a	0.88
Trpc5os	0.74
Ogt	0.71
Bcorl1	0.68

Taf1	0.59
Igsf1	0.58
Kdm5c	0.58
S100g	0.55
Eif2s3x	0.54
Pin4	0.48
Iqsec2	0.41
Utp14a	0.41
Drp2	0.41
Wnk3	0.39
Kdm6a	0.35
Suv39h1	0.34
Alas2	0.34

Table 3. Top autosomal DMRs

Gene symbol	Chromosome	Annotation	Change in methylation
Increased in male placentas			
Ube2k	5	Promoter-TSS	-36.70
Tiam2	17	Intron	-35.97
Map1b	13	Intron	-35.44
Ccdc116	16	3′ UTR	-35.31
Pygb	2	Intron	-35.00
Ccdc60	5	Intron	-34.52
Snord116l2	7	Intron	-33.61
Lrpprc	17	Intron	-33.26
Jdp2	12	TTS	-32.69
Col6a3	1	Intron	-32.53
Slc36a3	11	Exon	-31.99
Ddr1	17	Intron	-30.82
Mrpl45	11	3′ UTR	-29.56
Alg6	4	Intron	-29.31

Mir218-2	11	Intron	-28.90
Trhr2	8	Intron	-28.86
Tssc4	7	Exon	-28.82
Krtdap	7	TTS	-27.75
Gip	11	Exon	-27.73
Nuak1	10	Intron	-27.59
Increased in female placentas			
Proz	8	TTS	38.15
Tmem267	13	Promoter-TSS	36.91
Cdk5rap1	2	Intron	34.71
Stam2	2	Intron	34.66
Cdk5rap1	2	Exon	33.96
Clip4	17	Intron	33.56
Cacng3	7	Promoter-TSS	32.84
Tmem267	13	Promoter-TSS	32.32
Pbx1	1	Intron	32.25
Adamts2	11	Intron	30.96
Cdk5rap1	2	Intron	30.28
Dennd1c	17	Promoter-TSS	29.27
Tmem267	13	Promoter-TSS	29.02
Tmem267	13	Promoter-TSS	27.87
Mbp	18	Intron	27.65
Ppox	1	TTS	27.44
Phf19	2	Intron	25.47
Bcl2l11	2	Intron	25.26
Nckap5	1	Intron	25.05
Cdk5rap1	2	Intron	25.01

Table 4. Top X-chromosome DMRs

Gene symbol	Annotation	Change in methylation
Increased in male placentas		
Firre	Intron	-47.74
Firre	Intron	-46.93
Firre	Intron	-46.80
Xist	Non-coding	-45.23
Firre	Intron	-43.31
Firre	Intron	-42.18
Xist	Non-coding	-40.44
Firre	Intron	-40.22
Firre	Intron	-39.42
Xist	Non-coding	-39.07
Xist	Non-coding	-38.95
Ikbkg	Intron	-38.63
Firre	Intron	-38.53
Mir3620	Intron	-38.31
Xist	Promoter-TSS	-37.99
Firre	Intron	-37.88
Firre	Intron	-37.55
Firre	Intron	-36.76
Firre	Intron	-36.44
Firre	Intron	-36.39
Increased in female placentas		
Morf4l2	Intron	39.94
Pja1	Intron	39.38

Msl3	Intron	36.36
Efnb1	5′ UTR	36.02
Taf7l	Intron	35.63
Amer1	Intron	35.58
Ddx3x	Intron	35.23
Pja1	Intron	34.69
Atp6ap1	Intron	33.83
Las1l	Intron	32.74
Pgk1	Promoter-TSS	32.59
Sox3	3′ UTR	32.54
Mir1970	5′ UTR	31.52
Cnksr2	Intron	31.30
Sox3	Exon	31.29
Rab33a	Promoter-TSS	30.96
Msl3	Intron	30.44
Efnb1	Exon	30.43
Rai2	Intron	30.36
Gk	Promoter-TSS	30.31

FIGURES AND LEGENDS

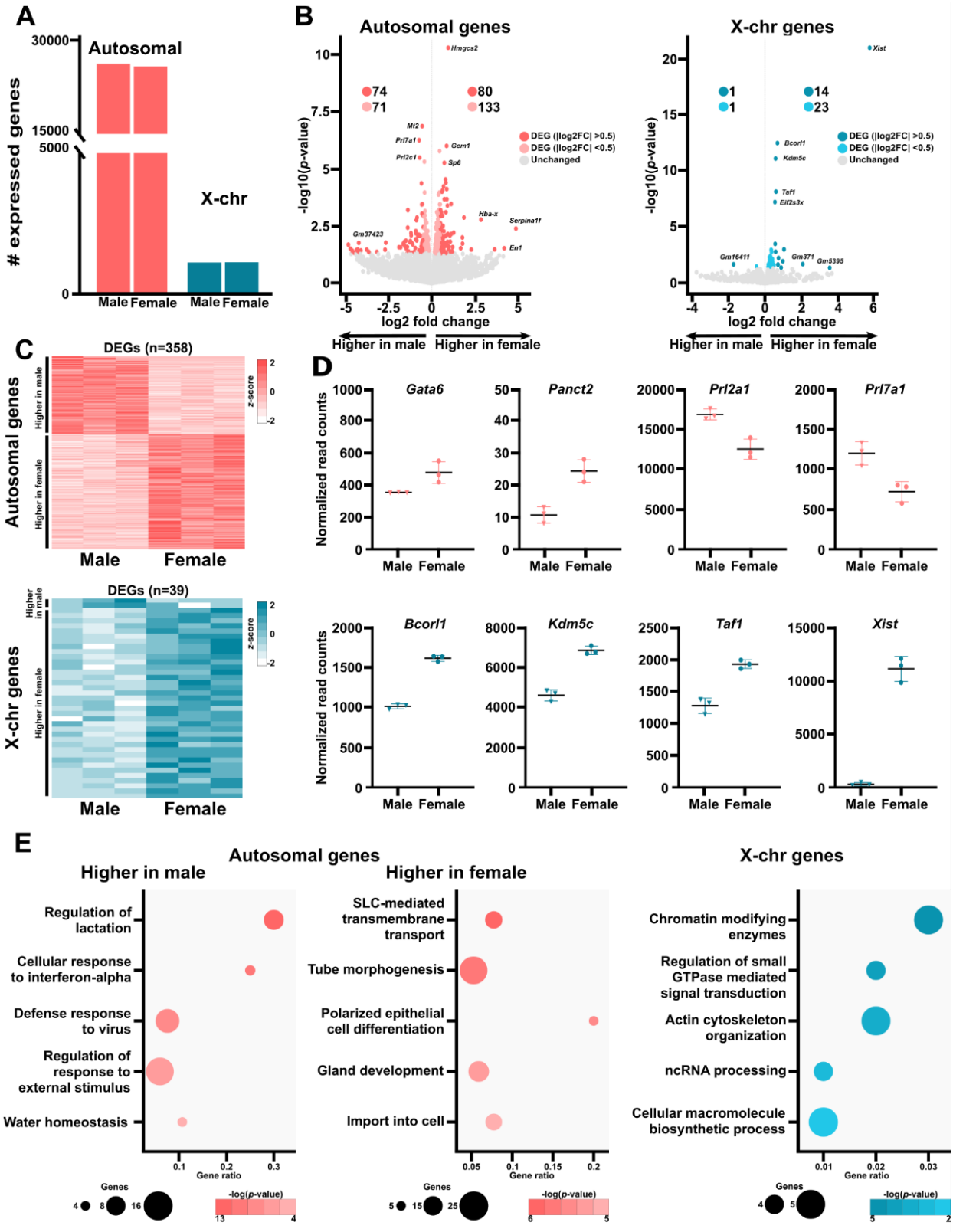
A
Autosomal
X-chr
expressed genes
30000
15000
5000
0
Male Female Male Female
B
Autosomal genes
X-chr genes
-log10(p-value)
log2 fold change
74
71
80
133
1
1
14
23
DEG (|log2FC| >0.5)
DEG (|log2FC| <0.5)
Unchanged
Hmgcs2
Mt2
Prl7a1
Prl2c1
Gcm1
Sp6
Hba-x
Serpina1f
En1
Gm37423
Xist
Bcorl1
Kdm5c
Taf1
Eif2s3x
Gm16411
Gm371
Gm5395
Higher in male
Higher in female
C
DEGs (n=358)
Autosomal genes
Higher in male
Higher in female
z-score
Male
Female
DEGs (n=39)
X-chr genes
D
Normalized read counts
Gata6
Panct2
Prl2a1
Prl7a1
Bcorl1
Kdm5c
Taf1
Xist
E
Autosomal genes
X-chr genes
Higher in male
Higher in female
Regulation of lactation
Cellular response to interferon-alpha
Defense response to virus
Regulation of response to external stimulus
Water homeostasis
SLC-mediated transmembrane transport
Tube morphogenesis
Polarized epithelial cell differentiation
Gland development
Import into cell
Chromatin modifying enzymes
Regulation of small GTPase mediated signal transduction
Actin cytoskeleton organization
ncRNA processing
Cellular macromolecule biosynthetic process
Gene ratio
Genes
-log(p-value)

Figure 1. Sex-specific DEGs occur throughout the genomes of late-gestation mouse placentas **A)** Genes expressed in male and female E18.5 placentas from the autosomes (male n = 26182, female n = 25758) and X chromosomes (male n = 1126, female n = 1139). Genes included had read counts > 0 in all samples of the relevant sex. **B)** Differential expression analysis of autosomal (n = 28194; left) and X chromosomal (n = 1286; right) genes in male and female placentas. Statistically significant DEGs are represented by colored dots ($p < 0.05$; n = 358 autosomal, n = 39 X chromosomal). Darker dots indicate genes with $|\log_2$ fold change$|$ values > 0.5 (n = 154 autosomal, n = 15 X chromosomal). **C)** Expression levels (z-scores) of 358 autosomal (top) and 39 X chromosomal (bottom) DEGs. **D)** Normalized read counts of genes with sex-specific expression. **E)** The top five pathways associated with the autosomal (left and middle) and X chromosome (right) DEGs.

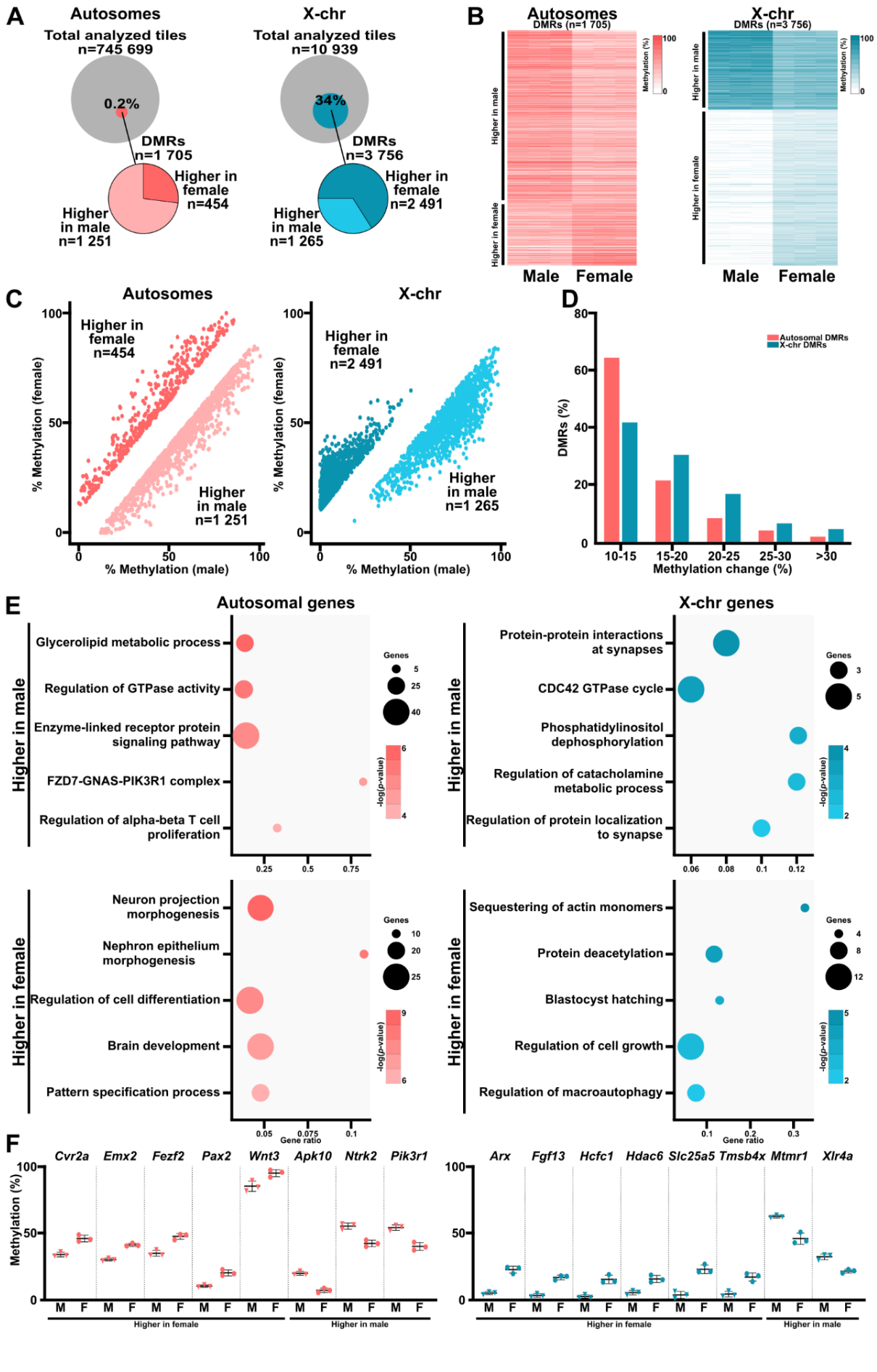
A
Autosomes
Total analyzed tiles
n=745 699
0.2%
DMRs
n=1 705
Higher in
female
n=454
Higher
in male
n=1 251
X-chr
Total analyzed tiles
n=10 939
34%
DMRs
n=3 756
Higher in
female
n=2 491
Higher
in male
n=1 265
B
Autosomes
DMRs (n=1 705)
Higher in male
Higher in female
Methylation (%)
100
0
Male Female
X-chr
DMRs (n=3 756)
Higher in male
Higher in female
Methylation (%)
100
0
Male Female
C
Autosomes
Higher in
female
n=454
Higher
in male
n=1 251
% Methylation (female)
% Methylation (male)
X-chr
Higher in
female
n=2 491
Higher
in male
n=1 265
% Methylation (female)
% Methylation (male)
D
Autosomal DMRs
X-chr DMRs
DMRs (%)
10-15
15-20
20-25
25-30
>30
Methylation change (%)
E
Autosomal genes
Higher in male
Glycerolipid metabolic process
Regulation of GTPase activity
Enzyme-linked receptor protein
signaling pathway
FZD7-GNAS-PIK3R1 complex
Regulation of alpha-beta T cell
proliferation
Genes
-log(p-value)
Higher in female
Neuron projection
morphogenesis
Nephron epithelium
morphogenesis
Regulation of cell differentiation
Brain development
Pattern specification process
Gene ratio
X-chr genes
Higher in male
Protein-protein interactions
at synapses
CDC42 GTPase cycle
Phosphatidylinositol
dephosphorylation
Regulation of catacholamine
metabolic process
Regulation of protein localization
to synapse
Higher in female
Sequestering of actin monomers
Protein deacetylation
Blastocyst hatching
Regulation of cell growth
Regulation of macroautophagy
F
Cvr2a Emx2 Fezf2 Pax2 Wnt3 Apk10 Ntrk2 Pik3r1
Methylation (%)
M F
Higher in female
Higher in male
Arx Fgf13 Hcfc1 Hdac6 Slc25a5 Tmsb4x Mtmr1 Xlr4a
Higher in female
Higher in male

Figure 2. Sex-specific DMRs are present throughout the genomes of late-gestation mouse placentas A) Schematic of the analyzed tiles in autosomes (left) and X chromosomes (right). DMRs exhibiting higher methylation levels in male or female placentas are indicated. **B)** DNA methylation levels of autosomal (left) and X chromosome (right) DMRs in male and female E18.5 placentas. Samples are clustered by methylation level. **C)** DMRs located on autosomes (left) and X chromosomes (right). Dark colors represent regions with ≥ 10% increased methylation in female placentas (higher in female), while light colors represent regions with ≥ 10% decreased methylation in female placentas (higher in male). **D)** The proportions of autosomal and X chromosomal DMRs that caused DNA methylation level changes of various magnitudes. **E)** The top five pathways enriched in autosomal (left) and X chromosomal (right) genes with DMRs that result in higher methylation levels in male (top) and female (bottom) placentas. **F)** DNA methylation levels of autosomal (left) and X chromosomal (right) DMRs associated with the top five enriched pathways in male and female placentas.

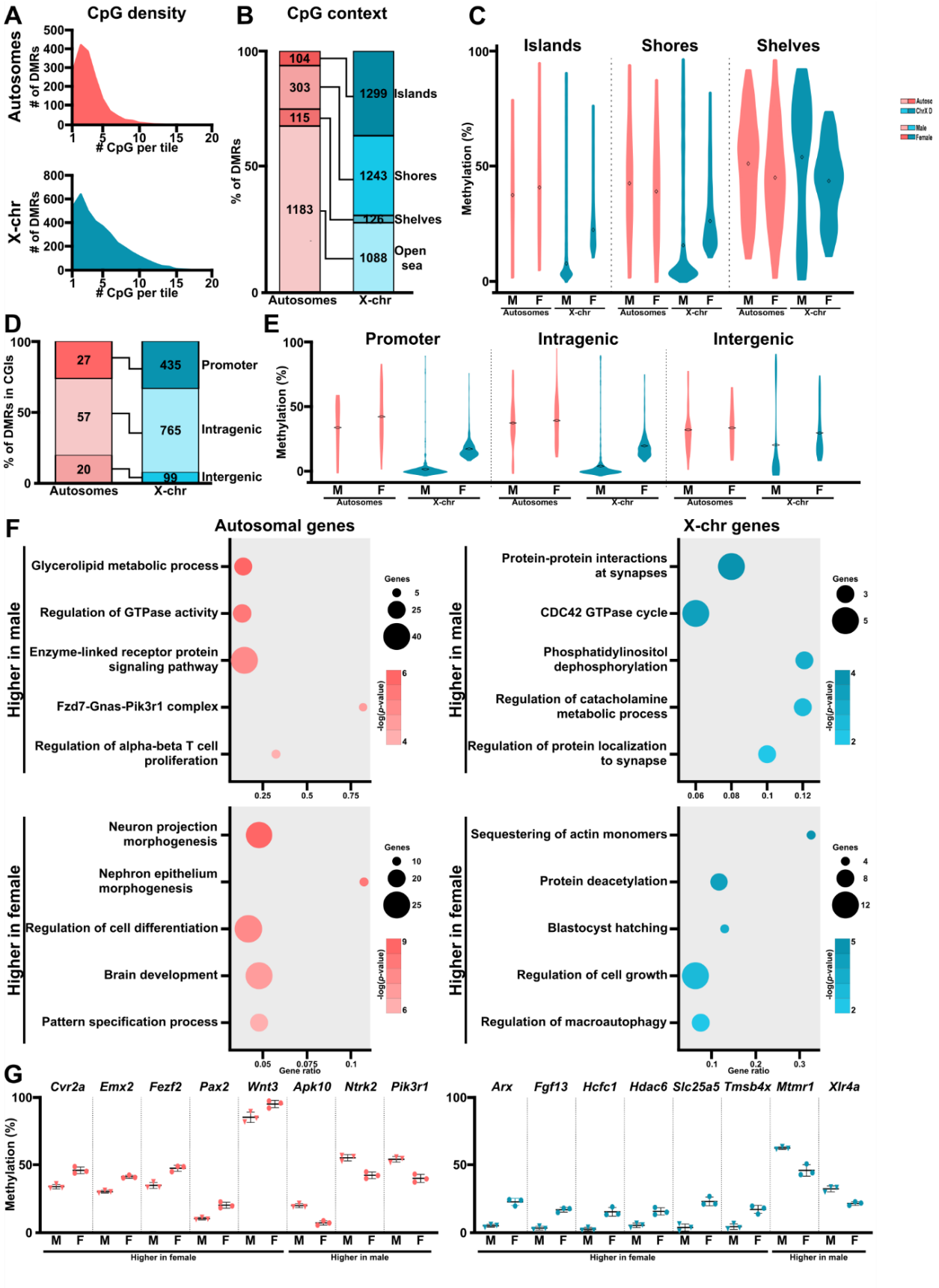
A
CpG density
Autosomes
# of DMRs
CpG per tile
X-chr
B
CpG context
% of DMRs
104
303
115
1183
1299
Islands
1243
Shores
126
Shelves
1088
Open sea
Autosomes
X-chr
C
Islands
Shores
Shelves
Methylation (%)
M F M F
Autosomes
X-chr
D
% of DMRs in CGIs
27
57
20
435
Promoter
765
Intragenic
99
Intergenic
E
Promoter
Intragenic
Intergenic
Methylation (%)
F
Autosomal genes
X-chr genes
Higher in male
Glycerolipid metabolic process
Regulation of GTPase activity
Enzyme-linked receptor protein signaling pathway
Fzd7-Gnas-Pik3r1 complex
Regulation of alpha-beta T cell proliferation
Protein-protein interactions at synapses
CDC42 GTPase cycle
Phosphatidylinositol dephosphorylation
Regulation of catacholamine metabolic process
Regulation of protein localization to synapse
Higher in female
Neuron projection morphogenesis
Nephron epithelium morphogenesis
Regulation of cell differentiation
Brain development
Pattern specification process
Sequestering of actin monomers
Protein deacetylation
Blastocyst hatching
Regulation of cell growth
Regulation of macroautophagy
Genes
-log(p-value)
Gene ratio
G
Cvr2a
Emx2
Fezf2
Pax2
Wnt3
Apk10
Ntrk2
Pik3r1
Arx
Fgf13
Hcfc1
Hdac6
Slc25a5
Tmsb4x
Mtmr1
Xlr4a
Methylation (%)
Higher in female
Higher in male

Figure 3. DMRs have divergent distributions on the autosomes and X chromosomes A) The frequency distributions of autosomal (top) and X chromosome (bottom) DMRs at various CpG densities (*i.e.*, numbers of CpGs per analyzed tile) in male and female E18.5 placentas. **B)** DMR distributions in male and female placentas based on their proximity to CpG islands (CGIs). Proximal regions are defined as shores (up to ±2 kb from a CGI), shelves (± 2–4 kb from a CGI), and open seas (± 4 kb or more from a CGI). **C)** DNA methylation levels on autosomal and X chromosome DMRs in male and female placentas by CGI proximity. **D)** Distributions of CGI-based DMRs into various genomic regions in male and female placentas. **E)** DNA methylation levels of CGI-based autosomal and X chromosome DMRs located in promoter, intragenic, and intergenic regions in male and female placentas.

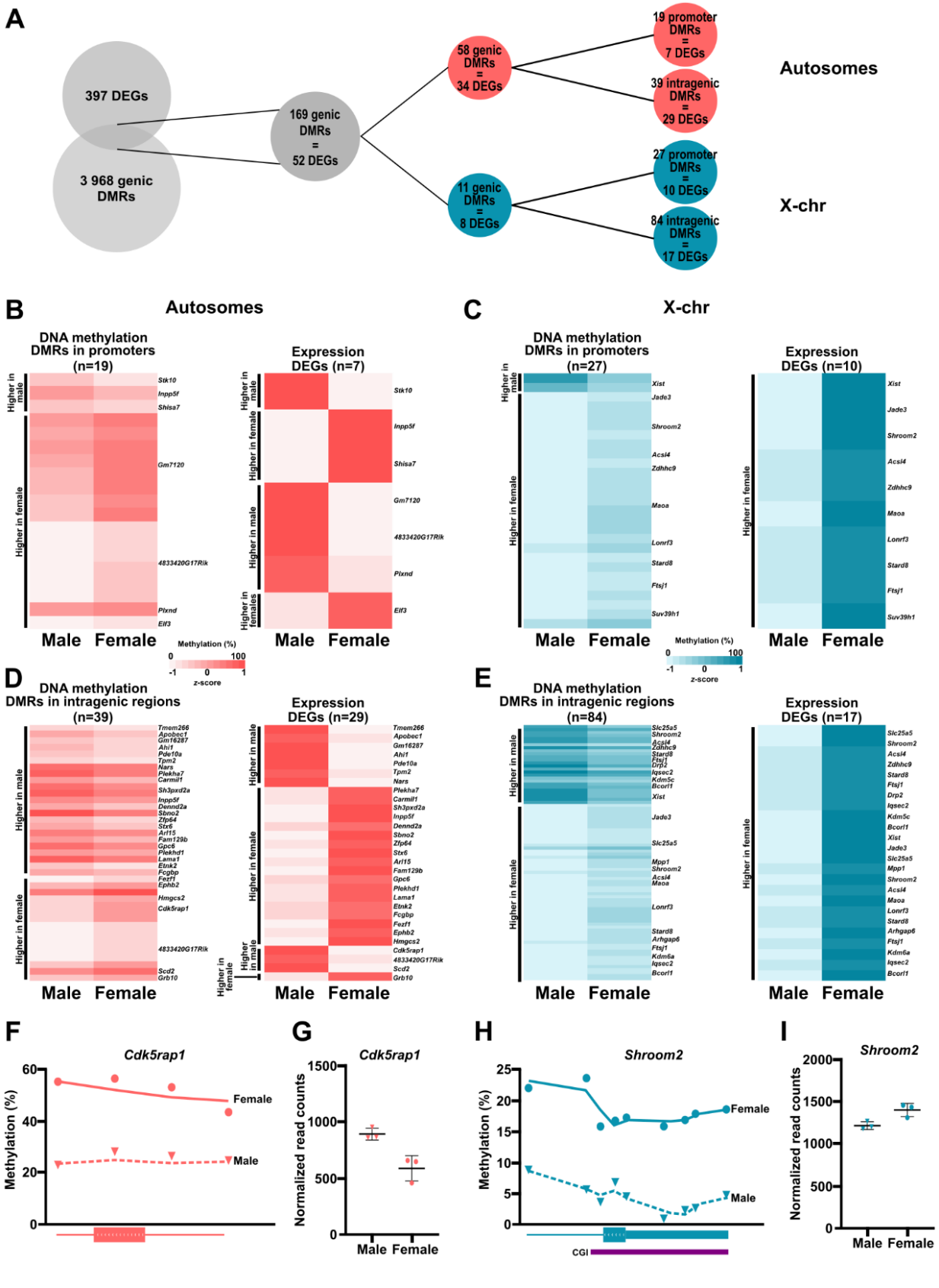
A
397 DEGs
3 968 genic DMRs
169 genic DMRs = 52 DEGs
58 genic DMRs = 34 DEGs
11 genic DMRs = 8 DEGs
19 promoter DMRs = 7 DEGs
39 intragenic DMRs = 29 DEGs
27 promoter DMRs = 10 DEGs
84 intragenic DMRs = 17 DEGs
Autosomes
X-chr
B
Autosomes
DNA methylation DMRs in promoters (n=19)
Expression DEGs (n=7)
Higher in male
Higher in female
Higher in females
Stk10
Inpp5f
Shisa7
Gm7120
4833420G17Rik
Plxnd
Elf3
Male Female
Methylation (%)
0 100
-1 0 1
z-score
C
X-chr
DNA methylation DMRs in promoters (n=27)
Expression DEGs (n=10)
Xist
Jade3
Shroom2
Acsl4
Zdhhc9
Maoa
Lonrf3
Stard8
Ftsj1
Suv39h1
D
DNA methylation DMRs in intragenic regions (n=39)
Expression DEGs (n=29)
Tmem266
Apobec1
Gm16287
Ahi1
Pde10a
Tpm2
Nars
Plekha7
Carmil1
Sh3pxd2a
Inpp5f
Dennd2a
Sbno2
Zfp64
Stx6
Arl15
Fam129b
Gpc6
Plekhd1
Lama1
Etnk2
Fcgbp
Fezf1
Ephb2
Hmgcs2
Cdk5rap1
4833420G17Rik
Scd2
Grb10
E
DNA methylation DMRs in intragenic regions (n=84)
Expression DEGs (n=17)
Slc25a5
Mpp1
Iqsec2
Kdm5c
Bcorl1
Arhgap6
Kdm6a
F
Cdk5rap1
Methylation (%)
Female
Male
G
Cdk5rap1
Normalized read counts
H
Shroom2
CGI
I
Shroom2

Figure 4. Correlations between sex-specific gene expression and DNA methylation changes in the E18.5 mouse placenta A) Overlap between DEGs and DMRs on the autosomes and X chromosomes and their locations in promoters and intragenic regions. **B)** and **C)** DNA methylation (left) and gene expression (*z*-scores; right) levels of promoter and gene regions with significant sex-specific DNA methylation and expression differences on the autosomes (**B**) and X chromosomes (**C**) of E18.5 placentas. **D)** and **E)** DNA methylation (left) and gene expression (*z*-scores; right) levels of intragenic regions (excluding promoters) with significant sex-specific DNA methylation and expression differences on the autosomes (**D**) and X chromosomes (**E**) of E18.5 placentas. **F)** *Cdk5rap1* DNA methylation levels in male and female placentas. Dots represent the mean methylation levels of individual DMRs in each sex. **G)** Normalized read counts for *Cdk5rap1* in male and female placentas. **H)** *Shroom2* DNA methylation levels in male and female placentas. Dots represent the mean methylation levels of individual DMRs in each sex. **I)** Normalized read counts for *Shroom2* in male and female placentas.

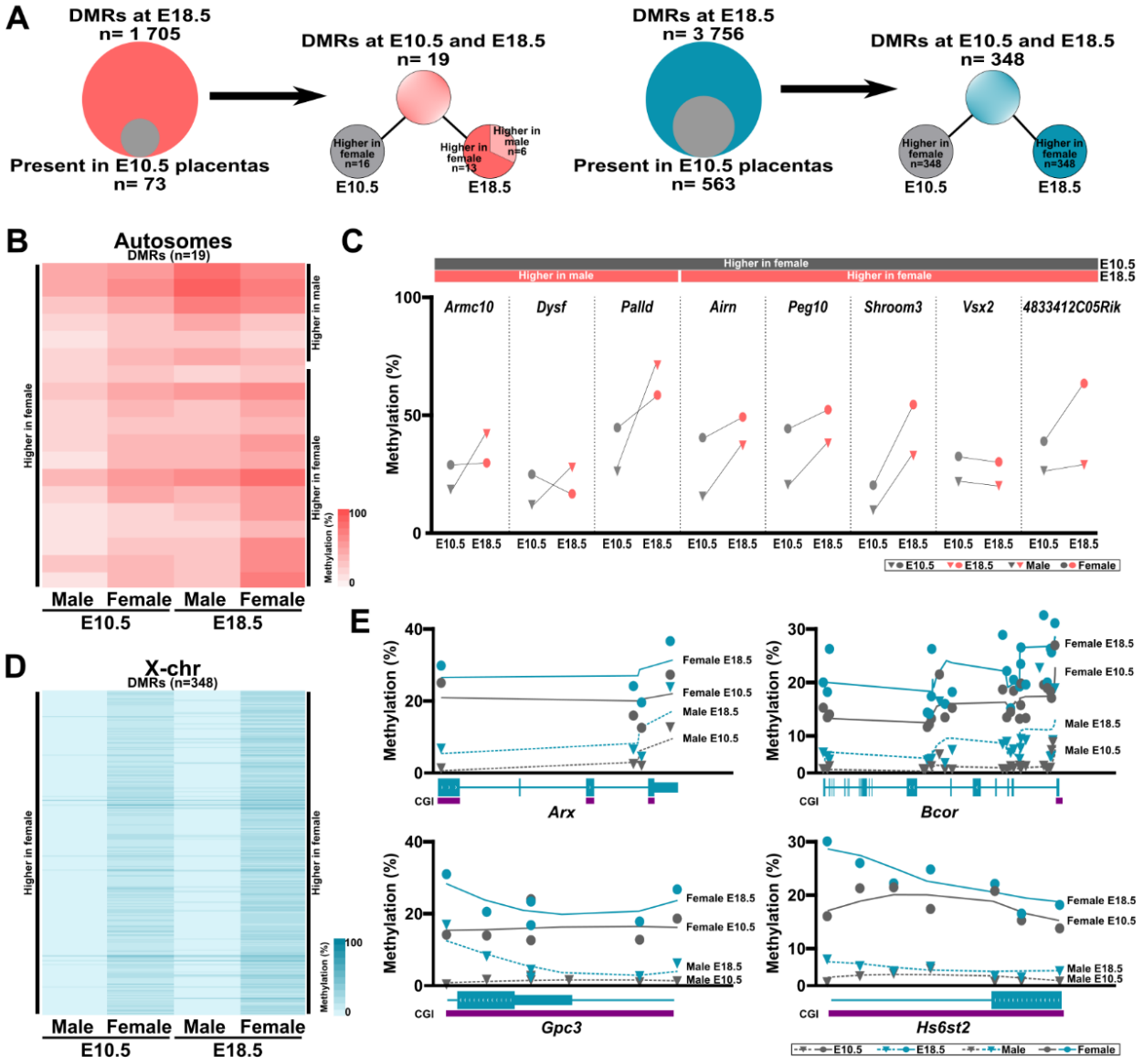

Figure 5. Selected DMRs between male and female E18.5 placentas are already established by mid-gestation A) Schematic of the overlap between autosomal (left) and X chromosomal (right) DMRs at E10.5 and E18.5. **B)** DNA methylation levels of DMRs present on autosomal chromosomes at both E10.5 and E18.5 in male and female placentas. **C)** Mean DNA methylation levels of selected autosomal DMRs in male and female placentas at E10.5 and E18.5. **D)** DNA methylation levels of DMRs present on the X chromosome at both E10.5 and E18.5 in male and female placentas. **E)** DNA methylation profiles of X chromosome DMRs in the indicated genes.

Supplemental figures and legends

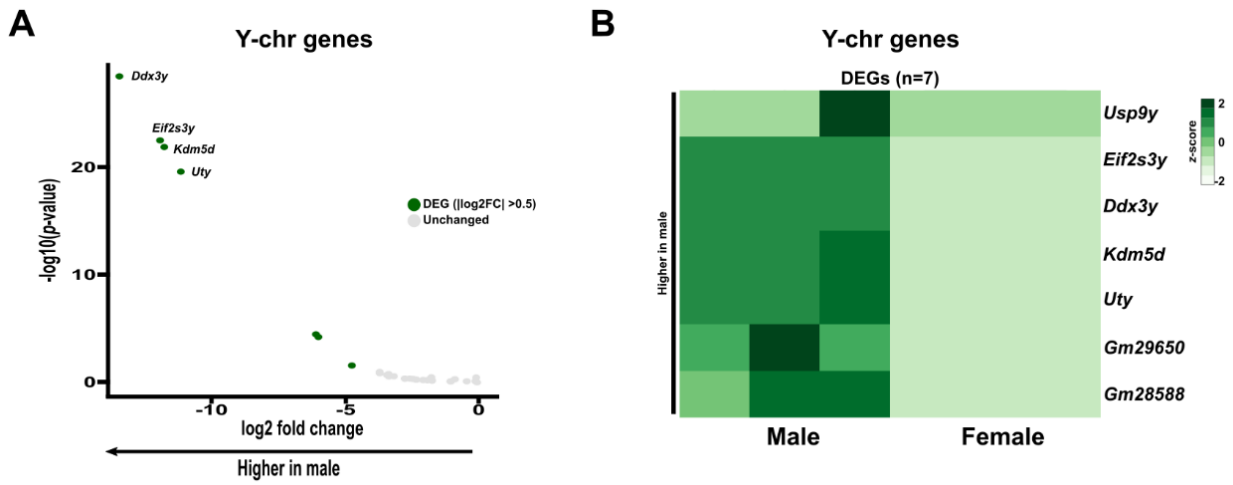

Supplemental Figure 1. Expression of Y chromosome genes in male placentas A) Differential expression analysis of Y chromosome genes in male and female E18.5 placentas ($n = 121$). Colored dots represent statistically significant DEGs ($p < 0.05$; $n = 7$) **B)** Expression levels (z-scores) of the Y chromosome DEGs.

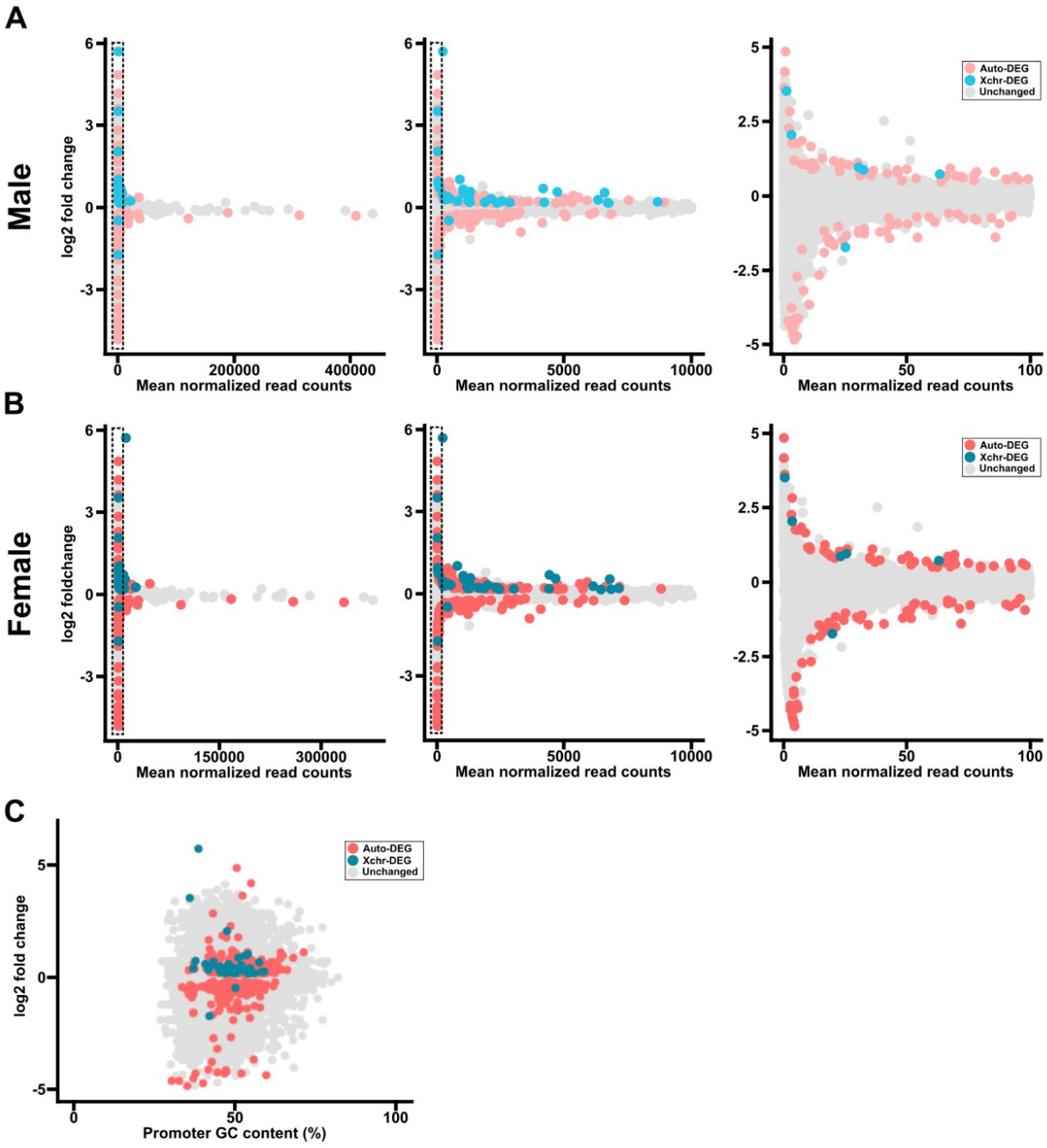

Supplemental Figure 2. DEG abundance in male and female placentas A–B) MA plot of the differential expression (log2 fold change) values of normalized read counts and their average expression levels in **A**) male and **B)** female E18.5 placentas. The plots include all analysed genes (left; *n* = 29480); genes with read counts > 10,000 (middle; *n* = 29165 and 29,160 in male and female placentas, respectively), and genes with read counts > 100 (right; *n* = 18160 and 18173 in male and female placentas, respectively). Colored dots represent significant DEGs on autosomes

(pink) and X chromosomes (blue). The dotted black rectangle indicates the subset of the graph shown on the right. **C)** Differential expression values of each analyzed gene) in male and female placentas relative to their promoter's GC content (%). Significant DEGs on autosomes and X chromosomes are shown in pink and blue, respectively.

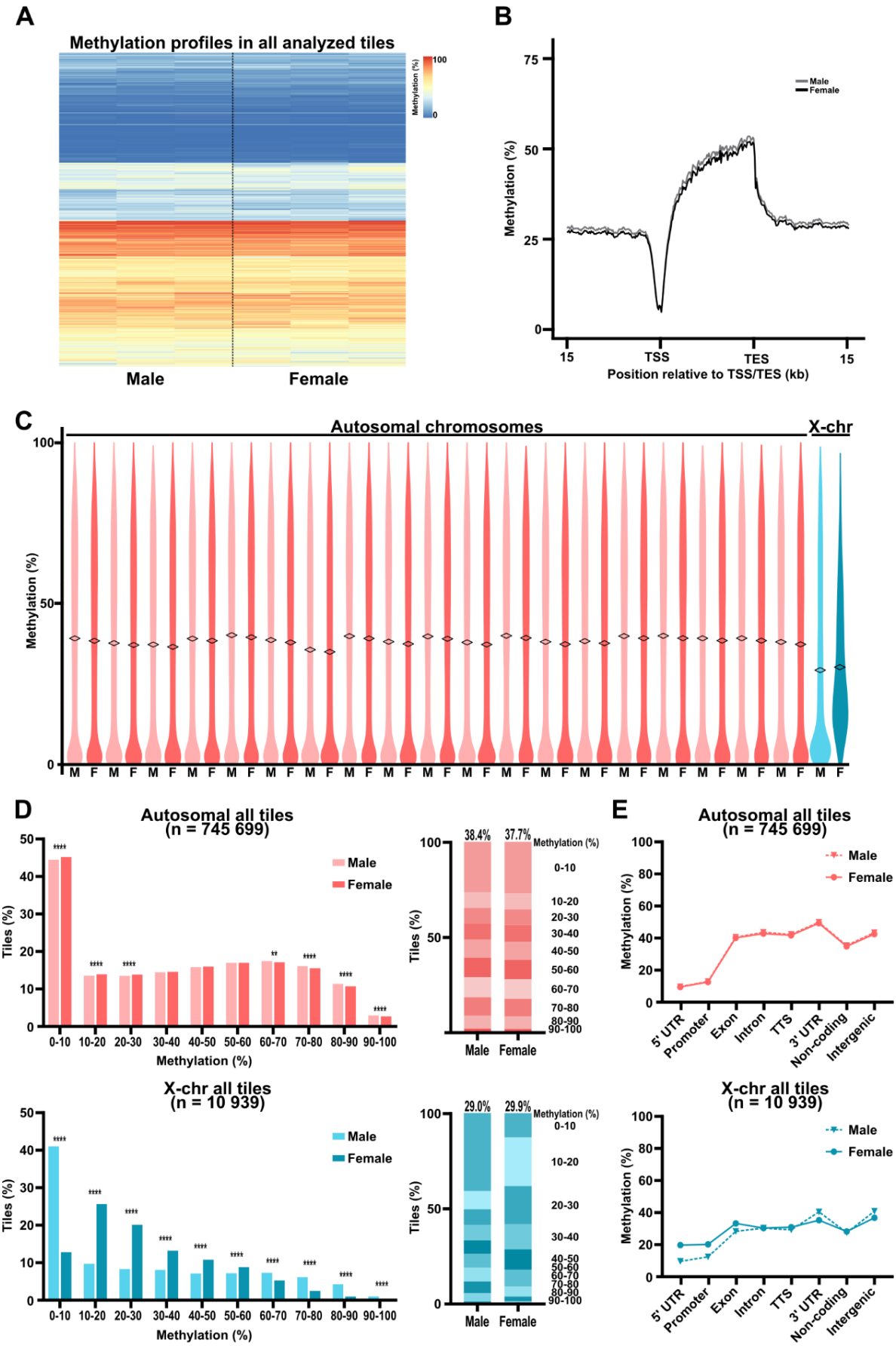
A
Methylation profiles in all analyzed tiles
Methylation (%)
100
0
Male
Female
B
Methylation (%)
75
50
25
0
Male
Female
15
TSS
TES
15
Position relative to TSS/TES (kb)
C
Autosomal chromosomes
X-chr
Methylation (%)
100
50
0
M F M F M F M F M F M F M F M F M F M F M F M F M F M F M F M F M F M F M F M F M F M F M F M F M F M F M F M F M F M F
D
Autosomal all tiles
(n = 745 699)
Male
Female
Tiles (%)
50
40
30
20
10
0
****
****
****
**
****
****
****
0-10
10-20
20-30
30-40
40-50
50-60
60-70
70-80
80-90
90-100
Methylation (%)
38.4%
37.7%
Methylation (%)
100
50
Tiles (%)
0-10
10-20
20-30
30-40
40-50
50-60
60-70
70-80
80-90
90-100
Male
Female
X-chr all tiles
(n = 10 939)
Male
Female
Tiles (%)
50
40
30
20
10
0
****
****
****
****
****
****
****
****
****
0-10
10-20
20-30
30-40
40-50
50-60
60-70
70-80
80-90
90-100
Methylation (%)
29.0%
29.9%
Methylation (%)
100
50
0
Tiles (%)
0-10
10-20
20-30
30-40
40-50
50-60
60-70
70-80
80-90
90-100
Male
Female
E
Autosomal all tiles
(n = 745 699)
Male
Female
Methylation (%)
100
80
60
40
20
0
5' UTR
Promoter
Exon
Intron
TTS
3' UTR
Non-coding
Intergenic
X-chr all tiles
(n = 10 939)
Male
Female
Methylation (%)
100
80
60
40
20
0
5' UTR
Promoter
Exon
Intron
TTS
3' UTR
Non-coding
Intergenic

Supplemental Figure 3. Sex-specific DMRs occur throughout the E18.5 placenta genome but are concentrated on the X chromosomes A) DNA methylation levels of a random subset of tiles in the individual male and female placenta samples. **B)** Mean DNA methylation levels within ±15 kb of a transcriptional start site (TSS) or transcriptional end site (TES) in all analyzed tiles from male and female placentas. **C)** Distributions of the DNA methylation levels of various chromosomes in male and female placentas. Median DNA methylation values are indicated with diamonds. **D)** DNA methylation levels in tiles associated with autosomes (top) and X chromosomes (bottom) in male and female placentas. ****$p < 0.0001$, ***$p < 0.001$ by two-proportion*z*-test . **E)** Average DNA methylation levels in tiles associated with various genomic features on the autosomal (top) and X (bottom) chromosomes of male and female placentas.

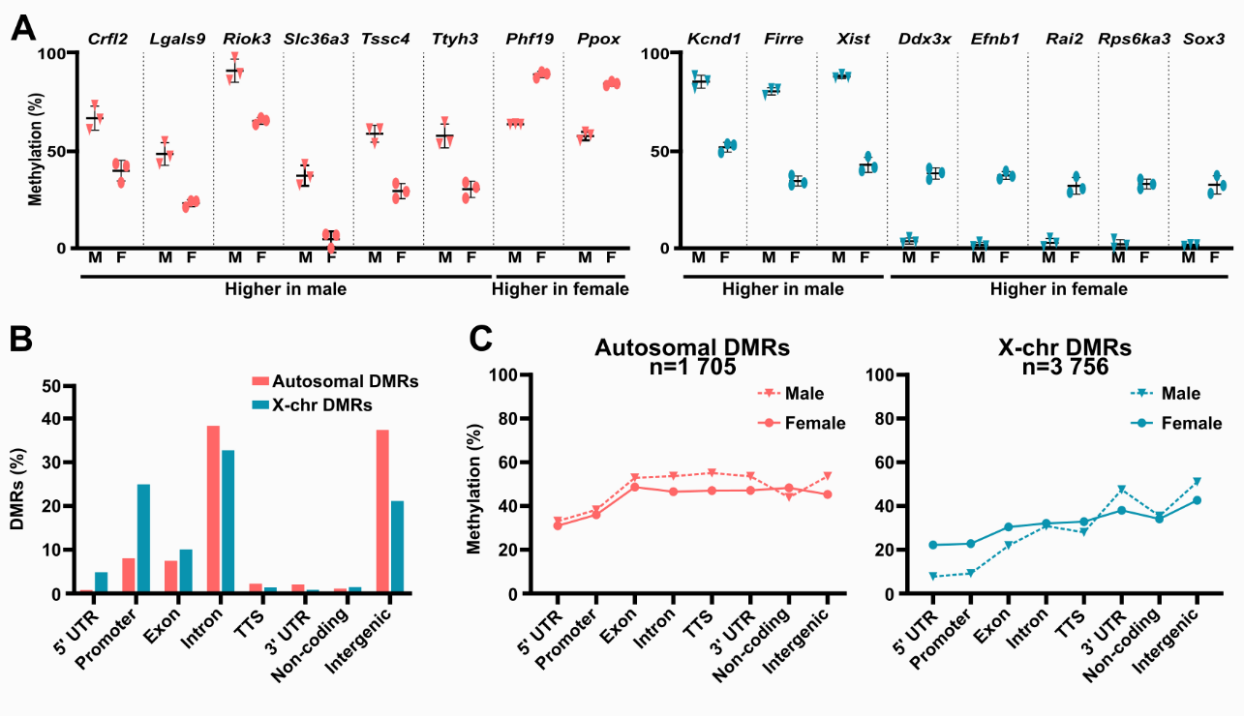

Supplemental Figure 4. Sex-specific DNA methylation differences in various genomic elements A) DNA methylation levels of top changed genes on the autosomes (left) and X chromosomes (right) of male and female placentas. **B)** Distributions of autosomal (pink) and X chromosome (blue) DMRs located in various genomic elements in male and female placentas. **C)** Average DNA methylation levels of sex-specific DMRs in autosomes (left) and X chromosomes (right) based on their location's genomic annotation.

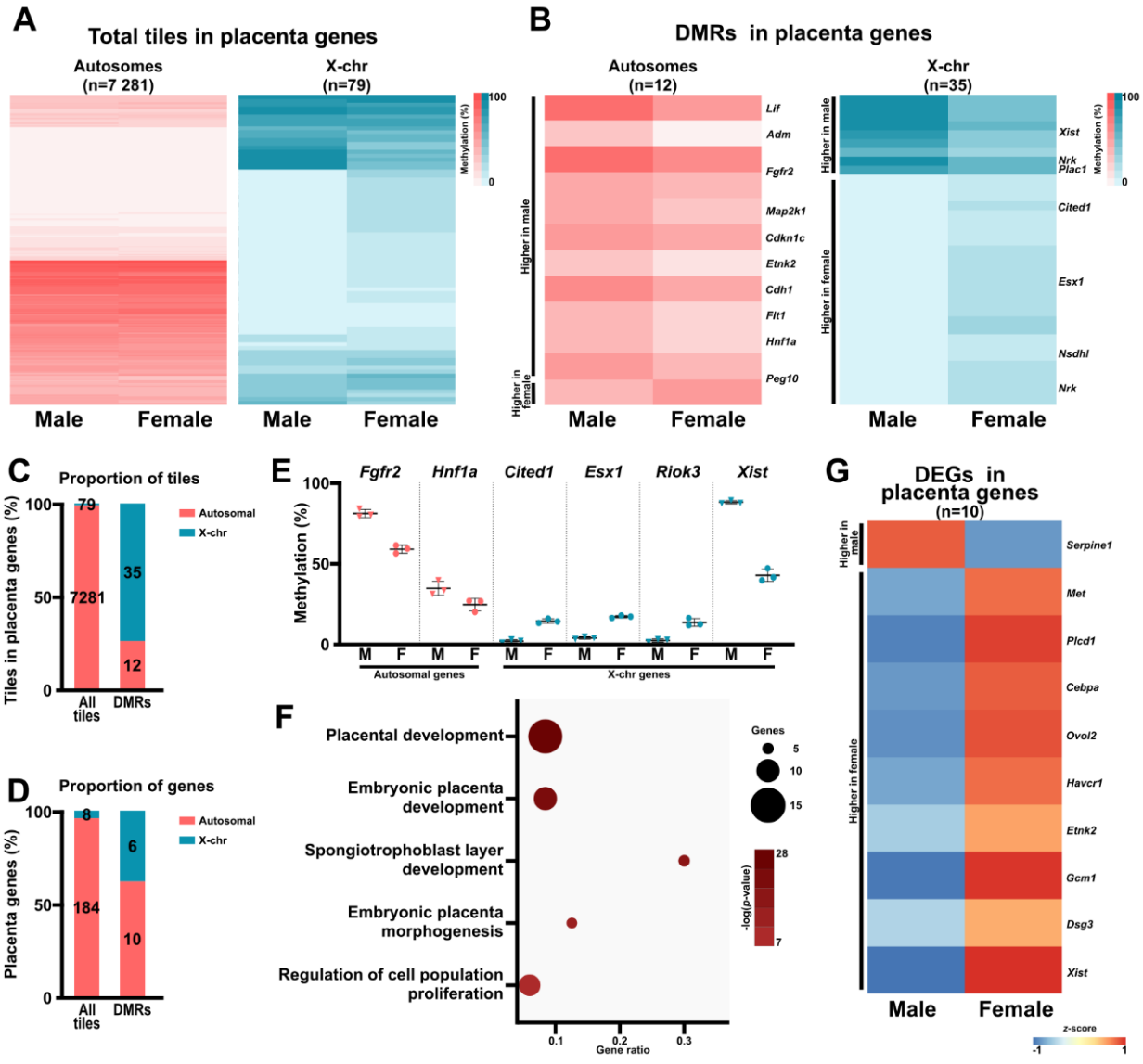

Supplemental Figure 5. DNA methylation and expression patterns of genes essential for placental development A) DNA methylation levels of autosomal (left) and X chromosomal (right) tiles associated with key placental developmental genes in male and female E18.5 placentas. **B)** DNA methylation levels of autosomal and X chromosomal DMRs associated with placental development genes in male and female placentas. **C)** Distributions of all analyzed tiles and DMRs located in essential placental development genes on the autosomes and X chromosomes. **D)** Distributions of individual placenta developmental genes on the autosomes and X chromosomes in the analyzed tiles and DMRs. **E)** DNA methylation levels of selected placenta developmental gene-related DMRs in male and female placentas. **F)** The top five pathways enriched for the

placental development-associated DMRs in B). **G)** Expression levels (*z*-scores) of differentially expressed essential placental development genes.

REFERENCES

1. Burton GJ, Fowden AL. The placenta: a multifaceted, transient organ. Philosophical transactions of the Royal Society of London Series B, Biological sciences. 2015;370(1663):20140066.
2. Treissman J, Yuan V, Baltayeva J, Le HT, Castellana B, Robinson WP, et al. Low oxygen enhances trophoblast column growth by potentiating differentiation of the extravillous lineage and promoting LOX activity. Development (Cambridge, England). 2020;147(2).
3. Weng J, Couture C, Girard S. Innate and Adaptive Immune Systems in Physiological and Pathological Pregnancy. Biology. 2023;12(3).
4. Coussons-Read ME. Effects of prenatal stress on pregnancy and human development: mechanisms and pathways. Obstetric medicine. 2013;6(2):52-7.
5. Wadhwa PD, Entringer S, Buss C, Lu MC. The contribution of maternal stress to preterm birth: issues and considerations. Clinics in perinatology. 2011;38(3):351-84.
6. Bale TL. The placenta and neurodevelopment: sex differences in prenatal vulnerability. Dialogues in clinical neuroscience. 2016;18(4):459-64.
7. Rosenfeld CS. Sex-Specific Placental Responses in Fetal Development. Endocrinology. 2015;156(10):3422-34.
8. Di Renzo GC, Rosati A, Sarti RD, Cruciani L, Cutuli AM. Does fetal sex affect pregnancy outcome? Gender medicine. 2007;4(1):19-30.
9. Eriksson JG, Kajantie E, Osmond C, Thornburg K, Barker DJ. Boys live dangerously in the womb. American journal of human biology : the official journal of the Human Biology Council. 2010;22(3):330-5.
10. Ingemarsson I. Gender aspects of preterm birth. BJOG : an international journal of obstetrics and gynaecology. 2003;110 Suppl 20:34-8.
11. Murji A, Proctor LK, Paterson AD, Chitayat D, Weksberg R, Kingdom J. Male sex bias in placental dysfunction. American journal of medical genetics Part A. 2012;158a(4):779-83.
12. Al-Qaraghouli M, Fang YMV. Effect of Fetal Sex on Maternal and Obstetric Outcomes. Frontiers in pediatrics. 2017;5:144.
13. Christians JK, Ahmadzadeh-Seddeighi S, Bilal A, Bogdanovic A, Ho R, Leung EV, et al. Sex differences in the effects of prematurity and/or low birthweight on neurodevelopmental outcomes: systematic review and meta-analyses. Biology of sex differences. 2023;14(1):47.
14. Christians JK, Chow NA. Are there sex differences in fetal growth strategies and in the long-term effects of pregnancy complications on cognitive functioning? Journal of developmental origins of health and disease. 2022;13(6):766-78.
15. Skinner MK. Role of epigenetics in developmental biology and transgenerational inheritance. Birth defects research Part C, Embryo today : reviews. 2011;93(1):51-5.
16. Joseph DB, Strand DW, Vezina CM. DNA methylation in development and disease: an overview for prostate researchers. American journal of clinical and experimental urology. 2018;6(6):197-218.

17. Lang Z, Wang Y, Tang K, Tang D, Datsenka T, Cheng J, et al. Critical roles of DNA demethylation in the activation of ripening-induced genes and inhibition of ripening-repressed genes in tomato fruit. Proceedings of the National Academy of Sciences of the United States of America. 2017;114(22):E4511-e9.
18. Smith ZD, Chan MM, Humm KC, Karnik R, Mekhoubad S, Regev A, et al. DNA methylation dynamics of the human preimplantation embryo. Nature. 2014;511(7511):611-5.
19. Legault LM, Doiron K, Lemieux A, Caron M, Chan D, Lopes FL, et al. Developmental genome-wide DNA methylation asymmetry between mouse placenta and embryo. Epigenetics. 2020;15(8):800-15.
20. Wang K, Liu S, Svoboda LK, Rygiel CA, Neier K, Jones TR, et al. Tissue- and Sex-Specific DNA Methylation Changes in Mice Perinatally Exposed to Lead (Pb). Frontiers in genetics. 2020;11:840.
21. Legault LM, Doiron K, Breton-Larrivée M, Langford-Avelar A, Lemieux A, Caron M, et al. Pre-implantation alcohol exposure induces lasting sex-specific DNA methylation programming errors in the developing forebrain. Clinical epigenetics. 2021;13(1):164.
22. Wanner NM, Colwell M, Drown C, Faulk C. Developmental cannabidiol exposure increases anxiety and modifies genome-wide brain DNA methylation in adult female mice. Clinical epigenetics. 2021;13(1):4.
23. Legault LM, Bertrand-Lehouillier V, McGraw S. Pre-implantation alcohol exposure and developmental programming of FASD: an epigenetic perspective. Biochemistry and cell biology = Biochimie et biologie cellulaire. 2018;96(2):117-30.
24. Inkster AM, Yuan V, Konwar C, Matthews AM, Brown CJ, Robinson WP. A cross-cohort analysis of autosomal DNA methylation sex differences in the term placenta. Biology of sex differences. 2021;12(1):38.
25. Martin E, Smeester L, Bommarito PA, Grace MR, Boggess K, Kuban K, et al. Sexual epigenetic dimorphism in the human placenta: implications for susceptibility during the prenatal period. Epigenomics. 2017;9(3):267-78.
26. Buckberry S, Bianco-Miotto T, Bent SJ, Dekker GA, Roberts CT. Integrative transcriptome meta-analysis reveals widespread sex-biased gene expression at the human fetal-maternal interface. Molecular human reproduction. 2014;20(8):810-9.
27. Cvitic S, Longtine MS, Hackl H, Wagner K, Nelson MD, Desoye G, et al. The human placental sexome differs between trophoblast epithelium and villous vessel endothelium. PloS one. 2013;8(10):e79233.
28. Sood R, Zehnder JL, Druzin ML, Brown PO. Gene expression patterns in human placenta. Proceedings of the National Academy of Sciences of the United States of America. 2006;103(14):5478-83.
29. Braun AE, Mitchel OR, Gonzalez TL, Sun T, Flowers AE, Pisarska MD, et al. Sex at the interface: the origin and impact of sex differences in the developing human placenta. Biology of sex differences. 2022;13(1):50.
30. Carter AM. Animal models of human placentation--a review. Placenta. 2007;28 Suppl A:S41-7.
31. Shaffer B, McGraw S, Xiao SC, Chan D, Trasler J, Chaillet JR. The DNMT1 intrinsically disordered domain regulates genomic methylation during development. Genetics. 2015;199(2):533-41.
32. Legault LM, Chan D, McGraw S. Rapid Multiplexed Reduced Representation Bisulfite Sequencing Library Prep (rRRBS). Bio-protocol. 2019;9(4):e3171.

33. Pierre WC, Legault LM, Londono I, McGraw S, Lodygensky GA. Alteration of the brain methylation landscape following postnatal inflammatory injury in rat pups. FASEB journal : official publication of the Federation of American Societies for Experimental Biology. 2020;34(1):432-45.
34. Bourgey M, Dali R, Eveleigh R, Chen KC, Letourneau L, Fillon J, et al. GenPipes: an open-source framework for distributed and scalable genomic analyses. GigaScience. 2019;8(6).
35. Love MI, Huber W, Anders S. Moderated estimation of fold change and dispersion for RNA-seq data with DESeq2. Genome biology. 2014;15(12):550.
36. Krueger F, Andrews SR. Bismark: a flexible aligner and methylation caller for Bisulfite-Seq applications. Bioinformatics (Oxford, England). 2011;27(11):1571-2.
37. Akalin A, Kormaksson M, Li S, Garrett-Bakelman FE, Figueroa ME, Melnick A, et al. methylKit: a comprehensive R package for the analysis of genome-wide DNA methylation profiles. Genome biology. 2012;13(10):R87.
38. Heinz S, Benner C, Spann N, Bertolino E, Lin YC, Laslo P, et al. Simple combinations of lineage-determining transcription factors prime cis-regulatory elements required for macrophage and B cell identities. Molecular cell. 2010;38(4):576-89.
39. Zhou Y, Zhou B, Pache L, Chang M, Khodabakhshi AH, Tanaseichuk O, et al. Metascape provides a biologist-oriented resource for the analysis of systems-level datasets. Nature communications. 2019;10(1):1523.
40. Karolchik D, Hinrichs AS, Furey TS, Roskin KM, Sugnet CW, Haussler D, et al. The UCSC Table Browser data retrieval tool. Nucleic acids research. 2004;32(Database issue):D493-6.
41. Canovas S, Ross PJ. Epigenetics in preimplantation mammalian development. Theriogenology. 2016;86(1):69-79.
42. Jones PL, Veenstra GJ, Wade PA, Vermaak D, Kass SU, Landsberger N, et al. Methylated DNA and MeCP2 recruit histone deacetylase to repress transcription. Nature genetics. 1998;19(2):187-91.
43. Ehrlich M, Lacey M. DNA methylation and differentiation: silencing, upregulation and modulation of gene expression. Epigenomics. 2013;5(5):553-68.
44. Hahn MA, Wu X, Li AX, Hahn T, Pfeifer GP. Relationship between gene body DNA methylation and intragenic H3K9me3 and H3K36me3 chromatin marks. PloS one. 2011;6(4):e18844.
45. Jones PA. Functions of DNA methylation: islands, start sites, gene bodies and beyond. Nature reviews Genetics. 2012;13(7):484-92.
46. Saoi M, Kennedy KM, Gohir W, Sloboda DM, Britz-McKibbin P. Placental Metabolomics for Assessment of Sex-specific Differences in Fetal Development During Normal Gestation. Scientific reports. 2020;10(1):9399.
47. Meakin AS, Cuffe JSM, Darby JRT, Morrison JL, Clifton VL. Let's Talk about Placental Sex, Baby: Understanding Mechanisms That Drive Female- and Male-Specific Fetal Growth and Developmental Outcomes. International journal of molecular sciences. 2021;22(12).
48. Hunter SK, Hoffman MC, D'Alessandro A, Noonan K, Wyrwa A, Freedman R, et al. Male fetus susceptibility to maternal inflammation: C-reactive protein and brain development. Psychological medicine. 2021;51(3):450-9.
49. Baines KJ, West RC. Sex differences in innate and adaptive immunity impact fetal, placental, and maternal health. Biology of reproduction. 2023.
50. Braun AE, Carpentier PA, Babineau BA, Narayan AR, Kielhold ML, Moon HM, et al. "Females Are Not Just 'Protected' Males": Sex-Specific Vulnerabilities in Placenta and Brain after Prenatal Immune Disruption. eNeuro. 2019;6(6).

51. Hanamsagar R, Bilbo SD. Sex differences in neurodevelopmental and neurodegenerative disorders: Focus on microglial function and neuroinflammation during development. The Journal of steroid biochemistry and molecular biology. 2016;160:127-33.
52. Ceasrine AM, Devlin BA, Bolton JL, Green LA, Jo YC, Huynh C, et al. Maternal diet disrupts the placenta-brain axis in a sex-specific manner. Nature metabolism. 2022;4(12):1732-45.
53. Rosenfeld CS. The placenta-brain-axis. Journal of neuroscience research. 2021;99(1):271-83.
54. Laufer BI, Neier K, Valenzuela AE, Yasui DH, Schmidt RJ, Lein PJ, et al. Placenta and fetal brain share a neurodevelopmental disorder DNA methylation profile in a mouse model of prenatal PCB exposure. Cell reports. 2022;38(9):110442.
55. Sutherland S, Brunwasser SM. Sex Differences in Vulnerability to Prenatal Stress: a Review of the Recent Literature. Current psychiatry reports. 2018;20(11):102.
56. Andrews SV, Yang IJ, Froehlich K, Oskotsky T, Sirota M. Large-scale placenta DNA methylation integrated analysis reveals fetal sex-specific differentially methylated CpG sites and regions. Scientific reports. 2022;12(1):9396.
57. Hall E, Volkov P, Dayeh T, Esguerra JL, Salö S, Eliasson L, et al. Sex differences in the genome-wide DNA methylation pattern and impact on gene expression, microRNA levels and insulin secretion in human pancreatic islets. Genome biology. 2014;15(12):522.
58. García-Calzón S, Perfilyev A, de Mello VD, Pihlajamäki J, Ling C. Sex Differences in the Methylome and Transcriptome of the Human Liver and Circulating HDL-Cholesterol Levels. The Journal of clinical endocrinology and metabolism. 2018;103(12):4395-408.
59. Oliva M, Muñoz-Aguirre M, Kim-Hellmuth S, Wucher V, Gewirtz ADH, Cotter DJ, et al. The impact of sex on gene expression across human tissues. Science (New York, NY). 2020;369(6509).
60. Khodursky S, Jiang CS, Zheng EB, Vaughan R, Schrider DR, Zhao L. Sex differences in interindividual gene expression variability across human tissues. PNAS nexus. 2022;1(5):pgac243.
61. Grant OA, Wang Y, Kumari M, Zabet NR, Schalkwyk L. Characterising sex differences of autosomal DNA methylation in whole blood using the Illumina EPIC array. Clinical epigenetics. 2022;14(1):62.
62. Bulka CM, Everson TM, Burt AA, Marsit CJ, Karagas MR, Boyle KE, et al. Sex-based differences in placental DNA methylation profiles related to gestational age: an NIH ECHO meta-analysis. Epigenetics. 2023;18(1):2179726.
63. Marks H, Kerstens HH, Barakat TS, Splinter E, Dirks RA, van Mierlo G, et al. Dynamics of gene silencing during X inactivation using allele-specific RNA-seq. Genome biology. 2015;16(1):149.
64. Cui Y, Cruz M, Palatnik A, Olivier-Van Stichelen S. O-GlcNAc transferase contributes to sex-specific placental deregulation in gestational diabetes. Placenta. 2023;131:1-12.
65. Howerton CL, Morgan CP, Fischer DB, Bale TL. O-GlcNAc transferase (OGT) as a placental biomarker of maternal stress and reprogramming of CNS gene transcription in development. Proceedings of the National Academy of Sciences of the United States of America. 2013;110(13):5169-74.